

---

# Performance Analysis of the HARQ Dynamic Decode-and-Forward Protocol

---

Author:

Stefan Maagh

A thesis submitted in partial fulfilment of the requirements of  
Edinburgh Napier University, for award of Doctor of Philosophy

April 2015

Contact: [s.maagh@napier.ac.uk](mailto:s.maagh@napier.ac.uk)

This document was set with the help of KOMA-Script and L<sup>A</sup>T<sub>E</sub>X

# Abstract

---

The explosive growth of data traffic in wireless communication systems comes together with the urgent need to minimize its environmental and financial impact. Therefore, the main objective in the field of green radio communication is to improve the energy efficiency of wireless communication systems with respect to the future performance demands on the wireless communication infrastructure. In this context, recent research in cooperative and cognitive communication techniques attracts particular attention.

While cognitive radio improves spectral efficiency by enhanced spectrum utilization, cooperative communication techniques achieve remarkable gains in spectral efficiency by enabling the terminals to share their resources. In particular, creating virtual multi-antenna arrays by antenna sharing enables exploitation of spatial diversity gains and multiplexing gains within a network of single antenna terminals. This technique is particularly attractive for mobile wireless networks, since power and space constraints often prohibit the integration of multiple antennas into mobile terminals.

This work studies the performance of the hybrid automatic repeat-request (HARQ) dynamic decode-and-forward (DDF) protocol in the half-duplex relay channel. The reason behind exploration of the HARQ-DDF protocol is that it achieves the optimal performance in terms of the diversity-multiplexing tradeoff (DMT) and the diversity-multiplexing-delay tradeoff (DMDT). However, DMT and DMDT are evaluated as the signal-to-noise ratio (SNR) approaches infinity.

In practice, key performance measures are the fixed-rate outage probability and delay-limited throughput achieved at the SNR expected during operation. To this end, it is common practice to give the performance of the DDF protocol as a function of the source-to-destination channel SNR (SD-SNR). In this dissertation the focus is to study the performance of the HARQ-DDF protocol measured as a function of the SNR as seen at the destination (D-SNR). This approach enables the performance comparison with the HARQ-SISO and the HARQ-MISO protocol from an energy efficiency perspective on the system level. Furthermore, a novel variant of the HARQ-MISO protocol, the hybrid repeat-with-diversity-request (HARDQ) MISO protocol, is introduced.

Considering outage probability as measure of reliability, closed-form solutions and simulation results show that the HARDQ-MISO and the HARQ-DDF protocol outperform the HARQ-MISO protocol from an energy efficiency point of view. From a delay-limited throughput point of view the HARQ-MISO protocol is beneficial. It is demonstrated that code-rate assignment allows to achieve significant performance gains in terms of delay-limited throughput. Furthermore, reducing the decoding cost using code-rate assignment techniques comes together with only negligible performance loss.

# Acknowledgement

---

First and foremost, I thank my parents, sister and brother for their love, support and motivation they gave me throughout my life.

I want to thank my supervisors Dr. T. David Binnie and Prof. John Sharp for their support, patience and guidance during the research process. Furthermore, I want to thank Dr. Mohammad Y. Sharif and Prof. Abid E. A. Almaini for their valuable discussion and support in the early stages of this research.

I would like to thank all the people who supported me during my research in so many various ways. In particular, I want to thank Marcus Holland-Moritz, Juer-gen Lenz and Tommaso Locatelli for helping me to stay sane during these difficult years. Furthermore, I am very grateful to Marcus Holland-Moritz, Thomas Schommer, Lily Petkova, Richard Nesnass and Nelly Juillet for proof-reading my conference papers. I would like to thank my flatmates Conor Cromie and Chris Bowden for their support and for making my life so much easier during the writing-up process.

I also would like to acknowledge my colleagues at odos-imaging ltd. for their patience and support throughout the last two years of this dissertation.

Without all this people (and many, many more) I would not have been able to pass the research process and to complete this dissertation.

# Contents

---

<b>List of Figures</b>	<b>VI</b>
<b>List of Abbreviations</b>	<b>XII</b>
<b>1 Motivation</b>	<b>1</b>
<b>2 Contribution and Outlook</b>	<b>7</b>
<b>3 Channel Models and Cooperative Communication</b>	<b>12</b>
3.1 Wireless Channel Models . . . . .	14
3.1.1 Single-Input Single-Output Channel . . . . .	17
3.1.2 Multiple-Input Multiple-Output Channel . . . . .	18
3.1.3 Half-Duplex Relay Channel . . . . .	19
3.2 Space-Time Block Codes . . . . .	20
3.2.1 Alamouti Code . . . . .	22
3.3 Performance Measures . . . . .	23
3.4 Cooperative Communication . . . . .	25
3.4.1 Protocols . . . . .	28
3.4.2 Dynamic Decode-and-Forward Protocol . . . . .	32
<b>4 Automatic Repeat-Request Protocols</b>	<b>34</b>
4.1 HARQ-SISO Protocol . . . . .	38
4.2 HARQ-MISO Protocol . . . . .	39
4.3 HARDQ-MISO Protocol . . . . .	40
4.4 HARQ-DDF Protocol . . . . .	41
4.5 Delay-limited throughput . . . . .	43
4.6 Signal-to-Noise Ratio . . . . .	44
4.7 Summary . . . . .	46

<b>5</b>	<b>Performance Analysis</b>	<b>48</b>
5.1	HARQ-SISO Protocol . . . . .	53
5.2	HARQ-MISO Protocol . . . . .	54
5.3	HARDQ-MISO Protocol . . . . .	55
5.4	HARQ-DDF Protocol . . . . .	56
5.5	SNR as Observed at the Destination . . . . .	58
5.6	Discrete Channel Inputs . . . . .	60
5.7	Verification using Monte Carlo Simulations . . . . .	62
5.7.1	Gaussian Channel Inputs . . . . .	63
5.7.2	Discrete Channel Inputs . . . . .	66
5.8	Summary . . . . .	67
<b>6</b>	<b>Numerical Results: Gaussian and Discrete Channel Inputs</b>	<b>70</b>
6.1	Outage Probability Analysis Considering SD-SNR and D-SNR . . . . .	72
6.2	Throughput Optimization Using Code Rate Assignment . . . . .	79
6.3	Performance Comparison of the NPA and the TPA HARQ Protocols . . . . .	83
6.4	Decoding Cost Reduction at the Relay for the HARQ-DDF Protocol . . . . .	86
6.5	Decoding Cost Reduction at the Relay and the Destination . . . . .	91
6.6	Summary . . . . .	97
<b>7</b>	<b>Numerical Results: RCPC Coding</b>	<b>100</b>
7.1	RCPC Coding for HARQ Protocols . . . . .	100
7.2	Simulation Set-up . . . . .	104
7.3	Outage Probability Analysis Considering SD-SNR and D-SNR . . . . .	105
7.4	Performance Comparison of the NPA and the TPA HARQ Protocols . . . . .	118
7.5	Decoding Cost Reduction at the Relay for the HARQ-DDF Protocol . . . . .	124
7.6	Decoding Cost Reduction at the Relay and the Destination . . . . .	125
7.7	Summary . . . . .	131
<b>8</b>	<b>Conclusion</b>	<b>133</b>
<b>9</b>	<b>Outlook Towards Future Work</b>	<b>136</b>
	<b>References</b>	<b>139</b>
<b>A</b>	<b>Outage Probability</b>	<b>152</b>

A.1	Outage Probability of the HARQ-MISO protocol . . . . .	152
A.2	Outage Probability of the HARDQ-MISO protocol . . . . .	155
A.2.1	Upper and lower bounds for $M$ . . . . .	157
<b>B</b>	<b>Comparison of Closed-Form and Simulation Results for the TPA HARQ Protocols</b>	<b>159</b>
<b>C</b>	<b>Numerical Performance Analysis Considering SD-SNR and D-SNR</b>	<b>161</b>
C.1	$C_{\text{non-opt}}$ and 16-QAM Channel Inputs . . . . .	161
C.2	$C_{\text{opt}}$ and Gaussian Channel Inputs . . . . .	166
C.2.1	HARDQ-MISO Protocol . . . . .	166
C.2.2	HARQ-DDF Protocol . . . . .	171
C.3	$C_{\text{opt}}$ and 16-QAM Channel Inputs . . . . .	171
<b>D</b>	<b>Performance of the RCPC Encoded HARQ Protocols With Increasing Memory</b>	<b>177</b>
<b>E</b>	<b>Publications</b>	<b>180</b>
E.1	On the Dynamic Decode-and-Forward Relay Listen-Transmit Decision Rule in Intersymbol Interference Channels . . . . .	180
E.2	RCPC Coding for the Dynamic Decode-and-Forward Channel . . . . .	185
E.3	The Dynamic Decode-and-Forward Channel: SNR Allocation For Fair Performance Analysis . . . . .	192

## List of Figures

---

3.1	Simplified block diagram of a digital communication system . . . . .	13
3.2	Multiple-input multiple-output channel with source S and destination D, each equipped with multiple antennas. . . . .	18
3.3	Half-duplex relay channel with source S, relay R and destination D together with channel coefficients $h_0$ , $h_{sr}$ and $h_1$ . . . . .	20
3.4	SER Comparison of the Rayleigh fading SISO and MISO channel using Alamouti encoding and BPSK modulation. . . . .	23
3.5	Set-up of a relay channel creating a virtual multi-antenna array; S: source; R: relay; D: destination . . . . .	26
3.6	Set-up of communication system providing user cooperation diversity	26
3.7	Orthogonal frequency-division medium access control ... . . . . .	30
4.1	Illustration of a communication system with one source and one destination employing the HARQ protocol. . . . .	37
4.2	Illustration of the half-duplex relay channel together with the HARQ-DDF protocol. . . . .	42
5.1	Mutual information of the discrete-input continuous-output AWGN channel for BPSK, 4-QAM and 16-QAM symbol constellations. . . . .	61
5.2	Outage probability of the NPA HARQ protocols measured as a function of the D-SNR. The Monte Carlo simulation results with $N = 10^8$ verify the closed-form expressions given in Chapter 5. . . . .	65
5.3	Delay-limited throughput of the NPA HARQ protocols measured as a function of the D-SNR. The Monte Carlo simulation results with $N = 10^8$ verify the closed-form expressions given in Chapter 5. . . . .	65

6.1	Comparison of the outage probability measured as a function of the SD-SNR and D-SNR for the HARDQ-MISO protocol considering Gaussian channel inputs and increasing $t$ . . . . .	73
6.2	Comparison of the delay-limited throughput as a function of the SD-SNR and the D-SNR for the HARDQ-MISO protocol considering Gaussian channel inputs and increasing $t$ . . . . .	74
6.3	Comparison of the outage probability measured as a function of the SD-SNR and the D-SNR for the HARQ-DDF protocol considering Gaussian channel inputs and increasing $\min\{D_r\}$ . . . . .	75
6.4	Comparison of the delay-limited throughput as a function of the SD-SNR and the D-SNR for the HARQ-DDF protocol considering Gaussian channel inputs and increasing $\min\{D_r\}$ . . . . .	76
6.5	Comparison of the outage probability of the code books $\mathcal{C}_{\text{non-opt}}$ and $\mathcal{C}_{\text{opt}}$ considering Gaussian distributed channel inputs. . . . .	80
6.6	Comparison of the delay-limited throughput of the code books $\mathcal{C}_{\text{non-opt}}$ and $\mathcal{C}_{\text{opt}}$ considering Gaussian distributed channel inputs. . . . .	80
6.7	Comparison of the outage probability of the code books $\mathcal{C}_{\text{non-opt}}$ and $\mathcal{C}_{\text{opt}}$ considering uniformly distributed 16-QAM channel inputs. . . . .	82
6.8	Comparison of the delay-limited throughput of the code books $\mathcal{C}_{\text{non-opt}}$ and $\mathcal{C}_{\text{opt}}$ considering uniformly distributed 16-QAM channel inputs. . . . .	82
6.9	Comparison of the outage probability and the delay-limited throughput of the NPA HARQ protocols and the TPA HARQ protocols considering Gaussian channel inputs. . . . .	84
6.10	Comparison of the outage probability and the delay-limited throughput of the NPA HARQ protocols and the TPA HARQ protocols considering 16-QAM channel inputs. . . . .	85
6.11	Comparison of the outage probability and delay-limited throughput of the HARQ-DDF protocol with reduced decoding cost at the relay considering Gaussian channel inputs. . . . .	88
6.12	Comparison of the outage probability and delay-limited throughput of the HARQ-DDF protocol with reduced decoding cost at the relay considering 16-QAM channel inputs. . . . .	89

6.13	Outage probability of the HARDQ-MISO and HARQ-DDF protocol with reduced decoding cost at the relay and the destination considering Gaussian channel inputs. . . . .	93
6.14	Delay-limited throughput of the HARDQ-MISO and HARQ-DDF protocol with reduced decoding cost at the relay and the destination considering Gaussian channel inputs. . . . .	94
6.15	Outage probability of the HARDQ-MISO and HARQ-DDF protocol with reduced decoding cost at the relay and the destination considering 16-QAM channel inputs. . . . .	95
6.16	Delay-limited throughput of the HARDQ-MISO and HARQ-DDF protocol with reduced decoding cost at the relay and the destination considering 16-QAM channel inputs. . . . .	96
7.1	Comparison of the outage probability measured as a function of the SD-SNR and D-SNR for the HARDQ-MISO protocol and increasing $t = x$ , considering uniformly distributed BPSK channel inputs. . . .	107
7.2	Comparison of the delay-limited throughput measured as a function of the SD-SNR and D-SNR for the HARDQ-MISO protocol and increasing $t = x$ , considering uniformly distributed BPSK channel inputs. . . . .	108
7.3	Comparison of the outage probability measured as a function of the SD-SNR and D-SNR for the RCPC encoded HARDQ-MISO protocol and increasing $t = x$ . . . . .	110
7.4	Comparison of the delay-limited throughput measured as a function of the SD-SNR and D-SNR for the RCPC encoded HARDQ-MISO protocol and increasing $t = x$ . . . . .	111
7.5	Comparison of the outage probability measured as a function of the SD-SNR and D-SNR for the HARQ-DDF protocol and increasing $\min\{\mathcal{D}_r\} = x$ , considering uniformly distributed BPSK channel inputs. . . . .	112
7.6	Comparison of the delay-limited throughput measured as a function of the SD-SNR and D-SNR for the HARQ-DDF protocol and increasing $\min\{\mathcal{D}_r\} = x$ , considering uniformly distributed BPSK channel inputs. . . . .	113
7.7	Comparison of the outage probability measured as a function of the SD-SNR and D-SNR for the RCPC encoded HARQ-DDF protocol and increasing $\min\{\mathcal{D}_r\} = x$ . . . . .	115

7.8	Comparison of the delay-limited throughput measured as a function of the SD-SNR and D-SNR for the RCPC encoded HARQ-DDF protocol and increasing $\min\{\mathcal{D}_r\} = x$ . . . . .	116
7.9	Comparison of the outage probability of the HARDQ-MISO protocol and the HARQ-DDF protocol measured as a function of the D-SNR considering Gaussian channel inputs and increasing $t = \min\{\mathcal{D}_r\} = x$ . . . . .	117
7.10	Comparison of the outage probability and the delay-limited throughput applying the NPA HARQ protocols and the TPA HARQ protocols, considering uniformly distributed BPSK channel inputs. . . . .	120
7.11	Comparison of the outage probability and the delay-limited throughput applying the RCPC encoded NPA HARQ protocols and the TPA HARQ protocols. . . . .	121
7.12	Comparison of the outage probability and the delay-limited throughput of the HARQ-DDF protocol with reduced decoding cost at the relay and considering uniformly distributed BPSK channel inputs. . . . .	122
7.13	Comparison of the outage probability and the delay-limited throughput of the RCPC encoded HARQ-DDF protocol with reduced decoding cost at the relay. . . . .	123
7.14	Outage probability of the HARDQ-MISO and HARQ-DDF protocol with reduced decoding cost at the relay and the destination considering uniformly distributed BPSK channel inputs. . . . .	126
7.15	Delay-limited throughput of the HARDQ-MISO and HARQ-DDF protocol with reduced decoding cost at the relay and the destination considering uniformly distributed BPSK channel inputs. . . . .	127
7.16	Outage probability of the RCPC encoded HARDQ-MISO and HARQ-DDF protocol with reduced decoding cost at the relay and the destination. . . . .	128
7.17	Delay-limited throughput of the RCPC encoded HARDQ-MISO and HARQ-DDF protocol with reduced decoding cost at the relay and the destination. . . . .	129
B.1	Outage probability of the TPA HARQ protocols measured as a function of the D-SNR. The Monte Carlo simulation results verify the closed-form expressions given in Chapter 5. . . . .	160

B.2	Delay-limited throughput of the TPA HARQ protocols measured as a function of the D-SNR. The Monte Carlo simulation results verify the closed-form expressions given in Chapter 5. . . . .	160
C.1	Comparison of the outage probability measured as a function of the SD-SNR and D-SNR for the HARDQ-MISO protocol considering uniformly distributed 16-QAM channel inputs and increasing $t = x$ . . .	162
C.2	Comparison of the outage probability measured as a function of the SD-SNR and D-SNR for the HARQ-DDF protocol considering uniformly distributed 16-QAM channel inputs and increasing $\min\{D_r\} = x$ . . . . .	163
C.3	Comparison of the delay-limited throughput measured as a function of the D-SNR and the SD-SNR for the HARDQ-MISO protocol considering uniformly distributed 16-QAM channel inputs and increasing $t$ . . . . .	164
C.4	Comparison of the delay-limited throughput measured as a function of the D-SNR and the SD-SNR for the HARQ-DDF protocol considering uniformly distributed 16-QAM channel inputs and increasing $\min\{D_r\}$ . . . . .	165
C.5	Comparison of the outage probability measured as a function of the SD-SNR and the D-SNR for the HARDQ-MISO protocol considering Gaussian channel inputs and increasing $t = x$ . . . . .	167
C.6	Comparison of the delay-limited throughput measured as a function of the SD-SNR and the D-SNR for the HARDQ-MISO protocol considering Gaussian channel inputs and increasing $t = x$ . . . . .	168
C.7	Comparison of the outage probability measured as a function of the SD-SNR and the D-SNR for the HARQ-DDF protocol considering Gaussian channel inputs and increasing $\min\{D_r\} = x$ . . . . .	169
C.8	Comparison of the delay-limited throughput measured as a function of the SD-SNR and the D-SNR for the HARQ-DDF protocol considering Gaussian channel inputs and increasing $\min\{D_r\} = x$ . . . . .	170
C.9	Comparison of the outage probability measured as a function of the SD-SNR and the D-SNR for the HARDQ-MISO protocol considering uniformly distributed 16-QAM channel inputs and increasing $t = x$ . . . . .	173

C.10	Comparison of the delay-limited throughput measured as a function of the SD-SNR and the D-SNR for the HARDQ-MISO protocol considering uniformly distributed 16-QAM channel inputs and increasing $t = x$ . . . . .	174
C.11	Comparison of the outage probability measured as a function of the SD-SNR and the D-SNR for the HARQ-DDF protocol considering uniformly distributed 16-QAM channel inputs and increasing $\min\{D_r\} = x$ . . . . .	175
C.12	Comparison of the delay-limited throughput measured as a function of the D-SNR and the SD-SNR for the HARQ-DDF protocol considering uniformly distributed 16-QAM channel inputs and increasing $\min\{D_r\} = x$ . . . . .	176
D.1	HARQ-SISO protocol: comparison of the achievable performance and the performance applying RCPC coding with memory $v = 2, 4, 6$ . . . . .	178
D.2	HARQ-MISO protocol: comparison of the achievable performance and the performance applying RCPC coding with memory $v = 2, 4, 6$ . . . . .	178
D.3	HARDQ-MISO protocol: comparison of the achievable performance and the performance applying RCPC coding with memory $v = 2, 4, 6$ . . . . .	179
D.4	HARQ-DDF protocol: comparison of the achievable performance and the performance applying RCPC coding with memory $v = 2, 4, 6$ . . . . .	179

## List of Abbreviations

---

ACK	.....	Acknowledge
AF	.....	Amplify-and-forward
ARQ	.....	Automatic-repeat-request
AWGN	.....	Additive white Gaussian noise
BER	.....	Bit error rate
BPCU	.....	BPCU
BPSK	.....	Binary phase-shift keying
CDMA	.....	Code-division multiple-access
CRC	.....	Cyclic-redundancy check
CSI	.....	Channel state information
D-SNR	.....	SNR of the channel as seen at the destination
DDF	.....	Dynamic decode-and-forward
DF	.....	Decode-and-forward
DFE	.....	Decision feedback equaliser
DL	.....	Delay-limited
DMDT	.....	Diversity-multiplexing-delay tradeoff
DMT	.....	Diversity-multiplexing tradeoff
FDMA	.....	Frequency-division multiple-access
FEC	.....	Forward error-correction

---

FER . . . . .	Frame error rate
HARDQ . . . . .	Hybrid automatic-with-diversity-request/FEC
HARQ . . . . .	Hybrid ARQ/FEC
i.i.d. . . . .	independent identically distributed
ICI . . . . .	Inter-channel interference
IRC . . . . .	Incremental-redundancy code
ISI . . . . .	Inter-symbol interference
LMS . . . . .	Least mean square
LOS . . . . .	Line-of-sight
LT . . . . .	Long-term
LTW . . . . .	Laneman, Tse and Wornell
MAC . . . . .	Multiple access channel
MIMO . . . . .	Multiple-input multiple-output
MISO . . . . .	Multiple-input single-output
ML . . . . .	Maximum likelihood
MMSE . . . . .	Minimum mean-square error
NACK . . . . .	Negative-acknowledge
NPA . . . . .	Native power allocation
QAM . . . . .	Quadrature-amplitude modulation
RCPC . . . . .	Rate-compatible punctured convolutional
SD-SNR . . . . .	Source-to-destination channel SNR
SER . . . . .	Symbol error rate
SISO . . . . .	Single-input single-output
SNR . . . . .	Signal-to-noise ratio

STBC . . . . .	Space-time block code
STC . . . . .	Space-time code
TDMA . . . . .	Time-division multiple-access
TPA . . . . .	Transmit power allocation
WLAN . . . . .	Wireless local area network

# CHAPTER 1

---

## Motivation

---

Mobile wireless communication plays a very decisive role in the daily life of modern society. Mobile terminals such as smart-phones, tablets and laptops are omnipresent. For popular applications, such as video-data streaming, service providers have to implement reliable high-rate communication channels in order to permit high picture quality without lagging effects. On an annual basis, the Cisco Visual Networking Index publishes a well-founded global mobile data traffic forecast illustrating that it will become more and more difficult for service providers to ensure the provision of reliable high-speed wireless communication channels. Important statements in the recent publication [1] are:

*Global mobile data traffic will increase nearly 11-fold between 2013 and 2018. Mobile data traffic will grow at a compound annual growth rate (CAGR) of 61 percent from 2013 to 2018, reaching 15.9 exabytes per month by 2018 [1].*

*By the end of 2014, the number of mobile-connected devices will exceed the number of people on earth, and by 2018 there will be nearly 1.4 mobile devices per capita.*

*There will be over 10 billion mobile-connected devices by 2018, including machine-to-machine (M2M) modules—exceeding the world’s population at that time (7.6 billion) [1].*

***Mobile network connection speeds will increase two-fold by 2018.*** *The average mobile network connection speed (1,387 Kbps in 2013) will exceed 2.5 megabits per second (Mbps) by 2018 [1].*

A simple approach to increase the achievable transmission rate is to increase the allocated bandwidth available for communication. But service providers have only limited bandwidth available and in regional conurbations, where the service provider has to serve a huge amount of mobile devices, this limitation in bandwidth presents a pervasive constraint. Furthermore, together with the explosive growth of the global mobile data traffic comes the need to minimize its financial and environmental impact. Therefore, the field of green communication has attracted major attention. The main objective of green communication is to reduce the financial and environmental impact by improving energy efficiency of communication networks while preserving their quality of service [2, 3, 4]. Therefore, in order to meet the future demands on the wireless network infrastructure with respect to green communication considerations, it is self-evident to investigate communication technologies allowing to make the most efficient use of the available bandwidth.

Conventional wireless communication systems allocate bandwidth statically and employ a single antenna at the source and at the destination. Thereby, communication is established across the so-called single-input single-output (SISO) channel. Due to static bandwidth allocation residual capacity of under-utilized frequency bands remains unused. Therefore, an emerging approach to meet the future performance demands of the wireless network infrastructure is the application of cognitive radio techniques. A cognitive radio is formally defined as a radio that can *change its transmitter parameters based on interaction with its environment and may involve active negotiation or communications with other spectrum users* [5, 6]. Mainly, research in the field of cognitive radio is concerned with dynamic spectrum allocation techniques to improve spectral efficiency by enabling unlicensed users to communicate in under-utilized licensed frequency bands [7, 4].

A further attractive means to improve spectral efficiency is to integrate multiple antennas at the source and at the destination. Thereby, communication is established across the so-called multiple-input multiple-output (MIMO) channel. MIMO channels are proven to allow reliable communication at higher transmission rates at the same transmit power by exploitation of spatial diversity [8, 9, 10]. However, due to power and space limitations it is often not feasible to integrate multiple antennas for cellular communication into a mobile terminal. A promising approach to overcome these constraints is to share the resources of the mobile terminals such as antennas, bandwidth and transmit power using cooperative communication techniques. In this case, the network enables the exploitation of so-called cooperative diversity to transmit information from the source to the destination. In their landmark papers [11, 12] Sendonaris et al. show that cooperative diversity techniques allow to achieve

*higher data rates at the same power level, or alternatively, reduced required transmit power at the same data rate [11].*

Sharing antennas and bandwidth among single antenna terminals using cooperative communication techniques results effectively in the implementation of a *virtual* multi-antenna array.

Due to their simplicity, amplify-and-forward (AF) and decode-and-forward (DF) protocols are the most practical cooperative communication protocols. A relay applying the AF technique amplifies the received signal and forwards it to the destination. A relay applying the DF protocol decodes the received information and forwards the re-encoded information to the destination. Assuming half-duplex operation, Laneman, Tse and Wornell (LTW) studied in [13, 14] several AF and DF protocols with fixed listen and transmit intervals at the relaying terminal<sup>1</sup>.

Furthermore, an important approach to improve spectral efficiency is the application of hybrid automatic repeat-request (HARQ) techniques. HARQ techniques allow the adjustment of the code-rate and the error correction capabilities to the communication channel during the transmission of a code word [15] and thereby enable to achieve high throughput.

Since cognitive radio improves spectrum efficiency by enhancing the spectrum utilization, cooperative communication by implementation of cooperative

---

<sup>1</sup>The half-duplex relay is restricted to transmit or receive.

diversity, and HARQ techniques by adjusting the channel code to the channel conditions it is attractive to combine these approaches. A comprehensive survey about the recent state of art in the field of cooperative cognitive radio including future research directions is given in [4]. HARQ in context of cognitive radio is investigated in [16].

Recent work in the field of cooperative cognitive radio such as [3, 17] apply the LTW DF protocols. However, in [18] Azarian et al. introduce the dynamic decode-and-forward (DDF) protocol and in [19] the DDF protocol is embedded into a HARQ protocol. In difference to the LTW protocols, the listen-transmit interval lengths at the DDF relay are determined by the source to relay channel conditions. It is shown that the DDF protocol outperforms all LTW AF and LTW DF protocols in terms of the diversity-multiplexing tradeoff (DMT).

The DMT, first introduced in [20], is an important tool to compare the performance of communication systems and defines the relationship between spatial-diversity gains and multiplexing gains as the signal-to-noise ratio (SNR) tends to infinity<sup>2</sup>. It is shown that both the DDF protocol and the HARQ-DDF protocol achieve the optimal DMT<sup>3</sup> for multiplexing rates  $0 \leq r \leq 0.5$ . However, in his dissertation Azarian states [22]:

*It should be noted, however, that there is no established relation, in the literature, between the DMT of a protocol and its fixed-rate outage probability. This may cause difficulties in comparing two protocols' performances based on their tradeoff curves.*

In other words, a superior DMT does not necessarily result in a superior fixed-rate outage probability at the SNR of interest. But, from a practical point of view, it is attractive to compare traditional performance measures such as reliability and throughput at the SNR expected during operation. Throughout this work, reliability is measured in terms of the fixed-rate channel outage probability, and throughput is measured in terms of the delay-limited throughput as introduced in [23]. However, particular care has to be taken to maintain comparability between communication protocols and system set-ups on the system level.

<sup>2</sup>This tool is of particular interest if the performance analysis in terms of reliability and throughput as a function of the SNR becomes mathematically intractable.

<sup>3</sup>In [21] it is shown that the compress-and-forward protocol is DMT optimal in the half-duplex relay channel.

Essentially, the DDF protocol upgrades the SISO channel to the multiple-input single-output (MISO) channel as soon as the relay can decode the received information successfully. Consequently, in order to study the performance advantages and disadvantages of the DDF protocol, it is attractive to consider non-cooperative communication across the SISO and the MISO channel for reference. The time at which the relay starts to participate the transmission of a code word is referred to as the listen-transmit decision-time.

In [24], Khormuji and Larsson give the closed-form expression for the outage probability of the DDF protocol and compare its performance against other DF protocols applying repetition coding. In [23], Narasimhan gives the closed-form expression for the outage probability and the delay-limited throughput of the HARQ-DDF protocol. In both [24] and [23], the performance is measured as a function of the source-to-destination channel SNR (SD-SNR). Furthermore, pertinent literature investigating coding schemes for the DDF protocol, such as [25, 26, 27, 28], gives the performance measured as a function of the SD-SNR. However, the comparison of these performances measures against the performance of the SISO channel gives the performance gains from the source perspective, neglecting that the relay introduces additional energy into the system. On the contrary, in order to evaluate the energy efficiency on the system level it is necessary to consider the total energy introduced into the system. Therefore, in order to maintain comparability with the SISO and MISO channel on the system level, it has to be taken into account that the relay introduces additional energy into the channel as seen at the destination and thereby increases the SNR as seen at the destination (D-SNR).

In [29], the performance comparison against the SISO channel and, in [18] the performance comparison against the LTW protocols is carried out by sharing the total available transmit power constraint,  $P$ , between the transmitting terminals. Thus, in the first phase of the DDF protocol, the source is allocated the transmit power  $P$ . In the second phase, the relay participates the transmission and both the source and the relay are allocated the transmit power  $\frac{P}{2}$ . Consequently, the transmit power into the channel as seen at the destination is constant and together with a known noise variance, the D-SNR can be obtained without prior knowledge about the listen-transmit decision-time at the relay. Throughout this work, this modification is referred to as the transmit

power allocation (TPA) protocol .

However, the application of the TPA protocol complicates the DDF protocol and might not be feasible in practice, since a feedback channel from relay to source is required. In comparison, it is more practical to assume that the transmit power constraints at the source and the relay are independent and do not change during the transmission of a code word. Throughout this work, this power allocation scheme is referred to as the native power allocation (NPA) protocol. In case of the NPA DDF protocol, statistical knowledge about the listen-transmit decision-time at the relay is required to obtain the D-SNR.

In the context of this dissertation, initial work towards the performance comparison of the TPA and NPA DDF protocol against the performance of the SISO and MISO channel is published in [30]. In this dissertation, focus is on the performance of the TPA and NPA HARQ-DDF protocol applied in the half-duplex relay channel and the comparison against the SISO and MISO channel. Considering the NPA protocol, it is required to have statistical knowledge about the listen-transmit decision-time at the relay *and* to have statistical knowledge about the time at which the destination stops to listen to the transmission of a code word.

Since the DDF protocol outperforms the LTW DF protocols, future research in the field of cooperative cognitive radio should consider the implementation of the DDF protocol together with HARQ techniques as a means to improve spectral efficiency. To this end, the results given within this dissertation can be used as benchmarks.

### Contribution and Outlook

---

The sequel gives the outline and the main contribution of this dissertation.

Chapter 3 gives an overview about the general properties and structures of digital communication systems and their mathematical description. Furthermore, it gives the channel models applied throughout this dissertation. The Alamouti code is given in context of space-time coding, since this coding scheme is of particular importance for the performance analysis. Furthermore, Section 3.4 provides a brief review of important cooperative communication protocols and their properties. This review includes the LTW protocols and the non-HARQ DDF protocol.

Chapter 4 gives the HARQ-SISO, HARQ-MISO and HARQ-DDF protocols considered throughout this work. Furthermore, a novel variant of the HARQ-MISO protocol, the hybrid automatic repeat-with-diversity-request (HARDQ) protocol is introduced. The performance analysis of the HARDQ-MISO protocol gives the performance of the HARQ-DDF protocol for a perfect source-to-relay channel. However, in Chapter 6 and Chapter 7 it is demonstrated that this protocol is also of interest in the non-cooperative communication context. Both the HARDQ-MISO and the HARQ-DDF protocol are embedded into the NPA

and the TPA protocol variants. In this context, the notion of the D-SNR is introduced.

The main contributions in this chapter can be summarized as:

- In comparison to the HARQ-DDF protocols investigated in [19, 23], these protocol formulations allow ARQ rounds with unequal symbol length. An unequal symbol length per ARQ round enables to assign a specific transmission rate to each ARQ round. In [31] Chen et al. investigate the optimal rate assignment in context of the HARQ-SISO channel and show that *the average rate performance can be dramatically improved* [31]. While the protocol formulations given in this chapter allow for rate assignment, the problem of *optimal* rate assignment is beyond the scope of this dissertation. However, the potential of rate assignment is demonstrated in Chapter 6.
- In [26, 25] the DDF protocol is modified by limiting the relay to decode at a finite number of decoding time instants in order to reduce the complexity of the communication system. Following this approach, the given HARQ-DDF protocol enables the relay *and* the destination to perform decoding attempts within a code word at symbol intervals selected from a finite decoding instant set. In the HARQ-MISO protocol, this property translates into the possibility of enabling the second antenna at any symbol interval within the transmission of a code word. Considering the size of the decoding instant sets to be a measure for the decoding complexity at the receiving terminals, the comparison of decoding cost against performance gives valuable information for system optimization. Furthermore, enabling the configuration of the decoding instant sets ensures scalability of the decoding cost at the receiving terminals<sup>1</sup>.
- Care is taken to maintain performance comparability on the system level across the HARQ protocols from a coding and system set-up perspective.

---

<sup>1</sup>The selection of the number of ARQ rounds together with rate assignment also enables the scalability of the decoding cost for the HARQ protocols. However, for the HARQ-DDF protocol the notion of decoding instant sets ensures *independent* scalability of the decoding cost at the relay *and* the destination. Using the notion of decoding instant sets for all HARQ protocols unifies their formulation.

The notion of the D-SNR enables the performance comparability from an energy efficiency perspective on the system level.

The main contributions in Chapter 5 are:

- Building upon the work in [32] and [23], this chapter gives the closed-form expressions for the fixed-rate outage probability and the delay-limited throughput as a function of the D-SNR for the HARQ-SISO, the HARQ-MISO protocol, the TPA HARQ-MISO and the TPA HARQ-DFP protocol. The derivations are based on the assumption of random Gaussian code ensembles and typical set decoding.
- Using these results, a two-step approach is proposed to measure the fixed-rate outage probability and the delay-limited throughput of the NPA HARQ-MISO protocol and the NPA HARQ-DFP protocol as a function of the D-SNR.

Note, the application of random Gaussian code ensembles gives the maximum achievable performance considering Alamouti encoding<sup>2</sup>. However, this assumption implies that the channel inputs are selected from an infinite continuous set. In practice, this assumption is not appropriate since the channel inputs are selected from a finite discrete set. Furthermore, in practical communication systems it is often assumed that the channel inputs are uniform distributed<sup>3</sup>. Therefore, as an important special case [34, 35, 36] the performance of the HARQ protocols assuming Gaussian distributed channel inputs is compared against the performance assuming uniform distributed channel inputs. Corresponding this assumption, the mathematical expressions required to perform the performance analysis using the Monte Carlo simulation method are given.

Chapter 6 provides a numerical performance analysis of the HARQ protocols considering Gaussian channel inputs and discrete channel inputs. The discrete channel inputs are selected from a quadrature amplitude modulation lattice with 16 symbols (16-QAM). Furthermore, two incremental redundancy codes are selected providing a high transmission rate of 4 bits per channel use (BPCU)

<sup>2</sup>As shown in [33], Alamouti encoding is not capacity achieving.

<sup>3</sup>As example, for the standard maximum-likelihood detector uniform distribution of the channel input symbols is assumed. However, in practice often non-uniform distribution of channel input symbols is desired to achieve optimal performance and can be achieved using constellation shaping techniques as investigated in [34, 35]

in the first ARQ round. For the non-optimized code  $\mathcal{C}_{\text{non-opt}}$ , the code rate of each ARQ round is assigned such that the ARQ rounds are of equal symbol length. For the optimized code  $\mathcal{C}_{\text{opt}}$ , an optimized rate assignment with high transmission rates in the early ARQ rounds is used. The main contributions of this chapter can be summarized as

- Comparing the performance measured as a function of the SD-SNR and as a function of the D-SNR reveals differences in the performance characteristics in the low SNR regime.
- Measuring the performance as a function of the D-SNR enables the performance comparison of the HARDQ-MISO protocol and the HARQ-DDF protocol against the HARQ-SISO protocol and the HARQ-MISO protocol on the system level. Using this feature it is demonstrated that the HARDQ-MISO protocol and the HARQ-DDF protocol outperform the HARQ-MISO protocol in terms of the fixed-rate outage probability at high D-SNR from an energy efficiency point of view. However, the HARQ-MISO protocol is beneficial in terms of delay-limited throughput.
- Comparing the performance of the non-optimized code  $\mathcal{C}_{\text{non-opt}}$  against the performance of the optimized code  $\mathcal{C}_{\text{opt}}$  it is demonstrated that rate assignment techniques enable to improve the delay-limited throughput function. This effect is even more remarkable considering discrete channel inputs.
- It is demonstrated that the application of the NPA protocol variant outperforms the TPA protocol variant in terms of the fixed-rate outage probability. But the TPA protocol variant outperforms the NPA protocol variant in terms of delay-limited throughput.
- Reducing the decoding cost at the relay by means of perforation of the decoding instant set results in a high performance loss in terms of fixed-rate outage probability for high degrees of perforation. For low degrees of perforation, the performance loss is negligible. For low and high degrees of perforation, the performance loss in terms of delay-limited throughput is negligible. Similar results are observed for the HARDQ-MISO protocol.

- Reducing the decoding cost at the destination by means of perforation of the decoding instant set results in negligible performance loss in terms of outage probability. However, the performance loss in terms of delay-limited throughput is significant. Similar results are observed for the HARDQ-MISO protocol.

Chapter 7 provides a performance analysis of the rate-compatible punctured convolutional (RCPC) encoded HARQ protocols. To this end, a convolutional mother code  $\mathcal{C}_{\text{RCPC}}$  with memory  $v = 2$  and a low transmission rate of 0.76389 BPCU in the first ARQ round is selected. Binary phase-shift keying (BPSK) modulation is used at the transmitting terminals.

In order to provide a comparison against theory, a further system set-up applying a mother code with the same rate assignment as given by  $\mathcal{C}_{\text{RCPC}}$  but using uniformly distributed channel inputs is considered. Excluding the results obtained for rate assignment optimization, the contributions in this chapter can be summarized as given for Chapter 6. Furthermore:

- It is demonstrated that RCPC encoding together with the HARDQ-MISO protocol and the HARQ-DDF protocol shows good performance. However, RCPC encoding with memory  $v = 2$  shows a significant performance loss compared against the theoretical measures. In Appendix D it is demonstrated that an increase in memory results in a significant performance gain.
- It is demonstrated that the RCPC code and the theoretical performance measures show the same characteristics.
- In comparison to Chapter 6, it can be observed that the application of the TPA protocol variant does not show a performance advantage in terms of delay limited throughput.

In the context of this dissertation, RCPC coding for the DDF protocol is published in [37].

Chapter 8 concludes this dissertation and Chapter 9 identifies interesting subjects to be considered for future research in the context of this dissertation.

# Channel Models and Cooperative Communication

---

In wireless communication systems, information is transmitted from the source to the destination by modulating the digital or analogue information on electromagnetic waves. Antennas at both ends of the communication channel couple transmitter and receiver to the propagation medium [38]. Wireless communication channels are impaired by many detrimental effects, such as fading and additive noise, which make it difficult to recover the information at the destination. Therefore, it is necessary to protect the information using appropriate error correction and error detection techniques.

Figure 3.1 shows the simplified block diagram of a digital communication system. Both transmitter and receiver have knowledge about the channel code  $\mathcal{C}$ , which is selected, such that the error correction and error detection capabilities are matched to the channel conditions and the application requirements [38, 15].

The information source passes the binary information sequence  $\mathbf{f}$  of length  $k$  bits to the channel encoder. The channel encoder  $\mathcal{C}(n, k)$  encodes this sequence into the binary output sequence  $\mathbf{m}$  of length  $n$  bits, referred to as code word. The ratio  $R = \frac{k}{n}$  is called the *code rate*.

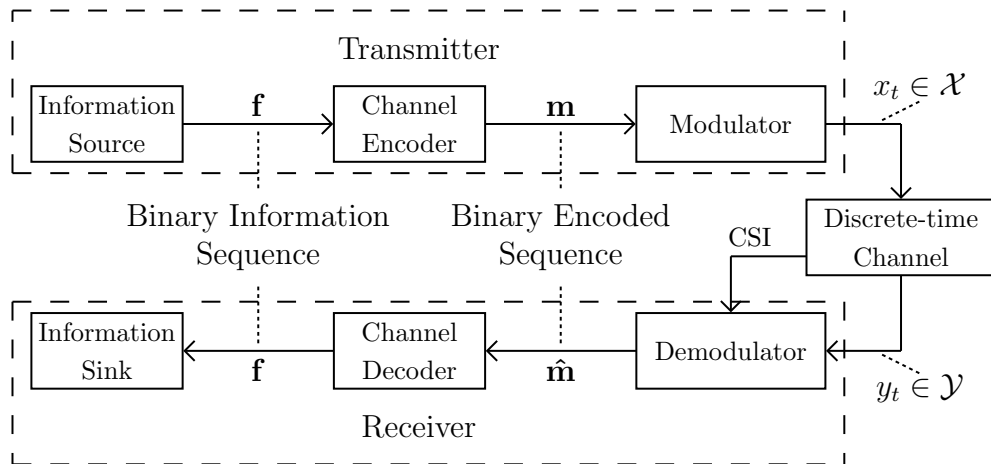


**Figure 3.1:** Simplified block diagram of a digital communication system

The modulator<sup>1</sup> parses  $\mathbf{m}$  into  $L$  subsequences  $\mathbf{s}_t$  of length  $K$  bits where  $0 \leq t < L$ . Then, the modulator maps each subsequence  $\mathbf{s}_t \in \mathcal{S}$  onto a symbol  $x_t \in \mathcal{X}$ , where  $\mathcal{X} \subset \mathbb{C}$  is called the channel input alphabet [38].

During transmission across the wireless channel, each symbol  $x_t$  is corrupted, where the degree of corruption depends on the channel state at time  $t$ . In wireless channels, the channel state is a random variable. Consequently, the channel output  $y_t \in \mathcal{Y}$  is a random variable drawn according to the transition probability density function  $p(y_t|x_t)$  from the channel output alphabet  $\mathcal{Y}$  [39, 38, 40]. In order to achieve reliable communication, it is common practice to provide knowledge about the channel state at the receiver and/or the transmitter. The channel state information (CSI) at the receiver can be obtained by probing the channel using an appropriate training sequence [41, 42, 43]. This information can then be transmitted to the source using a feedback channel. However, throughout this work it is assumed that perfect CSI is available at the receiver only. In this case, the receiver is called a *coherent* receiver.

At the receiver, the detector maps the observed signal  $\mathbf{y}$  to the binary information sequence  $\hat{\mathbf{f}}$  using the CSI. In terms of the optimal receiver, detection is concerned with the problem to minimize the probability that the detected information sequence  $\hat{\mathbf{f}}$  disagrees with the transmitted information sequence  $\mathbf{f}$  [38]. This task is addressed by the chain of the demodulator and the decoder. Once all  $L$  subsequences were received, the decoder attempts to recover the original

<sup>1</sup>Considering the union of channel encoder and modulator the channel codebook can be written as  $\mathcal{C} \subset \mathbb{C}^L$ . This notation is used extensively in Chapter 4 and Chapter 5.

information sequence  $\mathbf{f}$  using the information provided by the demodulator and the error correction capabilities of the channel code  $\mathcal{C}$ .

In the sequel, the wireless discrete-time channel is discussed. In particular, this model will be used to describe the SISO and MIMO channel. Then, these two channel models are combined to describe the half-duplex relay channel. On this basis, insights into space-time block coding used for communication in the MIMO channel are given in Section 3.2. In Section 4, these channel models are extended by a feedback channel to allow the application of ARQ, used as a method to increase throughput.

### 3.1 Wireless Channel Models

The most important detrimental effects of the wireless channel are:

- **Additive noise:** Thermal agitation of electrons in the electronic devices of the receiver front-end corrupts the received signal. This noise type is often called *thermal noise*. In general, thermal noise is modelled by a random stationary white Gaussian noise process with zero mean and variance  $\sigma^2 = N_0$  [38, 44]. Pertinent literature refers to this noise process as *additive white Gaussian noise* (AWGN).
- **Signal fading:** The radiated electro-magnetic wave is reflected and scattered by obstacles, such as houses and trees, in the propagation field. Thus, multiple reflected waves with different delays and different degrees of attenuation will be received at the destination. Due to the different propagation path delays, the multiple waves arrive at the receiving antenna with different phase. Thus, the superposition of the waves may be constructive or destructive, causing fluctuations in the signal amplitude. This effect is called signal fading [45].

In general, signal fading is *time-variant* due to changes in the propagation field, such as moving cars. In order to simplify mathematical tractability, a commonly used assumption is that fading is *time-invariant* over the channel *coherence-time*  $t_c$  [38].

Furthermore, signal fading can be considered to be *frequency flat* or *frequency selective*. For frequency flat fading, all spectral components of the

occupied bandwidth experience the same attenuation. On the other hand, if fading is frequency selective, the spectral components fade differently. The spectral range over which the the channel can be assumed to be frequency flat is called the coherence bandwidth  $f_c$  [38, 45].

- **Intersymbol interference:** In general, a wireless communication system is band-limited, i.e., only a given frequency range  $W$  is available for transmission. In this case, the channel can be modeled as lowpass filter with frequency response  $H(f)$  where  $H(f) = 0$  for  $|f| > W$ . Thus, the transmitted signals are distorted in time-domain, such that they are not distinguishable at the receiver. This effect is called intersymbol interference (ISI) [38].

A further source for intersymbol interference is the multipath propagation delay, causing the same pulse shape to arrive at the receiving antenna with different delays multiple times. In frequency domain, this results in a non-ideal frequency response [38].

- **Inter-channel interference:**

*Inter-channel interference* (ICI) occurs if the same transmission band is used by multiple users. At the destination, the superposition of the signals transmitted by the users will be received. Often, this effect is modelled as a further additive noise term [41, 46].

The destructive effect of additive noise can be overcome by increasing the signal power at the transmitter. Also, a powerful strategy is to apply multiple antennas at source and destination to increase diversity. But in particular for mobile terminals, the available transmission power and the available space for integration of antennas is limited. Signal fading and intersymbol interference can be reduced using appropriate pre-coding techniques at the source and/or by applying an equalizer at the receiver. For example, if CSI<sup>2</sup> is available at the source and the destination, Tomlinson-Harashima precoding can be applied [48, 49]. If CSI is available at the destination only, minimum-mean-square error equalization with decision feedback (MMSE-DFE) [50, 51, 52] can be used

---

<sup>2</sup>CSI can be obtained by probing the channel with an appropriate training sequence known at the receiver [41]. In time-variant channels, adaptive equalizers adjust the channel state information during operation [47].

for the time-invariant channel. For time-variant channels, adaptive equalization schemes such as the adaptive least-mean-squares equalizer with decision feedback (LMS-DFE) studied in [53, 54] can be used. Inter-channel interference can be minimized using appropriate multiple-access channel (MAC) techniques such as frequency-division (FDMA), code-division (CDMA) or time-division techniques (TDMA) [38].

In general, statistical models are used to characterize the fading process of wireless communication channels. For the land mobile radio channel most common are the Rician fading model and the Rayleigh fading model. The Rician fading model is typically used if it can be assumed that a line-of-sight (LOS) propagation path is available. The Rayleigh fading channel model is used to characterize a channel with small probability of occurrence of a LOS propagation path and is appropriate for urban environments. In order to take shadowing effects into account, caused by obstacles in the main propagation path, it is common practice to use the Suzuki process to model the random fading process. The Suzuki process is the product of the Rayleigh process and the lognormal process, where the Rayleigh process is used to model multipath propagation due to local scattering and the lognormal distribution to model slow variations in the local mean of the radio signal [55, 56]. Furthermore, the Rayleigh process is often used to model wireless local area network (WLAN) communication systems. However, in comparison with the mobile radio channel, bandwidth considerations, differences in multipath propagation delays as well as the high probability of presence of a strong LOS propagation path in the WLAN case suggest that a deterministic WLAN channel model is more appropriate [57]. In fact, the deterministic channel model used in [57] shows to achieve higher channel capacity than theoretical models. Consequently, the Rayleigh fading process can be considered as a worst case scenario for WLAN communication systems. Further statistical channel models are the Nakagami- $m$  channel model used to model rapid fading and the hyper-Rayleigh fading channel model for wireless sensors networks [58, 59].

Throughout this work, it is assumed that all channels are long-term quasi-static flat Rayleigh fading. In the long-term quasi-static fading channel the channel coherence time is assumed to be considerably larger than the code word interval. Thus, the channel state information remains constant over the channel

coherence-time and changes independently from coherence interval to coherence interval. Therefore, the long-term quasi-static paradigm states the worst-case scenario, since this channel model does not provide time diversity. As outlined in the previous paragraphs, this channel model does not satisfy real-world scenarios, but includes important properties of the mobile radio channel and the WLAN channel. This channel model is widely used within related literature such as [18, 22, 23, 25, 26, 31] and ensures reproducibility of the experiments in Chapter 7. Furthermore, this channel model is mathematically tractable and allowed to give closed-form solutions for information theoretic measures in Chapter 5. Comparability with related literature and reproducibility of experiments together with mathematical tractability is justification for its application in this dissertation.

### 3.1.1 Single-Input Single-Output Channel

In the discrete-time single-input single-output (SISO) channel model, both source and destination are equipped with a single antenna. Then, for a single code word of length  $T$  symbol intervals, the SISO channel can be written as

$$y_t = x_t h + n_t, \quad 0 \leq t < T. \quad (3.1)$$

where  $h$  denotes the complex flat fading channel coefficient. According to the quasi-static fading paradigm, the coherence interval  $t_c$  is assumed to be considerably larger than the code word length. Then, the channel coefficient  $h$  changes independently from code word to code word. In case of Rayleigh fading, the channel coefficient is an independent identical distributed (i.i.d) complex Gaussian random variable with zero mean and variance  $\sigma^2$ , i.e.  $h \sim \mathcal{CN}(0, \sigma^2)$ . Throughout this work, the Rayleigh fading channel is assumed to have unit variance, i.e.  $\sigma^2 = 1$ .

The additive noise component  $n_t$  is independently identical, circularly symmetric, complex white Gaussian distributed with zero mean and variance  $N_0/2$  per dimension, i.e.  $n_t \sim \mathcal{CN}(0, N_0)$ . Given the available transmit power constraint as

$$\mathbb{E}[|x_t|^2] = E, \quad (3.2)$$

where  $E$  denotes the average symbol energy available for transmission, the SNR

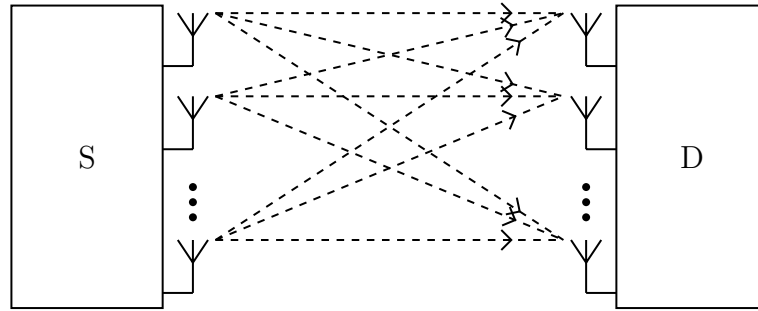


**Figure 3.2:** Multiple-input multiple-output channel with source S and destination D, each equipped with multiple antennas.

as seen at the destination is defined as

$$\rho = \frac{\mathbb{E}[|hx_t|^2]}{\mathbb{E}[|n_t|^2]} = \frac{E}{N_0}. \quad (3.3)$$

Using vector notation, the discrete-time SISO channel can be written as

$$\mathbf{y} = \mathbf{x}h + \mathbf{n}, \quad (3.4)$$

where the received symbols, the transmitted symbols and the additive noise sequence is represented by the vectors  $\mathbf{y}$ ,  $\mathbf{x}$  and  $\mathbf{n}$ , respectively, each of length  $T$  symbols.

### 3.1.2 Multiple-Input Multiple-Output Channel

Figure 3.2 depicts the MIMO channel with source S and destination D, both equipped with multiple antennas. Therefore, communication takes place across a spatial channel.

Let  $N$  denote the number of transmit antennas and  $M$  the number of receive antennas. Then, the input-output relation of the quasi-static fading discrete-time AWGN MIMO with the coherence interval  $t_c = T$  symbol intervals is given as [45]

$$\mathbf{Y}_{T \times M} = \mathbf{X}_{T \times N} \mathbf{H}_{N \times M} + \mathbf{N}_{T \times M}, \quad (3.5)$$

where the indices indicate the dimensions of the matrices,  $\mathbf{Y}$  denotes the output matrix of the channel,  $\mathbf{X}$  the channel input matrix and  $\mathbf{N}$  the additive noise.

The channel matrix  $\mathbf{H}_{N \times M}$  is given as [45]

$$\mathbf{H}_{N \times M} = \begin{pmatrix} h_{11} & h_{12} & \dots & h_{1M} \\ h_{21} & h_{22} & \dots & h_{2M} \\ \vdots & \vdots & \ddots & \vdots \\ h_{N1} & h_{N2} & \dots & h_{NM} \end{pmatrix}, \quad (3.6)$$

where  $h_{ij}$  denotes the channel coefficient for the link from the  $i$ -th transmit antenna to the  $j$ -th receive antenna. Furthermore, the additive noise components  $n_{t,m}$  with  $1 \leq m \leq M$  are mutually independent, circularly symmetric, complex white Gaussian distributed with zero mean and variance  $N_0/2$  per dimension [45, 8].

In general, the elements of  $\mathbf{X}$  are considered to be i.i.d Gaussian distributed with zero mean. Then, applying the average per symbol transmit power constraint  $E$  given in 3.2 to each antenna, the total average transmit power per symbol interval  $t$  is given by<sup>3</sup>

$$\text{tr}(E[\mathbf{X}_k \mathbf{X}_k^\dagger]) = NE. \quad (3.7)$$

Consequently, the SNR per receive antenna is given as

$$\rho = \frac{NE}{N_0}. \quad (3.8)$$

For comparison with the relay channel, the multiple-input single-output (MISO) channel with  $N = 2$  transmit antennas and  $M = 1$  receive antennas is of particular interest.

### 3.1.3 Half-Duplex Relay Channel

As depicted in Figure 3.3, the half-duplex relay channel consists of the source S, the relay R and the destination D. Due to the half-duplex constraint, the relay can either transmit or receive, but not transmit and receive simultaneously. This constraint is motivated by the fact that the incoming signal is typically much smaller than the outgoing signal [18, 14]. Furthermore, each terminal is equipped with a single antenna.

<sup>3</sup> $\text{tr}(\mathbf{X})$  denotes the trace of matrix  $\mathbf{X}$

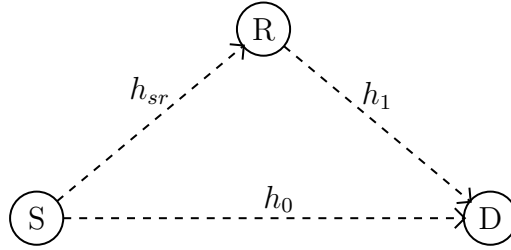


**Figure 3.3:** Half-duplex relay channel with source S, relay R and destination D together with channel coefficients  $h_0$ ,  $h_{sr}$  and  $h_1$ .

The channel coefficients  $h_0$ ,  $h_{sr}$  and  $h_1$  are mutually independent, circularly symmetric, complex Gaussian random variables with zero mean and variances  $\sigma_0^2$ ,  $\sigma_{sr}^2$  and  $\sigma_1^2$ , respectively. The additive noise at the relay and the destination is mutually independent, circularly symmetric, complex Gaussian distributed with zero mean and variances  $N_r$  and  $N_d$ , respectively.

While the source-to-relay channel is described by the SISO channel, the expression for the received signal at the destination needs to take the half-duplex constraint into account. However, it can be observed that the channel as seen at the destination is the MISO channel with  $N = 2$  transmit antennas and  $M = 1$  receive antennas. Thus, the signal  $y_t$  received at the destination during symbol interval  $t$  can be written

$$y_t = \begin{pmatrix} x_{t,s} \\ x_{t,r} \end{pmatrix} \begin{pmatrix} h_0 & h_1 \end{pmatrix} + n_t, \quad (3.9)$$

where  $x_{t,s}$  and  $x_{t,r}$  denote the symbols transmitted from source and relay, respectively. If the relay does not participate in transmission during symbol interval  $t$ , then  $x_{t,r} = 0$  should be defined as 0.

Furthermore, the received signal depends on the forwarding protocol applied at the relay such as AF, DF and DDF.

## 3.2 Space-Time Block Codes

*Severe attenuation makes it impossible for the receiver to determine the transmitted signal unless some less-attenuated replica of the transmitted signal is provided to the receiver. This resource is called diversity and it is the single most important contributor to*

*reliable wireless communications [60].*

As outlined in Section 3.1, communication across the wireless channel suffers from multiple detrimental impacts, such as multipath fading and additive noise. Therefore, in general the receiver will not be able to recover information from the transmitted signal until a hardly corrupted replica of the signal is received. Consequently, in order to achieve reliable communication across the wireless channel, the signal has to be provided at the receiver in redundant form, i.e., in diverse form. The degree of redundancy in the received signal is called *diversity gain* or *diversity*. The most common diversity techniques are [60]

- **Temporal diversity:** Appropriate channel coding may be used to provide redundant data at the receiver in temporal domain. For example, a transmitter applying the repetition code repeats to send the same symbol interleaved in time for a certain number of times.
- **Frequency diversity:** Signals transmitted on different carrier frequencies experience different channel characteristics. Consequently, transmitting the same signal on several carrier frequencies provides diversity in frequency domain.
- **Spatial diversity:** In MIMO systems, multiple spatially separated antennas at transmitter and/or receiver are used to realise reliable communication. Since the propagation paths depend on the physical environment, signals radiated and/or received from spatially separated antennas experience different channel characteristics. Thus, redundancy is achieved in spatial domain. In contrast to temporal diversity and frequency diversity, spatial diversity can be achieved without sacrificing bandwidth.

Consider the quasi-static MIMO channel with  $N$  transmit antennas and  $M$  receive antennas discussed in Section 3.1.2. In this channel, the spatial diversity order is given by the number of independent fading channels<sup>4</sup>  $N \times M$ . Space-time codes (STC) exploit the diversity provided by the channel by performing coding in space and time domain [60, 61].

---

<sup>4</sup>As in Section 3.1.2, it is assumed that the MIMO channel operates on the base-band and each code word is transmitted within a single coherence interval. Therefore, temporal diversity and frequency diversity cannot be exploited.

In this work space-time block codes (STBC) are of particular interest [62, 10, 63, 64]. A STBC  $\mathcal{C}$  is given by a finite set of matrices  $\mathbf{X}$ , each of dimension  $T \times N$ , where  $|\mathcal{C}|$  denotes the cardinality of the codebook.

### 3.2.1 Alamouti Code

The most famous STBC is the Alamouti code introduced in [10] for the  $N = 2$  MIMO channel given as<sup>5,6</sup>

$$\mathbf{X} = \begin{pmatrix} x_0 & -x_1^* \\ x_1 & x_0^* \end{pmatrix}. \quad (3.10)$$

Then, for the MISO channel with  $N = 2$  and  $M = 1$  the channel input-output relation given in (3.5) becomes

$$\begin{pmatrix} y_0 \\ y_1 \end{pmatrix} = \begin{pmatrix} x_0 & -x_1^* \\ x_1 & x_0^* \end{pmatrix} \begin{pmatrix} h_0 \\ h_1 \end{pmatrix} + \begin{pmatrix} n_0 \\ n_1 \end{pmatrix}. \quad (3.11)$$

The combiner decouples the signals received from the transmit antennas as [10]

$$\tilde{y}_0 = h_0^* y_0 + h_1 y_1^*, \quad (3.12)$$

$$\tilde{y}_1 = h_1^* y_0 - h_0 y_1^*, \quad (3.13)$$

which results in [10]

$$\tilde{y}_0 = (|h_0|^2 + |h_1|^2)x_0 + h_0^* n_0 + h_1 n_1^*, \quad (3.14)$$

$$\tilde{y}_1 = (|h_0|^2 + |h_1|^2)x_1 - h_0 n_1^* + h_1^* n_0. \quad (3.15)$$

Finally, the combiner passes the symbols  $\tilde{y}_0$  and  $\tilde{y}_1$  to the maximum likelihood (ML) symbol detector where the factor  $|\tilde{h}|^2 = |h_0|^2 + |h_1|^2$  is used as CSI. Consequently, the SNR at the demodulator is

$$\rho_{AM} = \frac{E}{N_0} \mathbb{E} \left[ |\tilde{h}|^2 \right] = \frac{2E}{N_0}. \quad (3.16)$$

<sup>5</sup>In [10] the encoding matrix is given as  $\mathbf{X}'$ . Here the encoding matrix is rearranged such that the unaltered symbol sequence  $\{x_0, x_1\}$  is transmitted by a single antenna. In the relay channel this property ensures that the source transmits the unaltered symbol sequence.

<sup>6</sup>Symbol  $x^*$  denotes the complex conjugate of  $x$ .

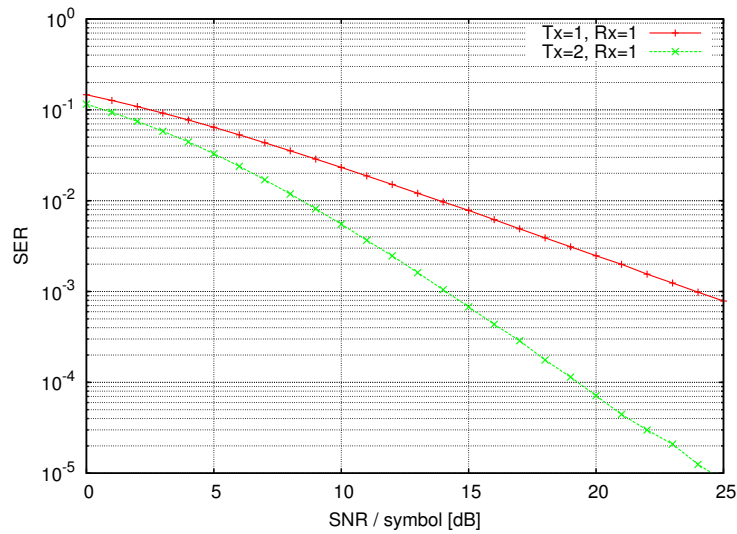


**Figure 3.4:** SER Comparison of the Rayleigh fading SISO and MISO channel using Alamouti encoding and BPSK modulation.

Figure 3.4 compares the symbol error rate (SER) performance of BPSK in the SISO and MISO channel. For the MISO channel, two transmit antennas at the source and one receive antenna at the destination are used together with Alamouti encoding. All channels are i.i.d. quasi-static Rayleigh fading with unit variance and zero mean. The performance was measured by simulation over a total of  $10^7$  symbol transmission. This graph shows that the SER curve of the MISO channel achieves a gradient of  $-2$  which corresponds to the diversity gain of the channel.

### 3.3 Performance Measures

*The characterization of the channel capacity ... as the maximum mutual information is the central and most famous success of information theory [65].*

In 1948, C.E. Shannon published his celebrated paper 'A Mathematical Theory of Communication' [39] which constitutes the most important work in information theory. The importance of information theory originates from the fact that it not only provides a tool to measure and compare performance, but also to compute the achievable performance of communication systems. Beneath oth-

ers, Shannon introduced the entropy as a measure of information, the channel capacity and proofed the coding theorem.

The most important performance measures are:

- **Channel capacity:** The channel capacity  $C$  denotes the maximum rate at which reliable communication over the communication channel is possible [39, 65].
- **Outage probability:** In the quasi-static fading channel, the channel capacity is a random variable, depending on the probability distribution of the channel coefficient. Considering a single coherence interval, reliable communication is not possible if the channel capacity is below the transmission rate. In this case, the transmitted message cannot be successfully decoded and an outage is declared. The outage probability  $P_{\text{out}}$  denotes the probability that the channel capacity is lower than the transmission rate [38, 41].
- **Outage capacity:** Considering the quasi-static fading channel, in strict Shannon sense, the channel capacity seen over a single coherence interval is zero. This results from the fact, that it is not possible to find a code for every possible channel realization allowing reliable communication. Observing that the channel capacity is a random variable drawn independently for each coherence interval, the  $\epsilon$ -outage capacity  $C_\epsilon$  is defined as the highest achievable transmission rate with an outage probability below  $\epsilon$  [38, 41].
- **Ergodic capacity:** Considering communication over a larger number of coherence intervals, reliable communication is possible up to rates given in terms of the average capacity  $C_{\text{avg}}$  of the channel [38, 41].
- **Diversity-multiplexing tradeoff:** In Section 3.2, coding for the MIMO channel was considered from a diversity point of view. However, the MIMO channel can also be seen as multiple parallel spatial channels. Therefore, multiple independent information streams can be transmitted in parallel. In this case, the channel provides *spatial multiplexing gain*. Both gains can be achieved in parallel but there is a tradeoff between how much of each gain can be achieved. Higher diversity gain results in lower multiplexing

gain and vice versa. The optimal diversity-multiplexing tradeoff (DMT) is investigated in [20].

- **Diversity-multiplexing delay tradeoff:** The DMT was extended in [66] to the diversity-multiplexing-delay (DMDT) for the ARQ case. The DMDT takes into account the fact that the allowed decoding delay  $L$  can be exploited to increase diversity.
- **Throughput:** The average transmission rate achieved by a communication system is the so-called throughput. Two common definitions of throughput are the long-term throughput  $R_{LT}$  and the delay-limited throughput  $R_{DL}$ . These measures are discussed in detail in Section 4.5.

In practice symbol-error rate (SER), bit-error rate (BER), frame-error rate (FER) and throughput are further important performance measures. The BER denotes the probability  $P_b$  that an information bit  $f$  is transmitted but an information bit  $\hat{f} \neq f$  is received. Similarly, the SER denotes the probability that a symbol  $x$  is transmitted but a symbol  $\hat{x} \neq x$  is received. The FER denotes the probability that an information sequence  $\mathbf{f}$  is transmitted but an information sequence  $\hat{\mathbf{f}} \neq \mathbf{f}$  is received. In this work, it is assumed that the quasi-static channel has a coherence time considerably larger than the code word length and changes independently from code word to code word. Consequently, outage probability and FER can be compared against each other.

This dissertation studies the performance of HARQ code properties and the comparability of the performance measures across different channel models from an energy efficiency point of view, rather than the channel properties themselves. Therefore, the fixed-rate outage probability, delay-limited throughput and FER are the relevant performance measures. Delay-limited throughput and FER, rather than long-term throughput and BER, are selected since modern communication systems are packet oriented. However, in this context outage capacity is also an interesting measure but excluded from this dissertation for conciseness.

### 3.4 Cooperative Communication

Due to space and power limitations, it is often infeasible to integrate multiple antennas for cellular communication into a mobile terminal. But, within

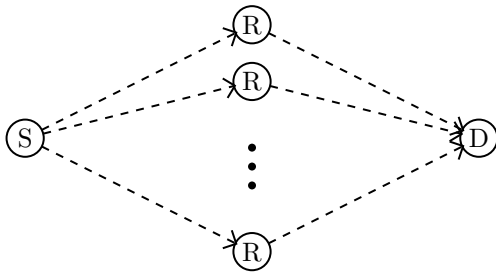


**Figure 3.5:** Set-up of a relay channel creating a virtual multi-antenna array; S: source; R: relay; D: destination

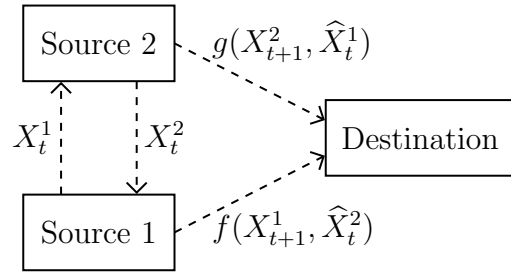


**Figure 3.6:** Set-up of communication system providing user cooperation diversity

a network of single-antenna terminals, it is still desirable to exploit transmit diversity in order to achieve reliable communication<sup>7</sup>. The idea of cooperative communication is to share resources such as antennas, power and bandwidth, among a group of mobile terminals. For example, consider the wireless network with a single source S, multiple relays R and a single destination D depicted in Figure 3.5. Let the source and the relays be equipped with a single antenna, while the destination can be equipped with an arbitrary number of antennas. The relays receive the information from the source and forward it to the destination. Consequently, the destination effectively sees the multiple-input channel which provides transmit diversity gain. In this case, the relays create a so-called virtual multi-antenna array.

Figure 3.6 shows a more advanced cooperative communication system studied by Sendonaris et al. in [11, 12]. At time instant  $t$  source 1 and source 2 transmit their own information  $X_t^1$  and  $X_t^2$ , respectively, to one another and to the destination. Let  $\hat{X}_t^2$  and  $\hat{X}_t^1$  denote the signal received at source 1 and source 2, respectively. Then, at time instant  $t + 1$  the sources form the cooperative transmit messages as a function of their own information and the received information according to  $f(X_{t+1}^1, \hat{X}_t^2)$  and  $g(X_{t+1}^2, \hat{X}_t^1)$ , and transmit these messages to the destination. Therefore, the sources do not only create a virtual multi-antenna array but also share bandwidth. Furthermore, the sources have control concerning the degree of cooperation offered to one another by partitioning their available transmit power and the transmission rate on the parts in the cooperative message. This communication system provides so-called user

<sup>7</sup>The recent iPhone 5 and iPhone 6 implement two transmit antennas. However, only a single antenna a time can be used for transmission [67, 68].

cooperation diversity.

Note, the communication system shown in Figure 3.6 operates in the multiple-access channel (MAC). In general, the MAC is considered to be non-cooperative, i.e., the sources do not communicate with each other. However, in [11] it is shown that in comparison to communication in the non-cooperative MAC, the implementation of user cooperation allows to achieve increased data rates or increased cellular coverage of mobile networks while keeping the average transmit power per terminal constant, or vice versa.

In the cooperative MAC, the sources serve as relays for each other, where the functions  $f$  and  $g$  determine the operating mode of the relaying process. Due to their simplicity, the most common relaying modes are amplify-and-forward (AF) and decode-and-forward (DF). A relay operating in the AF mode receives the message from the source, amplifies and forwards it to the destination. No further processing of the received signal is performed at the relay. Contrarily, a relay operating in the DF mode decodes the received message and forwards the re-encoded message. In general, implementation complexity of the AF mode at the relay is significantly lower compared to the DF mode [69].

As outlined in [11], an interesting problem is concerned with resource allocation within a cooperative network, since it is likely that a participant in the network shares its bandwidth and transmission power only if cooperation is beneficial for himself. In [70, 71] this problem is addressed using a game theoretical approach. Assuming complete information about available resources and CSI in [70] and assuming incomplete information in [71] it is shown that all participants can benefit from cooperative communication strategies.

However, in this work focus is on the dynamic DF (DDF) protocol, in particular because the DDF protocol outperforms all AF protocols in terms of DMT<sup>8</sup> and achieves the optimal DMT for multiplexing gains  $0 \leq r \leq 0.5$ . In the DDF protocol, communication takes place over a single code word of length  $N$  symbols. The relay attempts to assist the transmission of this block as soon it decodes successfully during the symbol interval  $d$ , where  $1 \leq d < N$  [18].

Section 3.4.1 gives the classification of cooperative protocols in terms of the degree of broadcasting and the degree of receive collision. Furthermore, simple

---

<sup>8</sup>As the objective of user cooperation is not only to achieve spatial diversity but also to share bandwidth, i.e. to achieve multiplexing gains, the DMT is the tool of choice to evaluate and compare the performance of cooperative protocols.

Time slot\Protocol	I	II	III
1	S-R,S-D	S-R,S-D	S-R
2	S-D,R-D	R-D	S-D,R-D

**Table 3.1:** Three cooperative protocols; S: source; R: relay; D: destination; A-B: terminal A transmits to terminal B [69].

protocols for the multi-user cooperative protocols are summarized. However, for the analysis of cooperative communication systems, the simplification of the cooperative MAC to the single relay channel given in Section 3.1.3 constitutes a convenient method. Moreover, in order to develop practical communication protocols and coding techniques it is adequate to consider the half-duplex constraint. Therefore, Section 3.4.2 details the DF protocol for the half-duplex relay channel.

### 3.4.1 Protocols

In [69] Nabar et al. analyse the ergodic channel capacity and the outage probability of several cooperative protocols for AF and DF relaying considering the single relay channel model given in Section 3.1.3. These protocols realize different degrees of broadcasting and receive collision. Due to the half-duplex constraint, transmission is divided into two timeslots. The degree of broadcasting is equal to the number of listeners during the same time-slot and the degree of receive collision is given by the number of terminals transmitting during the same time-slot. The protocols are summarized in Table 3.1. In detail [69]:

- **Protocol I** In the first time-slot, the source message is received by the relay and the destination. During the second time-slot, the source and the relay transmit to the destination simultaneously. Thus, this protocol implements the maximum degree of broadcasting during time-slot 1 and maximum degree of receive collision during time-slot 2.
- **Protocol II** In the first time-slot the source message is received by the relay and the destination. During the second time-slot only the relay transmits to the destination. Thus, this protocol implements the maximum degree of broadcasting during time-slot 1 but not the maximum degree of receive collision.

- **Protocol III** In the first time-slot, the source message is received only by the relay. During the second time-slot, the source and the relay transmit to the destination simultaneously. Thus, this protocol does not implement the maximum degree of broadcasting but the maximum degree of receive collision during time-slot 2.

Assuming the flat Rayleigh fading channel model, it is shown in [69] that protocol I outperforms protocol II and III in terms of the ergodic channel capacity<sup>9</sup> and outage capacity, considering both AF and DF relaying. Protocol I and III are also called non-orthogonal cooperative protocols since the source and the relay are allowed to transmit simultaneously. On the contrary, protocol II is an orthogonal protocol since either the source or the relay transmit within a timeslot.

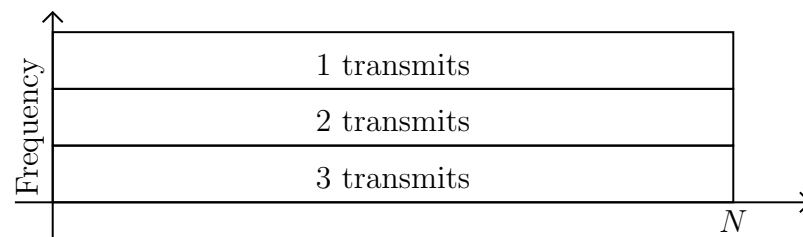
Laneman and Wornell proposed in [13, 14] several cooperative protocols of type II for AF and DF relaying considering multiple sources. To this end, the sources share the available bandwidth using orthogonal FDMA (OFDMA). Figure 3.7a illustrates the non-cooperative OFDMA technique, where the three sources transmit simultaneously over block length  $N$ , each source in its own frequency band.

In contrast, in Figure 3.7b the block length is partitioned between the sources. In the first block, all sources transmit their own information to one another and to the destination. During the successive blocks, the sources act as relays for each other by repeating the received information, while only one relay is active per frequency band. For this channel model, Laneman et al. investigate three repetition based protocols in [14]:

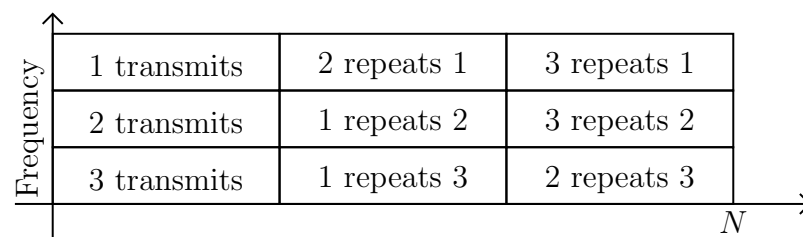
- **Fixed relaying** This protocol is akin the type II protocol given in Table 3.1, while the sources transmit according to the transmission scheme given in Figure 3.7b. It is shown in [69, 14] that AF relaying, in comparison to DF relaying, allows to achieve full spatial diversity gain.
- **Selection relaying** A common assumption is that the receivers have knowledge about their channel coefficients and that the sources are able

---

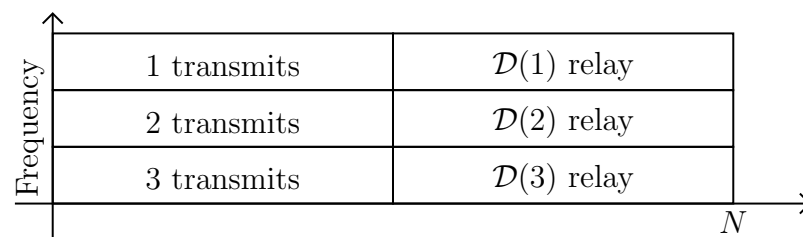
<sup>9</sup>In the derivation for the ergodic channel capacity for the protocols I to III, coding was assumed to be performed over an infinite number of coherence intervals. Throughout this work, it is assumed that coding is performed over a single coherence interval, but in this case the ergodic channel capacity is zero.



(a) ... without cooperation



(b) ... with repetition based cooperation



(c) ... with space-time coded cooperation

**Figure 3.7:** Orthogonal frequency-division medium access control ...

to sense activity in the frequency bands. Consider that the channel gain of the source 1 to source 2 link falls below a certain threshold. In this case, source 2 rejects to relay for source 1 in the second time-slot. Sensing the frequency bands, source 1 observes silence on its frequency band and re-transmits its information itself.

It is shown in [14] that this protocol enables to achieve full spatial diversity gain applying DF relaying.

- **Incremental relaying** A disadvantage of the fixed relaying protocol and the selection relaying protocol is the reduction of throughput. But if the channel between a source and the destination is good, relaying might not be necessary. Therefore, Laneman et al. introduce an incremental relaying protocol where the source transmits its message in the first time slot. In case that the destination is not able to decode the direct transmission successfully, it sends a negative-acknowledge signal. Only in this case, the corresponding relay retransmits the message in the next time slot. If the destination is still not able to decode the message successfully, it again sends the repeat request and the next relay retransmits the message.

This protocol enables to exploit full spatial diversity gain applying AF relaying and outperforms the selection relaying protocol and the fixed relaying protocol in terms of throughput.

Laneman and Wornell propose in [13] a further orthogonal protocol for the DF relay based on unitary space-time codes investigated in [62]. In pertinent literature, this protocol is known as the Laneman-Wornell orthogonal protocol. In comparison to selection relaying and incremental relaying, this protocol allows to achieve full spatial diversity gain with higher spectral efficiency.

The Laneman-Wornell orthogonal protocol is illustrated in Figure 3.7c. Let  $\mathcal{D}(i)$  denote the set of relays that are able to decode the message transmitted from source  $i$  in the first time-slot. Furthermore, the columns of the employed STBC matrix are distributed over the relays. These relays re-encode the received message using the STBC and forward their columns to the destination in the frequency band of source  $i$ .

One drawback is that before transmission, the columns of the code matrix have to be assigned to the relays. In a group of relays, where the set of par-

icipating relays is not constant, this might not be possible. In [72] it is shown that assigning the code matrix columns randomly to the relays allows to achieve full diversity gain for an infinite number of relays. But for a finite number of relays, the probability that all relays select the same column is finite and thus, diversity gain is achieved only if the SNR between source and relays is below a certain threshold.

### 3.4.2 Dynamic Decode-and-Forward Protocol

The DDF protocol is a type I protocol allowing for non-orthogonal communication in the half-duplex relay channel. Its dynamic feature stems from the ability of the relay to determine its listen-transmit decision time dependent on the channel conditions rather than listening to the source for a fixed symbol interval duration.

According to the DDF protocol given in [18, 73, 74] the source encodes a message of  $b$  bits into a code word of length  $N$  symbols using a random Gaussian codebook. The relay listens to the source until it can successfully decode the code word during symbol interval  $d$ , where  $1 \leq d < N$ . Using an independent random Gaussian codebook, it then re-encodes the information and assists the transmission during the remaining symbol intervals of the code word. The relay does not assist the transmission if it cannot decode the information successfully during symbol interval  $d = N - 1$ .

In [18] it is shown that the DDF protocol achieves the optimal DMT for multiplexing gains  $0 \leq r \leq 0.5$  using independent random Gaussian codebooks at the source and the relay. But, this *approach may not be practically feasible due to the prohibitive decoding complexity required at the destination* [26]. In order to reduce the decoding complexity at the destination a modified DDF protocol is investigated in [26] where the relay uses the source codebook to re-encode the information such that the destination sees an Alamouti code word. It is shown in [26] that this modification does not degrade the achievable DMT. A further source of complexity is the requirement to encode the information such that it is decodable after each symbol interval. Therefore, in [26] complexity is further reduced by segmenting the code word into a finite number of  $L$  blocks after which the relay is allowed to assist the transmission and it is shown that this modification degrades the DMT significantly if  $L$  is small. But the loss in

performance is negligible if the number of segments  $L$  is high<sup>10</sup>.

---

<sup>10</sup>In fact, it is shown in [26] that no loss of DMT is entailed if the relay is allowed to assist the transmission after any symbol interval  $d \geq \frac{N}{2}$ .

### Automatic Repeat-Request Protocols

---

In conventional communication systems a source transmits encoded data at a fixed rate to the destination. To ensure reliable communication, data rate and error correction capabilities of the channel code are matched to the channel conditions. However, in presence of a feedback channel from destination to source, it is beneficial to implement an automatic-repeat request / forward error-correction (ARQ/FEC) protocol. This technique allows to adapt data rate and error correction capabilities to the channel during transmission of a message [15].

To this end, the transmission of a message is divided into  $L$  blocks, where  $L$  is called the allowed decoding delay. The source transmits sequentially the blocks  $\mathbf{x}_l$  to the destination, where  $1 \leq l \leq L$ . In this context,  $l$  is called the ARQ round. After each block transmission, the destination attempts to decode the received information and the source listens to the feedback channel for negative-acknowledge (NACK) or acknowledge (ACK) signals. These signals are generated by the destination, where a NACK signal indicates that the destination was not able to decode the message successfully. In this case, the source transmits the next block. An ACK signal indicates that the destination

decoded the message successfully. In this case, the source discards the remaining blocks and starts the transmission of the next message, thereby allowing the communication system to achieve high throughput.

If the receiver cannot decode the received information successfully in ARQ round  $L$  a so-called outage event occurs. There are several application dependent techniques to handle an outage event. For example, in case of time sensitive information the allowed decoding delay  $L$  is short and the receiver discards the current message. However, in case that it is critical that the message is received successfully at the destination the source retransmits the message [15, 32].

For the performance analysis of HARQ protocols it is crucial to take the channel coherence time  $t_c$  into account. In this context, the most common channel models considered in pertinent literature [66, 75, 76, 77] are the short-term quasi-static channel and the long-term quasi-static channel. In the short-term quasi-static channel the channel coefficients are assumed to change independently from ARQ round to ARQ round. In the long-term quasi-static channel, the channel coefficients are assumed to remain constant during the transmission of a code word but to change independently from code word to code word. The long-term quasi-static channel can be considered as the worst-case scenario since it does not provide time-diversity [31, 78]. Therefore, throughout this work all channels are assumed to be long-term quasi-static .

Several coding and decoding techniques are considered in combination with the ARQ protocol. Such as the Aloha protocol [32, 79, 80], the Type-I ARQ/FEC protocol [81, 82, 83] and the more advanced Type-II ARQ/FEC protocol [15, 82, 83]. The type-II ARQ/FEC hybrid protocol uses an incremental redundancy code (IRC), which enables transmission of the information at a high data rate in the first ARQ round and transmission of small redundant information packets in the remaining ARQ rounds. Thus, the source incrementally reduces the data rate and increases the error correction capabilities of the code until they are adapted to the channel conditions. The type-II ARQ/FEC hybrid (HARQ) protocol allows the achievement of a higher throughput compared with type-I protocols [15, 82, 83].

Throughout this work, the type-II ARQ/FEC protocol is employed. Furthermore, it is assumed that the source comes with an infinite message buffer, where each message is of length  $b$  bits. In the event of an outage, the source transmits

the next message on the buffer. For simplicity, it is assumed that all feedback channels are delay and error free.

Section 4.1 introduces the HARQ protocol for the SISO channel, where both the source and the destination are equipped with a single antenna. The HARQ-MISO protocol given in Section 4.2 assumes that the source is equipped with two antennas. Therefore, this protocol allows to exploit transmit diversity to achieve higher throughput and lower outage probability. Section 4.3 introduces a novel variant of the HARQ-MISO protocol, the hybrid automatic repeat-with-diversity-request (HARDQ) MISO protocol. In this protocol, the source transmits the blocks  $\mathbf{x}_t$  with a single antenna up to ARQ round  $t$ . If the destination was not able to decode successfully in ARQ round  $t$ , the source continues to transmit with two antennas. At high SNR, this protocol is more energy efficient than the HARQ-MISO protocol and provides transmit diversity.

Of particular interest is the application of HARQ techniques in combination with the DDF protocol. The DMDT for the long-term quasi-static and short-term quasi-static half-duplex HARQ relay channel was investigated in [75] where communication takes place over a variable number of blocks. The relay is allowed to assist the transmission once it is able to decode successfully after reception of a block. This protocol is referred to as the TDK protocol. Using the DDF protocol and communication over a variable number of blocks, the DMDT derived in [76] showed to outperform the TDK protocol in the short-term quasi-static channel. For the long-term quasi-static channel, it is shown in [19, 76] that the DDF protocol achieves the optimal DMDT. Therefore, Section 4.4 introduces the HARQ protocol operating in the DDF relay channel. The DDF protocol formulation used throughout this work is based on the HARQ-DDF protocol given in [75, 23]. A comprehensive study of capacity and throughput for cooperative AF protocols is given in [84].

Similar to [26, 25], the receiving terminals are restricted to perform the decoding attempts within a code word at symbol intervals selected from a finite decoding instant set. Considering the size of the decoding instant set to be a measure for the decoding cost at the receiving terminals, this approach allows for scalability of decoding cost at the relay and destination. Furthermore, these protocols give rise for an information theoretic (Chapter 5, Chapter 6) and a simulation based (Chapter 7) performance analysis of the protocols given

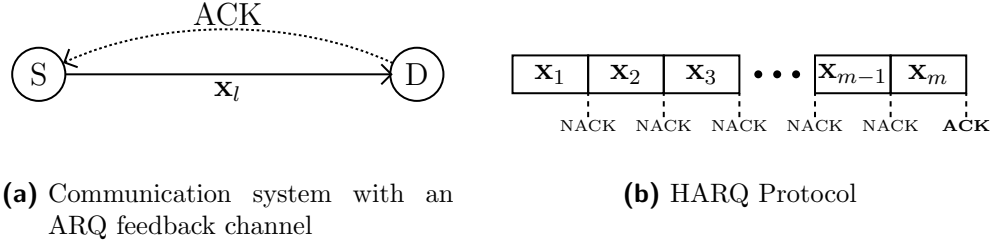


**Figure 4.1:** Illustration of a communication system with one source and one destination employing the HARQ protocol.

in [15, 32, 18, 19, 75, 23, 76] within a unified framework.

### Notation

Let  $\mathcal{A} \subseteq \mathbb{Z}^+$  where each element  $a \in \mathcal{A}$  is associated with a code rate  $R(a)$ , where  $R(a_1) > R(a_2)$  for  $a_1 < a_2$ . In order to simplify mathematical notation define:

- The minimum and maximum element of  $\mathcal{A}$  is written as

$$a_{\min} = \min \{ \mathcal{A} \}, \quad (4.1)$$

$$a_{\max} = \max \{ \mathcal{A} \}, \quad (4.2)$$

respectively. Furthermore, let

$$a_{\max}^- = \max \{ a \in \mathcal{A} : R(a) > R(a_{\max}) \}. \quad (4.3)$$

- For a given  $b \in \mathcal{B} \subseteq \mathcal{A}$  write

$$b_{\mathcal{A}}^- = \max \{ a \in \mathcal{A} : R(a) > R(b) \}, \quad (4.4)$$

$$b_{\mathcal{A}}^+ = \min \{ a \in \mathcal{A} : R(a) \leq R(b) \}. \quad (4.5)$$

Note,  $b_{\mathcal{A}}^-$  does not exist if  $b \leq a_{\min}$  and  $b_{\mathcal{A}}^+$  does not exist if  $b > a_{\max}$ .

## 4.1 HARQ-SISO Protocol

Figure 4.1 shows the HARQ communication system with a single source and single destination together with an illustration of the HARQ protocol. Both source and destination are equipped with a single antenna. The source-to-destination channel is assumed to be long-term quasi-static Rayleigh fading as given in Section 3.1.1. The destination has perfect knowledge about the CSI. A feedback channel from destination to source is available to transmit the ACK and NACK signals.

Following the communication protocol in [32], the source encodes the next message on the buffer into a code word  $\mathbf{x} \in \mathcal{C}^{N(L)}$ , where  $\mathcal{C}^{N(L)}$  denotes the codebook with symbol length  $N(L)$ . The code word consists of  $L$  blocks  $\mathbf{x}_l$  such that  $\mathbf{x} = \{\mathbf{x}_1 \mathbf{x}_2 \dots \mathbf{x}_L\}$ . Let  $n(l)$  denote the symbol length<sup>1</sup> of block  $\mathbf{x}_l$ . In this context,  $l$  also denotes the ARQ round. The source transmits these blocks sequentially, starting with the first block. Therefore, in ARQ round  $l$  the total number of channel uses is

$$N(l) = \sum_{i=1}^l n(i), \quad (4.6)$$

and the corresponding code rate in BPCU is

$$R(l) = \frac{b}{N(l)}, \quad (4.7)$$

with  $R(l) > R(l+1)$ . The effective codebook used in ARQ round  $l$  is given by  $\mathcal{C}_l^{N(l)}$  obtained from  $\mathcal{C}^{N(L)}$  by deleting the last  $N(L) - N(l)$  symbols. Hence, block  $\mathbf{x}_1$  is encoded at a high rate and each block  $\mathbf{x}_l$  with  $l > 1$  contains incremental redundancy only. This technique of obtaining a high rate codebook from a low rate codebook is called puncturing.

After encoding, the source transmits the first block of the message to the destination. The destination attempts to decode the received information. If decoding failed<sup>2</sup> the destination sends a NACK signal to the source. In this case, the source transmits the following packet. If decoding at the destination was successful in ARQ round  $l \leq L$ , the destination sends an ACK signal to

<sup>1</sup>Note, in comparison to [32], the blocks  $\mathbf{x}_l$  are not necessarily of equal symbol length.

<sup>2</sup>Cyclic redundancy check (CRC) codes are used commonly as inner FEC code to allow the destination to validate the received information.

the source and the transmission is complete. This procedure continues until the source either receives an ACK signal or all  $L$  blocks are transmitted. Then, the source starts to transmit the next information message in the queue.

In general, decoding at the destination is computationally expensive. Therefore, in order to decrease protocol complexity and computational cost, source and destination can be configured to use only a subset of the punctured codebooks offered by the mother codebook. Let  $\mathcal{D} = \{1, 2, \dots, L\}$  denote the set of decoding time instants defined by the number of punctured codebooks obtained from the mother codebook  $\mathcal{C}^{N(L)}$ . Then, the source is configured with the set of allowed decoding time instants  $\mathcal{D}_s \subseteq \mathcal{D}$ . The source sequentially transmits the packets  $l \in \mathcal{D}$  with  $l \leq \max\{\mathcal{D}_s\}$  but listens to the feedback channel only after each ARQ round  $l \in \mathcal{D}_s$ . The destination has knowledge about the set  $\mathcal{D}_s$  and is configured to perform a decoding attempt only in the ARQ rounds  $l \in \mathcal{D}_d \subseteq \mathcal{D}_s$  with  $\max\{\mathcal{D}_d\} = \max\{\mathcal{D}_s\}$ . However, the destination sends a NACK signal after every ARQ round  $l \in \mathcal{D}_s$  until it decoded the message successfully<sup>3</sup>.

Throughout this work, this protocol is denoted as the HARQ-SISO protocol and parameter affiliation is indicated by the superscript <sup>(1)</sup>.

## 4.2 HARQ-MISO Protocol

Essentially the HARQ-MISO protocol adopts the HARQ-SISO protocol, but the source is equipped with two antennas. The source-to-destination MISO channel is assumed to be long-term quasi-static Rayleigh fading as given in Section 3.1.2. The source encodes each message into the code word<sup>4</sup>  $\mathbf{X} = \{\mathbf{X}_1; \mathbf{X}_2; \dots; \mathbf{X}_L\}$  using the space-time mother codebook  $\mathcal{C}^{N(L) \times 2}$  where each pair of adjacent rows is encoded using the Alamouti code. The punctured codebooks  $\mathcal{C}_l^{N(l) \times 2}$  are obtained by deleting the last  $N(L) - N(l)$  rows of codebook  $\mathcal{C}^{N(L) \times 2}$ . Due to Alamouti encoding the block length  $n(l)$  is restricted to be even. Each block consists of two columns  $\mathbf{X}_l = \{\mathbf{x}_{0,l}, \mathbf{x}_{1,l}\}$ , each transmitted by a different antenna.

Throughout this work, affiliation of parameters to the HARQ-MISO protocol

<sup>3</sup>Allowing  $\mathcal{D}_d \subseteq \mathcal{D}_s$  enables the destination to perform optimizations on the set  $\mathcal{D}_d$  without the requirement to synchronize this set with the source. Optimizations on  $\mathcal{D}_d$  could consider the source-to-destination channel quality, decoding cost and decoding delay considerations. However, this optimization is beyond the scope of this work.

<sup>4</sup>The operator ; denotes the row wise concatenation of the matrices  $\mathbf{X}_l$ .

is indicated by the superscript <sup>(2)</sup>.

### 4.3 HARDQ-MISO Protocol

#### Motivation

Consider each antenna to be subject to the average per symbol power constraint  $E$ , unit variance Rayleigh fading channel coefficients and AWGN noise with variance  $N_0$ . Then, according to (3.3) and (3.8), the SNR of the HARQ-SISO protocol  $\rho^{(1)}$  and SNR of the HARQ-MIMO protocol  $\rho^{(2)}$  is related as

$$\rho^{(2)} = \frac{\rho^{(1)}}{2}, \quad (4.8)$$

where the divisor 2 originates from the fact that the source introduces twice as much energy into the MISO channel than into the SISO channel. Furthermore, consider the noise variance to be very low such that for both protocols the probability is high that the destination decodes successfully in the first ARQ round. Then, assuming equal block lengths  $n^{(1)}(1) = n^{(2)}(1)$ , both protocols achieve the same transmission rate  $R(1)$ , while according to (4.8) the HARQ-SISO protocol is two times more power efficient than the HARQ-MISO protocol. This observation motivates the application of the hybrid automatic repeat-with-diversity-request (HARDQ) protocol which represents a novel variant of the HARQ-MISO protocol.

#### Protocol Definition

The HARDQ-MISO protocol essentially adopts the HARQ-MISO protocol, but transmits up to ARQ round  $t \in \mathcal{D}$  only one column of  $\mathcal{C}^{N(L) \times 2}$ . Consequently, during ARQ round  $l \leq t$  the destination effectively sees the SISO channel. If the destination was not able to decode the message successfully within this interval, the source continues the transmission using the MISO channel. Therefore, during ARQ round  $l > t$  the destination can exploit the diversity advantage of the MISO channel. For  $t = 0$  this protocol represents the HARQ-MISO protocol.

Let  $\mathbf{X}_{l,k} = (\mathbf{X}_l ; \mathbf{X}_{l+1} ; \dots ; \mathbf{X}_k)$  denote the concatenation of the code word blocks of ARQ round  $l$  to ARQ round  $k$  with  $l \leq k$ . Then, the signal received

at the destination up to ARQ round  $l$  can be written as

$$\mathbf{y}_l = \begin{cases} \mathbf{X}_{1,t} \begin{pmatrix} h_0 \\ 0 \end{pmatrix} + \mathbf{n}, & t \geq l, \\ \left( \mathbf{X}_{1,t} \begin{pmatrix} h_0 \\ 0 \end{pmatrix} ; \mathbf{X}_{t+1,l} \begin{pmatrix} h_0 \\ h_1 \end{pmatrix} \right) + \mathbf{n}, & t < l, \end{cases} \quad (4.9)$$

where the vector  $\mathbf{y}_l \in \mathbb{C}^{N(l)}$  denotes the received signal and  $\mathbf{n} \in \mathbb{C}^{N(l)}$  denotes the additive noise vector.

In comparison to the HARQ-SISO and the HARQ-MISO protocol, the feedback channel does not only increase the achievable throughput but also changes the channel configuration in ARQ round  $t$ . In particular, in the ARQ rounds  $l \leq t$  the destination effectively sees the SISO channel and in the ARQ rounds  $l > t$  the destination effectively sees the MISO channel. Therefore, let  $\rho_1$  denote the SNR as observed at the destination in the ARQ rounds  $l \leq t$  and  $\rho_2$  the SNR as observed at the destination in ARQ rounds  $l > t$ . Then, the total SNR as observed at the destination up to ARQ round  $l$  is

$$\rho = \begin{cases} \rho_1, & t \geq l, \\ \frac{t}{l}\rho_1 + \frac{l-t}{l}\rho_2, & t < l. \end{cases} \quad (4.10)$$

Note,  $t$  is a design parameter and therefore subject to optimization. An attractive approach to determine  $t$  is to optimize the tradeoff between power efficiency and outage probability with respect to throughput. However, the optimization of  $t$  is beyond the scope of this work.

Throughout this work, affiliation of parameters to the HARQ-MISO protocol is indicated by the superscript <sup>(3)</sup>.

## 4.4 HARQ-DDF Protocol

Consider the half-duplex relay channel depicted together with the HARQ-DDF protocol in Figure 4.2. Let source and relay use the HARQ-MISO mother codebook  $\mathcal{C}^{N(L) \times 2}$ . Furthermore, the decoding time instants allowed at the relay are given as  $\mathcal{D}_r \subseteq \mathcal{D}_s$  with  $\max(\mathcal{D}_r) = \max(\mathcal{D}_s)$ . Let  $t \in \mathcal{D}_r$  and  $T \in \mathcal{D}_d$  denote

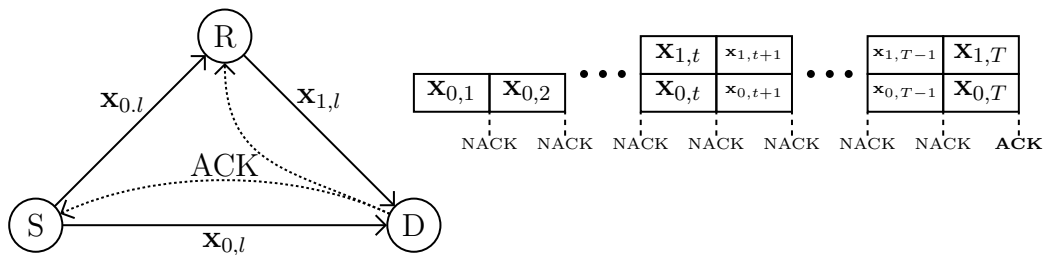


**Figure 4.2:** Illustration of the half-duplex relay channel together with the HARQ-DDF protocol.

the ARQ round in which the relay and the destination decode the code word successfully, respectively. During ARQ round  $l$ , where  $l \leq T \leq T_{\max}$ , the source transmits the code word blocks  $\mathbf{x}_{0,l}$  to the relay and to the destination. The relay listens to the source until it can decode the information successfully in ARQ round<sup>5</sup>  $t$ , where  $t \leq T$ . Then, with knowledge about the mother codebook  $\mathcal{C}^{N(L) \times 2}$  it re-encodes the information and assists the transmission during the remaining ARQ rounds  $t+1 \leq l \leq T$ , by transmitting the code word blocks  $\mathbf{x}_{1,l}$  to the destination. If  $t \geq T$  the relay does not participate in the transmission.

Essentially, the destination performs according to the HARDQ-MISO protocol, where the parameter  $t$  is given by the decoding time at the relay. The destination listens to the source and the relay until it can decode the code word successfully in ARQ round  $T \leq T_{\max}$  and sends an ACK signal to the source and the relay to request the transmission of the next code word. If the destination does not decode the code word successfully in ARQ round  $l \leq T_{\max}$  it sends an NACK signal to the source and the relay to request the transmission of the next code block  $\mathbf{X}_{l+1}$ . If the destination does not decode successfully in ARQ round  $T_{\max}$  an outage event is declared and the source starts to transmit the next code word on the buffer. Throughout this work, it is assumed that the destination has knowledge about the listen-transmit decision-time  $t$  at the relay. Evidently, this protocols allows to adopt the DDF protocol modifications investigated in [26].

The SNR as observed at the destination up to ARQ round  $T$  is given by (4.10) where  $\rho_1$  denotes the SNR during the ARQ rounds the relay listens to the source and  $\rho_2$  denotes the SNR during the ARQ rounds the relay participates

<sup>5</sup>Actually, in ARQ round  $T_{\max}$  it is not necessary for the relay to listen to the source. However, this notation simplifies the mathematical notations in Chapter 5.

the transmission.

Throughout this work, affiliation of parameters to the HARQ-DDF protocol is indicated by the superscript <sup>(4)</sup>.

## 4.5 Delay-limited throughput

The frequently used metric to measure the throughput of ARQ communication systems is the long-term (LT) average throughput<sup>6</sup>. Let  $P_{\text{out}}(l)$  denote the probability of outage in ARQ round  $l \in \mathcal{D}_d$  and  $P_{\text{out}}(0) = 1$ . Then, according [32], the LT throughput in BPCU is defined as

$$R_{\text{LT}} = \frac{b}{N(l_{\text{max}})P_{\text{out}}(l_{\text{max}}^-) + \sum_{l=l_{\text{min}}}^{l_{\text{max}}} N(l)[P_{\text{out}}(l_{\mathcal{D}_d}^-) - P_{\text{out}}(l)]}, \quad (4.11)$$

where the term  $P_{\text{out}}(l_{\mathcal{D}_d}^-) - P_{\text{out}}(l)$  denotes the probability that decoding was successful in ARQ round  $l$ . This definition assumes that  $P_{\text{out}}(l)$  is constant for infinite-time, i.e., steady-state behaviour for infinite message transmissions [23]. Furthermore, this definition does not differ between successfully transmitted information and the outage event. In fact, it is a measure for the average transmitted code word length, instead for the average time required to transmit information.

A more flexible definition of throughput is the delay-limited (DL) throughput introduced in [23]. Let  $G$  denote the throughput of a single message with the probability density function

$$\Pr(G = g) = \begin{cases} P_{\text{out}}(l_{\mathcal{D}_d}^-) - P_{\text{out}}(l), & g = R(l), \\ P_{\text{out}}(l_{\text{max}}), & g = 0, \\ 0, & \text{otherwise.} \end{cases} \quad (4.12)$$

Then, according [23], the DL throughput is defined as the throughput of a single

---

<sup>6</sup>For the non-ARQ case, throughput can be obtained by restricting the decoding set at the destination as  $\mathcal{D}_d = \max\{D\}_s$ . This configuration restricts the destination to perform a decoding attempt only in the last ARQ round.

message in BPCU as

$$R_{\text{DL}} = \mathbb{E}[G] = \sum_{l=1}^{l_{\max}} \frac{b}{N(l)} [P_{\text{out}}(l_{\mathcal{D}_d}^-) - P_{\text{out}}(l)]. \quad (4.13)$$

As can be seen, the outage event contributes with a rate  $R = 0$  BPCU to the DL throughput. This is intuitively right, since no information is transmitted if the receiver can decode the message. Therefore, the DL throughput is a measure for the average time required to transmit information. Furthermore, in [23] it is shown that the LT throughput underestimates the throughput of an individual message for small outage probabilities. Therefore, throughout this work the delay-limited throughput is considered.

## 4.6 Signal-to-Noise Ratio

The exact outage probability and delay-limited throughput of the HARQ-DDF protocol was investigated in [23] as a function of the SNR of the direct source-to-destination channel. However, for a performance comparison with the HARQ-SISO and the HARQ-MISO protocol on the system level, it needs to be taken into account that the relay introduces additional energy into the channel as seen at the destination. Therefore, the approach in [23] does not enable direct comparison of outage probability and delay-limited throughput on the system level with the HARQ-SISO and the HARQ-MISO protocol. Similarly, in the HARQ-MISO protocol the SNR as seen at the destination varies from message to message, since only on request the second antenna introduces energy into the channel. Throughout this work, the SNR of the channel as seen at the destination will be referred to as D-SNR.

For the HARQ-MISO protocol, let  $E_{0,i}$  and  $E_{1,i}$  denote the energy introduced into the channel by the first and the second antenna, respectively. Similarly, for the HARQ-DDF let  $E_{0,i}$  and  $E_{1,i}$  denote the energy introduced into the channel by the source and the relay, respectively. The subscript  $i$  counts the messages on the buffer. Then, the D-SNR is defined as

$$\rho_{\text{D-SNR}} = \frac{E_{\text{avg}}}{N_d} = \frac{\mathbb{E}[E_{0,i} + E_{1,i}]}{N_d}, \quad (4.14)$$

where  $E_{avg}$  denotes the average signal power introduced into the channel as seen at the destination and  $N_d$  denotes the noise variance at the destination.

In [18] the DDF protocol is modified such that the total average signal energy seen at the destination is constant over all symbol intervals. To this end, the average per symbol transmit power constraint at the source and the relay is adjusted at the moment the relay participates in the transmission as

$$\mathbb{E}[x_{0,t}] = \mathbb{E}[x_{1,t}] = \begin{cases} E, & 1 \leq l \leq t, \\ \frac{E}{2}, & t < l \leq T. \end{cases} \quad (4.15)$$

This energy allocation protocol can also be applied to the HARDQ-MISO protocol. Consequently, for both protocols this method results in  $\rho_1 = \rho_2$  and therefore the corresponding D-SNR is given as

$$\rho_{D-SNR} = \rho_{TPA} = \frac{E}{N_d}. \quad (4.16)$$

For the application of this method, the symbol detector at the destination has to be adjusted in ARQ round  $t$ . Additionally, for the HARQ-DDF protocol provision of the relay decoding time at the source is required. While this approach enables the performance comparison on the system level with the HARQ-SISO and HARQ-MISO protocol, these requirements increase the complexity of the communication protocol and might not be desired, nor feasible, in practice. However, throughout this work this modification is referred to as the transmit power allocation (TPA) protocol.

Conversely, in a real-world scenario the average per symbol transmission power  $E$  at the source and the relay will remain constant over all symbol intervals. Then, for the HARQ-DDF protocol the total signal energy per code word seen at the destination is a function of two random variables, the decoding time  $t$  at the relay and the decoding time  $T$  at the destination. In case of the HARDQ-MISO protocol, the average per symbol transmission power  $E$  is assigned to both antennas at the source. Then, the total signal energy is a random variable depending on the decoding time  $T$  at the destination and the choice of  $t$ .

Let

$$E(l, t) = \begin{cases} E \left( 1 + \frac{N(T) - N(t)}{N(T)} \right), & t < T, \\ E, & \text{otherwise,} \end{cases} \quad (4.17)$$

denote the total signal energy of a code word transmitted up to ARQ round  $l$ . Consequently, the corresponding D-SNR is given as

$$\rho_{D-SNR} = \rho_{NPA} = \frac{\mathbb{E} \left[ E(T, t) \right]}{N_d}. \quad (4.18)$$

Then, for performance analysis the noise variance can be used to adjust the D-SNR. Since the application of this method does not require a modification of the HARQ-MISO and the HARQ-DDF protocol, throughout the remaining chapters of this work, these protocols are referred to as *native* power allocation (NPA) protocols in order to highlight the differentiation against the TPA protocols.

Measuring the performance of the *non-HARQ* DDF protocol as a function of the D-SNR was published in [30] as a result of the research towards this dissertation.

## 4.7 Summary

Section 4.1 introduces the HARQ protocol operating in the SISO channel, where both the source and the destination are equipped with a single antenna. Subsequently, Section 4.2 extends this protocol for operation in the MISO channel, where the source is equipped with two antennas. Therefore, the HARQ-MISO protocol allows to exploit transmit diversity for decoding at the destination. Consequently, a higher throughput and a lower outage probability can be achieved.

However, in Section 4.3 it is pointed out, that at high SNR the HARQ-SISO protocol is more energy efficient than the HARQ-MISO protocol while achieving the same delay-limited throughput. Therefore, the HARQ-MISO protocol introduced in Section 4.3 allows the source to operate in the SISO channel up to ARQ round  $t$ , but to operate in the MISO channel in the ARQ rounds  $l > t$ . At high SNR, the probability is high that the destination can

decode successfully in ARQ round  $l < t$ . Therefore, at high SNR the HARDQ-MISO protocol is as energy efficient as the HARQ-SISO protocol and provides transmit diversity if the destination cannot decode successfully in ARQ round  $t$ .

Section 4.4 gives the HARQ protocol for operation in the DDF relay channel. This protocol can be seen as a variant of the HARDQ-MISO, where the parameter  $t$  is determined by the listen-transmit decision-time at the relay.

In general, the computational decoding complexity at the destination is high. In order to enable scalability of the decoding complexity, the given protocol formulations permit the relay and the destination to select a subset of the decoding time instants offered by the mother codebook. Furthermore, as given in Chapter 5 and Chapter 7, the protocol formulations enable to perform a performance analysis and a performance comparison among these protocols within a unified framework.

Respective HARQ protocols, the achievable throughput is of particular interest. In general, the long-term throughput is considered. However, the delay-limited throughput [23] is the more reasonable performance measure as it takes into account that no information was transmitted if the destination cannot decode successfully in the last ARQ round. These measures are discussed in Section 4.5.

In comparison to the HARQ-SISO protocol and the HARQ-MISO protocol, for the HARDQ-MISO and the HARQ-DDF protocol the average symbol energy introduced into the channel as seen at the destination varies from code word to code word. Therefore, in order to enable the performance comparison on the system level the D-SNR is introduced in Section 4.6

### Performance Analysis

---

*The fundamental problem of communication is that of reproducing at one point either exactly or approximately a message selected at another point. Frequently the messages have meaning; ... These semantic aspects of communication are irrelevant to the engineering problem [39].*

This part investigates the information theoretic performance of the

- HARQ protocol operating in the SISO channel,  
(Section 4.1, 3.1.1)
- HARQ protocol operating in the MISO channel,  
(Section 4.2, 3.1.2)
- HARDQ protocol operating in the MISO channel,  
(Section 4.3, 3.1.2)
- HARQ-DDF protocol operating in the half-duplex relay channel,  
(Section 4.4, 3.1.3)

in terms of the *fixed-rate outage probability* and the *delay-limited throughput* measured as functions of the SNR as observed at the destination (D-SNR). All channels are subject to AWGN and long-term quasi-static Rayleigh fading with mutually i.i.d. channel coefficients.

In [32] the long-term throughput of HARQ protocols in the multi-user channel is investigated considering the short-term quasi-static<sup>1</sup> multi-user channel together with ARQ rounds of equal symbol length. It is shown that the HARQ using incremental redundancy coding outperforms the ALOHA and Type-I ARQ/FEC protocol. Furthermore, the tools derived in [32] to obtain the closed-form throughput formulas for these protocols are essential for the theoretical analysis throughout this part. Therefore, these tools will be discussed in Section 5.

Using incremental redundancy codes, in [31] the outage probability and long-term throughput of the rate-optimized ARQ protocol applied to the long-term quasi-static SISO channel is derived together with the optimal power allocation. In the rate-optimized ARQ protocol, the source transmits the information at a very high code rate in the first ARQ round and incrementally reduces the code rate in the following ARQ rounds. Furthermore, rate-optimization considers the optimization of the average transmission rate by optimal selection of the code rates assigned to the ARQ rounds. Therefore, consistent with the HARQ protocol formulations in Chapter 4, the ARQ rounds are not necessarily of equal symbol length. The results in [31] are compared to single-layer and multi-layer protocols which do not utilize ARQ. In the multi-layer protocol, multi-user coding techniques are applied to a single user to increase throughput. To this end, the information is encoded multiple times using different code rates. The resulting code words are superposed into the transmit signal using different signal power for each code word. It is shown that the application of ARQ together with incremental redundancy coding outperforms single-layer and multi-layer communication. Furthermore, it is shown that optimal power allocation results in significant gain at low SNR but negligible gain at high SNR. Throughout this part no limitations are given on the code rate of the first ARQ round and the code rate adjustment of the following ARQ rounds. Therefore, the theoretical analysis in Chapter 5 can be applied to the rate-optimized ARQ

---

<sup>1</sup>In [32] slotted multi-user communication is considered. To this end, it is defined that the channel gains are constant during each slot.

protocol. The optimal power allocation derived in [31] is performed from ARQ round to ARQ round. Throughout this work, it is assumed that the average transmit power constraint is constant, thus optimal power allocation is beyond the scope of this work.

In [8, 9] it is shown that the MIMO channel capacity is achieved for circularly symmetric Gaussian channel inputs. However, for the derivations in Chapter 5, it is necessary to consider that STBC codes are not capacity achieving [33].

In [85] the outage probability of the MISO channel applying the Alamouti code is derived for several channel configurations. However, for the derivation of the outage probability analysis in Section 5.2, a different approach is used. The detailed derivation is given in Appendix A.1. Considering the long-term quasi-static MIMO channel, in [78, 86] the optimum space-time code design criterion for the HARQ-MIMO channel is derived for the type-I and the type-II ARQ/FEC protocols. Furthermore, information-theoretic measures are used to optimize the long-term throughput performance.

In [87] the outage probability and the delay-limited throughput for the type-I and the type-II decode-and-forward channel is derived. While the outage probability for the non-ARQ DDF protocol is investigated in [24], the outage probability and delay-limited throughput for the HARQ-DDF protocol is investigated in [23].

The derivations given in Section 5.3 and Section 5.4 are closely related to the derivations in [23]. However, the analysis in Section 5.3 and Section 5.4 enables to assign a specific code rate to each ARQ round and the configuration of the allowed sets of decoding time instants  $\mathcal{D}_s$ ,  $\mathcal{D}_r$  and  $\mathcal{D}_d$  at the source, the relay and the destination, respectively. Furthermore, in [23] the outage probability is measured as a function of the source-to-destination channel SNR (SD-SNR) only. In comparison, the closed-form expressions in Section 5.4 enable the application of the TPA protocols. A method to measure the outage probability as a function of the D-SNR considering the application of the NPA protocols is given in Section 5.5.

Note, the analysis in Section 5 gives the achievable performance considering Gaussian channel inputs together with Alamouti encoding. In order to enable further performance comparison with the simulation results given in Chapter 7, the method to obtain the achievable performance considering uniformly dis-

tributed discrete channel inputs using Monte Carlo simulations is discussed in Section 5.6 and Section 5.7. In [88], the mutual information considering power-allocation for the Gaussian vector channel with discrete-channel inputs is considered. It is shown that so-called waterfilling methods lead to a significant loss in mutual information compared with communication systems without power allocation. However, also a cross-channel power allocation method is presented which outperforms communication systems without power allocation. In [89], it is shown that a finite number of  $2^{C+1}$  channel inputs is sufficient to achieve approximately optimal performance in terms of mutual information, where  $C$  denotes the channel capacity. Discrete channel inputs were also considered in [77] in context of the throughput-diversity-delay tradeoff in MIMO ARQ channels. Upper and lower bounds on the capacity and the outage probability for discrete channel inputs are investigated in [90] for the Rayleigh fading channel, and in [91] for the Nakagami- $m$  blockfading channel. For Gaussian channel inputs, bounds on the capacity of the full-duplex relay channel are studied in [92], and for half-duplex relay channel in [93]. For both Gaussian and discrete channel inputs, the effect of ISI on the listen-transmit decision-time at the DDF relay was published in [94] as a result of the research towards this dissertation.

The outage probability  $P_{\text{out}}$  of a communication channel is defined as [38]

$$P_{\text{out}} = \Pr(I < R), \quad (5.1)$$

where  $I$  denotes the mutual information between the source and the destination, and  $R$  the code rate. The unit of  $I$  and  $R$  is BPCU.

Consider the HARQ protocol defined in Section 4.1 operating in the quasi-static Rayleigh fading SISO channel given in Section 3.1.1. For the sake of mathematical tractability, the source is assumed to use a random Gaussian mother codebook  $\mathcal{C}$  to encode a message of  $b$  bits into  $L$  blocks of length  $n(l)$  symbols with  $1 \leq l \leq L$ . Then, using typical set decoding and assuming  $n(l)$  to be sufficiently large, it is shown [32] that codebooks  $\mathcal{C}$  with an arbitrarily small decoding error probability  $P_{\text{out}}$  for all punctured codebooks  $\mathcal{C}_l$  exist. To prove this result, it is shown in [32] that the mutual information between the source and destination in ARQ round  $l$  is given by the accumulation of the mutual

information  $I_i$  of each ARQ round  $i$  with  $1 \leq i \leq l$  as

$$I(l) = \sum_{i=1}^l \frac{n(i)}{N(l)} I_i. \quad (5.2)$$

and that for  $n(l) \rightarrow \infty$  the probability of erroneous decoding at the destination is

$$P_{\text{out}}(l|I(l) > R(l)) < \epsilon, \quad (5.3)$$

$$P_{\text{out}}(l|I(l) \leq R(l)) \rightarrow 1, \quad (5.4)$$

where  $\epsilon > 0$  is arbitrarily small. Therefore, in the regime of very large  $n(l)$  it is assumed for all  $l$  [32]

$$P_{\text{out}}(l|I(l) > R(l)) = 0, \quad (5.5)$$

$$P_{\text{out}}(l|I(l) \leq R(l)) = 1, \quad (5.6)$$

and the probability of an undetected error is assumed as [32]

$$P_{\text{out,undetected}} = 0. \quad (5.7)$$

Considering this result, it is not directly evident that codebooks  $\mathcal{C}^{N(L) \times 2}$ , with an arbitrarily small decoding error probability for all punctured codebooks  $\mathcal{C}_i^{N(l) \times 2}$  also exist<sup>2</sup>. However, in [33] it is shown that the space-time block encoded MISO channel effectively results in a scaled SISO AWGN channel with SNR

$$\rho = \frac{E}{N_0} \|\mathbf{H}\|^2. \quad (5.8)$$

Therefore, postulating  $n(l)$  to be even, for the HARQ and HARDQ protocol operating in the MISO channel, and for the HARQ-DDF protocol operating in the half-duplex relay channel, the encoding rule

$$A : \mathcal{C} \rightarrow \mathcal{C}^{N(L) \times 2} \quad (5.9)$$

is used where the encoder  $A$  encodes each code word  $\mathbf{x} \in \mathcal{C}$  into a code word

---

<sup>2</sup>Considering the random Gaussian i.i.d. code ensemble this is shown rigorously in [66].

$\mathbf{x}' \in \mathcal{C}^{N(L) \times 2}$  such that the first column of  $\mathbf{x}'$  represents the code word  $\mathbf{x}$  and such that each pair of adjacent columns of  $\mathbf{x}'$  are Alamouti encoded. Consequently, the assumptions (5.5), (5.6) and (5.7) are valid for the  $\mathcal{C}^{N(L) \times 2}$  codebook.

Using these results, Sections 5.1 to 5.4 give the closed-form expressions for the outage probability  $P_{out}(l)$  in ARQ round  $l$  as a function of the D-SNR for the relevant HARQ protocols. To this end, it is assumed that the channel inputs are circularly symmetric, i.i.d. complex Gaussian distributed with zero mean and variance  $E$ . Furthermore, perfect CSI is available at the receiving terminals. For mathematical tractability define  $l \in \mathcal{D}_d$  throughout this chapter. Within the derivations, care is taken to permit the measurement of the outage probability and the delay-limited throughput as a function of the D-SNR considering the application of the NPA and the TPA protocols as discussed in Section 5.5.

The results in Sections 5.1 to 5.4 give the necessary tools to calculate the delay-limited throughput according to (4.13). Furthermore, since the destination declares an outage event only if it was not able to decode the received information successfully in the last ARQ round, the effective outage probability is given by

$$P_{out} = P_{out}(l_{\max}). \quad (5.10)$$

## 5.1 HARQ-SISO Protocol

Due to the long-term quasi-static channel paradigm, the mutual information of the SISO channel does not change from one ARQ round to another. Therefore, the mutual information of the SISO channel accumulated up to ARQ round  $l$  is given as [38, 32]

$$I^{(1)} = I^{(1)}(l) = \log_2(1 + \rho\gamma), \quad (5.11)$$

where the channel gain  $\gamma = |h|^2$  is exponentially distributed with mean  $\sigma^2$ . Therefore, for  $\rho > 0$  the outage probability in ARQ round  $l$  is [38]

$$P_{out}^{(1)}(l) = \Pr\left(\gamma < \frac{2^{R(l)} - 1}{\rho}\right) \quad (5.12)$$

$$= \begin{cases} 1, & \sigma^2 = 0, \\ \frac{2^{R(l)} - 1}{\rho\sigma^2}, & \sigma^2 > 0. \end{cases} \quad (5.13)$$

## 5.2 HARQ-MISO Protocol

Also in the long-term quasi static MISO channel, the mutual information does not change from one ARQ round to another. Therefore, the mutual information accumulated up to ARQ round  $l$  is given as [33]

$$I^{(2)} = I^{(2)}(l) = \log_2 (1 + \rho(\gamma_0 + \gamma_1)), \quad (5.14)$$

where the channel gains  $\gamma_0 = |h_0|^2$  and  $\gamma_1 = |h_1|^2$  are exponentially distributed with respective mean  $\sigma_0^2$  and  $\sigma_1^2$ . Therefore, for  $\rho > 0$  the outage probability in ARQ round  $l$  is (see also [85])

$$P_{\text{out}}^{(2)}(l) = \Pr \left( \gamma_0 + \gamma_1 < \frac{2^{R(l)-1}}{\rho} \right) \quad (5.15)$$

$$= \begin{cases} 1, & \sigma_0^2 = \sigma_1^2 = 0, \\ 1 - e^{-\frac{2^{R(l)-1}}{\rho\sigma_0^2}}, & \sigma_0^2 > 0, \sigma_1^2 = 0, \\ 1 - e^{-\frac{2^{R(l)-1}}{\rho\sigma_1^2}}, & \sigma_0^2 = 0, \sigma_1^2 > 0, \\ 1 - \left(1 + \frac{2^{R(l)-1}}{\rho\sigma^2}\right) e^{-\frac{2^{R(l)-1}}{\rho\sigma^2}}, & \sigma^2 = \sigma_0^2 = \sigma_1^2 > 0, \\ 1 - e^{-\frac{M}{\sigma_0^2}} - \frac{\sigma_0^2}{\sigma_1^2 - \sigma_0^2} e^{-\frac{M}{\sigma_1^2}} \left[ 1 - e^{-M \frac{\sigma_1^2 - \sigma_0^2}{\sigma_0^2 \sigma_1^2}} \right], & \sigma_0^2 > 0, \sigma_1^2 > 0, \sigma_0^2 \neq \sigma_1^2, \end{cases} \quad (5.16)$$

where

$$M = \frac{2^{R(l)} - 1}{\rho}. \quad (5.17)$$

As can be seen for  $\sigma_0^2 = 0$  and  $\sigma_1^2 = 0$  no communication is possible. For  $\sigma_0^2 > 0$  or  $\sigma_1^2 > 0$  the MISO channel reduces to the SISO channel. In case  $\sigma_0^2 = \sigma_1^2 > 0$  equation (5.15) can be solved using the Erlang distribution. Appendix A.1 gives the detailed derivation of the outage probability for the last case, where  $\sigma_0^2 \neq \sigma_1^2$  with  $\sigma_0^2 > 0$  and  $\sigma_1^2 > 0$ .

### 5.3 HARDQ-MISO Protocol

Since the HARDQ protocol upgrades the SISO channel in ARQ round  $t$  to the MISO channel, the mutual information accumulated up to ARQ round  $l$  is given as

$$I^{(3)}(l) = \begin{cases} I^{(1)}, & t \geq l, \\ \frac{R(l)}{R(t)}I^{(1)} + \frac{R(t)-R(l)}{R(t)}I^{(2)}, & t < l. \end{cases} \quad (5.18)$$

Therefore, for  $l \leq t$  the outage probability is given by (5.13) as

$$P_{\text{out}}^{(3)}(l|l \leq t) = 1 - e^{-\frac{2^{R(l)}-1}{\rho_1 \sigma_0^2}}, \quad (5.19)$$

and for  $l > t$  as

$$P_{\text{out}}^{(3)}(l|l > t) = 1 - e^{-\frac{M}{\sigma_0^2}} - \frac{1}{\sigma_0^2} \int_{\gamma_0}^M e^{-\frac{\gamma_0}{\sigma_0^2} - \frac{\beta(\gamma_0)}{\sigma_1^2}} d\gamma_0, \quad (5.20)$$

with

$$M = \left\{ \gamma : R(l) = \frac{R(l)}{R(t)} \log_2(1 + \rho_1 \gamma) + \left(1 - \frac{R(l)}{R(t)}\right) \log_2(1 + \rho_2 \gamma) \right\}, \quad (5.21)$$

and

$$\beta(\gamma_0) = \frac{2^{\frac{R(l)R(t)}{R(t)-R(l)}}}{\rho_2 (1 + \rho_1 \gamma_0)^{\frac{R(l)}{R(t)-R(l)}}} - \frac{1}{\rho_2} - \gamma_0 = \gamma_1. \quad (5.22)$$

The integral in (5.20) can be solved using a numerical integration method. To find the integration limit (5.21), a root finding algorithm such as Brent's method [95] is appropriate, which solves

$$0 = \frac{R(l)}{R(t)} \log_2(1 + \rho_1 \gamma) + \left(1 - \frac{R(l)}{R(t)}\right) \log_2(1 + \rho_2 \gamma) - R(l) \quad (5.23)$$

by searching for  $\gamma$ . An appropriate search interval for  $\rho_1 < \rho_2$  is

$$\frac{2^{R(l)} - 1}{\rho_2} < \gamma < \frac{2^{\frac{R(l)R(t)}{R(t)-R(l)}} - 1}{\rho_2}. \quad (5.24)$$

and for  $\rho_1 > \rho_2$

$$\frac{2^{\frac{R(l)R(t)}{R(t)+R(l)}} - 1}{\rho_1} < \gamma < \frac{2^{R(l)} - 1}{\rho_2}. \quad (5.25)$$

For  $\rho = \rho_1 = \rho_2$  the solution of (5.21) is

$$M = \frac{2^{R(l)} - 1}{\rho}. \quad (5.26)$$

The detailed derivation of (5.20) and (5.22) is given in Appendix A.2 and the detailed derivation of the search intervals (5.24) and (5.25) is given in Appendix A.2.1.

For simplicity define for a given  $t$

$$P_{\text{out}}^{(3)}(l) = \begin{cases} P_{\text{out}}^{(3)}(l|l \leq t), & l \leq t, \\ P_{\text{out}}^{(3)}(l|l > t), & l > t. \end{cases} \quad (5.27)$$

## 5.4 HARQ-DDF Protocol

The HARQ-DDF protocol can be seen as a variant of the HARQ-MISO protocol where the source represents the first antenna and the relay represents the second antenna. Then, the design parameter  $t$  is given by the listen-transmit decision-time of the relay. Consequently, in this protocol define  $t \in \mathcal{D}_r$ . In order to derive the outage probability of the HARQ-DDF protocol define  $\mathcal{X} = t$  as the earliest listen-transmit decision-time instant that decodes the information received at the relay successfully.

### Listen-Transmit Decision-Time $t$

The mutual information of the source-to-relay channel is given by the mutual information of the SISO channel (5.11) as

$$I_{\text{sr}}^{(4)} = \log_2(1 + \rho_r \gamma_{\text{sr}}), \quad (5.28)$$

where  $\rho_r$  denotes the SNR at the relay and  $\gamma_{sr}$  the exponentially distributed channel gain of the source-to-relay link with mean  $\sigma_{sr}^2$ . Then,  $t$  is given as

$$t = \begin{cases} \min\{l \in \mathcal{D}_r : R(l) \leq I_{sr}^{(4)}\}, \\ t_{\max}, \quad \text{if } l \text{ does not exist,} \end{cases} \quad (5.29)$$

and consequently, for a known  $t$  the mutual information of the relay channel in ARQ round  $l$  is given by (5.18).

### Probability Distribution $\Pr(\mathcal{X})$

For  $t = t_{\min}$  the probability of successful decoding at the relay is

$$\Pr(\mathcal{X} = t_{\min}) = \Pr[I_{sr}^{(4)} \geq R(t_{\min})] \quad (5.30)$$

$$= 1 - \Pr[I_{sr}^{(4)} < R(t_{\min})] \quad (5.31)$$

$$= e^{-\frac{2^{R(t_{\min})}-1}{\rho_r \sigma_{sr}^2}}. \quad (5.32)$$

For  $t_{\max} > t > t_{\min}$  the probability is

$$\Pr(\mathcal{X} = t) = \Pr[I_{sr}^{(4)} < R(t_{\mathcal{D}_r}^-), I_{sr}^{(4)} > R(t)] \quad (5.33)$$

$$= \Pr[I_{sr}^{(4)} < R(t_{\mathcal{D}_r}^-)] - \Pr[I_{sr}^{(4)} < R(t)] \quad (5.34)$$

$$= e^{-\frac{2^{R(t)}-1}{\rho_r \sigma_{sr}^2}} - e^{-\frac{2^{R(t_{\mathcal{D}_r}^-)}-1}{\rho_r \sigma_{sr}^2}}. \quad (5.35)$$

If  $t = t_{\max}$  the relay does not assist the transmission. For mathematical tractability, the probability  $\Pr(\mathcal{X} = t_{\max})$  is defined as the probability that the relay cannot assist the transmission as

$$\Pr(\mathcal{X} = t_{\max}) = \Pr[I_{sr}^{(4)} < R(t_{\mathcal{D}_r}^-)] \quad (5.36)$$

$$= 1 - e^{-\frac{2^{R(t_{\mathcal{D}_r}^-)}-1}{\rho_r \sigma_{sr}^2}}. \quad (5.37)$$

Therefore,  $\Pr(\mathcal{X} = t)$  has the probability distribution

$$\Pr(\mathcal{X} = t) = \begin{cases} e^{-\frac{2^{R(t_{\min})}-1}{\rho_r \sigma_{sr}^2}}, & t = t_{\min}, \\ e^{-\frac{2^{R(t)}-1}{\rho_r \sigma_{sr}^2}} - e^{-\frac{2^{R(t_{\mathcal{D}_r^-})}-1}{\rho_r \sigma_{sr}^2}}, & t_{\max} > t > t_{\min}, \\ 1 - e^{-\frac{2^{R(t_{\mathcal{D}_r^-})}-1}{\rho_r \sigma_{sr}^2}}, & t = t_{\max}. \end{cases} \quad (5.38)$$

### Outage Probability

For any  $t_{\min} \geq l$  the relay cannot participate in transmission. Therefore, for this range, the outage probability is given by the outage probability of the direct source-to-destination link as

$$P_{\text{out}}^{(4)}(l|l \leq t_{\min}) = 1 - e^{-\frac{2^{R(l)}-1}{\rho_1 \sigma_0^2}}. \quad (5.39)$$

For  $l > t_{\min}$  the outage probability of the relay channel can be evaluated as

$$P_{\text{out}}^{(4)}(l|l > t_{\min}) = \sum_{t=t_{\min}}^{l_{\mathcal{D}_r}^-} P_{\text{out}}^{(3)}(l|l > t) \Pr(\mathcal{X} = t) + \sum_{t=l_{\mathcal{D}_r}^+}^{t_{\max}} P_{\text{out}}^{(3)}(l|l \leq t) \Pr(\mathcal{X} = t). \quad (5.40)$$

For simplicity define

$$P_{\text{out}}^{(4)}(l) = \begin{cases} P_{\text{out}}^{(4)}(l|l \leq t_{\min}), & l \leq t_{\min}, \\ P_{\text{out}}^{(4)}(l|l > t_{\min}), & l > t_{\min}. \end{cases} \quad (5.41)$$

## 5.5 SNR as Observed at the Destination

As discussed in Section 4.6 the D-SNR depends on the energy introduced into the channel as seen at the destination and the noise variance  $N_d$  at the destination. In comparison to the HARQ-SISO and the HARQ-MISO protocol, the energy introduced into the channel according to the HARDQ-MISO and the HARQ-DDF protocol is a random variable depending on the parameters  $t$  and  $T$  and the per antenna average per symbol transmit power constraints given by the application of the NPA and the TPA protocols variants.

In order to obtain the average energy introduced into the channel as seen at the destination according to

$$E_{\text{avg}} = \mathbb{E} \left[ E(T, t) \right], \quad (5.42)$$

define  $\mathcal{Y}$  as the event that the destination decodes successfully in ARQ round  $l$  with probability

$$\Pr^{(x)}(\mathcal{Y} = l) = P_{\text{out}}^{(x)}(l-1) - P_{\text{out}}^{(x)}(l), \quad (5.43)$$

and define  $\bar{\mathcal{Y}}$  as the event that the destination cannot decode successfully in ARQ round  $l$  given by the outage probability as

$$\Pr^{(x)}(\bar{\mathcal{Y}} = l) = P_{\text{out}}^{(x)}(l). \quad (5.44)$$

Then, the average energy introduced into the channel as seen at the destination for the HARDQ-MISO protocol is

$$E_{\text{avg}}^{(3)} = \Pr^{(3)}(\bar{\mathcal{Y}} = T_{\text{max}})E(T_{\text{max}}, t) + \sum_{T=T_{\text{min}}}^{T_{\text{max}}} \Pr^{(3)}(\mathcal{Y} = T)E(T, t), \quad (5.45)$$

and for the HARQ-DDF protocol

$$E_{\text{avg}}^{(4)} = \sum_{t=t_{\text{min}}}^{t_{\text{max}}} \left( \Pr^{(4)}(\bar{\mathcal{Y}} = T_{\text{max}})\Pr(\mathcal{X} = t)E(T_{\text{max}}, t) + \sum_{T=T_{\text{min}}}^{T_{\text{max}}} \Pr^{(4)}(\mathcal{Y} = T)\Pr(\mathcal{X} = t)E(T, t) \right). \quad (5.46)$$

For the TPA protocol variant, the per antenna average per symbol power constraint is given by (4.15). Therefore, for a given target SNR  $\rho_{\text{D-SNR}}$  the SNR parameters relate as

$$\rho_1 = 2\rho_2 = \rho_{\text{D-SNR}}. \quad (5.47)$$

For the NPA protocol variant, the closed-form expression of the outage probability in ARQ round  $l$  for the HARDQ-MISO and the HARQ-DDF protocol is unknown. Therefore, the proposed method to obtain these performance measures for these protocols as a function of the D-SNR is

1. In the first step, the performance is measured according to (5.10) and

(4.13) as a function of the source-to-destination channel SNR. To this end, let  $\rho_1 = \rho_2 = \frac{E}{N_d}$ .

2. Since  $E$  and  $N_d$  are known, the corresponding D-SNR is obtained using (4.14) together with (5.45) and (5.46).

## 5.6 Discrete Channel Inputs

The analysis in Sections 5.1 to 5.4 considers Gaussian distributed channel inputs. Therefore, this analysis is valid for the discrete-time *continuous-input* continuous-output channel and gives an upper bound on the achievable outage probability<sup>3</sup>. In practice, the channel inputs are selected from a discrete symbol constellation  $\mathcal{X} \subset \mathbb{C}$  such as PSK and QAM. Therefore, in order to obtain further insights about the performance of communication protocols the discrete-time discrete-input continuous-output channel has to be considered. This is of particular interest since the mutual-information of the SISO channel tends to infinity for high SNR while the maximum information that can be transmitted across the channel per symbol is limited by the size of the discrete channel input set at  $\log_2(M)$  bits, where  $M = |\mathcal{X}|$ . It is demonstrated in Section 7.4 that this property has a major impact on the achievable diversity gain of the HARDQ-MISO protocol and the HARQ-DDF protocol for certain protocol configurations.

Let  $x_i \in \mathcal{X}$  with  $1 \leq i \leq M$  denote the symbols of the channel input set. Furthermore, let  $\mathcal{Y} = \mathbb{C}$  denote the continuous channel output ensemble, where  $y_R = \Re\{y\}$  and  $y_I = \Im\{y\}$  denote the real and imaginary part for each symbol  $y \in \mathcal{Y}$ , respectively. Given the probability of the channel input symbols as  $\Pr(x_i)$  and the conditional probability  $p(y_R, y_I|x_i)$  of the channel output symbol  $y$ , given the channel input symbol  $x_i$ , the mutual information for the discrete-time discrete-input continuous-output channel is [40]

$$I = \sum_{i=1}^M \int_{y_R=-\infty}^{\infty} \int_{y_I=-\infty}^{\infty} \Pr(x_i) p(y_R, y_I|x_i) \log \frac{p(y_R, y_I|x_i)}{p(y_R, y_I)} dy_R dy_I, \quad (5.48)$$

---

<sup>3</sup>Note, since the STBC codes are not capacity achieving, the analysis in Sections 5.1 to 5.4 gives an upper bound on the outage probability considering the Alamouti code and Gaussian code ensembles.

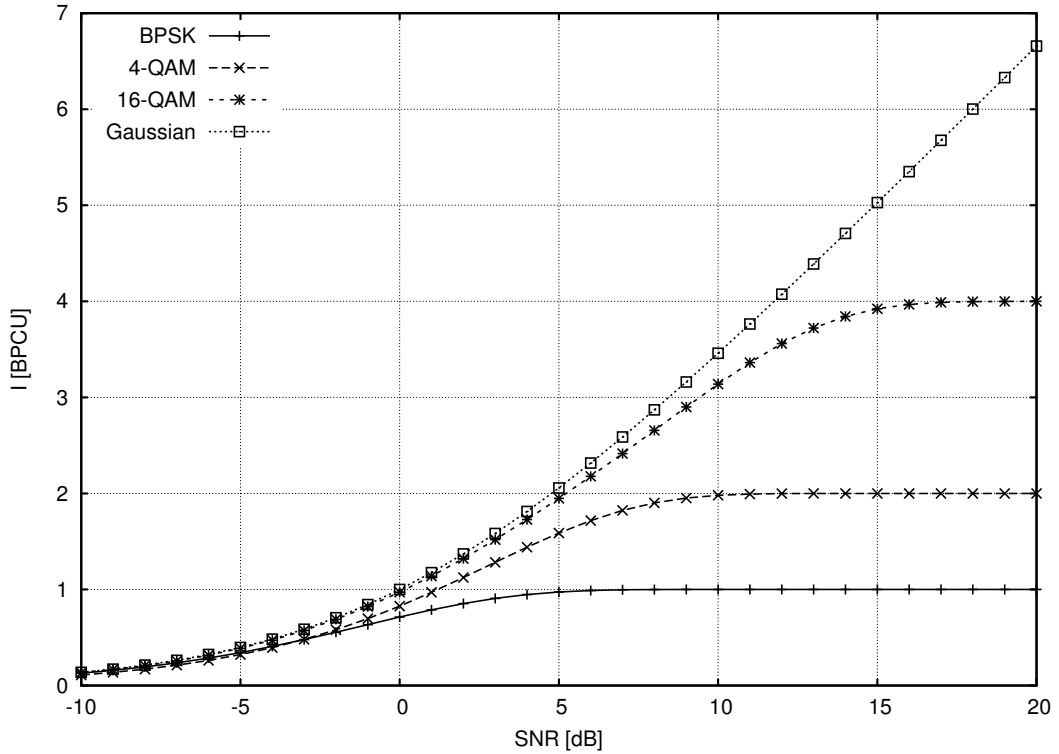


**Figure 5.1:** Mutual information of the discrete-input continuous-output AWGN channel for BPSK, 4-QAM and 16-QAM symbol constellations.

where the probability  $p(y_R, y_I)$  is [40]

$$p(y_R, y_I) = \sum_{i=1}^M \Pr(x) p(y_R, y_I | x_i). \quad (5.49)$$

Since the closed-form expression of the outage probability of the HARQ protocols considering discrete channel inputs is unknown, the numerical analysis in Chapter 7 is carried out using Monte Carlo simulations as described in Chapter 5.7. To this end, the mutual information of the discrete-input AWGN SISO channel<sup>4</sup> is required. For the AWGN channel with zero mean and variance  $\sigma^2$  the conditional probability  $p(y_R, y_I | x_i)$  is given by the complex Gaussian distri-

<sup>4</sup>Since the MISO channel applying STBC codes results in a scaled SISO AWGN channel [33] the mutual information of the Rayleigh fading MISO channel with discrete channel inputs can be obtained by scaling the noise variance using (5.8).

bution with mean  $x_i$  as

$$p(y_R, y_I | x_i) = \frac{1}{2\pi\sigma^2} e^{-\frac{(y_R - x_R)^2 + (y_I - x_I)^2}{2\sigma^2}}, \quad (5.50)$$

where  $x_R = \Re\{x_i\}$  and  $x_I = \Im\{x_i\}$  denote the real and imaginary part of  $x_i$ . Furthermore, in practice it is reasonable to assume the channel input symbols to be uniformly distributed with  $\Pr(x_i) = \frac{1}{M}$ . Correspondingly, Figure 5.1 depicts the mutual information of the discrete-input continuous-output AWGN channel considering the BPSK, 4-QAM and 16-QAM symbol constellations together with the Shannon channel capacity. In order to obtain these graphs, the integrals in (5.48) were solved using the VEGAS algorithm [96] implementation of the GNU Scientific Library [97] written for the programming language C.

## 5.7 Verification using Monte Carlo Simulations

*... the Monte Carlo simulation (MCS) method is a powerful modelling tool for the analysis of complex systems, due to its capability of achieving a closer adherence to reality. It may be generally defined as a methodology for obtaining estimates of the solution of mathematical problems by means of random numbers [98].*

The Monte Carlo simulation method is a powerful tool to approximate the expected value  $\mathbb{E}[g(X)]$  of a function  $g(X)$  according to the integral [99]

$$\mathbb{E}[g(X)] = \int_{\mathcal{X}} g(x)f(x) dx, \quad (5.51)$$

where the argument  $X \in \mathcal{X}$  is a random variable with probability density function  $f$ . To this end, a random number generator<sup>5</sup> is used to draw a sample  $[X_1, X_2, \dots, X_N]$  according to the probability density function  $f$  to compute the approximation [99]

$$\bar{g}_N = \frac{1}{N} \sum_{i=1}^N g(X_i), \quad (5.52)$$

---

<sup>5</sup>Throughout this work, the pseudo-random number generators provided by `boost::random` library v1.0 [100] written for the programming language C++ are used.

which, according to the Strong Law of Large Numbers, converges almost surely to  $\mathbb{E}[g(X)]$  [99].

The Monte Carlo simulation method is a frequently used tool [101, 102, 103, 104, 105] to assess the accuracy of approximations and closed-form expressions of information theoretic measures such as outage probability and outage capacity. Therefore, in this work, the Monte Carlo simulation method is used to validate the closed-form expressions given in Chapter 5. Furthermore, this method is used to obtain the outage probability and delay-limited throughput of the HARQ protocols considering discrete channel input constellations in Chapter 6, and to measure the performance of the RCPC encoded communication systems in Chapter 7, since the closed-form solutions for these systems are unknown.

### 5.7.1 Gaussian Channel Inputs

This section describes the application of the Monte Carlo simulation method to approximate the performance of the HARQ-SISO protocol considering continuous channel input constellations. Similar simulations are performed for the HARQ-MISO, HARQ-MISO and the HARQ-DDF protocol but their structure is excluded from this chapter for conciseness. The results are compared to the performance measures obtained using the closed-form expressions in Chapter 5 to verify their correctness.

Recall, according to (5.11) the mutual information of the SISO channel is for all ARQ rounds  $l$  given as

$$I^{(1)} = \log_2(1 + \gamma\rho), \quad (5.53)$$

where  $\gamma = |h_0|^2$  is an exponentially distributed random variable with mean  $\sigma^2$ , and  $\rho$  denotes the SNR. However, the measure of interest is the outage probability in HARQ round  $l$  defined according to (5.10) as

$$P_{\text{out}}(l) = \Pr(I^{(1)} < R(l)) = \Pr(\log_2(1 + \gamma\rho) < R(l)). \quad (5.54)$$

In order to approximate  $\mathbb{E}[P_{\text{out}}(l)]$  define the function

$$g_{\text{O}}(R, \rho, \gamma) = \begin{cases} 1, & \log_2(1 + \gamma\rho) < R, \\ 0, & \text{otherwise.} \end{cases} \quad (5.55)$$

Furthermore, consider a random number generator to sample the vector  $[\gamma_1, \gamma_2, \dots, \gamma_N]$  with independent identically exponentially distributed elements and mean  $\sigma^2$ . Then, given the function  $R(l)$  and  $\rho$  the outage probability in ARQ round  $l$  can be approximated according to (5.52) as

$$\bar{P}_{\text{out}}(l) = \frac{1}{N} \sum_{i=1}^N g_{\text{O}}(R(l), \rho, \gamma_i). \quad (5.56)$$

Similarly, in order to approximate the delay-limited throughput define the function

$$g_{\text{T}}(\gamma, \rho) = \begin{cases} \max\{R(l) : \log_2(1 + \gamma\rho) \geq R(l)\}, \\ 0, & \text{if } R(l) \text{ does not exist.} \end{cases} \quad (5.57)$$

Then, given the function  $R(l)$  and  $\rho$  the delay-limited throughput can be approximated (5.52) as

$$\bar{R}_{\text{DL}} = \frac{1}{N} \sum_{i=1}^N g_{\text{T}}(\gamma_i, \rho). \quad (5.58)$$

Note,  $N$  has to be large to obtain accurate approximations at high SNR.

Considering Gaussian channel inputs, Figure 5.2 and Figure 5.3 depict the outage probability and delay-limited throughput of the NPA HARQ protocols as a function of the D-SNR and compare the results obtained using the closed-form expressions against the results obtained using the Monte Carlo simulation method. To this end<sup>6</sup> an incremental redundancy  $\mathcal{C}$  code with  $L = 14$  punctured code books  $\mathcal{C}_l$  and rate assignment

$$R(l) = \begin{cases} \frac{32}{8+(l-1)}, & 1 \leq l < 8, \\ \frac{32}{16+8(l-8)}, & 8 \leq l \leq 14, \end{cases} \quad (5.59)$$

is used. Note, this configuration of the code rates implies unequal symbol length

---

<sup>6</sup>Note, this configuration is used to demonstrate the agreement of the numerical results and the simulation results only. Other system configurations could also have been considered.

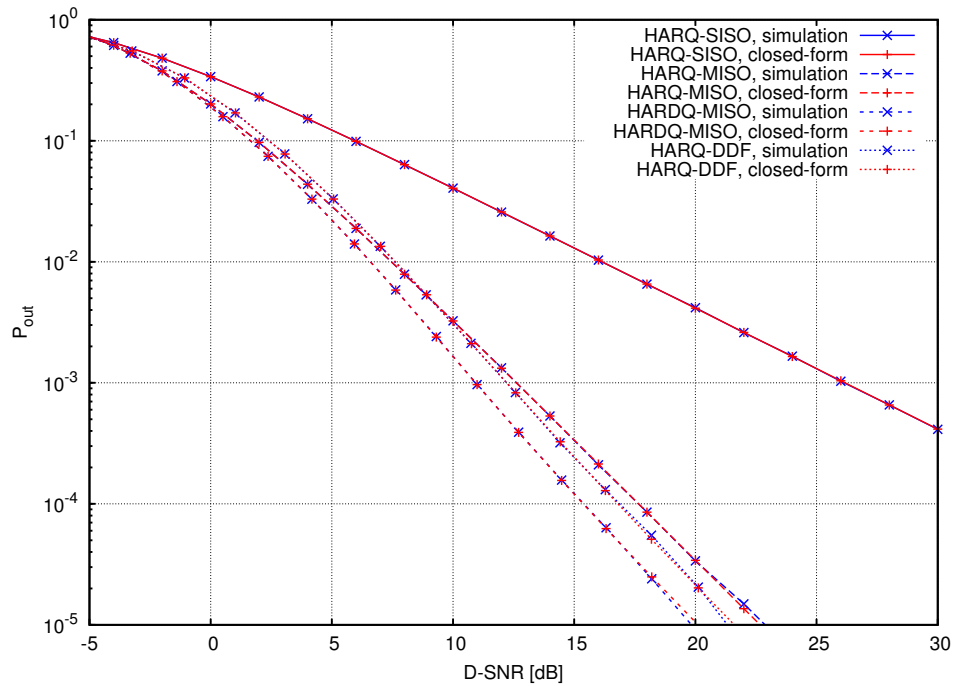


**Figure 5.2:** Outage probability of the NPA HARQ protocols measured as a function of the D-SNR. The Monte Carlo simulation results with  $N = 10^8$  verify the closed-form expressions given in Chapter 5.

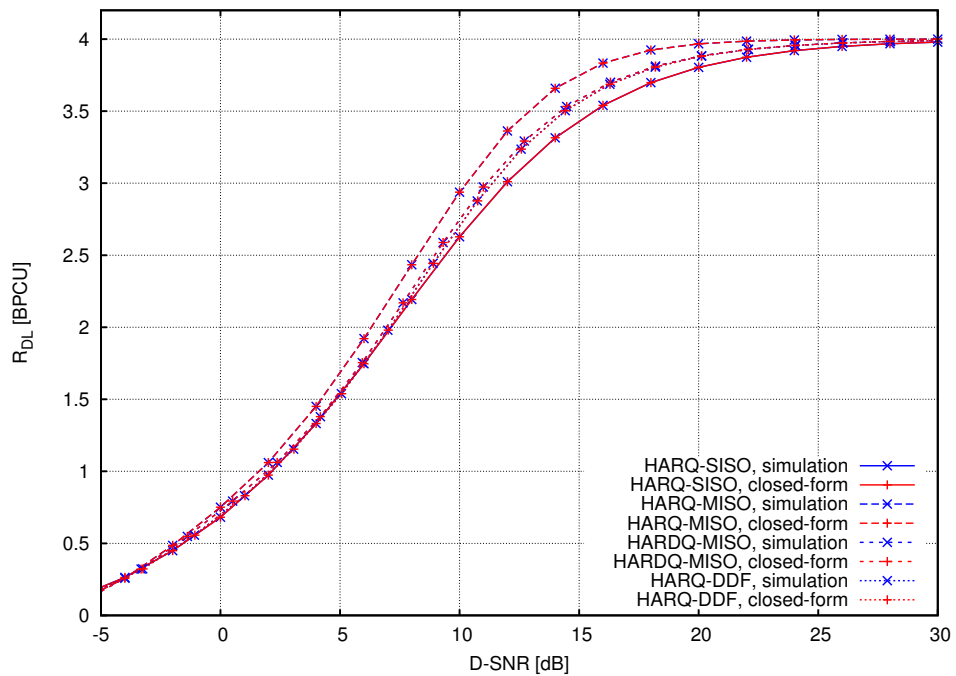


**Figure 5.3:** Delay-limited throughput of the NPA HARQ protocols measured as a function of the D-SNR. The Monte Carlo simulation results with  $N = 10^8$  verify the closed-form expressions given in Chapter 5.

ARQ rounds<sup>7</sup>. Furthermore, the decoding-time instant sets are configured as  $\mathcal{D} = \mathcal{D}_s = \mathcal{D}_r = \mathcal{D}_d$  with  $\mathcal{D} = \{1, 2, \dots, 14\}$ . For the HARDQ-MISO protocol, the transmission ARQ round of the second antenna is selected as  $t = 1$ . For the HARQ-DDF protocol, the noise variance at the relay  $N_r$  is selected to be half of the noise variance at the destination<sup>8</sup>  $N_d$ , i.e.,  $N_r = \frac{N_d}{2}$ . The number of samples is selected as  $N = 10^8$ . Both figures demonstrate the agreement of the results obtained using the closed-form expressions to the results obtained using the Monte Carlo simulation method.

Appendix B gives the results considering the TPA protocol variants and demonstrates the agreement of the results obtained using the closed-form results to the results obtained using the Monte Carlo simulation method.

All numerical results obtained according to Chapter 5 and presented throughout this work have been validated using the Monte Carlo simulation method. However, for conciseness these validations are excluded from this work.

### 5.7.2 Discrete Channel Inputs

This section describes the application of the Monte Carlo simulation method to approximate the performance of the HARQ-SISO protocol considering discrete channel input constellations. Similar simulations were performed for the HARQ-MISO, HARDQ-MISO and the HARQ-DDF protocol but their structure is excluded from this section for conciseness. Chapter 6 provides a comparison of the outage probability and delay-limited throughput considering continuous and discrete channel inputs. In Chapter 7, further results are compared to the performance measures obtained for the RCPC encoded communication systems in order to quantify their distance to the performance considering uniformly distributed BPSK channel inputs and to validate the correctness of the simulations.

Consider the function  $I_d(\rho)$  to give the mutual information of discrete-input AWGN channel with SNR  $\rho$  and channel input constellation  $\mathcal{X}$  as discussed in

<sup>7</sup>For  $b = 32 \times x$  information bits, the first ARQ round has symbol length  $n = 8 \times x$ , the ARQ rounds  $2 \leq l < 8$  have symbol length  $n = x$  and the ARQ rounds  $8 \leq l \leq 14$  have symbol length  $n = 8 \times x$ , where  $x \in \mathbb{Z}^+$ .

<sup>8</sup>This system set-up is also used in [25, 26, 18] where the SNR of the source-to-relay channel is defined to be 3dB better than the SD-SNR. However, using the noise variance to select the SNR levels maintains comparability of the TPA and the NPA protocol variants.

Section 5.6. Furthermore, the coherent maximum-likelihood detector is given as [38]

$$\hat{x} = \arg \min_{x_i \in \mathcal{X}} \|xh + n - hx_i\| \equiv \arg \min_{x_i \in \mathcal{X}} \left\| x + \frac{n}{h} - x_i \right\|. \quad (5.60)$$

As can be seen, at detection time the AWGN noise sample  $n$  is scaled by the channel input coefficient. Therefore, for a given channel coefficient  $h$  and AWGN noise variance  $N_0$  the effective SNR is

$$\rho_d(\gamma = |h|^2, \rho) = \mathbb{E} \left[ \left| \frac{Eh}{n} \right|^2 \right] = \gamma\rho, \quad (5.61)$$

where  $E$  denotes the average per symbol power constraint. Consequently, for a given channel gain  $\gamma$  the mutual information of the fading discrete-input SISO channel with SNR  $\rho$  can be obtained as  $I_d(\rho_d(\gamma, \rho))$ . Therefore, define the functions

$$g_O(R, \rho, \gamma) = \begin{cases} 1, & I_d(\rho_d(\gamma, \rho)) < R, \\ 0, & \text{otherwise,} \end{cases} \quad (5.62)$$

and

$$g_T(\gamma, \rho) = \begin{cases} \max\{R(l) : I_d(\rho_d(\gamma, \rho)) \geq R(l)\}, \\ 0, & \text{if } R(l) \text{ does not exist.} \end{cases} \quad (5.63)$$

Then, outage probability and delay-limited throughput of the discrete-time discrete-input continuous-output channel applying the HARQ-SISO protocol can be obtained using (5.56) and (5.58), respectively.

## 5.8 Summary

Sections 5.1 to 5.4 give the outage probability  $P_{\text{out}}(l)$  of the HARQ-SISO, HARQ-MISO, HARDQ-MISO and the HARQ-DDF protocol in ARQ round  $l \in \mathcal{D}_d$ . Using these results, the delay-limited throughput  $R_{\text{DL}}$  and the outage probability  $P_{\text{out}}$  of each protocol can be computed according to (4.13) and (5.10), respectively.

The key to these derivations is the observation that the mutual information of each ARQ round can be accumulated according to (5.2) which forms the basis of the assumptions (5.5), (5.6) and (5.7) [32]. Furthermore, the structure

of the derivations clearly reveals the interrelation of the HARQ-SISO and the HARQ-MISO protocol with the HARDQ-MISO protocol and the propinquity of the HARDQ-MISO to the HARQ-DDF protocol. These observations once more legitimize the performance analysis by comparison across the relevant protocols.

In order to enable the performance analysis and the performance comparison, care is taken that the same assumptions are valid across the protocols by applying a unified incremental redundancy coding approach. Since the derivations for the HARDQ-MISO and the HARQ-DDF protocol respect the change of the channel configuration in ARQ round  $t$ , the performance comparison on the system level is maintained by the consideration of the D-SNR as outlined in Section 4.6 and Section 5.5.

The analysis given in [32, 23] considers equal symbol length ARQ rounds. In comparison, the derivations given in this chapter consider to assign a specific code rate to each ARQ round. Therefore, it can be seen that the outage probability depends on the ratio between the achievable rates  $R(l)$ , rather than block length specification, i.e., two mother codes  $\mathcal{C}_a$  and  $\mathcal{C}_b$  with block lengths  $n_a(l) \neq n_b(l)$  achieve the same performance as long as  $R_a(l) = R_b(l)$ .

The definitions  $\mathcal{D}_r \subseteq \mathcal{D}_s$  and  $\mathcal{D}_d \subseteq \mathcal{D}_s$  enable to maintain comparability and scalability of the decoding cost at the relay and the destination across the protocols.

The results derived in the Sections 5.1 to 5.4 give the achievable outage probability considering a Gaussian distributed continuous ensemble of channel inputs. In practice, the channel input constellation is assumed to be discrete with uniformly distributed symbols and finite. Therefore, Section 5.6 gives the necessary tools to obtain the mutual information for the discrete-input continuous-output SISO AWGN channel. These results are used to obtain the achievable outage probability considering uniformly distributed finite channel input constellations using the Monte Carlo simulation method as discussed in Section 5.7.

In Section 5.7.1, the simulation structure considering continuous channel inputs is given in order to validate the closed-form expressions. A particular HARQ protocol configuration is used to demonstrate the agreement of the simulation results and the results obtained using the closed-form expressions. All numerical results presented throughout this work are validated using the Monte Carlo simulation method but most of the validations are excluded for concise-

ness.

Furthermore, in Section 5.6, the simulation structure is given considering discrete channel inputs. Corresponding simulation results are presented in Chapter 6 and in Chapter 7.

### Numerical Results: Gaussian and Discrete Channel Inputs

---

This chapter provides a discussion of the outage probability and the delay-limited throughput for the HARQ protocols introduced in Section 4. To this end, consider two mother code books<sup>1</sup>  $\mathcal{C}_{\text{non-opt}}$  and  $\mathcal{C}_{\text{opt}}$  associated with the non-optimized code rate function

$$R_{\text{non-opt}}(l) = \frac{32}{8 + 8(l - 1)}, \quad 1 \leq l \leq 8, \quad (6.1)$$

and the optimized code rate function

$$R_{\text{opt}}(l) = 4 - 0.5(l - 1), \quad 1 \leq l \leq 8, \quad (6.2)$$

---

<sup>1</sup>The non-optimized and optimized codebook used throughout this chapter are examples only, and enable to reveal important performance characteristics. These codebooks could also have been selected differently. Furthermore, it is noteworthy, that the optimized codebook does not necessarily represent the optimal codebook. The optimization of the mother codebook is beyond the scope of this work.

respectively. The non-optimized codebook  $\mathcal{C}_{\text{non-opt}}$  has equal symbol length ARQ rounds. Consequently, the decrement  $R_{\text{non-opt}}(l) - R_{\text{non-opt}}(l-1)$  decreases for increasing  $l$ . In contrast, the optimized code  $\mathcal{C}_{\text{opt}}$  is chosen such that the decrement  $R_{\text{opt}}(l) - R_{\text{opt}}(l-1) = 0.5$  BPCU is constant and therefore, the symbol length of each ARQ round increases for increasing  $l$ . Both codebooks offer  $L = 8$  ARQ rounds. Consequently, the decoding instant set offered by the mother codebook is given as  $\mathcal{D} = \{1, 2, \dots, 8\}$ . Both codebooks have a maximum code rate of  $R_{\text{max}} = 4$  BPCU in ARQ round  $l = 1$  and a minimum code rate  $R_{\text{min}} = 0.5$  BPCU in ARQ round  $l = 8$ .

The numerical results discussed throughout this chapter consider the long-term quasi-static Rayleigh fading channel with AWGN. The Rayleigh distributed channel coefficients have unit variance and zero mean. Furthermore, the noise variance at the relay  $N_r$  is selected to be half of the noise variance at the destination<sup>2</sup>  $N_d$ , i.e.,  $N_r = \frac{N_d}{2}$ . This channel set-up ensures comparability with related work such as [25, 26, 18].

The analysis considers Gaussian distributed channel inputs and uniformly distributed 16-QAM channel inputs. For the Gaussian distributed channel inputs the closed-form expressions given in Section 5 were used. In order to obtain the results considering the 16-QAM channel input constellation, the Monte Carlo simulation method is applied as discussed in Section 5.7. To this end, the simulation was configured to perform  $N = 10^8$  iterations per D-SNR level.

Applying the non-optimized codebook, Section 6.1 demonstrates that the performance measurement of the HARQ protocols as function of the D-SNR reveals several performance characteristics which cannot be observed if the performance is measured as a function of the SD-SNR. Section 6.2 provides a comparison of the performance of the non-optimized and the optimized codebook. Then, Section 6.3 compares the performance of the NPA HARDQ-MISO and the NPA HARQ-DDF protocol against the performance of the corresponding TPA protocol variants applying the optimized codebook. Section 6.4 and Section 6.5 consider the decoding cost reduction at the relay only and the decoding cost reduction at the relay *and* at the destination, respectively.

---

<sup>2</sup>This system set-up is also used in [25, 26, 18] where the SNR of the source-to-relay channel is defined to be 3dB better than the SD-SNR. However, using the noise variance to select the SNR levels maintains comparability of the TPA and the NPA protocol variants.

## 6.1 Outage Probability Analysis Considering SD-SNR and D-SNR

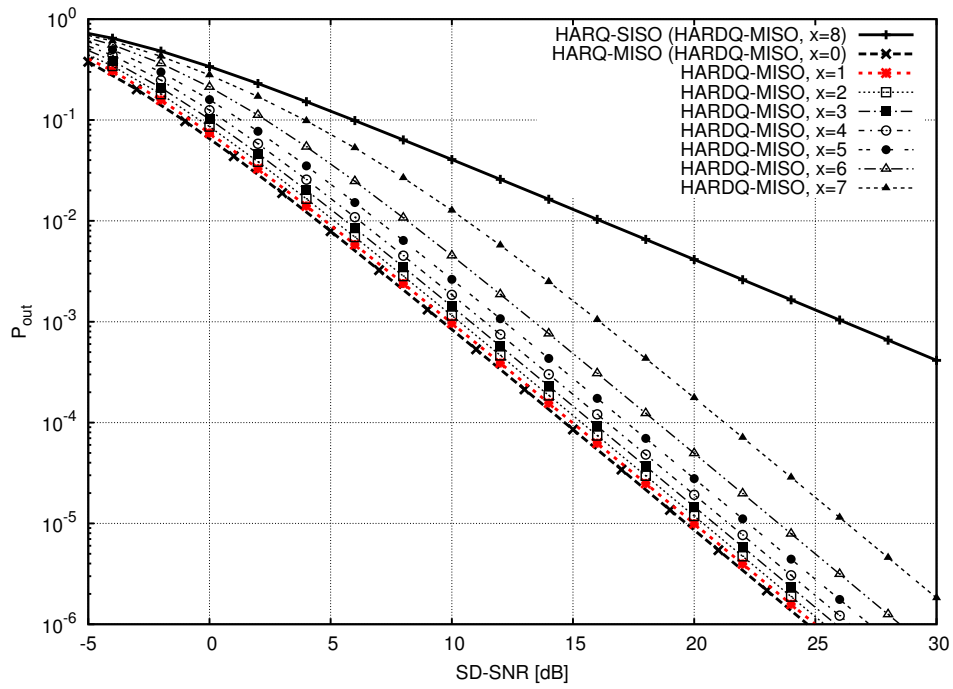
In [23, 25, 26, 27, 28], the performance of the DDF protocol is measured as a function of the SD-SNR. However, this approach does not enable the performance comparison with the SISO and the MISO channel on the system level, since the relay introduces additional energy into the channel and thereby changes the D-SNR as discussed in Section 4.6.

In this section, the outage probability and the delay limited throughput of the HARQ protocols introduced in Chapter 4 is given as a function of the SD-SNR and the D-SNR. The comparison reveals several differences in the performance characteristics and thereby justifies the performance analysis as a function of the D-SNR.

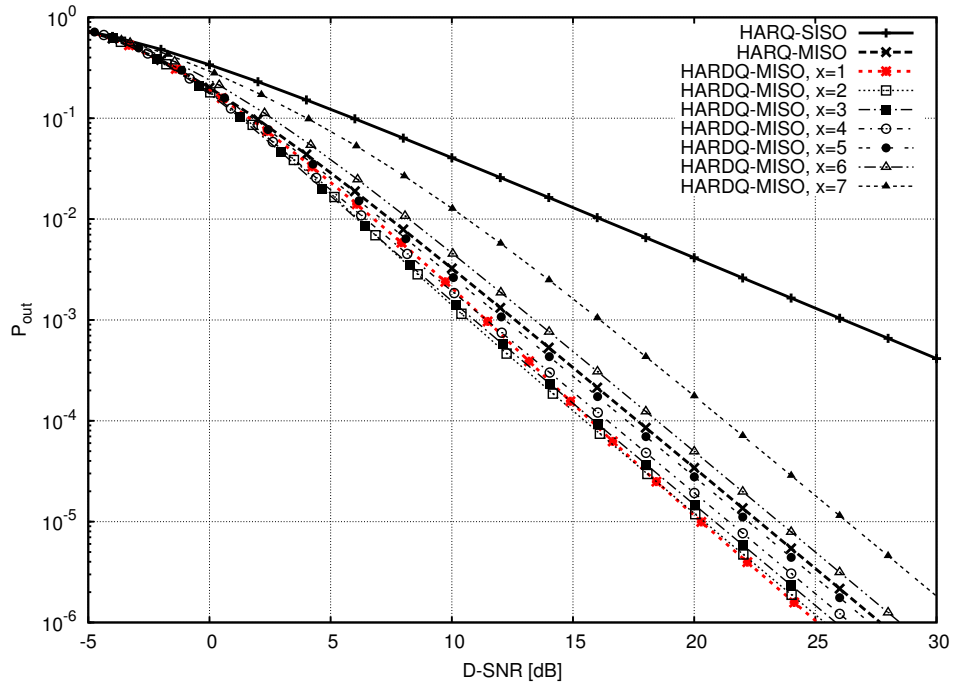
Throughout this section, consider the non-optimized codebook  $\mathcal{C}_{\text{non-opt}}$ , Gaussian channel inputs and the NPA protocol variants. For completeness, Appendix C depicts the graphs corresponding to those shown in this section but considering the optimized codebook and 16-QAM channel inputs, these graphs are excluded from this section for conciseness since they do not reveal further insights considering performance analysis as a function of the SD-SNR and D-SNR.

For the HARDQ-MISO and the HARQ-DDF protocol, the decoding instant sets at the source and the destination are selected as  $\mathcal{D} = \mathcal{D}_s = \mathcal{D}_d$ . For the HARQ-DDF protocol, the decoding instant set at the relay is selected as  $\mathcal{D}_r = \{x, x+1, \dots, 8\}$  and for the HARDQ-MISO protocol the ARQ round after which the second antenna starts to assist the transmission is given as  $t = x$ , where  $x \in \mathcal{D}$ . I.e., for increasing  $x$  the relay and the second antenna start to assist the transmission later.

For comparison, the performance measures for the HARQ-SISO and the HARQ-MISO protocols are given. The HARQ-SISO and the HARQ-MISO protocols are given by the HARDQ-MISO protocol with  $t = 8$  and  $t = 0$ , respectively. For the HARQ-MISO protocol the SD-SNR is measured across a single source antenna to destination antenna channel.

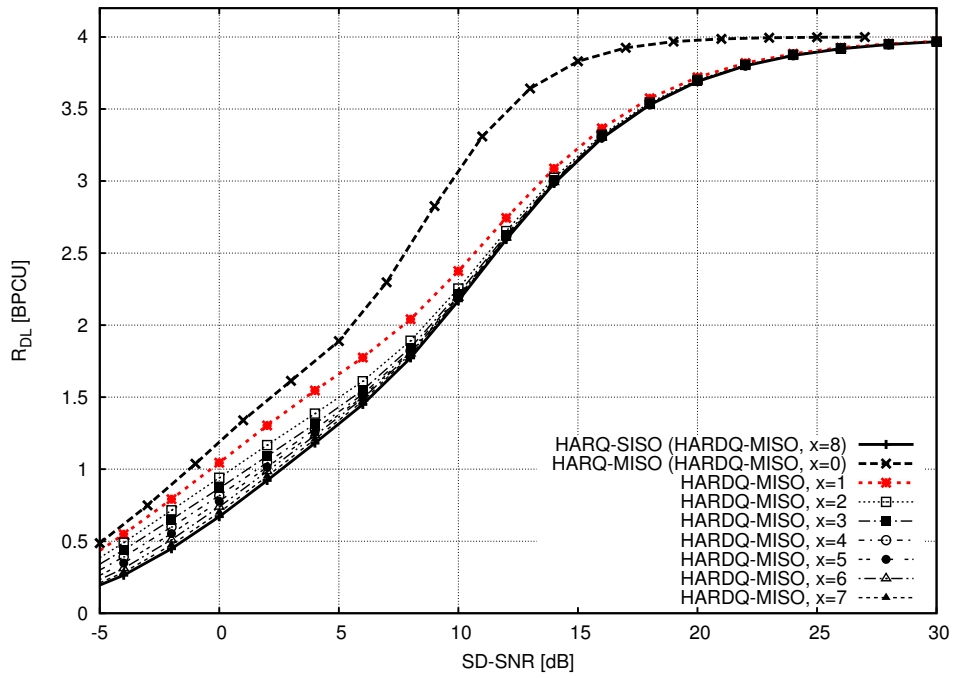


(a) Outage probability as a function of the SD-SNR

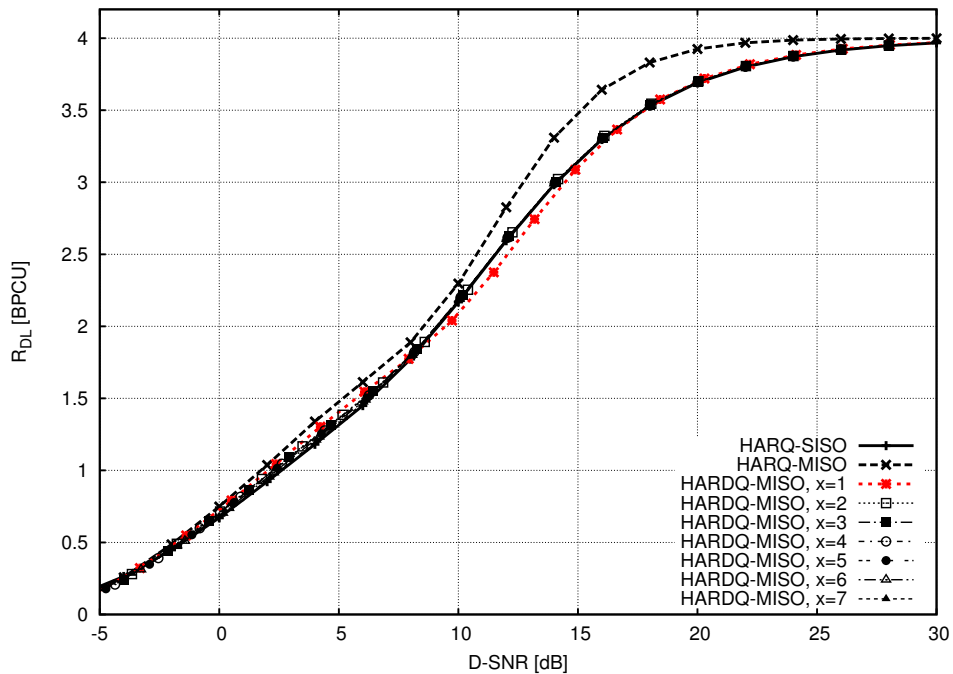


(b) Outage probability as a function of the D-SNR

**Figure 6.1:** Comparison of the outage probability measured as a function of the SD-SNR and D-SNR for the HARQ-MISO protocol considering Gaussian channel inputs and increasing  $t$ .

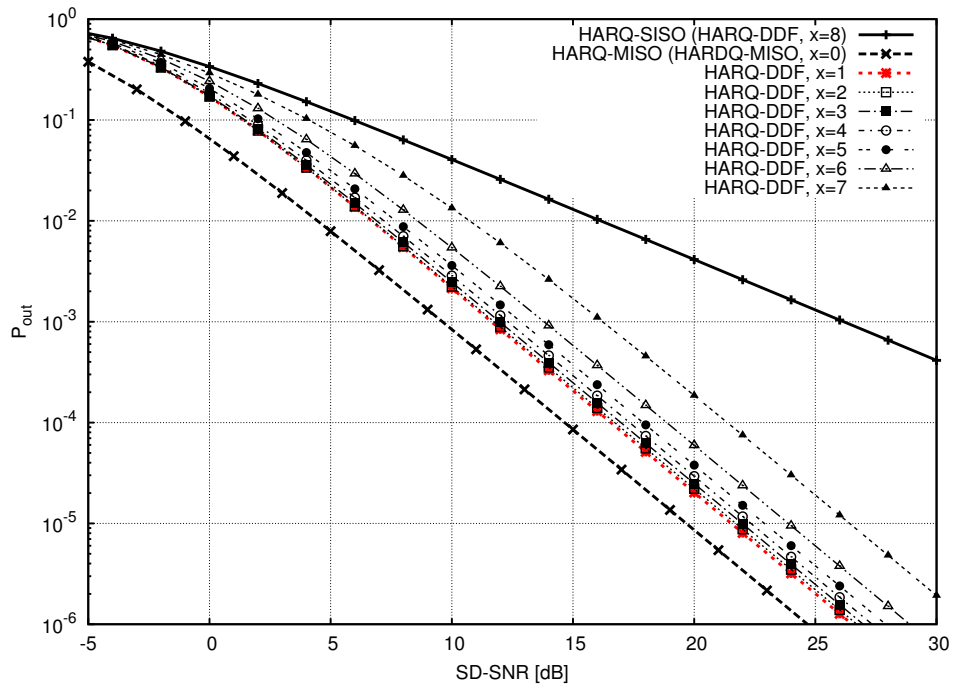


(a) Delay-limited throughput as a function of the SD-SNR

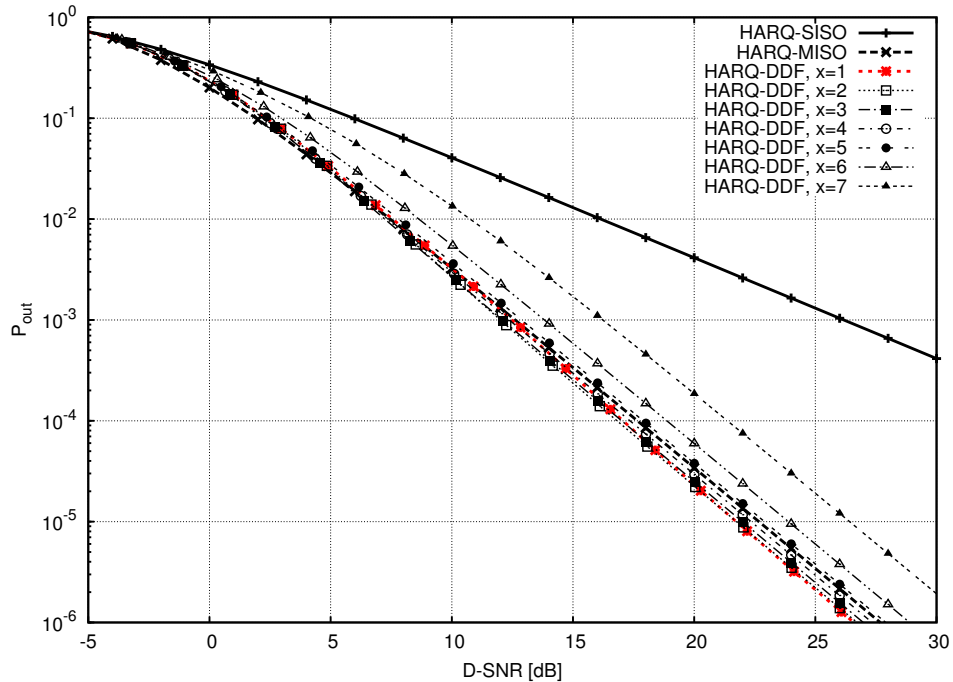


(b) Delay-limited throughput as a function of the D-SNR

**Figure 6.2:** Comparison of the delay-limited throughput as a function of the SD-SNR and the D-SNR for the HARQ-MISO protocol considering Gaussian channel inputs and increasing  $t$ .

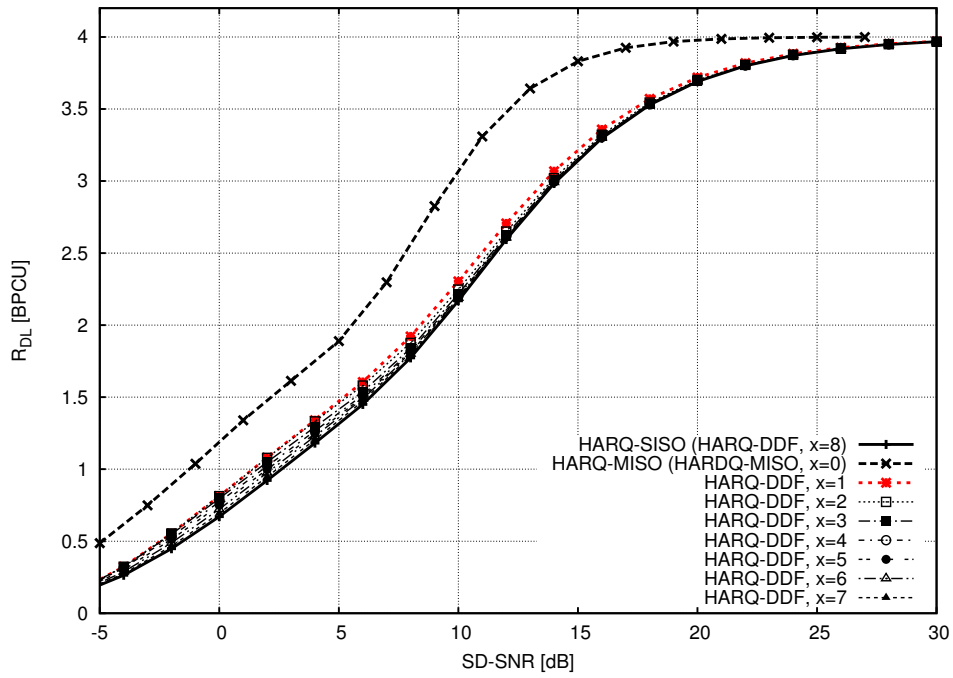


(a) Outage probability as a function of the SD-SNR

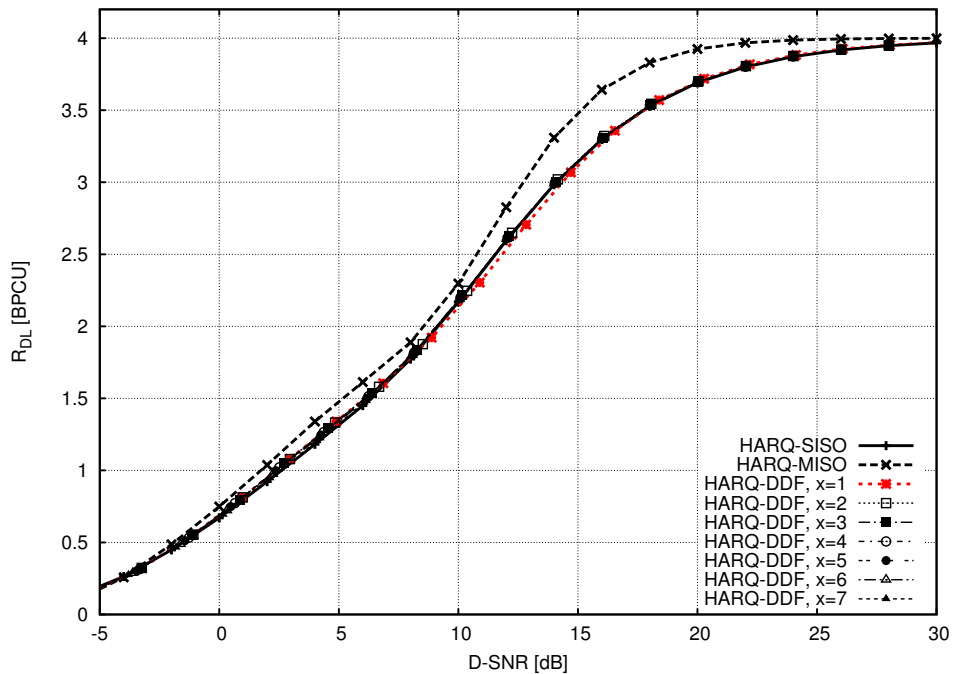


(b) Outage probability as a function of the D-SNR

**Figure 6.3:** Comparison of the outage probability measured as a function of the SD-SNR and the D-SNR for the HARQ-DDF protocol considering Gaussian channel inputs and increasing  $\min\{D_r\}$ .



(a) Delay-limited throughput as a function of the SD-SNR



(b) Delay-limited throughput as a function of the D-SNR

**Figure 6.4:** Comparison of the delay-limited throughput as a function of the SD-SNR and the D-SNR for the HARQ-DDF protocol considering Gaussian channel inputs and increasing  $\min\{D_r\}$ .

### HARDQ-MISO Protocol

Figure 6.1 depicts the outage probability of the HARDQ-MISO protocol as a function of the SD-SNR and as a function of the D-SNR.

In Figure 6.1a, the outage probability is shown as a function of the SD-SNR. It can be observed that the performance loss for increasing  $x$  is constant at medium to high SD-SNR. Furthermore, the HARQ-MISO protocol outperforms the HARDQ-MISO protocol. In Figure 6.1b, the outage probability is shown as a function of the D-SNR and it can be observed that the performance loss is not constant for each  $x$  at medium D-SNR but at high D-SNR. At high D-SNR, the probability is high that the destination decodes the received information successfully in the first ARQ round. Therefore, the second antenna does rarely assist the transmission and for high SD-SNR and D-SNR an equivalent outage probability can be observed.

However, for low to medium D-SNR, the probability is high that the destination decodes successfully in a late ARQ round, or never. Thus, with high probability the second antenna is used and introduces additional energy into the channel. In Figure 6.1a and Figure 6.1b, observe the functions for  $x = 1$  depicted as a red line for easier tracking. In Figure 6.1a, this function shows a better outage probability performance than for  $x > 1$  over the complete shown SD-SNR range. In contrast, for medium D-SNR, e.g. D-SNR = 12dB, it can be observed in Figure 6.1b that the function for  $x = 1$  has a higher outage probability than the functions shown for  $x = 2$  and  $x = 3$ . Note, the configurations  $x = 2$  and  $x = 3$  show better performance, although the second antenna assists the transmission in later ARQ rounds than for the configuration  $x = 1$ . The configuration  $x = 4$  achieves a performance very close to  $x = 1$ . Only if the second antenna assists the transmission in very late ARQ rounds, i.e., for  $x \geq 5$  the configuration  $x = 1$  shows higher reliability.

Furthermore, Figure 6.1b shows the outage probability performance of the HARQ-SISO and HARQ-MISO channel for comparison with the HARDQ-MISO channel. It can be observed that the HARDQ-MISO channel achieves the same diversity as the HARQ-MISO channel at high SNR. For all  $x \in \mathcal{D}$ , with  $x \neq 8$ , the HARDQ-MISO protocol outperforms the HARQ-SISO protocol. In difference to the SD-SNR measure given in Figure 6.1a, the HARDQ-MISO protocol outperforms the HARQ-MISO protocol for  $x \leq 5$  only.

Figure 6.2a and Figure 6.2b show the delay-limited throughput as a function of the SD-SNR and the D-SNR, respectively. In Figure 6.2a, the HARDQ-MISO configuration with  $x = 1$  outperforms the configurations with  $x \geq 2$  for low to medium SD-SNR significantly. Furthermore, with increasing  $x$  the delay-limited throughput decreases. However, measuring the delay-limited throughput as a function of the D-SNR as shown in Figure 6.2b, it can be observed that the configuration of  $x$  allows to achieve only a negligible performance advantage. Furthermore, for rates  $2 \leq R_{\text{DL}} \leq 3.4$  BPCU it can be observed that the HARQ-SISO channel and the configurations  $x \geq 2$  outperform the configuration  $x = 1$ .

Comparing the performance difference of the HARQ-MISO and the HARDQ-MISO protocol in Figure 6.2a and Figure 6.2b shows that the HARQ-MISO protocol always outperforms the HARDQ-MISO protocol in terms of delay-limited throughput. However, Figure 6.2b reveals that the performance difference is small from an energy efficiency point of view.

Consequently, considering a medium SNR level, it is beneficial to configure the source to assist the transmission after ARQ round  $t = 2$  since the configuration  $x = 2$  is more reliable and achieves as least comparable throughput as the configuration  $x = 1$ . This performance advantage is not revealed if the outage probability is measured as a function of the SD-SNR.

### **HARQ-DDF Protocol**

Figure 6.3a and Figure 6.3b depict the outage probability of the HARQ-DDF protocol as a function of the SD-SNR and the D-SNR, respectively. Correspondingly, Figure 6.4a and Figure 6.4b depict the delay-limited throughput as a function of the SD-SNR and the D-SNR, respectively.

In comparison with the HARDQ-MISO protocol, it can be observed that the HARQ-DDF protocol shows very similar performance, but the performance gains are smaller. This effect results from the fact, that the ARQ round in which the relay starts to assist the transmission is a random variable depending on the source-to-relay channel realisation. At high D-SNR, the HARQ-DDF protocol does not show to achieve the performance of the HARDQ-MISO protocol.

## 6.2 Throughput Optimization Using Code Rate Assignment

This section demonstrates the effect of code rate assignment on the delay-limited throughput function ( $R_{\text{DL}}$ ) measured as a function of the D-SNR using the optimized code book  $\mathcal{C}_{\text{opt}}$  and the NPA HARQ protocols. To this end, the decoding instant sets are chosen as  $\mathcal{D} = \mathcal{D}_s = \mathcal{D}_r = \mathcal{D}_d$ , where  $\mathcal{D} = \{1, 2, \dots, 8\}$ . I.e., relay and destination perform a decoding attempt in each ARQ round offered by the mother codebook. Therefore, the HARDQ-MISO protocol gives the outage probability of the HARQ-DDF protocol achieved if the SNR of the source-to-relay channel tends to infinity.

### Gaussian Channel Inputs

Figure 6.5 depicts the outage probability of the HARQ protocols considering Gaussian distributed channel inputs for both codebooks. It can be observed that the selection of the codebook does not change the outage probability for the HARQ-SISO and the HARQ-MISO protocol. For the HARDQ-MISO protocol, a negligible performance advantage can be observed for the optimized codebook. The non-optimized codebook outperforms the optimized codebook from an outage probability point of view considering the HARQ-DDF protocol.

Furthermore, it can be observed that the HARDQ-MISO protocol clearly outperforms the HARQ-MISO protocol for both codebooks for medium to high D-SNR. At low D-SNR, the HARDQ-MISO protocol achieves the performance of the HARQ-MISO protocol. At high D-SNR, also the HARQ-DDF protocol outperforms the HARQ-MISO protocol for both codebooks, but considering the optimized codebook, the performance advantage is negligible. At medium to low D-SNR, the HARQ-MISO protocol outperforms the HARQ-DDF protocol. It is also important to point out that both the HARDQ-MISO and the HARQ-DDF protocol achieve the same diversity as the HARQ-MISO protocol at high D-SNR.

However, for both codebooks, the HARDQ-MISO protocol and the HARQ-DDF protocol show a very good outage probability performance which is at least equivalent or superior to the performance of the HARQ-MISO protocol at

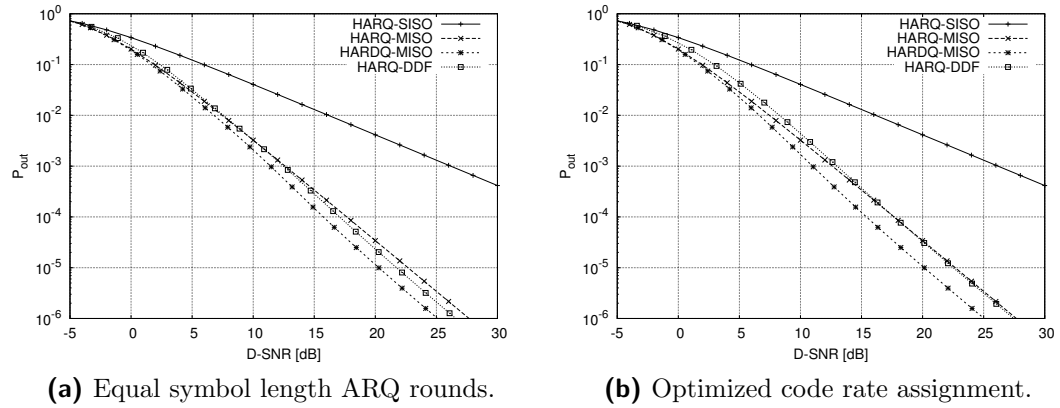


**Figure 6.5:** Comparison of the outage probability of the code books  $\mathcal{C}_{\text{non-opt}}$  and  $\mathcal{C}_{\text{opt}}$  considering Gaussian distributed channel inputs.

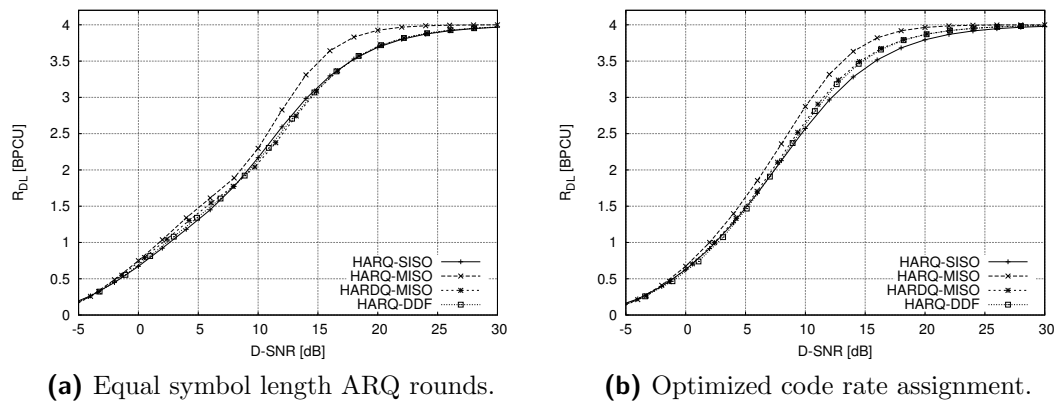


**Figure 6.6:** Comparison of the delay-limited throughput of the code books  $\mathcal{C}_{\text{non-opt}}$  and  $\mathcal{C}_{\text{opt}}$  considering Gaussian distributed channel inputs.

high D-SNR.

Figure 6.6 depicts the corresponding delay-limited throughput measured as a function of the D-SNR for the HARQ protocols. For both codebooks, all protocols achieve the maximum throughput at high D-SNR. But it can be observed that the optimized codebook outperforms the non-optimized codebook over almost the complete shown D-SNR range. At very low D-SNR, both codebooks show equivalent performance. The HARDQ-MISO protocol outperforms the HARQ-DDF protocol, but the performance difference is negligible. Furthermore, it can be observed that the HARQ-MISO protocol outperforms the remaining protocols for both codebooks.

Considering the non-optimized codebook, it can be observed that the HARDQ-MISO protocol and the HARQ-DDF protocol outperform the HARQ-SISO protocol for rates up to  $R_{DL} = 2$ . For higher rates, the HARQ-SISO protocol is superior. In comparison, the optimized codebook allows to achieve at least the performance of the HARQ-SISO protocol and is superior for rates  $R_{DF} > 2$ .

Furthermore, an interesting observation is that the delay-limited throughput functions show a kink at  $R_{DL} = 2$  BPCU. This observation will be revisited considering 16-QAM channel inputs in the subsequent analysis.

The comparison of the delay-limited throughput as a function of the D-SNR demonstrates that the optimization of the achievable code rates of the mother codebook offers significant performance gains in terms of delay-limited throughput. From a reliability point of view, equal symbol length ARQ rounds offer a remarkable outage probability measured as a function of the D-SNR for the HARQ-DDF protocol only.

### 16-QAM Channel Inputs

Figure 6.7 and Figure 6.8 show the outage probability and the delay-limited throughput measured as functions of the D-SNR for the HARQ protocols.

In general, the outage probability functions are very similar in performance to the Gaussian channel inputs. However, the performance advantage of the HARDQ-MISO and the HARQ-DDF protocol over the HARQ-MISO protocol is reduced.

Considering the delay-limited throughput functions in Figure 6.8 and Figure 6.6, major differences can be observed. Primarily, it can be observed that

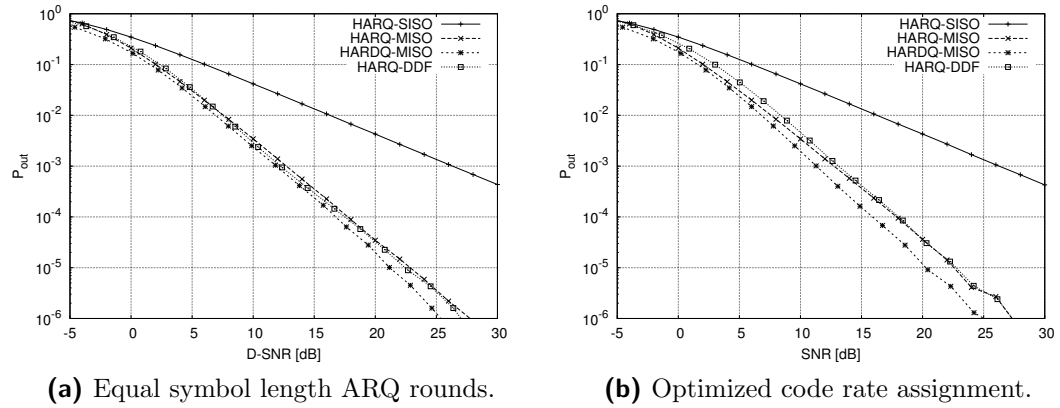


**Figure 6.7:** Comparison of the outage probability of the code books  $\mathcal{C}_{non-opt}$  and  $\mathcal{C}_{opt}$  considering uniformly distributed 16-QAM channel inputs.

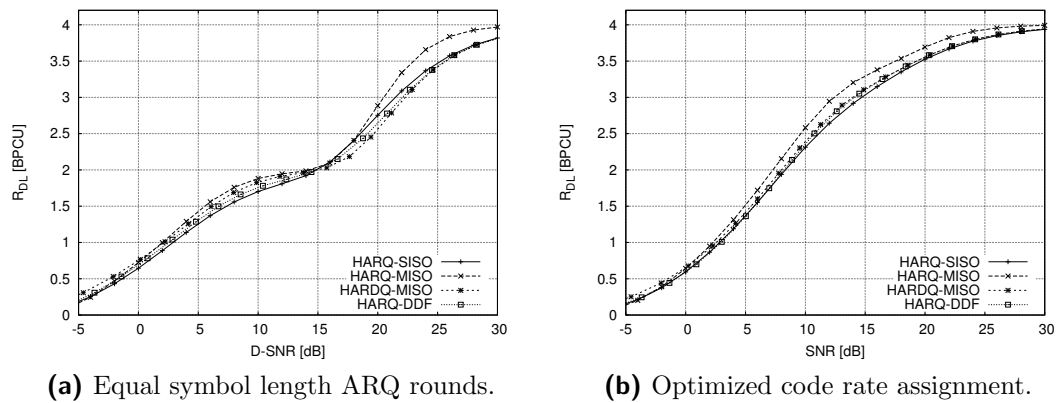


**Figure 6.8:** Comparison of the delay-limited throughput of the code books  $\mathcal{C}_{non-opt}$  and  $\mathcal{C}_{opt}$  considering uniformly distributed 16-QAM channel inputs.

the functions considering Gaussian channel inputs significantly outperform the functions obtained due to 16-QAM channel inputs. Furthermore, as mentioned earlier, a kink can be observed around  $R_{\text{DL}} = 2$  BPCU for Gaussian channel inputs and the non-optimized codebook. Considering 16-QAM channel inputs, this kink takes a more significant form. This kink stems from the fact the distance between the code rate of the first and the second ARQ round is large. This distance can be overcome only if the D-SNR is high. However, in the optimized codebook, the distance to the next achievable code rate higher than  $R = 2$  BPCU is smaller and can be overcome at lower D-SNR levels. Therefore, the delay-limited throughput function considering the optimized codebook is smooth.

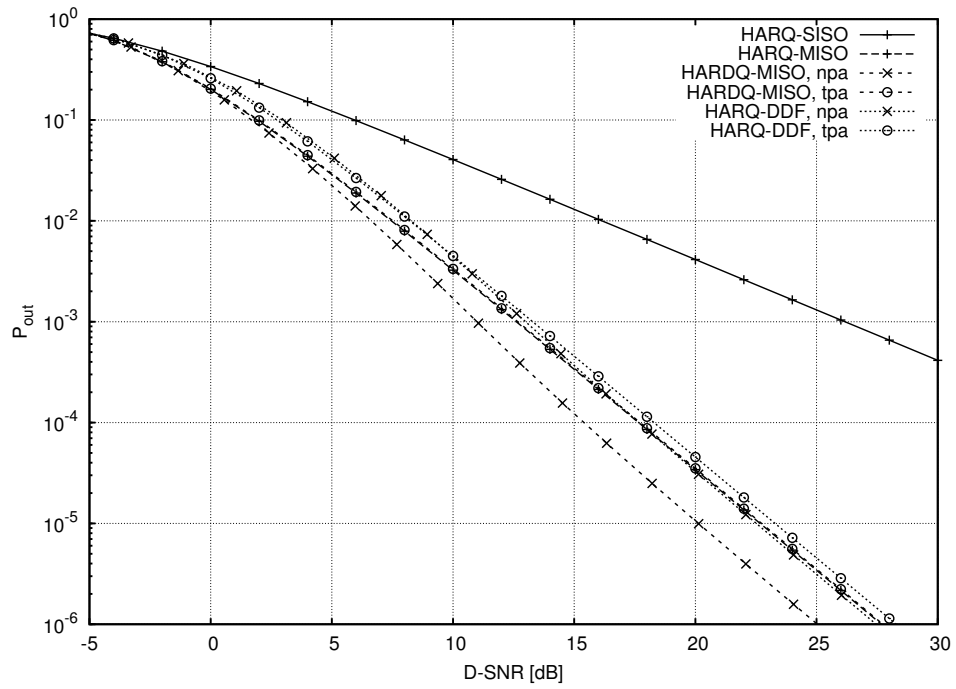
It can be observed that the optimization of the mother codebook allows significant throughput performance gains considering 16-QAM channel inputs. But the performance gain of the HARDQ-MISO and HARQ-DDF protocol over the HARQ-SISO protocol is less significant than considering Gaussian channel inputs.

### 6.3 Performance Comparison of the NPA and the TPA HARQ Protocols

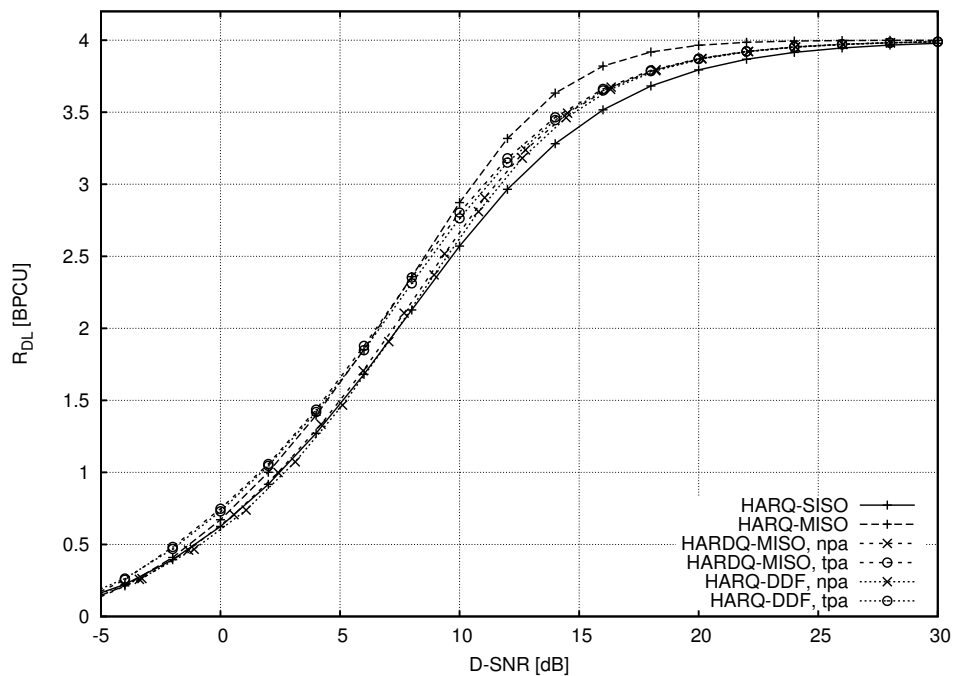
This section compares the performance of the NPA HARQ protocols against the corresponding TPA protocol variants. To this end, outage probability and the delay-limited throughput are measured as a function of the D-SNR. Throughout this section, the optimized codebook  $\mathcal{C}_{\text{opt}}$  with  $\mathcal{D} = \mathcal{D}_s = \mathcal{D}_d$  and  $\mathcal{D} = \mathcal{D}_r$  for the HARQ-DDF protocol and  $t = \min\{\mathcal{D}\}$  for the HARDQ-MISO protocol is used.

#### Gaussian Channel Inputs

Figure 6.9 depicts the outage probability and the delay-limited throughput of the HARQ protocols considering Gaussian channel inputs. As can be observed in Figure 6.9a, the HARDQ-MISO protocol and the HARQ-DDF protocol show an equivalent outage probability at low D-SNR levels. For medium to high D-SNR, the application of the NPA protocol variant achieves a lower outage probability

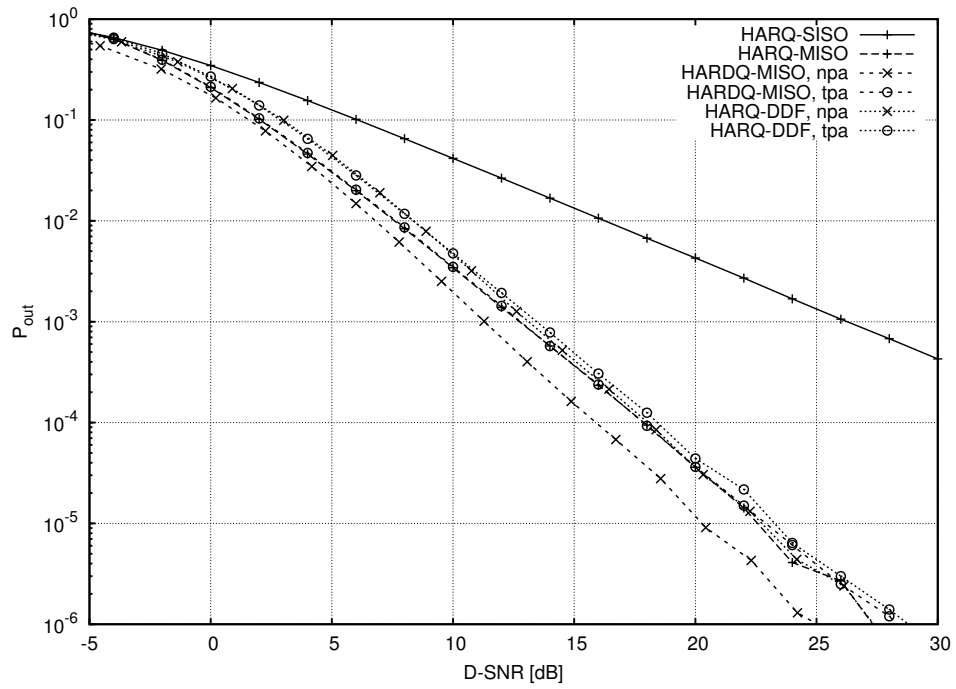


(a) Outage probability

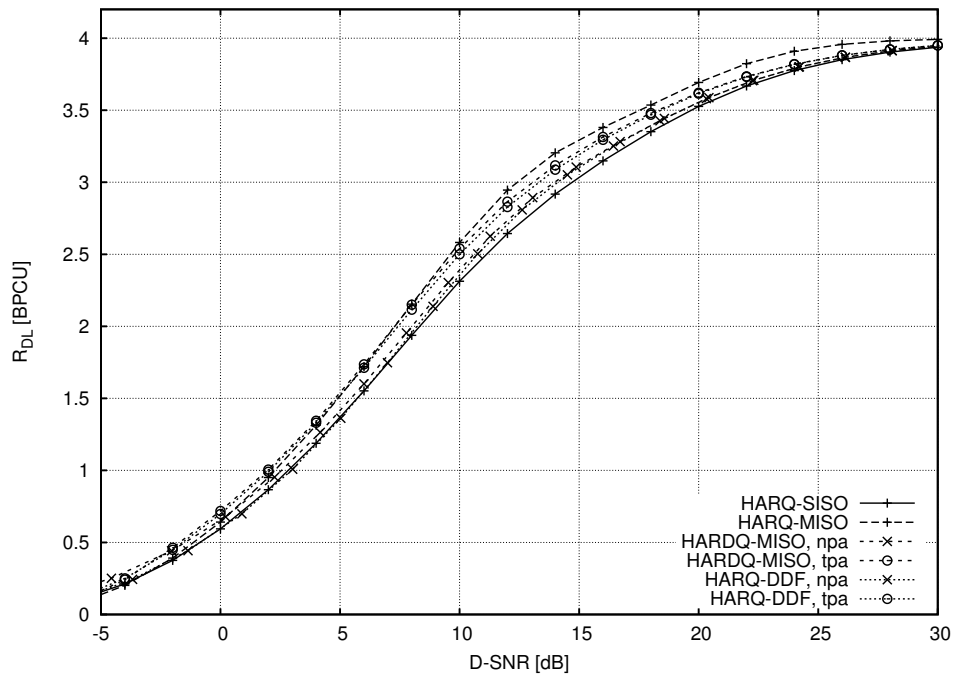


(b) Delay-limited throughput

**Figure 6.9:** Comparison of the outage probability and the delay-limited throughput of the NPA HARQ protocols and the TPA HARQ protocols considering Gaussian channel inputs.



(a) Outage probability



(b) Delay-limited throughput

**Figure 6.10:** Comparison of the outage probability and the delay-limited throughput of the NPA HARQ protocols and the TPA HARQ protocols considering 16-QAM channel inputs.

than the application of the TPA protocol variant for both the HARDQ-MISO and the HARQ-DDF protocol. However, for the HARQ-DDF protocol, the performance gain is smaller than for the HARDQ-MISO protocol. Furthermore, in comparison with the HARQ-MISO protocol, it can be observed that the TPA HARDQ-MISO protocol achieves an equivalent performance while the TPA HARQ-DDF protocol shows a constant performance loss.

In Figure 6.9b, it can be observed at low to medium D-SNR that the TPA HARDQ-MISO protocol and the TPA HARQ-DDF protocol achieve a higher delay-limited throughput than the corresponding NPA protocols. However, at high D-SNR, the NPA and the TPA protocols show equivalent performance. Furthermore, at low D-SNR, the TPA protocols outperform the HARQ-MISO protocol, while the HARQ-SISO protocol outperforms the application of NPA protocol variants. For both protocol variants, the HARDQ-MISO protocol shows a negligible performance gain over the HARQ-DDF protocol.

### 16-QAM Channel Inputs

Correspondingly, Figure 6.10 depicts the outage probability and the delay-limited throughput of the HARQ protocols considering uniformly distributed 16-QAM channel inputs. In general, it can be observed that all protocols show very similar performance as considering Gaussian channel inputs. However, considering the delay-limited throughput depicted in Figure 6.10b, it can be observed that the performance gains are smaller than considering Gaussian channel inputs.

## 6.4 Decoding Cost Reduction at the Relay for the HARQ-DDF Protocol

This section provides a discussion of the performance of the NPA HARQ-DDF protocol considering decoding cost reduction at the relay. Outage probability and delay-limited throughput are measured as a function of the D-SNR. The source, the destination and the relay apply the optimized codebook  $\mathcal{C}_{\text{opt}}$ . Furthermore, source and destination use the complete decoding instant set offered by the mother codebook, i.e.  $\mathcal{D} = \mathcal{D}_s = \mathcal{D}_d$ . But the relay uses perforated

decoding instant sets  $\mathcal{D}_r(z)$  given as

$$\mathcal{D}_r(1) = \mathcal{D}, \quad (6.3)$$

$$\mathcal{D}_r(2) = \{1, 2, 3, 5, 6, 7, 8\}, \quad (6.4)$$

$$\mathcal{D}_r(3) = \{1, 2, 5, 7, 8\}, \quad (6.5)$$

$$\mathcal{D}_r(4) = \{1, 5, 8\}, \quad (6.6)$$

$$\mathcal{D}_r(5) = \{1, 8\}, \quad (6.7)$$

where the decoding cost at the relay decreases with increasing  $z$ . In order to quantify the decoding cost reduction, assume the decoding cost in each ARQ round to be constant<sup>3</sup>. Then, in relation to the complete decoding instant set  $\mathcal{D}$ , the decoding cost factor<sup>4</sup> is defined as

$$c_r(z) = \frac{|\mathcal{D}_r(z)| - 1}{|\mathcal{D}_r(1)| - 1}. \quad (6.8)$$

where the subtrahend  $-1$  in the numerator and denominator results from the fact that the relay does not perform a decoding attempt in the last ARQ round<sup>5</sup>  $l = 8$ . Therefore, the decoding cost factors are given as

$$c_r(1) = 1, \quad c_r(2) = \frac{6}{7}, \quad c_r(3) = \frac{5}{7}, \quad c_r(4) = \frac{3}{7}, \quad \text{and} \quad c_r(5) = \frac{1}{7}.$$

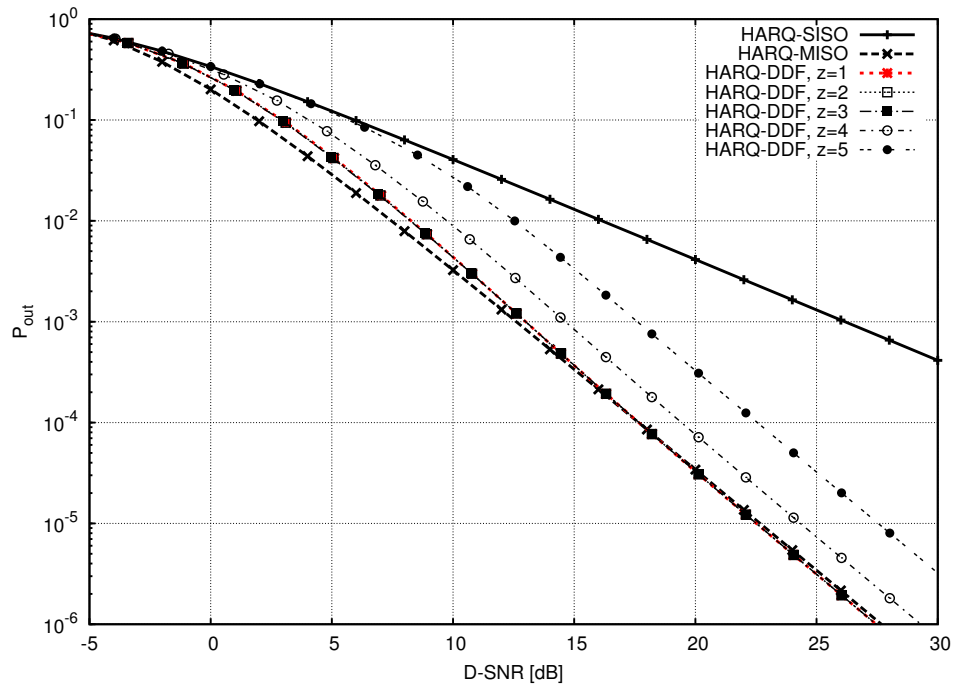
### Gaussian Channel Inputs

Figure 6.11 depicts the outage probability and delay-limited throughput of the HARQ-DDF protocol for the decoding instant sets  $\mathcal{D}_r(1)$  to  $\mathcal{D}_r(5)$  considering Gaussian channel inputs. In Figure 6.11a, it can be observed that the application of the decoding instant sets  $\mathcal{D}_r(z)$  with  $z = 1, 2, 3$  does not result in performance loss. But, in comparison with  $z = 1$ , for the decoding instant sets with  $z = 4, 5$

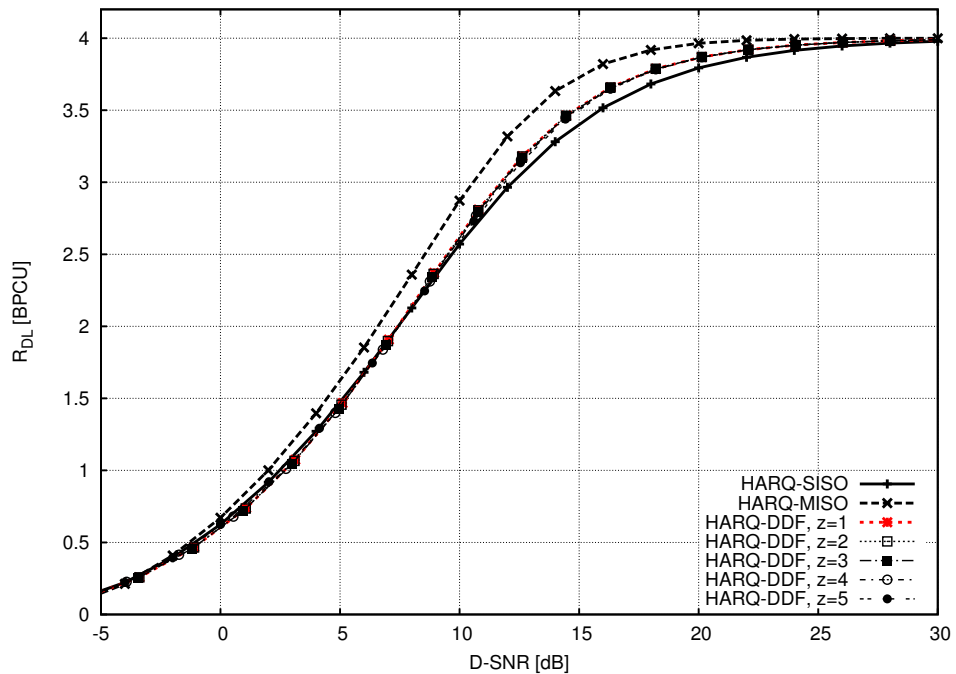
<sup>3</sup>The RCPC coding scheme applied in Section 7.1 has an approximately constant decoding cost since the computational cost for additions and depuncturing can be considered to be negligible in comparison with multiplications.

<sup>4</sup>The decoding cost factor given in (6.8) is the worst-case decoding cost at the relay. For a more sophisticated decoding cost analysis, the probability that the relay decodes in a particular ARQ round has to be taken into account.

<sup>5</sup>Note, in Section 4.4 the decoding instant set at the relay is defined to satisfy  $\max\{\mathcal{D}_r\} = \max\{\mathcal{D}_s\}$  in order to simplify mathematical tractability. However, the relay does not participate in the transmission if it cannot decode successfully before the last ARQ round.

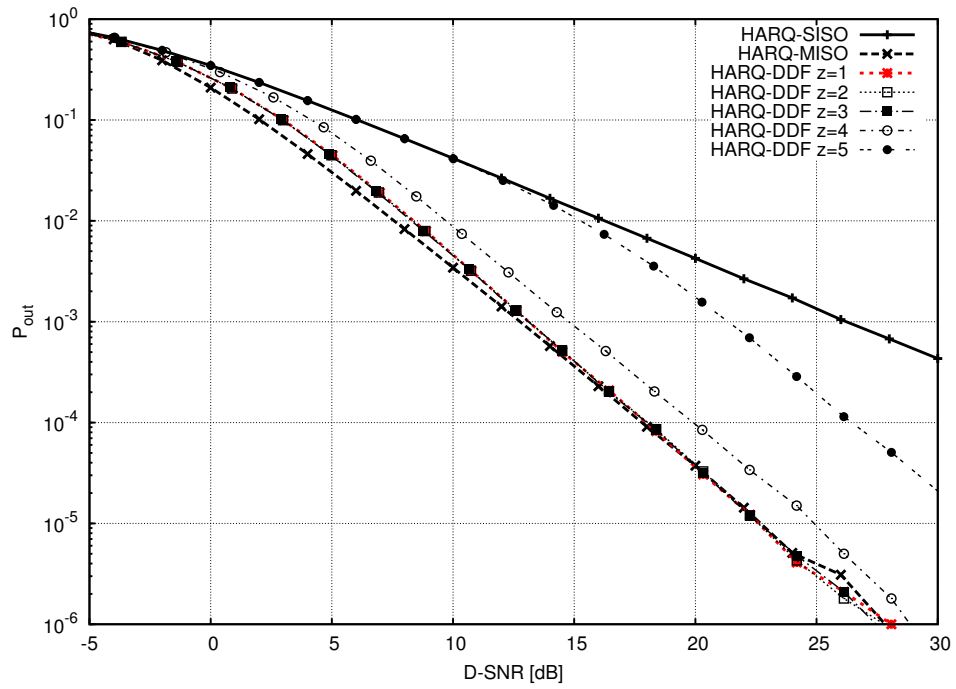


(a) Outage probability

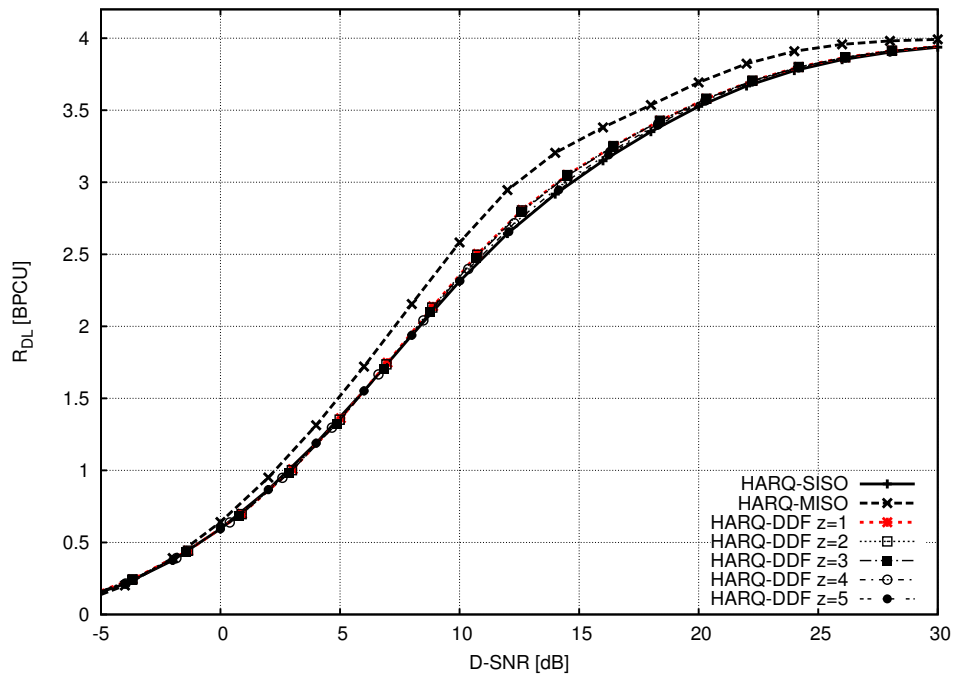


(b) Delay-limited throughput

**Figure 6.11:** Comparison of the outage probability and delay-limited throughput of the HARQ-DDF protocol with reduced decoding cost at the relay considering Gaussian channel inputs.



(a) Outage probability



(b) Delay-limited throughput

**Figure 6.12:** Comparison of the outage probability and delay-limited throughput of the HARQ-DDF protocol with reduced decoding cost at the relay considering 16-QAM channel inputs.

a constant performance loss can be observed. However, for all decoding instant sets, the HARQ-DDF protocol shows the achievement of the diversity of the HARQ-MISO protocol at high D-SNR.

In Figure 6.11b, it can be observed that the reduction of the decoding cost at the relay does not result in performance loss from a delay-limited throughput point of view. Only at low D-SNR levels, a negligible performance loss for  $z = 5$  can be observed.

Consequently, considering Gaussian channel inputs, the decoding cost can be reduced by a factor of  $c(3) = \frac{5}{7}$  without a loss of outage probability and delay-limited throughput in the depicted D-SNR range. Furthermore, if the figure of merit is the delay-limited throughput, the decoding cost can be reduced to a factor of  $c(5) = \frac{1}{7}$  while the outage probability still achieves maximum diversity at high D-SNR.

### Discrete Channel Inputs

Figure 6.12 depicts the outage probability and delay-limited throughput of the HARQ-DDF protocol for the decoding instant sets  $\mathcal{D}_r(1)$  to  $\mathcal{D}_r(5)$  considering uniformly distributed 16-QAM channel inputs. In general, it can be observed that the outage probability and delay-limited throughput perform very similarly as considering Gaussian channel inputs. However, in comparison with Figure 6.11a it can be observed in Figure 6.12a that the performance loss for  $z = 5$  is higher.

In Figure 6.12b, it can be observed that the decoding instant set  $\mathcal{D}_r(4)$  suffers from a negligible delay-limited throughput loss in comparison with  $\mathcal{D}_r(1)$ . Furthermore, applying the decoding instant set  $\mathcal{D}_r(5)$  results in a delay-limited throughput equivalent to that of the HARQ-SISO protocol. However, the performance loss of the HARQ-DDF protocol applying the decoding instant sets  $\mathcal{D}_r(4)$  and  $\mathcal{D}_r(5)$  is not of significant importance since the delay-limited throughput gain of the HARQ-DDF protocol applying the decoding instant sets with  $z = 1, 2, 3$  over the HARQ-SISO protocol is negligible.

## 6.5 Decoding Cost Reduction at the Relay and the Destination

This section provides a discussion of the performance of the NPA HARDQ-MISO protocol and the NPA HARQ-DDF protocol considering decoding cost reduction at the relay *and* at the destination. Outage probability and delay-limited throughput are measured as a function of the D-SNR. The source, the destination and the relay apply the optimized codebook  $\mathcal{C}_{\text{opt}}$ . Furthermore, the source uses the complete decoding instant set offered by the mother codebook, i.e.,  $\mathcal{D} = \mathcal{D}_s$ . But the destination and the relay use the perforated decoding instant sets given in (6.3) to (6.7) with<sup>6</sup>  $\mathcal{D}_d(z) = \mathcal{D}_r(z)$ . Note, in comparison to (6.8) the decoding cost factor<sup>7</sup> for the destination is defined as

$$c_d(z) = \frac{|\mathcal{D}_d(z)|}{|\mathcal{D}_d(1)|}, \quad (6.9)$$

since the destination attempts to decode the received information in the last ARQ round. Therefore, the decoding cost factors are given as

$$c_d(1) = 1, \quad c_d(2) = \frac{7}{8}, \quad c_d(3) = \frac{6}{8}, \quad c_d(4) = \frac{4}{8}, \quad \text{and} \quad c_d(5) = \frac{2}{8}.$$

Throughout this section, for the HARDQ-MISO protocol, the ARQ round after which second antenna of the source participates the transmission is given as  $t = \min\{\mathcal{D}\} = 1$ .

For comparison, the worst-case performance measure of the HARQ-SISO protocol achieved with  $z = 5$  and the best-case performance measure of the HARQ-MISO protocol achieved with  $z = 1$  is given.

---

<sup>6</sup>Note, since the relay and the destination apply the same decoding instant set for a given  $z$ , this configuration can also be seen as a reduction of the number of allowed ARQ rounds together with a reassignment of the achievable code rates. However, throughout this section, this modification will be discussed from a decoding cost point of view.

<sup>7</sup>The decoding cost factor given in (6.9) is the worst-case decoding cost at the destination. For a more sophisticated decoding cost analysis, the probability that the destination decodes in a particular ARQ round has to be taken into account.

### Gaussian Channel Inputs

Figure 6.13 depicts the outage probability of the HARDQ-MISO and the HARQ-DDF protocol applying the perforated decoding instant sets  $\mathcal{D}_r(z)$  and  $\mathcal{D}_d(z)$  with  $z = 1, 2, \dots, 5$  considering Gaussian channel inputs.

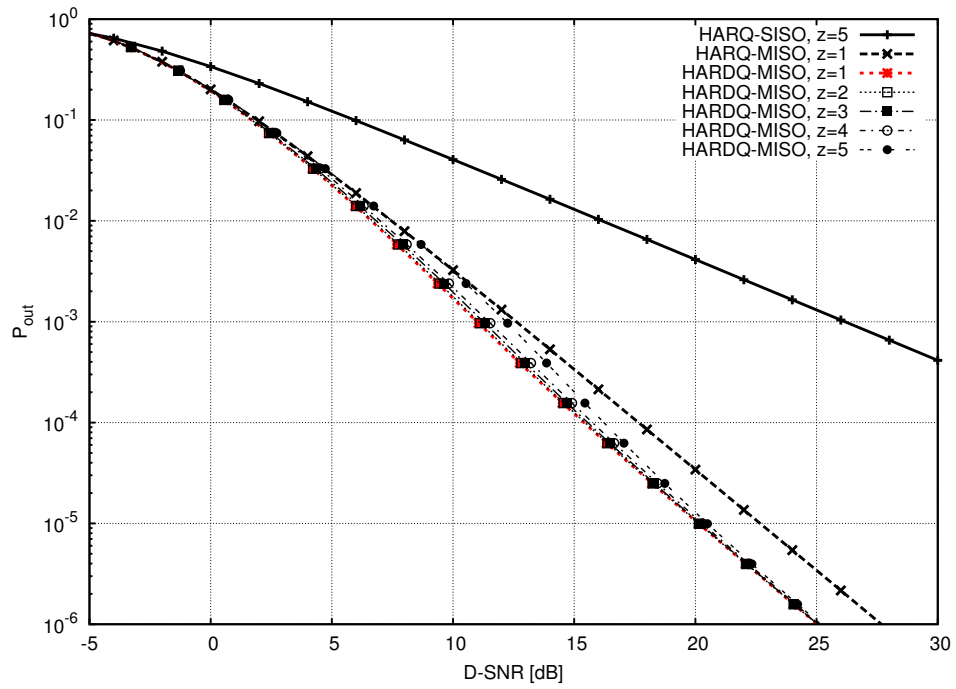
For the HARDQ-MISO protocol, it can be observed in Figure 6.13a that the decoding cost reduction does not result in a performance loss from an outage probability point of view at low and high D-SNR levels. At medium D-SNR levels, a negligible performance loss can be observed for  $z = 1, 2, 3, 4$ . The application of the decoding instant set  $\mathcal{D}_d(z) = 5$  results in a small but significant performance loss. Furthermore, it can be seen that the HARDQ-MISO protocol outperforms the HARQ-MISO protocol with  $z = 5$  for all  $z = 1, 2, \dots, 5$  at high D-SNR. At low D-SNR the HARDQ-MISO protocol achieves the same performance as the HARQ-MISO protocol for all  $z = 1, 2, \dots, 5$ .

For the HARQ-DDF protocol, in Figure 6.13b a significant performance loss can be observed for  $z = 4$  and  $z = 5$ . Furthermore, the HARQ-MISO protocol outperforms the HARQ-DDF protocol for  $z = 1, 2, \dots, 4$ . However, in Section 6.4 it is demonstrated that this performance loss results from the decoding cost reduction at the relay.

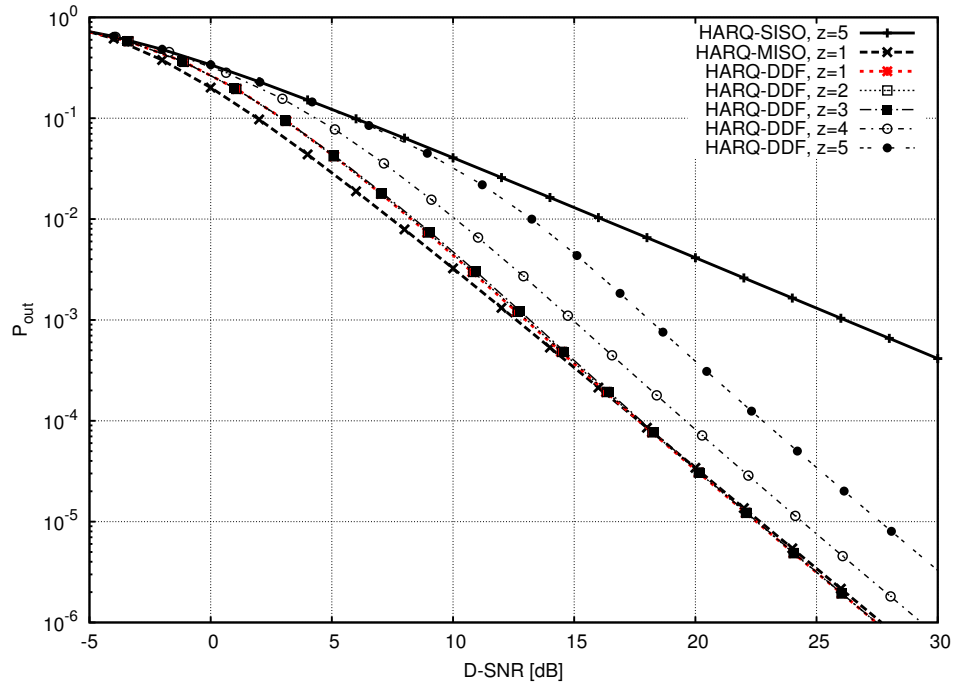
Figure 6.14 depicts the delay-limited throughput of the HARDQ-MISO and the HARQ-DDF protocol applying the perforated decoding instant sets  $\mathcal{D}_r(z)$  and  $\mathcal{D}_d(z)$  with  $z = 1, 2, \dots, 5$  considering Gaussian channel inputs.

For the HARDQ-MISO protocol, it can be observed in Figure 6.14a that the reduction of the decoding cost at the destination results in significant performance loss. Only for  $z = 2$  the performance loss is small. Furthermore, the the HARDQ-MISO protocol outperforms the HARQ-SISO protocol with  $z = 1$  for  $z=1, 2, \dots, 4$ . But for  $z = 5$  the HARQ-SISO protocol outperforms the HARDQ-MISO protocol. Similar performance can be observed in Figure 6.14b for the HARQ-DDF protocol.

Therefore, from a delay-limited throughput point of view, the application of the decoding time sets  $\mathcal{D}_d(1)$  and  $\mathcal{D}_d(2)$  is desirable, since the delay-limited throughput suffers from a significant loss for  $z = 3, 4, 5$ . In case that reliability is more important than throughput, the decoding instant sets with  $z = 1, 2, 3, 4$  are sufficient.

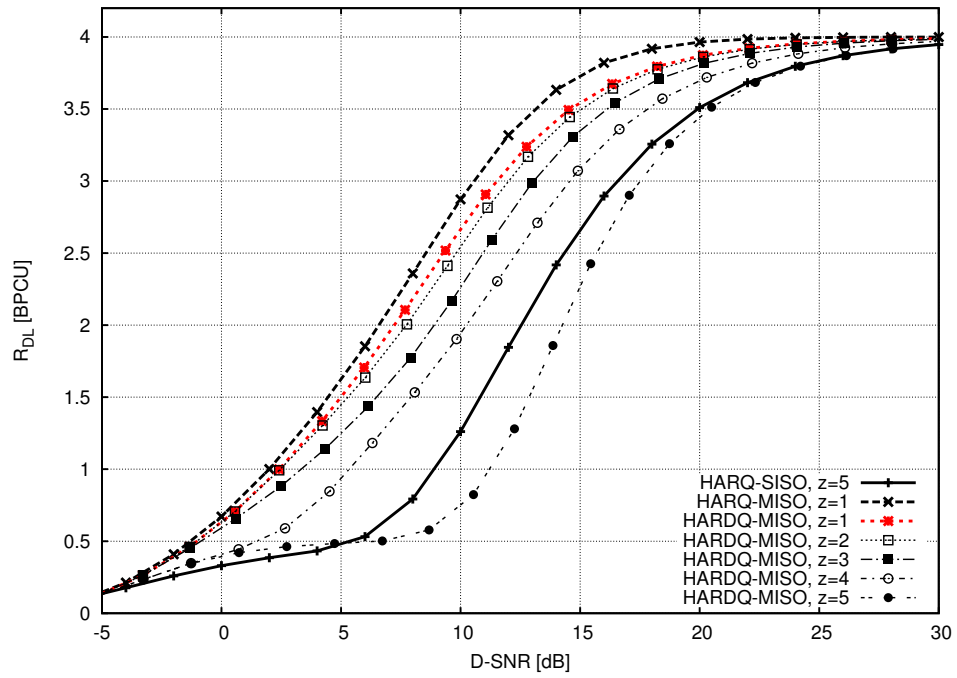


(a) HARQ-MISO protocol

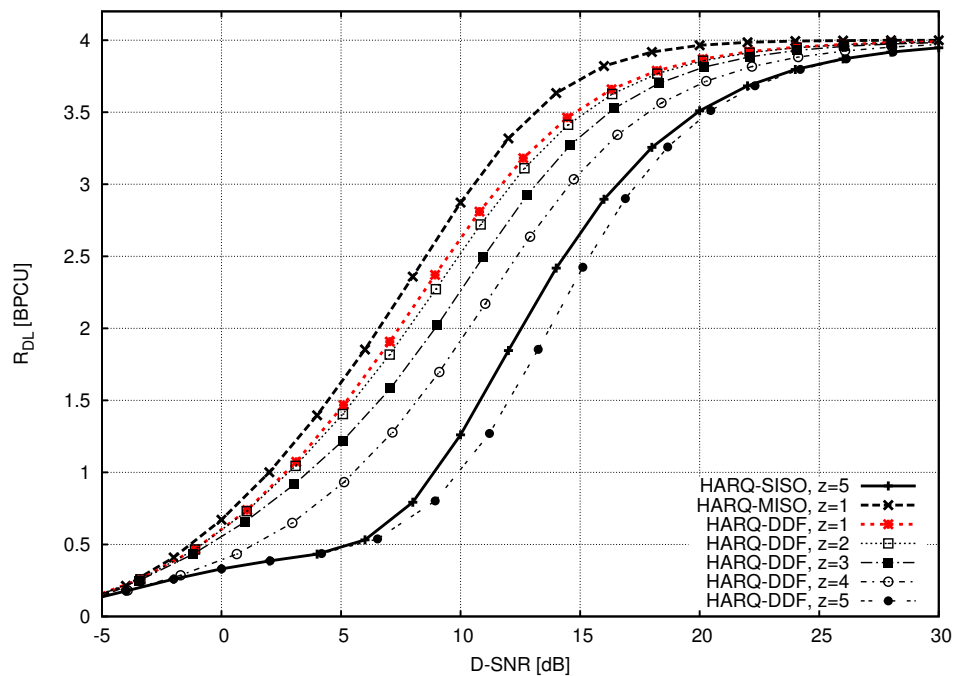


(b) HARQ-DDF protocol

**Figure 6.13:** Outage probability of the HARQ-MISO and HARQ-DDF protocol with reduced decoding cost at the relay and the destination considering Gaussian channel inputs.

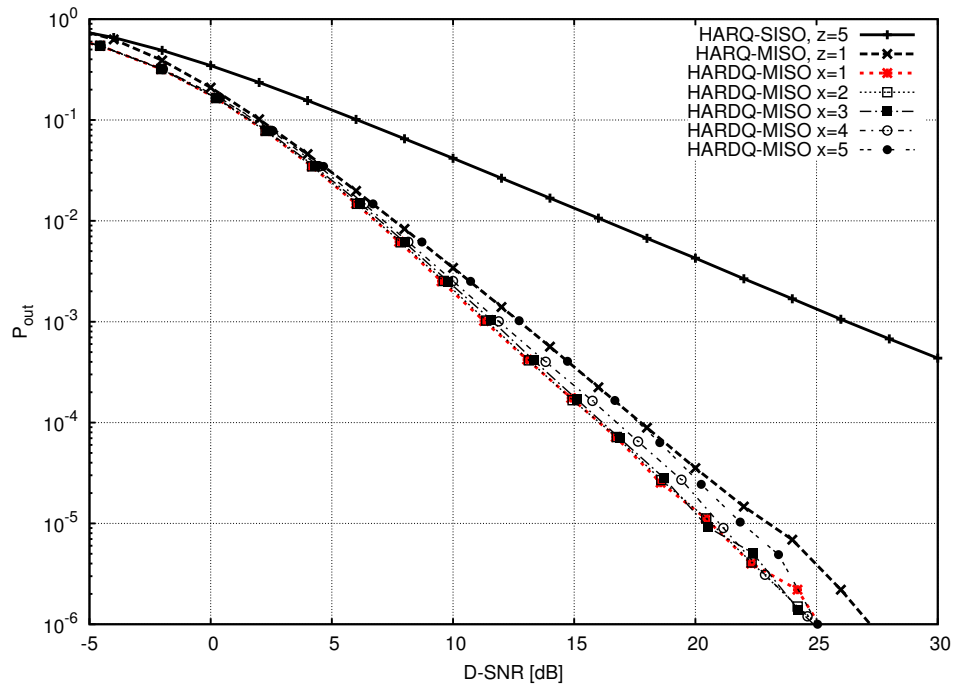


(a) HARDQ-MISO protocol

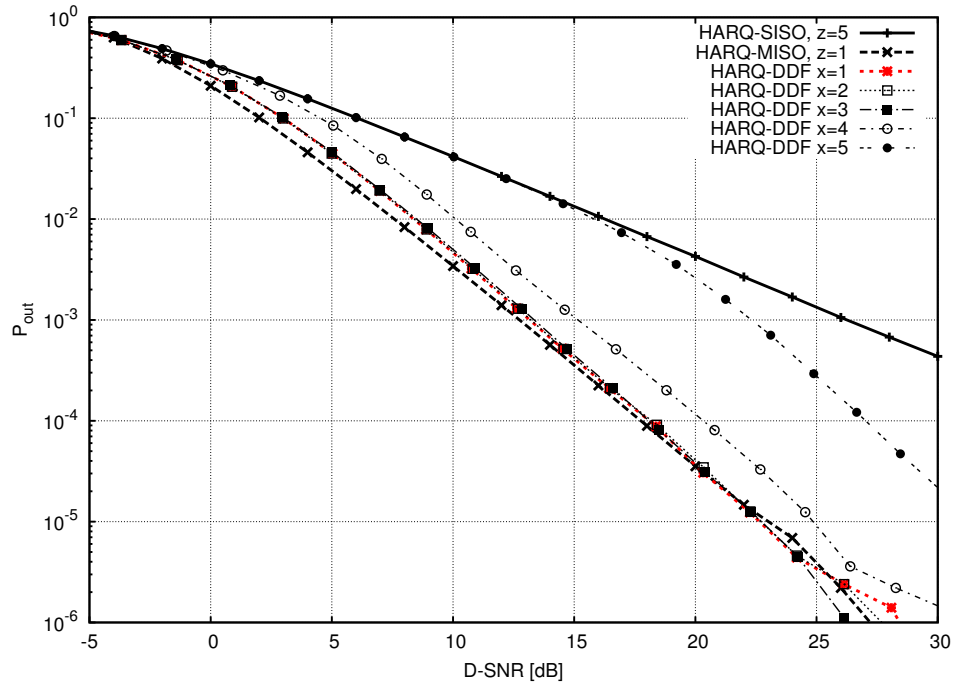


(b) HARQ-DDF protocol

**Figure 6.14:** Delay-limited throughput of the HARDQ-MISO and HARQ-DDF protocol with reduced decoding cost at the relay and the destination considering Gaussian channel inputs.

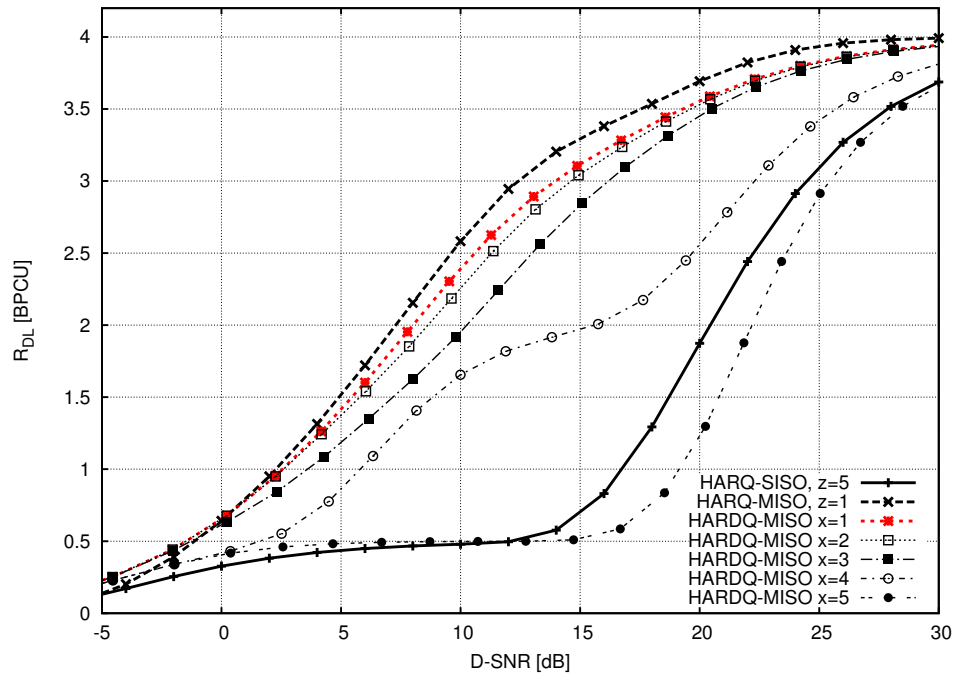


(a) HARQ-MISO protocol

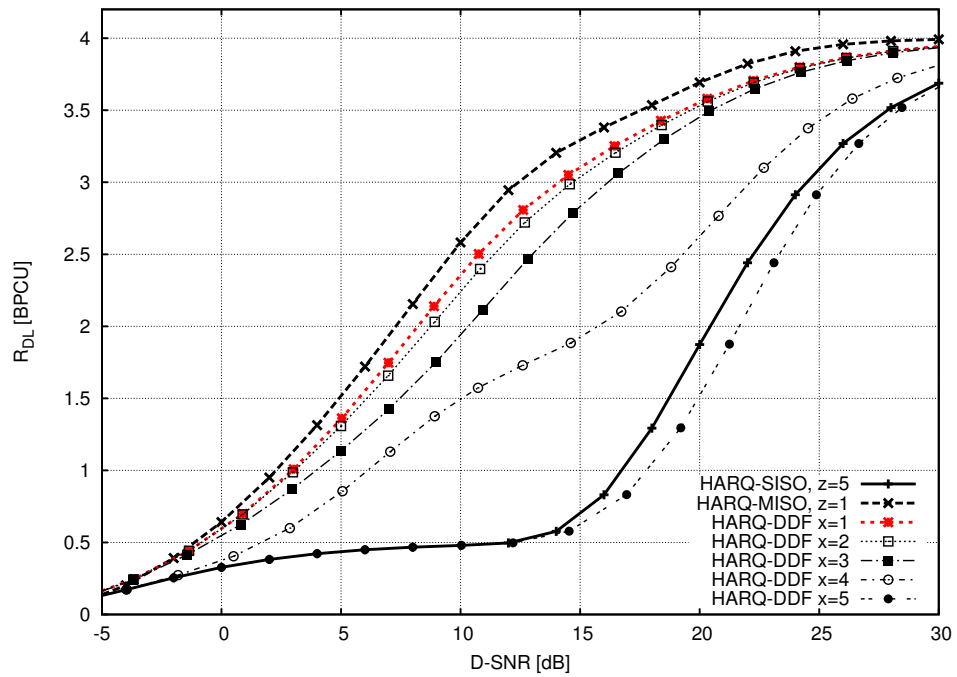


(b) HARQ-DDF protocol

**Figure 6.15:** Outage probability of the HARQ-MISO and HARQ-DDF protocol with reduced decoding cost at the relay and the destination considering 16-QAM channel inputs.



(a) HARQ-MISO protocol



(b) HARQ-DDF protocol

**Figure 6.16:** Delay-limited throughput of the HARQ-MISO and HARQ-DDF protocol with reduced decoding cost at the relay and the destination considering 16-QAM channel inputs.

### Discrete Channel Inputs

Figure 6.15 depicts the outage probability of the HARQ-MISO and the HARQ-DDF protocol applying the perforated decoding instant sets  $\mathcal{D}_r(z)$  and  $\mathcal{D}_d(z)$  with  $z = 1, 2, \dots, 5$  considering uniformly distributed 16-QAM channel inputs.

In general, it can be observed, that the outage probability of the HARQ-MISO and the HARQ-DDF protocol performs very similar to the outage probability considering Gaussian channel inputs as depicted in Figure 6.13. However, for  $z = 4$  and  $z = 5$  it can be observed at high D-SNR that the outage probability does not result in the outage probability achieved for  $z = 1$ . Instead, in comparison with  $z = 1$ , a constant performance loss can be observed for medium to high D-SNR. Correspondingly, Figure 6.16 depicts the delay-limited throughput of the HARQ-MISO and the HARQ-DDF protocol. In general, it can be observed, that the delay-limited throughput performs very similar to the delay-limited throughput considering Gaussian channel inputs as depicted in Figure 6.14. However, the performance loss for increasing  $z$  is larger. An interesting difference is the kink at  $R_{DL} = 2$  BPCU for  $z = 4$ . Note, effectively the perforated decoding instant set  $\mathcal{D}_d(4)$  results in a codebook with achievable code rates similar to the non-optimized codebook  $\mathcal{C}_{\text{non-opt}}$ . Therefore, as for the the delay-limited throughput function of the non-optimized codebook shown in Figure 6.8, this kink results from the fact that the distance between the code rates corresponding to the consecutive decoding attempts at the destination in ARQ round  $l = 1$  and  $l = 5$  is large.

## 6.6 Summary

This chapter provides a performance analysis and comparison of the HARQ protocols introduced in Chapter 4 in terms of fixed-rate outage probability and delay-limited throughput, considering Gaussian distributed channel inputs and uniformly distributed 16-QAM channel inputs. To this end, the non-optimized codebook  $\mathcal{C}_{\text{non-opt}}$  and the optimized codebook  $\mathcal{C}_{\text{opt}}$  associated with the code rate functions (6.1) and (6.2), respectively, are selected. The codebook  $\mathcal{C}_{\text{non-opt}}$  is an example for an incremental redundancy codebook with equal symbol length ARQ rounds. In comparison, the codebook  $\mathcal{C}_{\text{opt}}$  has unequal symbol length ARQ rounds.

In Section 6.1, the performance is measured as a function of the SD-SNR and the D-SNR using the NPA protocol variant. Furthermore, the performance measures are given for increasing  $t$  for the HARDQ-MISO protocol and for increasing  $\min\{\mathcal{D}_r\}$  for the HARQ-DDF protocol. Measuring the performance as a function of the SD-SNR indicates that  $t$  and  $\min\{\mathcal{D}_r\}$  should always be selected such that the second antenna or the relay are allowed to participate in the transmission after the first ARQ round. However, measuring the performance as a function of the D-SNR reveals for low to medium D-SNR levels that it can be more energy efficient to select later ARQ rounds. As example, for the non-optimized codebook  $\mathcal{C}_{\text{non-opt}}$  it is beneficial at low to medium D-SNR levels to select  $t = \min\{\mathcal{D}_r\} = 2$ . Furthermore, measuring the performance as a function of the D-SNR enables the comparison with the HARQ-SISO and HARQ-MISO protocol. It is shown that the HARDQ-MISO and the HARQ-DDF protocol outperform the HARQ-MISO protocol at high D-SNR.

Section 6.2 compares the outage probability and the delay-limited throughput of the HARQ protocols considering the non-optimized codebook  $\mathcal{C}_{\text{non-opt}}$  and optimized codebook  $\mathcal{C}_{\text{opt}}$ . It is demonstrated that the selected codebooks show almost equivalent outage probability performance for the HARQ-SISO, HARQ-MISO and HARDQ-MISO protocol. At high D-SNR, the non-optimized codebook provides a lower outage probability for the HARQ-DDF protocol. However, the optimized codebook shows significant delay-limited throughput performance gains for all HARQ protocols.

The performance of the HARDQ-MISO protocol and the HARQ-DDF protocol considering the NPA and the TPA protocol variants is discussed in Section 6.3. It is shown that the application of the NPA protocol provides significant performance gains in terms of outage probability. But in terms of delay-limited throughput the TPA protocol variant is beneficial.

Section 6.4 considers the reduction of the decoding cost at the relay. To this end, the outage probability and delay-limited throughput is measured using perforated decoding instant sets  $\mathcal{D}_r(z)$ , where the degree of perforation increases with  $z$ . Considering the application of the given perforated decoding instant sets, no performance loss can be observed for low degrees of perforation in terms of outage probability. However, at high degrees of perforation, the performance loss is significant. In terms of delay-limited throughput, no performance can be

observed for low and high degrees of perforation.

Similarly, Section 6.5 considers the reduction of the decoding cost at the relay together with the reduction of the decoding cost at the destination, using the same perforated decoding instant sets. Only negligible outage probability performance loss can be observed at high degrees of perforation at medium D-SNR. However, in terms of delay-limited throughput, significant performance loss can be observed with an increasing degree of perforation.

In general it can be observed, that the assumption of Gaussian channel inputs and 16-QAM channel inputs results in very similar performance measures. But for 16-QAM channel inputs the observable levels of performance gains are smaller and the levels of performance loss are higher.

## Numerical Results: RCPC Coding

---

### 7.1 RCPC Coding for HARQ Protocols

A convolutional encoder [38, 82, 106]  $\mathcal{C}(n, k, v)$  encodes a sequence of binary input blocks  $\mathbf{s}_t$  of length  $k$  bits into a sequence of binary output blocks  $\mathbf{m}_t$  of length  $n$  bits where the output block  $\mathbf{m}_t$  depends on  $\mathbf{s}_t$  and the  $v$  previous input blocks. Such an encoder is called to have a memory of order  $v$ . The resulting code rate is given as

$$R = \frac{k}{n}. \quad (7.1)$$

While the encoded output sequence is infinite, in practice finite sequences are preferred. To obtain a finite encoded sequence, a so-called termination method has to be used. The three most common termination methods are truncation, tail-biting and termination [106, 82]. For simplicity, in this work code termination is used. To this end, after encoding of  $T$  input blocks,  $v \times k$  so-called termination bits are fed to the encoder such that the encoder returns to a known final state. Consequently, the length of the binary information sequence per code word is given as  $b = kT$ . This method results in low error probabilities at the end of the sequence and is computationally simple. The disadvantage is that

truncation decreases code rate to [82]

$$R = \frac{k}{n} \frac{M}{M+v}, \quad (7.2)$$

where the factor  $\frac{M}{M+v}$  denotes the fractional code rate loss [106, 82]. For large  $M$  the fractional loss is negligible.

Puncturing a convolutional code is a technique to construct high-rate codes from a  $\mathcal{C}(n, 1, v)$  mother code using a puncturing pattern  $A_l$  of period  $P$  [15, 107]. Puncturing a convolutional code enables to use ML decoders with significantly reduced complexity compared to a convolutional  $\mathcal{C}(n, k, v)$  code which achieves the same resulting code rate [108].

The puncturing patterns is applied at the output of the convolutional encoder and periodically deletes  $L-l$  bits of the encoded output block  $\mathbf{m}_l$ . Consequently, codes of rate [15]

$$R(l) = \frac{P}{P+l}, \quad l = 1, \dots, L \quad (7.3)$$

are obtained, where  $L = P(n-1)$  and  $R(L) = 1/N$  is the rate of the convolutional mother code.

Rate-compatible punctured convolutional (RCPC) codes are investigated in [15] in context of automatic repeat-request (ARQ) techniques and unequal error protection schemes. A RCPC code is a family of punctured convolutional codes  $\mathcal{A} = \{A_1, A_2, \dots, A_L\}$  where the higher-rate codes are embedded in the lower-rate codes [15].

It is noteworthy, that puncturing reduces the free distance of the code and is therefore not necessarily optimal [106, 108]. Thus, the task of finding good RCPC codes is concerned with the problem of finding a family of puncturing patterns with good code properties associated with each puncturing pattern. A comprehensive list of RCPC mother codes and their associated puncturing patterns is given in [109].

A communication system with an ARQ feedback channel from destination to source can exploit these properties to adjust code rate and error correction capabilities to the channel and the application requirements as follows [15]:

1. Both source and destination employ the same set of puncturing patterns.
2. The source encodes the information sequence using the highest rate punc-

turing pattern and stores the punctured bits. Then, the source transmits the corresponding code word to the destination.

3. At the destination, the decoder attempts to decode the code word. If decoding was successful it sends an acknowledge (ACK) signal to the source and the communication procedure is continued from 2. If decoding failed, the destination sends a negative-acknowledge (NACK) signal to the source.
4. Let  $A_l$  denote the puncturing pattern used during ARQ round  $l$ . Once the source received a NACK signal it is necessary to differ between two cases:
  - $A_l$  corresponds to the mother code: Communication failed in the last ARQ round. In this case, a higher layer of the communication protocol has to take the appropriate action. In general, this action depends on the application requirements. For example, if the information is critical, the source will attempt to transmit the code word again. Otherwise, the source can decide to transmit the next information sequence.
  - $A_l$  does not correspond to the mother code: In this case, the source transmits the bits punctured by  $A_l$  from  $A_{l+1}$  during the next ARQ round  $l + 1$ . Consequently, the code rate is reduced from  $R(l)$  to  $R(l + 1)$ . The communication protocol continues from 3.

Thus, the resulting code word  $\mathbf{x}$  of the convolutional mother code is transmitted in  $L$  blocks  $\{\mathbf{x}_1, \mathbf{x}_2, \dots, \mathbf{x}_L\}$  with accumulated block lengths  $N(l) = \frac{b}{R(l)}$ . Consequently, RCPC coding can be applied together with the HARQ protocols discussed in Chapter 4.

At the receiver it is common practice to perform soft-decision decoding using the Viterbi algorithm [110] or the Fano algorithm [111]. The Viterbi algorithm is the maximum likelihood decoder in terms of minimizing the code word error probability. The Fano algorithm is a suboptimal decoder which achieves comparable code word error rates. A further commonly used decoding algorithm is the BCJR algorithm [112] which minimizes the symbol error rate. Throughout this chapter the Viterbi algorithm is applied in order to minimize the FER. For a given RCPC code the destination uses the same

decoder for all ARQ rounds [107]. Furthermore, as decoding is in general computationally expensive the communication system can decide to employ only a subset of  $\mathcal{A}$  to reduce the computational effort.

In this work, *cyclic redundancy check* (CRC) codes are used at the receiver to validate whether a received code word was decoded successfully. The application of CRC codes for error detection was first introduced in [113]. Consequently, the resulting channel code consists of an outer CRC code  $\mathcal{B}(n_1, k_1)$  and an inner convolutional code  $\mathcal{C}(n_2, k_2, v)$ .

For the selection of an appropriate CRC code, the probability of an undetectable error  $P_u$  is the performance measure of interest. Optimized CRC codes with 16, 24 and 32 bit parity are given in [114, 115]. These codes can be adjusted to the desired code word length using shortening techniques [82, 106]. One disadvantage is that the application of CRC codes comes together with a further reduction of the resulting code rate. Considering RCPC coding with termination and 16-bit CRC coding, the code rate in ARQ round  $l$  is given as

$$R(l) = \frac{P}{P+l} - \frac{16+v}{N(l)}, \quad l = 1, \dots, L, \quad (7.4)$$

where the subtrahent  $\frac{16+v}{N(l)}$  denotes the code rate loss in ARQ round  $l$ .

A further drawback is that the application of CRC codes results in a suboptimal DMDT. These drawbacks can be overcome using Forney's decision rule for decoding at the source as investigated in [25]. However, the application of Forney's decision rule is computationally significantly more expensive than decoding verification by CRC.

Since RCPC coding is not systematic, it is not possible to achieve the code rate of the modulator in the first ARQ round. This drawback can be overcome by the application of turbo codes [116, 32] or the application of the lattice codes given in [25, 26]. In this dissertation, the design decision in favour of RCPC codes is motivated by the facts that the encoding and the decoding engines are simple to implement and that RCPC codes show good FER performance.

In [15] interleaving is used to exploit time-diversity. However, in this work, it is assumed that the Rayleigh fading channel is quasi-static over the complete code word length, i.e., the channel is assumed to be long-term quasi-static. Therefore, this channel model does not provide time-diversity [66, 117]. Consequently, the

application of interleaving structures does not affect the system performance.

For simplicity, throughout this work it is assumed that all terminals are perfectly synchronized and that the ACK feedback channels are error and delay free. Synchronization and channel estimation for the cooperative decode-and-forward channel is studied [42]. Furthermore, considering the HARQ-DDF it is assumed that the destination has perfect knowledge about the listen-transmit decision-time. Therefore, for a real-world system application the communication protocol has to provide synchronization headers within the code word to synchronize the terminals and to provide the listen-transmit decision-time. Furthermore, ACK/NACK time slots are required to communicate the ACK/NACK signal [75, 23]. In order to obtain the channel coefficients, it is common practice to probe the channels using training sequences [41, 42, 43]. Further coding techniques for the DDF protocol are investigated in [25, 26, 27, 28].

## 7.2 Simulation Set-up

This chapter gives the fixed-rate outage probability and the delay-limited throughput of the HARQ protocols introduced in Chapter 4 applying RCPC codes. To this end, the performance is measured using the Monte Carlo simulation method discussed in Section 5.7, assuming uniformly distributed BPSK channel inputs and maximum-likelihood decoding. These results are compared against the performance of the RCPC encoded HARQ communication systems. To this end, a Monte Carlo simulation has been implemented in the C++ programming language. For both simulations, the Rayleigh fading channel coefficients are chosen to have unit variance and zero mean. In order to model the Rayleigh fading AWGN channels, the pseudo-random number generators of the *Boost* library [100] are used. Furthermore, the noise variance at the relay  $N_r$  is selected to be half of the noise variance at the destination<sup>1</sup>  $N_d$ , i.e.,  $N_r = \frac{N_d}{2}$ . This channel set-up ensures comparability with related work such as [25, 26, 18].

The inner RCPC code is selected as  $\mathcal{C}_{\text{RCPC}}(3, 1, 2)$  with puncturing period  $P = 8$  using the high-rate optimized puncturing patterns and the corresponding generator polynomial given in [109]. An appropriate outer 16-bit CRC code

<sup>1</sup>This system set-up is also used in [25, 26, 18] where the SNR of the source-to-relay channel is defined to be 3dB better than the SD-SNR. However, using the noise variance to select the SNR levels maintains comparability of the TPA and the NPA protocol variants.

is selected from [114]. A pseudo-random number generator of the *Boost* library is used to generate the uniformly distributed binary information sequences  $\mathbf{f}$  of length 110 bits. Consequently, together with 2 bits for code termination<sup>2</sup> and 16 bits CRC information, the input sequence  $\mathbf{f}_{\text{CRC}}$  to the convolutional encoder is of length 128 bits. The symbol mapper at the source maps the incoming information sequences  $\mathbf{m}'_l$  onto the BPSK symbol constellation. Therefore, the sequences  $\mathbf{m}'_l$  are of length 1 bit. The simulation is configured to measure the outage probability and the delay-limited throughput over  $10^7$  information sequences per SD-SNR and D-SNR level.

The selected mother code  $\mathcal{C}_{\text{RCPC}}(3, 1, 2)$  comes with 16 puncturing patterns. Consequently, the number of allowed ARQ rounds is  $L = 16$  and the decoding instant set offered by the mother code is  $\mathcal{D} = \{1, 2, \dots, 16\}$ . Furthermore, the associated code rate function is given according to (7.4) as

$$R(l) = \frac{8}{8+l} - \frac{18}{128+16 \times l} = \frac{110}{128+16 \times l}, \quad l \in \mathcal{D}. \quad (7.5)$$

Therefore, the maximum achievable code rate is  $R(1) = 0.76$  BPCU and the minimum code rate is  $R(16) = 0.29$  BPCU.

### 7.3 Outage Probability Analysis Considering SD-SNR and D-SNR

This section provides a discussion of the outage probability and the delay-limited throughput measured as a function of the SD-SNR and measured as a function of the D-SNR. Since the relay introduces additional energy into the channel as seen at the destination, the performance measured as function of the SD-SNR is not compared against the HARQ-SISO and HARQ-MISO protocol. However, the performance measured as function of the D-SNR provides a comparison with these protocols. Throughout this section the NPA protocol variants are applied.

To this end, the decoding instant sets at the source and at the destination are

---

<sup>2</sup>In fact, the convolutional encoder is implemented to generate the termination sequence, since the modules in front the encoder do not necessarily have knowledge about the memory  $v$  of the applied convolutional code.

selected as  $\mathcal{D} = \mathcal{D}_s = \mathcal{D}_d$ . For the HARQ-DDF protocol, the decoding instant set at the relay is selected as  $\mathcal{D}_r = \{x, x + 1, \dots, 16\}$  and for the HARDQ-MISO protocol the ARQ round after which the second antenna assists the transmission is given as  $t = x$ .

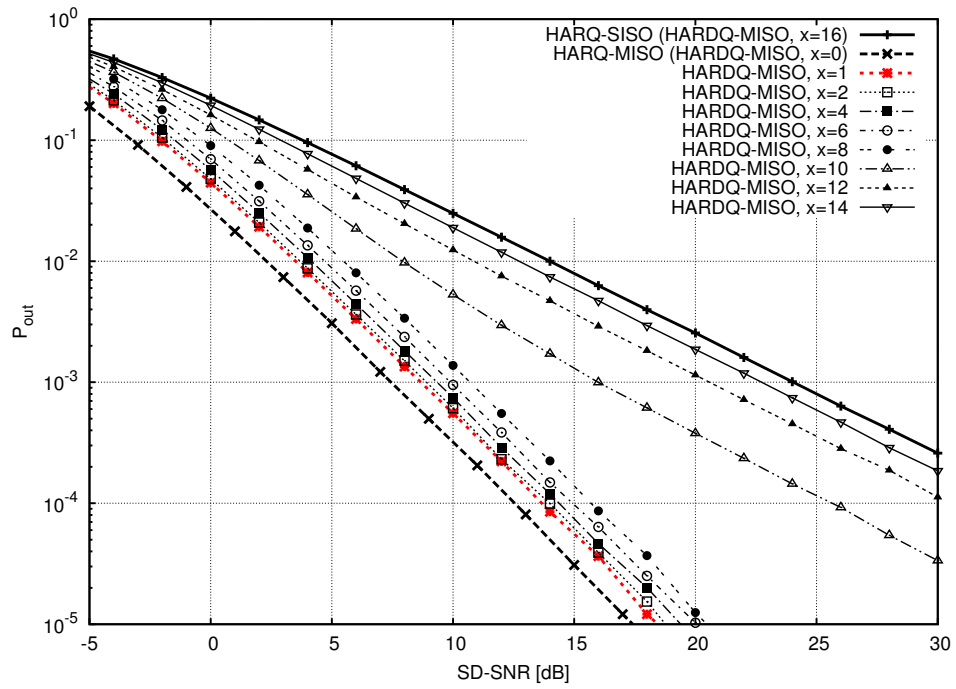
For comparison, the performance measures for the HARQ-SISO and the HARQ-MISO protocols are given. The HARQ-SISO and the HARQ-MISO protocols are given by the HARDQ-MISO protocol with  $t = 8$  and  $t = 0$ , respectively. For the HARQ-MISO protocol the SD-SNR is measured across a single source antenna to destination antenna channel.

Similar performance measures assuming a high-rate mother code are given in Section 6.1.

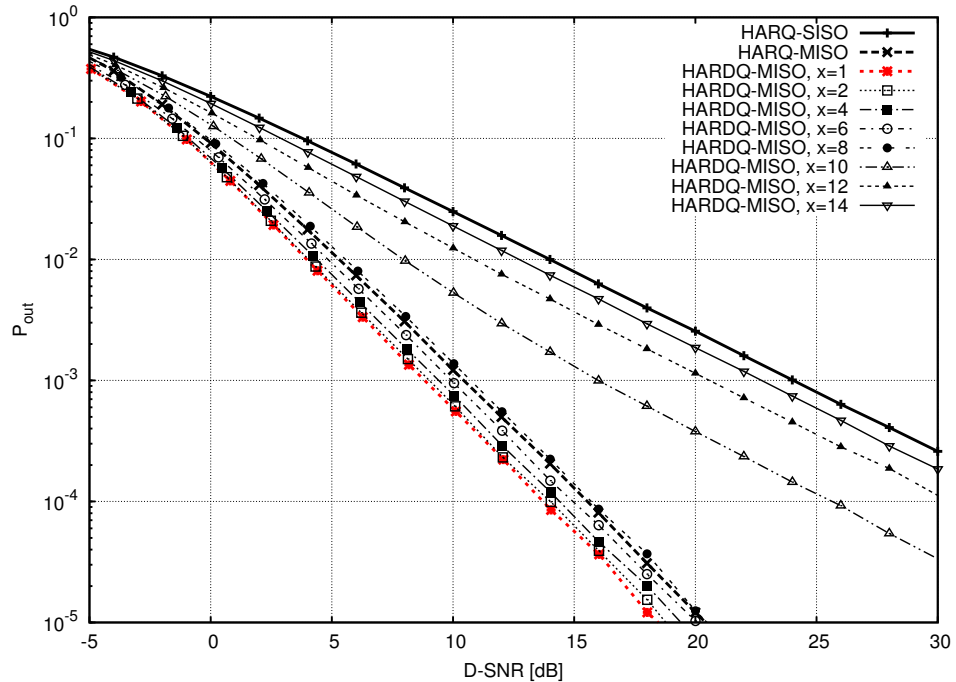
### **HARDQ-MISO Protocol**

Figure 7.1 depicts the outage probability of the HARDQ-MISO protocol measured as a function of the SD-SNR and as a function of the D-SNR, considering uniformly distributed BPSK channel inputs. Measuring the outage probability as a function of the SD-SNR shows a constant performance loss for the medium to high SD-SNR range caused by increasing  $x = 1$  to  $x = 8$ . However, for the configurations  $x = 1$  to  $x = 8$  it can be observed that the outage probability achieves the maximum diversity gain. For the configurations  $x = 10, 12, 14$ , a significant loss of diversity gain can be observed. Furthermore, the HARQ-MISO protocol outperforms the HARQ-MISO protocol.

Measuring the outage probability as a function of the D-SNR as depicted in Figure 7.1b shows similar performance. However, at low D-SNR it can be observed that the configurations  $x = 1, 2, 3, 4$  show equivalent outage probability. But at high D-SNR, the configurations  $x = 2, 3, 4$  show significant performance loss in comparison with  $x = 1$ . Furthermore, it can be observed that the configurations  $x = 1$  to  $x = 8$  achieve the same diversity as the HARQ-MISO protocol. In difference to Figure 7.1a it can be seen that the configurations  $x = 1$  to  $x = 6$  outperform the HARQ-MISO protocol from an energy efficiency point of view. For the configuration  $x = 8$ , a negligible performance loss in comparison with the HARQ-MISO protocol can be observed. The configurations  $x = 10, 12, 14$  achieve only the diversity of the HARQ-SISO protocol but show a significant performance gain over the HARQ-SISO protocol.

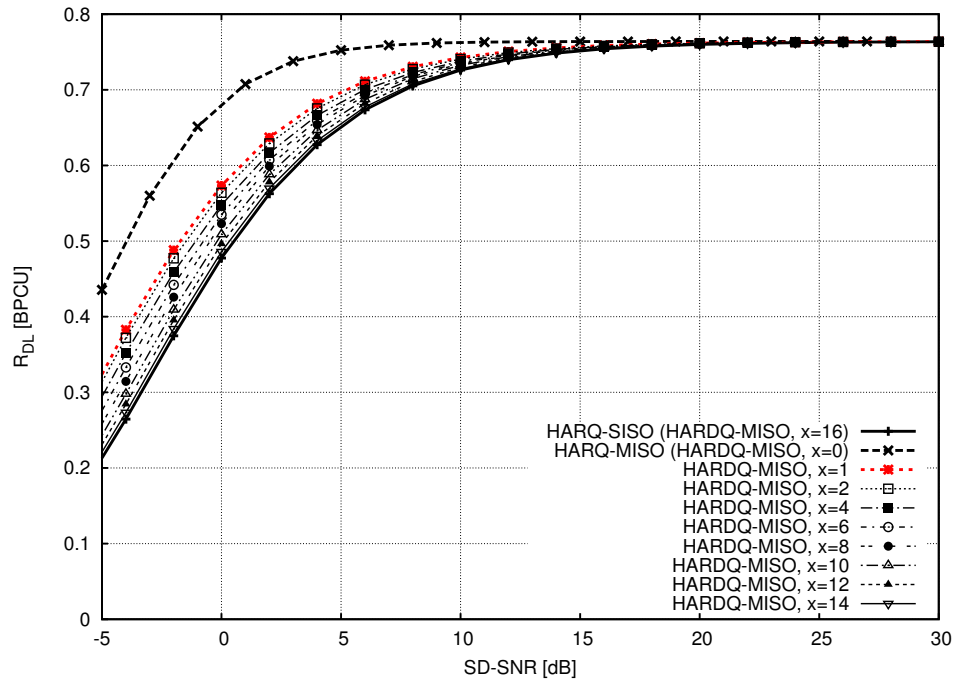


(a) Outage probability as a function of the SD-SNR

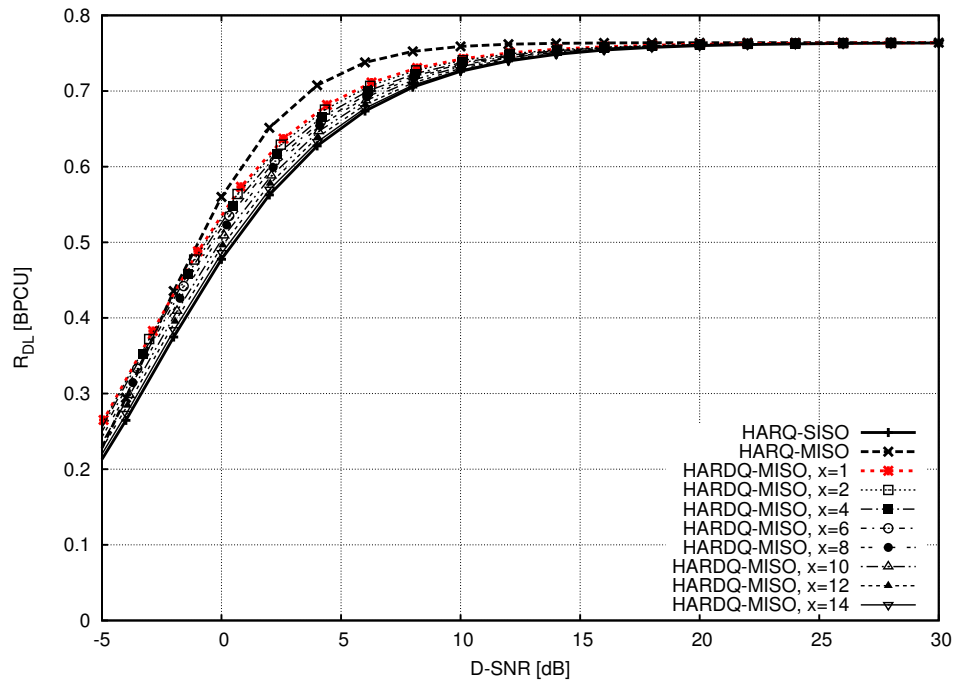


(b) Outage probability as a function of the D-SNR

**Figure 7.1:** Comparison of the outage probability measured as a function of the SD-SNR and D-SNR for the HARQ-MISO protocol and increasing  $t = x$ , considering uniformly distributed BPSK channel inputs.



(a) Delay-limited throughput as a function of the SD-SNR



(b) Delay-limited throughput as a function of the D-SNR

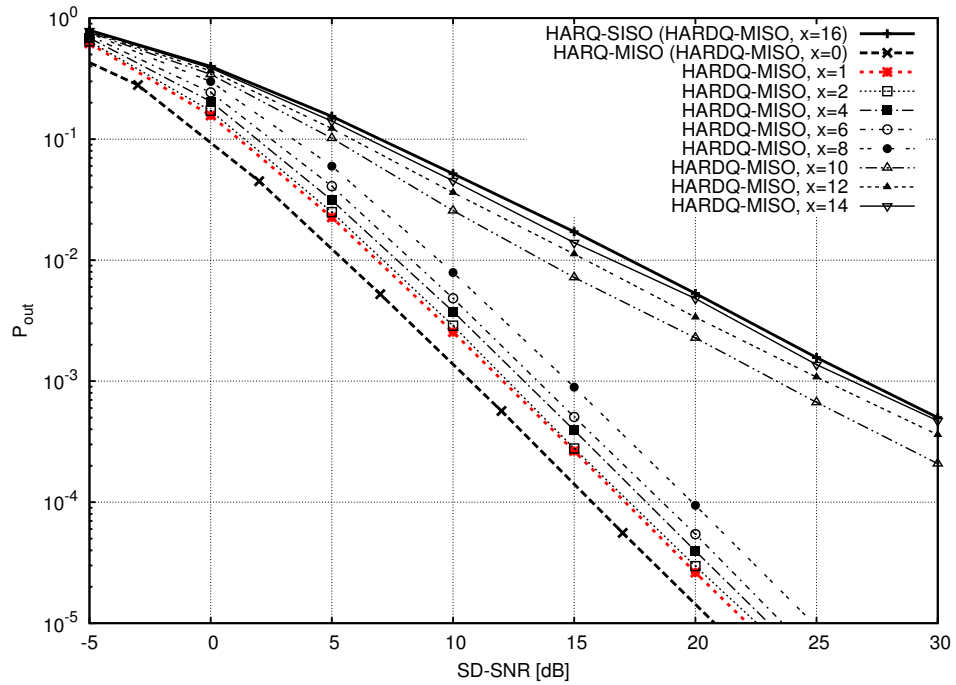
**Figure 7.2:** Comparison of the delay-limited throughput measured as a function of the SD-SNR and D-SNR for the HARQ-MISO protocol and increasing  $t = x$ , considering uniformly distributed BPSK channel inputs.

Figure 7.2 depicts the delay-limited throughput of the HARDQ-MISO protocol measured as a function of the SD-SNR and as a function of the D-SNR, considering uniformly distributed BPSK channel inputs. At low SD-SNR, significant performance gains for decreasing  $x$  can be observed. Measuring the delay-limited throughput as a function of the D-SNR shows lower performance gains. Furthermore, it can be observed in Figure 7.2b that the HARDQ-MISO protocol outperforms the HARQ-MISO protocol at low D-SNR. At medium to high D-SNR, the HARQ-MISO protocol outperforms the HARDQ-MISO protocol. Furthermore, the delay-limited throughput decreases with increasing  $x$ . For  $x = 14$ , the HARDQ-MISO protocol achieves a delay-limited throughput equivalent to that of the HARQ-SISO protocol.

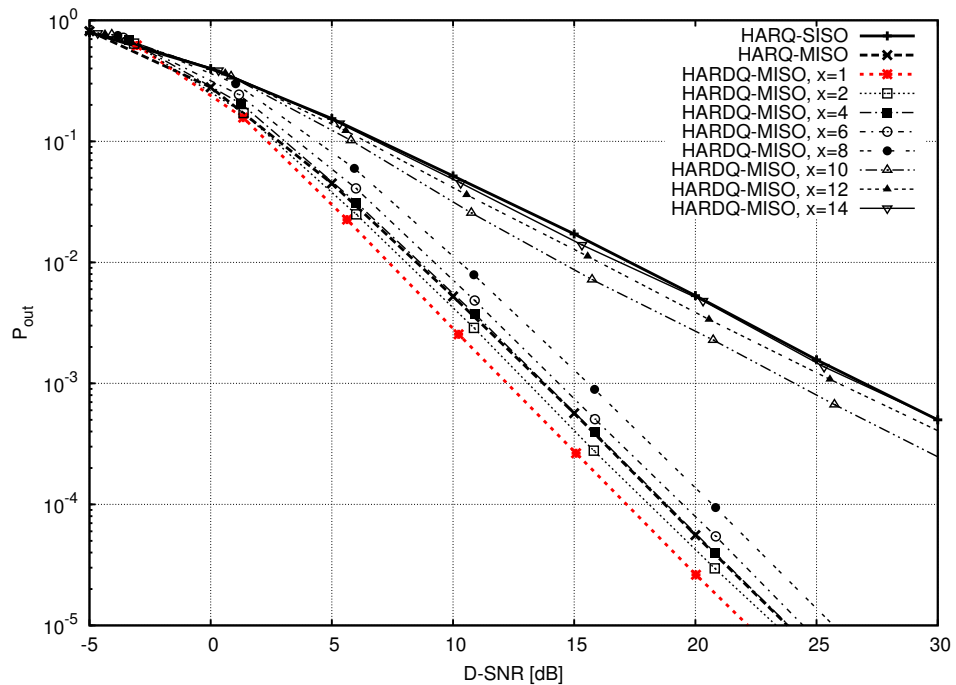
Comparing the performance difference of the HARQ-MISO and the HARDQ-MISO protocol in Figure 7.1a and Figure 7.1b shows that the HARQ-MISO protocol outperforms the HARDQ-MISO protocol in terms of delay-limited throughput at medium to high D-SNR. However, Figure 7.1a reveals that the performance difference is small from an energy efficiency point of view.

Similar performance gains, measured using the RCPC encoded simulation systems, can be observed in Figure 7.3 and in Figure 7.4. But it can be observed that the RCPC encoded communication systems do not achieve the theoretical performance. Furthermore, while the HARDQ-MISO protocol outperforms the HARQ-MISO protocol in terms of delay-limited throughput at low D-SNR for uniformly distributed BPSK channel inputs, it can be observed in Figure 7.4b that these performance gains are not achieved using the RCPC encoded HARQ protocols. In fact, in this case the HARQ-SISO protocol outperforms both the HARQ-MISO and the HARDQ-MISO protocol.

However, the performance considering uniformly distributed BPSK channel inputs as well as the performance of the RCPC encoded HARQ protocols shows that the HARDQ-MISO protocol achieves for low  $t$  significant gains over the HARQ-MISO protocol in the depicted D-SNR range in terms of outage probability. For medium D-SNR, the HARDQ-MISO protocol outperforms the HARQ-SISO protocol in terms of delay-limited throughput.

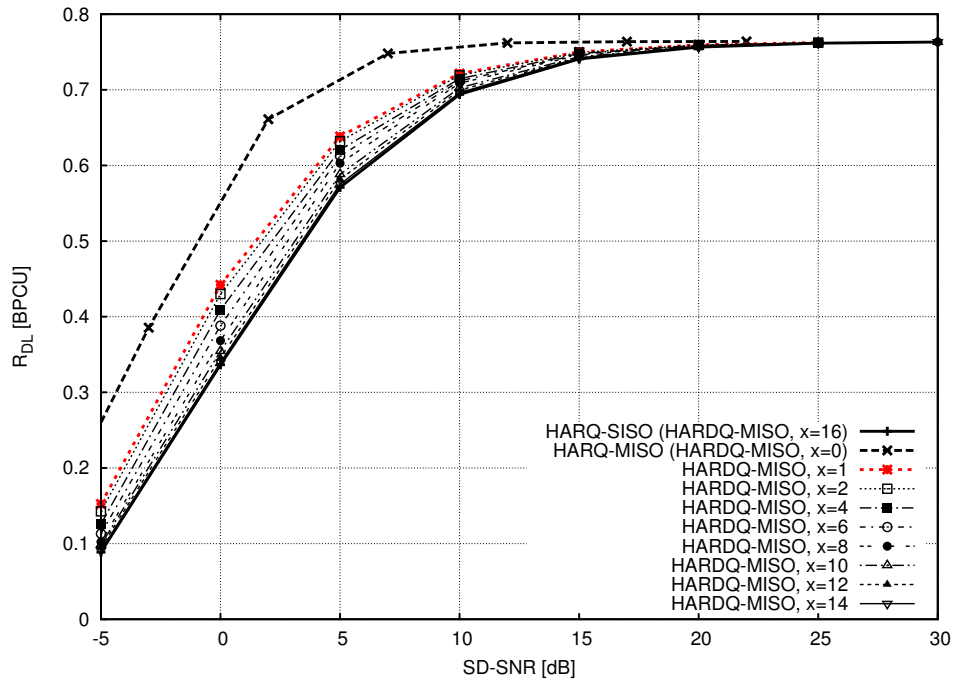


(a) Outage Probability as a function of the SD-SNR

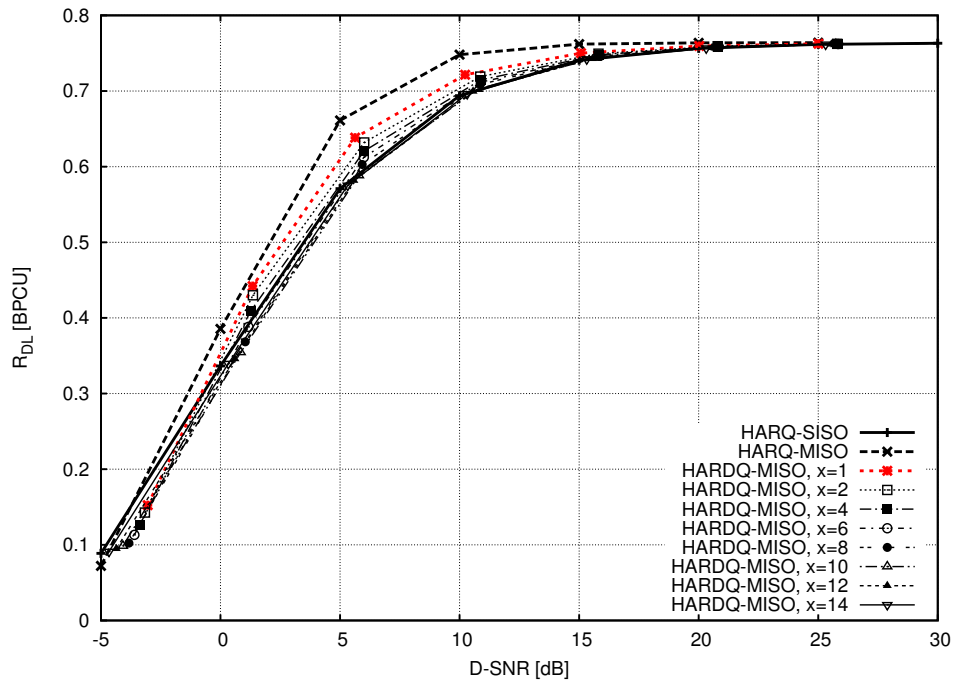


(b) Outage Probability as a function of the D-SNR

**Figure 7.3:** Comparison of the outage probability measured as a function of the SD-SNR and D-SNR for the RCPC encoded HARQ-MISO protocol and increasing  $t = x$ .

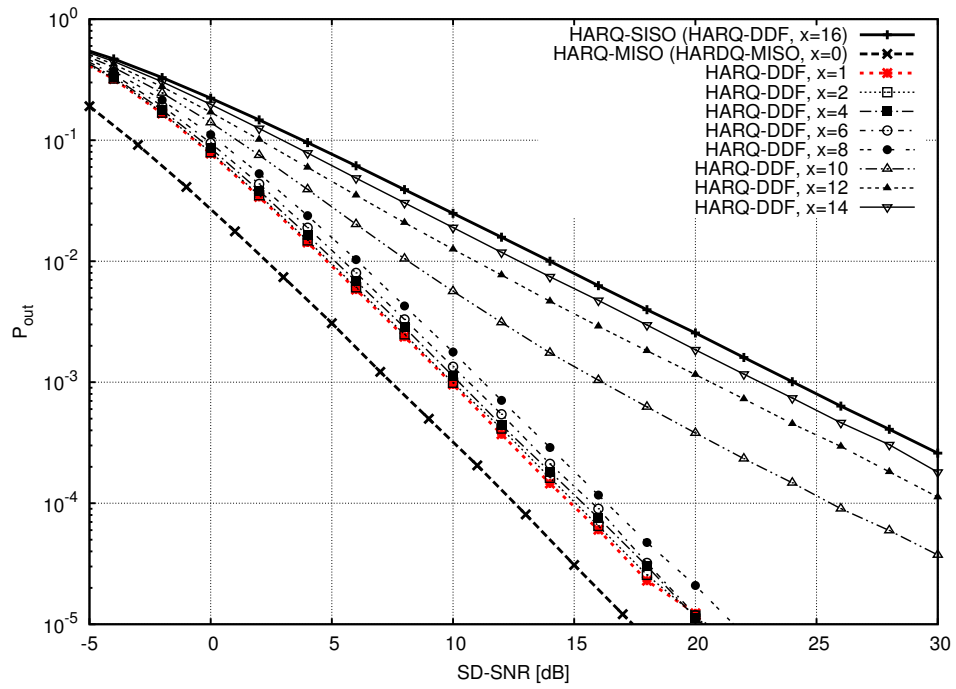


(a) Delay-limited throughput as a function of the SD-SNR

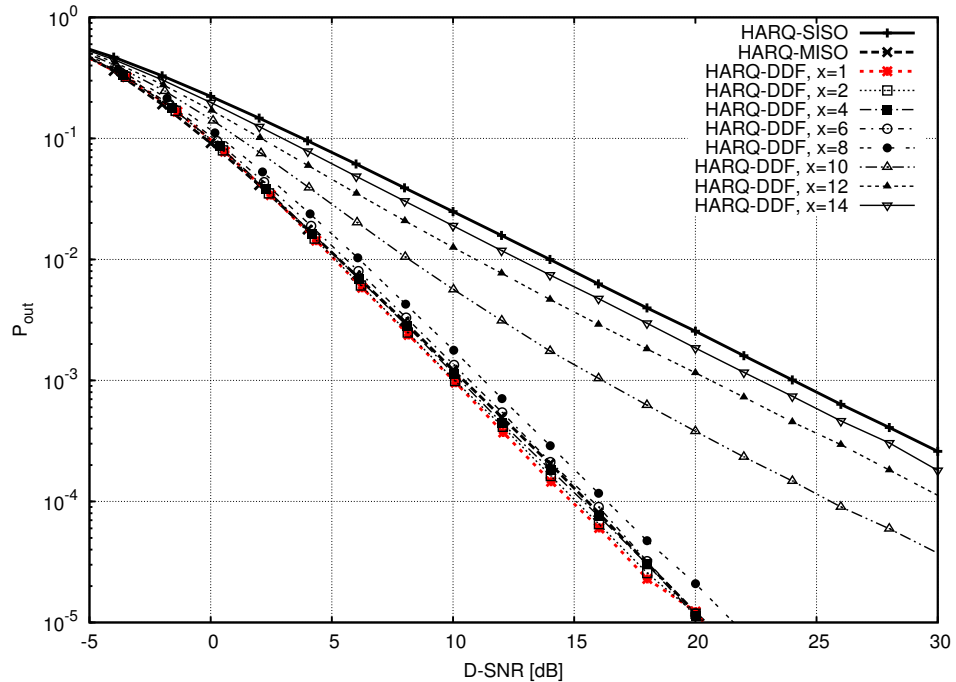


(b) Delay-limited throughput as a function of the D-SNR

**Figure 7.4:** Comparison of the delay-limited throughput measured as a function of the SD-SNR and D-SNR for the RCPC encoded HARQ-MISO protocol and increasing  $t = x$ .

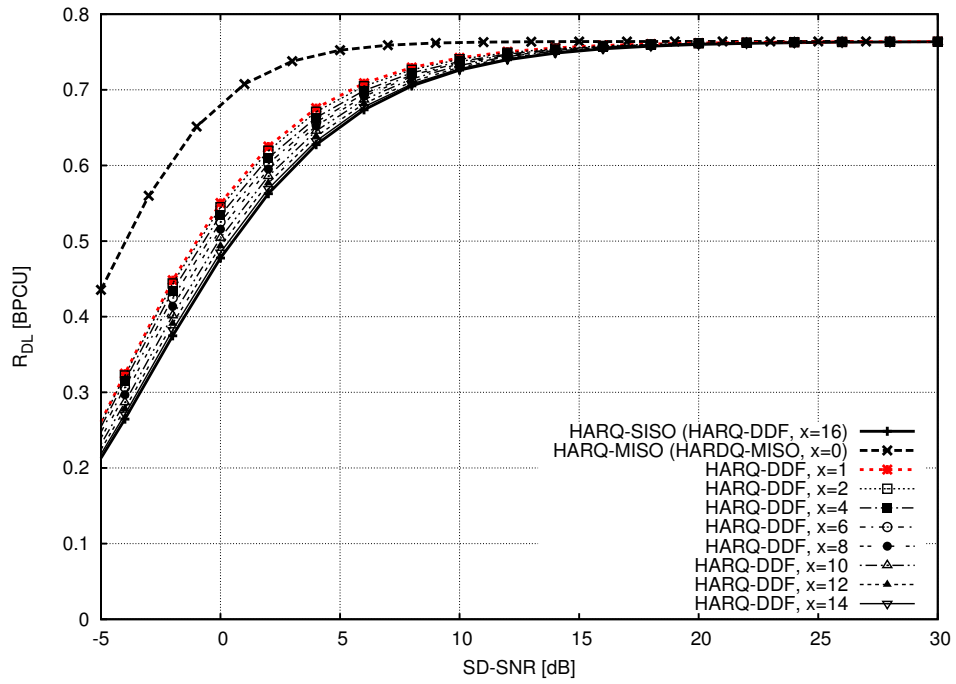


(a) Outage probability as a function of the SD-SNR

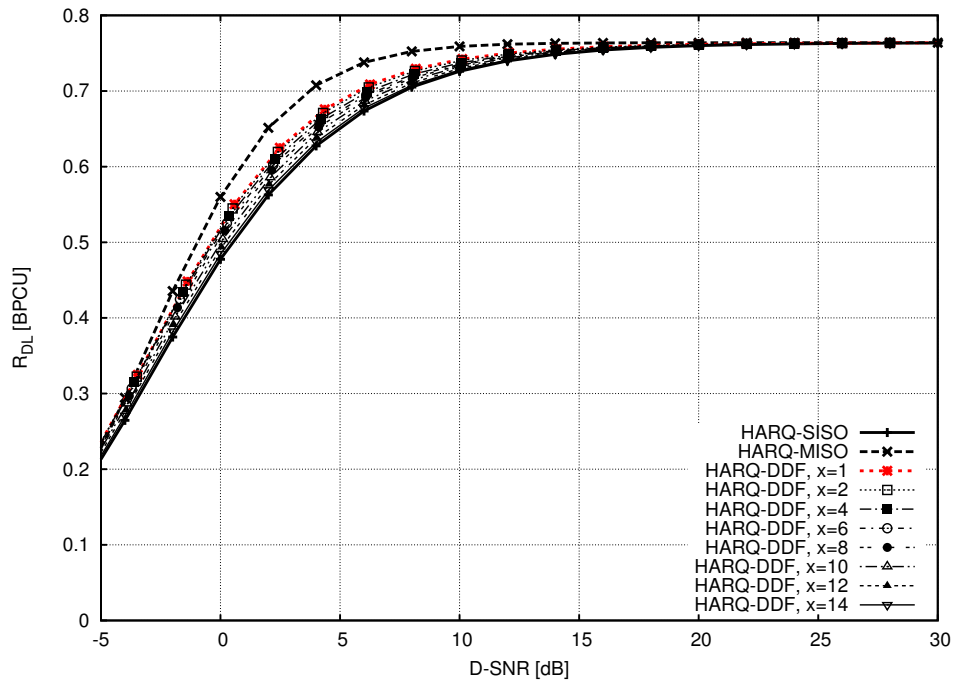


(b) Outage probability as a function of the D-SNR

**Figure 7.5:** Comparison of the outage probability measured as a function of the SD-SNR and D-SNR for the HARQ-DDF protocol and increasing  $\min\{\mathcal{D}_r\} = x$ , considering uniformly distributed BPSK channel inputs.



(a) Delay-limited throughput as a function of the SD-SNR



(b) Delay-limited throughput as a function of the D-SNR

**Figure 7.6:** Comparison of the delay-limited throughput measured as a function of the SD-SNR and D-SNR for the HARQ-DFD protocol and increasing  $\min\{\mathcal{D}_r\} = x$ , considering uniformly distributed BPSK channel inputs.

### HARQ-DDF Protocol

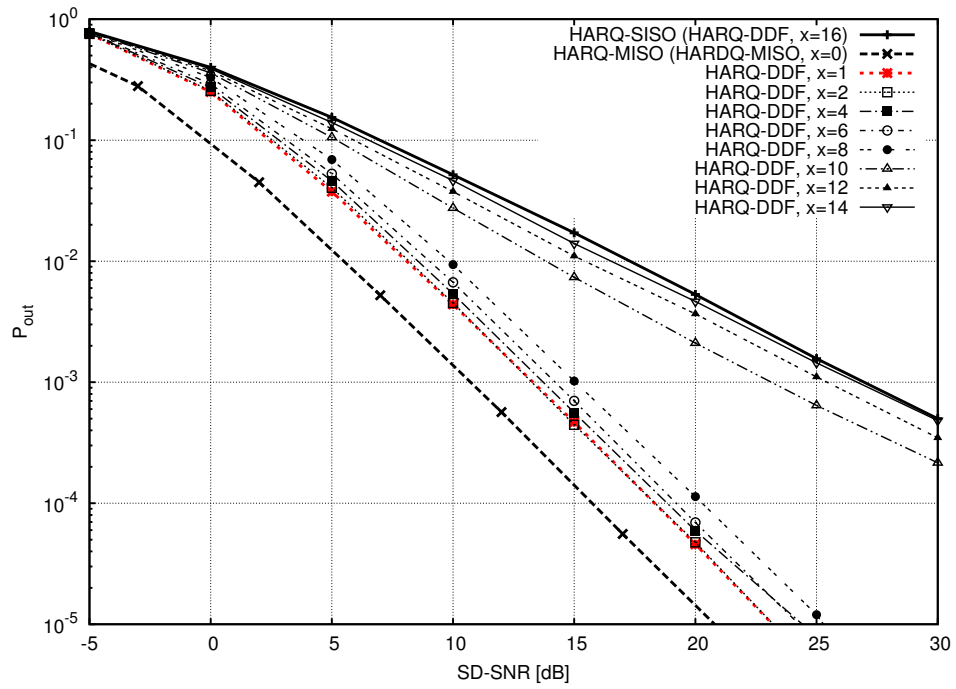
Considering uniformly distributed BPSK channel inputs, Figure 7.5 and Figure 7.6 depict the outage probability and the delay-limited throughput of the HARQ-DDF protocol measured as a function of the SD-SNR and as a function of the D-SNR for increasing  $\min\{\mathcal{D}_r\} = x$ , respectively. In general, it can be observed that the HARQ-DDF protocol shows similar performance as the HARQ-MISO protocol. However, in comparison with the HARQ-MISO protocol the HARQ-DDF protocol shows smaller performance gains than the HARQ-MISO protocol for  $x < 10$ . In comparison with the HARQ-SISO protocol, the configuration  $x \geq 10$  shows equivalent performance gains to these of the HARQ-MISO protocol.

In terms of outage probability it can be seen at high D-SNR that the HARQ-DDF protocol outperforms the HARQ-MISO protocol for the configuration  $x = 1$  and  $x = 2$  only. For  $x = 4$ , the HARQ-DDF protocol shows an equivalent outage probability as the HARQ-MISO protocol at medium to high D-SNR. For  $x > 8$ , the HARQ-DDF protocol does not achieve the diversity gain of the HARQ-MISO protocol but provides significant performance gains over the HARQ-SISO protocol.

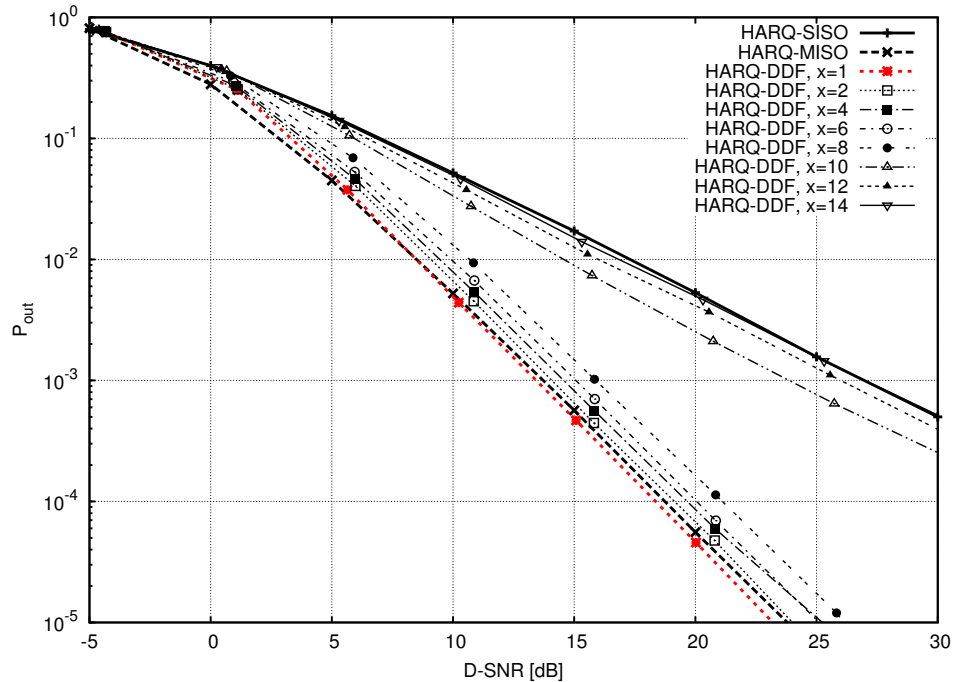
While the HARQ-MISO protocol outperforms the HARQ-MISO protocol in terms of the delay-limited throughput, it can be seen in Figure 7.6b that the HARQ-DDF protocol achieves only an equivalent performance as the HARQ-MISO protocol in the low D-SNR range for  $x = 1, 2$ . However, at medium D-SNR, the HARQ-DDF protocol shows significant performance gains over the HARQ-SISO protocol for  $x = 1$ . These performance gains decrease for increasing  $x$ . The HARQ-MISO protocol outperforms the HARQ-DDF protocol over the complete D-SNR range.

Figure 7.7 and Figure 7.8 depict the outage probability and delay limited throughput measured as a function of the SD-SNR and as a function of the D-SNR for the RCPC encoded communication systems. In general, it can be seen that RCPC encoded HARQ protocols show similar performance as measured considering uniformly distributed BPSK channel inputs.

Furthermore, only the HARQ-DDF protocol with the configuration  $x = 1$  outperforms the HARQ-MISO protocol at high D-SNR. For  $x > 1$ , a significant performance loss can be observed in comparison with the HARQ-MISO proto-

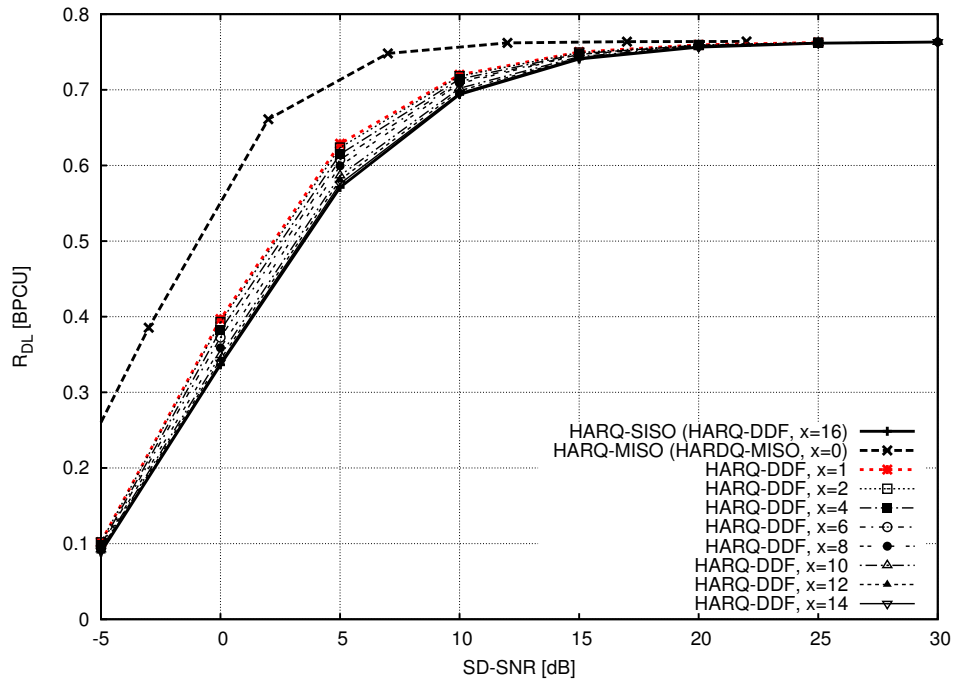


(a) Outage Probability as a function of the SD-SNR

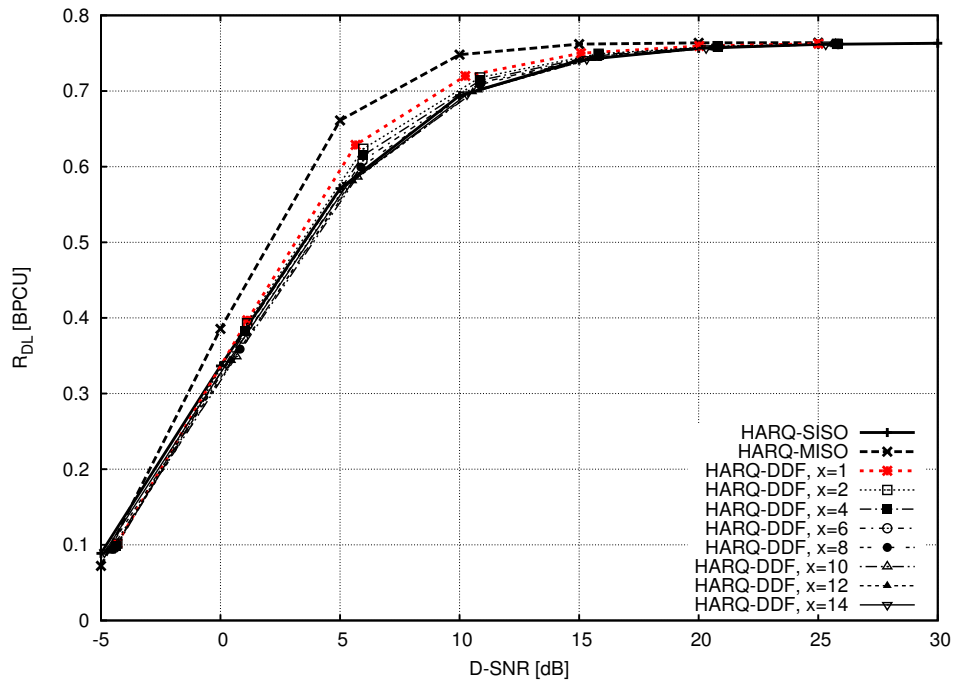


(b) Outage Probability as a function of the D-SNR

**Figure 7.7:** Comparison of the outage probability measured as a function of the SD-SNR and D-SNR for the RCPC encoded HARQ-DFD protocol and increasing  $\min\{\mathcal{D}_r\} = x$ .

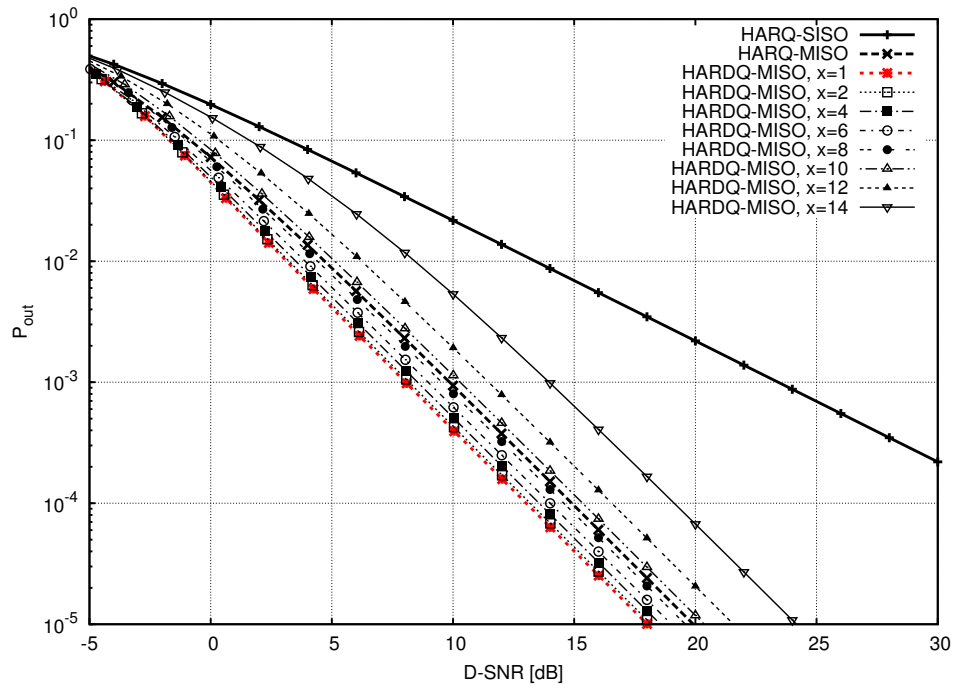


(a) Delay-limited throughput as a function of the SD-SNR

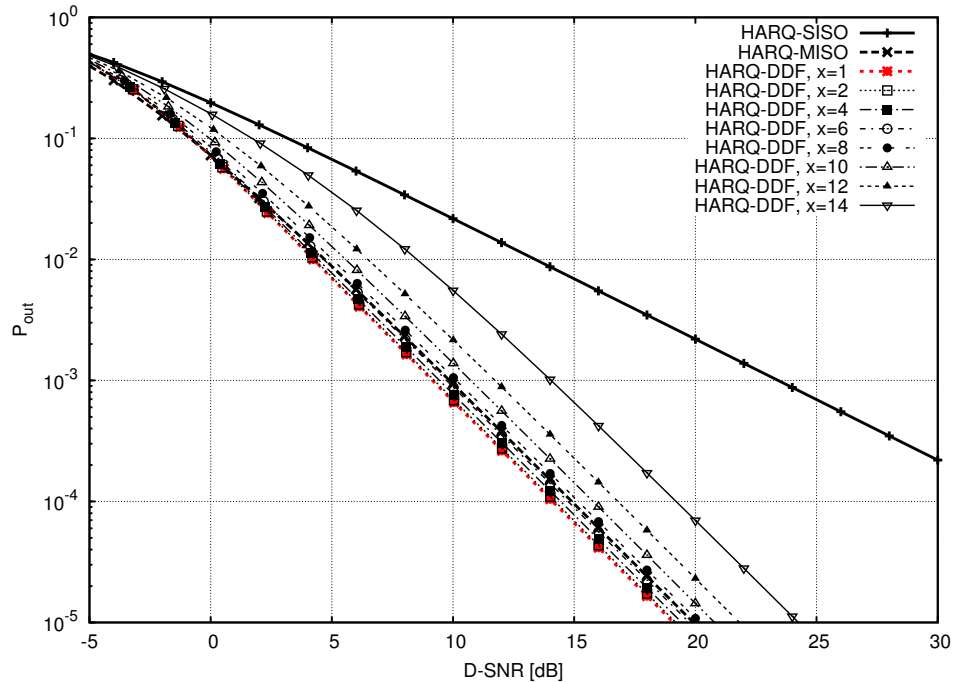


(b) Delay-limited throughput as a function of the D-SNR

**Figure 7.8:** Comparison of the delay-limited throughput measured as a function of the SD-SNR and D-SNR for the RCPC encoded HARQ-DFD protocol and increasing  $\min\{\mathcal{D}_r\} = x$ .



(a) Outage probability as a function of the D-SNR



(b) Outage probability as a function of the D-SNR

**Figure 7.9:** Comparison of the outage probability of the HARQ-MISO protocol and the HARQ-DDF protocol measured as a function of the D-SNR considering Gaussian channel inputs and increasing  $t = \min\{D_r\} = x$ .

col. For  $x > 8$ , the HARQ-DDF protocol does not achieve the diversity gain of the HARQ-MISO protocol but shows performance gains over the HARQ-SISO protocol. For  $x = 14$ , the HARQ-DDF protocol achieves an equivalent performance as the HARQ-SISO protocol.

In terms of delay-limited throughput, it can be observed in Figure 7.8b that the HARQ-DDF protocol is outperformed by the HARQ-SISO protocol at low D-SNR but shows significant performance gains at medium D-SNR for the configuration  $x = 1$ .

### Outage Probability Considering Gaussian Channel Inputs

Both the HARQ-MISO protocol and the HARQ-DDF protocol do not achieve the diversity gain of the HARQ-MISO protocol for  $x > 8$ . This effect is noteworthy, since it cannot be observed for the high-rate mother code configuration investigated in Section 6.1. In order to investigate this effect, Figure 7.9 depicts the outage probability of the HARQ protocols measured as a function of the D-SNR considering Gaussian distributed channel inputs. It can be observed that the HARQ-MISO protocol and the HARQ-DDF protocol achieve the diversity gain of the HARQ-MISO protocol for  $x > 8$ , while the performance loss in comparison with the HARQ-MISO protocol increases with increasing  $x$ . Therefore, it can be reasoned that the loss in diversity gain is caused by the upper limit of the mutual information between the source and destination given by the application of discrete channel inputs.

## 7.4 Performance Comparison of the NPA and the TPA HARQ Protocols

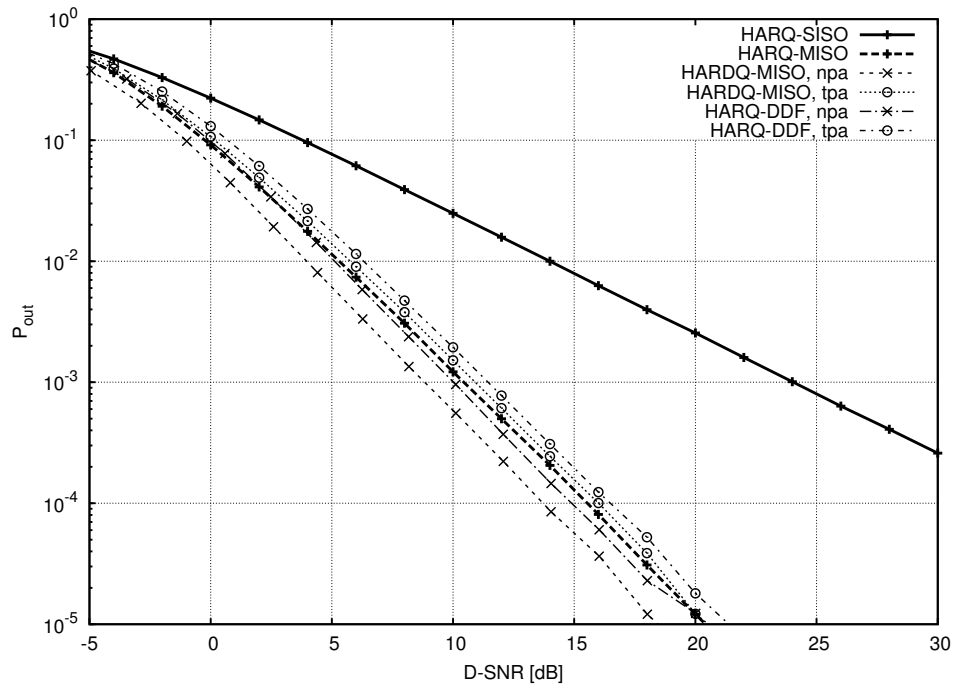
This section details the outage probability and delay-limited throughput of the HARQ-MISO and the HARQ-DDF protocol applying the NPA and the TPA protocol variants. To this end, the source and the destination apply the decoding instant sets  $\mathcal{D} = \mathcal{D}_s = \mathcal{D}_d$ , respectively. The HARQ-MISO protocol is configured to assist the transmission using the second antenna after the first ARQ round, i.e., the HARQ-MISO protocol is configured with  $t = 1$ . The HARQ-DDF protocol is configured to apply the decoding instant set  $\mathcal{D} = \mathcal{D}_r$  at

the relay, i.e., the relay attempts to decode the received information after each ARQ round.

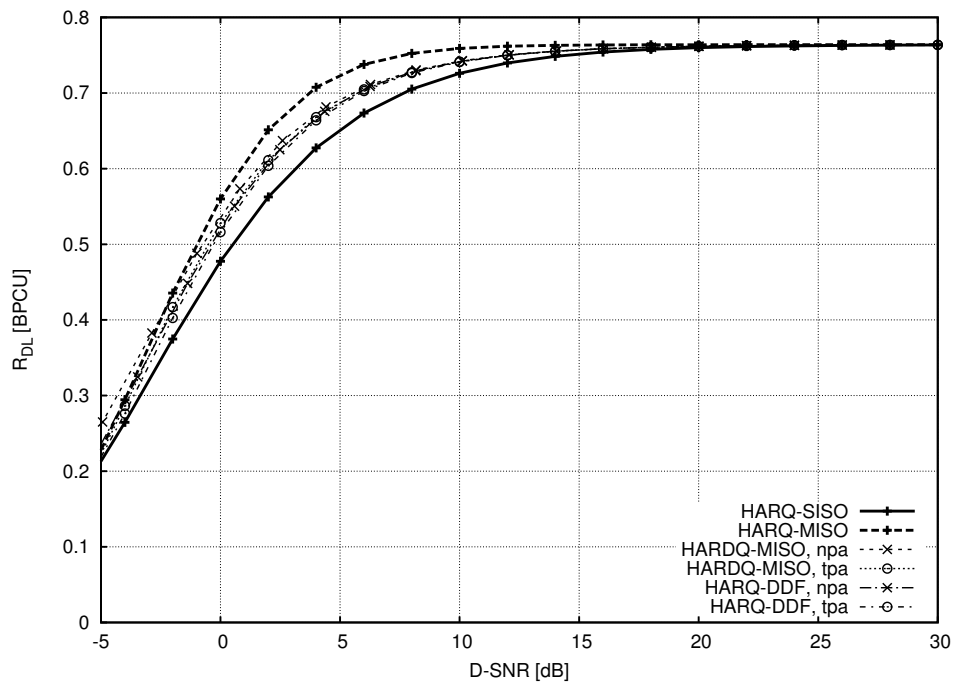
Figure 7.10 depicts the performance of the HARQ protocols considering uniformly distributed BPSK channel inputs. In terms of outage probability, it can be observed in Figure 7.10a that the application of the NPA protocol achieves higher performance gains than the application of the TPA protocols. Furthermore, it can be seen that the NPA HARDQ-MISO protocol outperforms the HARQ-MISO protocol over the depicted D-SNR range, while the NPA HARQ-DDF protocol outperforms the HARQ-MISO protocol for medium to high D-SNR.

Considering the application of a high-rate mother code, it is demonstrated in Section 6.3 that the TPA protocol outperforms the NPA protocol in terms of the delay-limited throughput considering Gaussian channel inputs. However, considering the code rate function (7.5) defined by the RCPC mother codebook, it can be observed in Figure 7.10b that the TPA protocol does not provide an advantage over the NPA protocol. In fact, the NPA HARDQ-MISO protocol outperforms the TPA protocol variant at low D-SNR. Furthermore, both the HARDQ-MISO protocol and the HARQ-DDF protocol show to outperform the HARQ-SISO protocol over the depicted D-SNR range for both the NPA and the TPA protocol variants.

Figure 7.11 depicts the performance of the HARQ protocols measured by the simulation of the RCPC encoded communication systems. Besides significant performance offsets, it can be observed that the RCPC encoded HARQ protocols show similar performance as the performance measured considering uniformly distributed BPSK channel inputs. However, at low D-SNR it is shown in Figure 7.11b that the NPA HARDQ-MISO protocol does not outperform the corresponding TPA protocol. Furthermore, at low D-SNR the HARQ-SISO protocol outperforms both the HARDQ-MISO and the HARQ-DDF protocol for both the NPA and the TPA protocol variants.

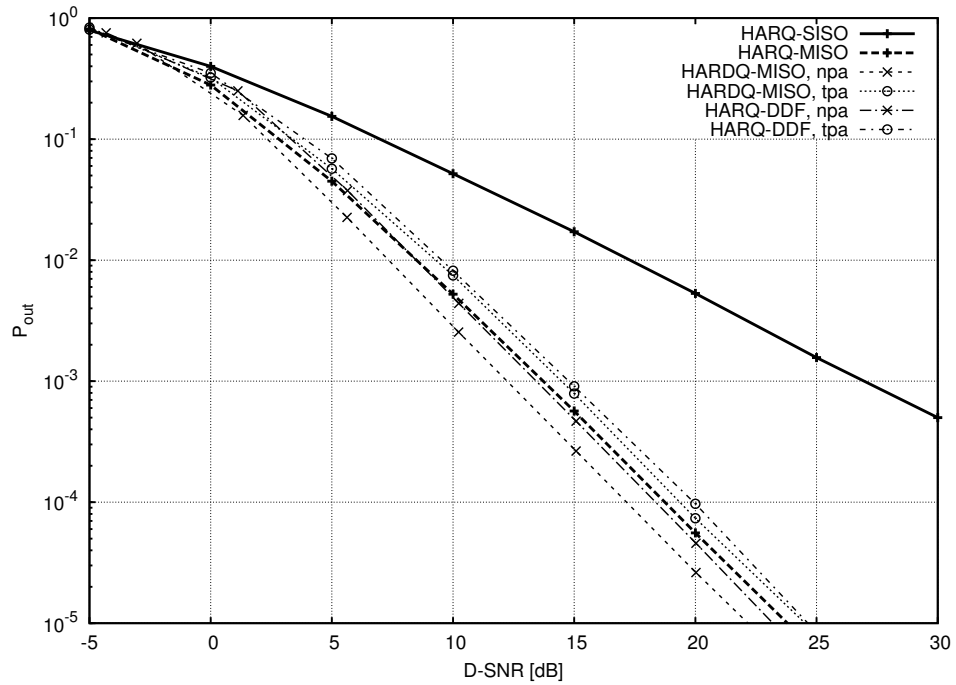


(a) Outage probability

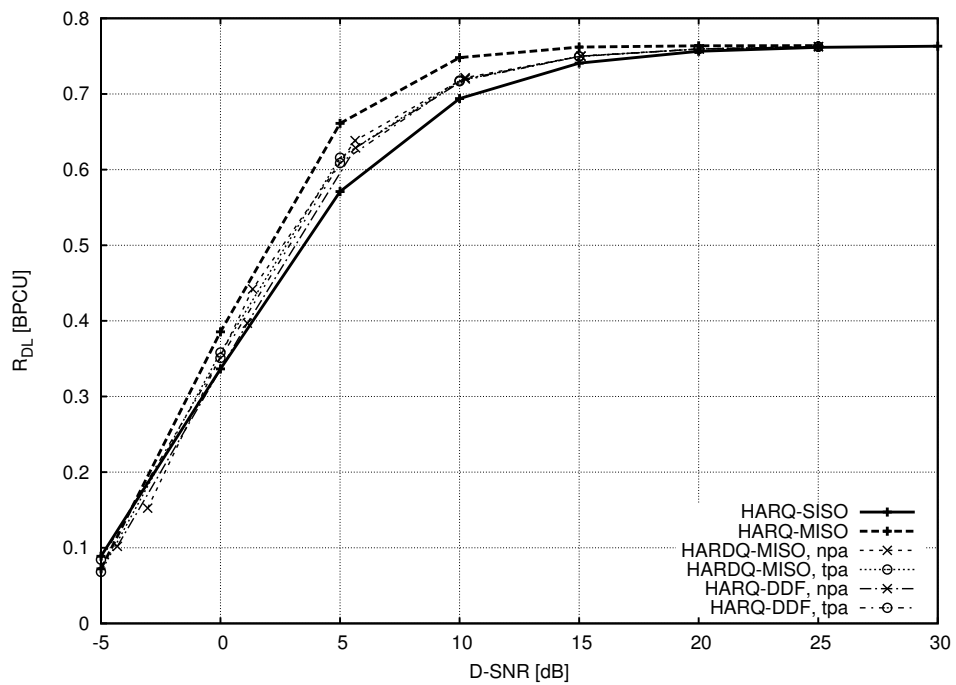


(b) Delay-limited throughput

**Figure 7.10:** Comparison of the outage probability and the delay-limited throughput applying the NPA HARQ protocols and the TPA HARQ protocols, considering uniformly distributed BPSK channel inputs.

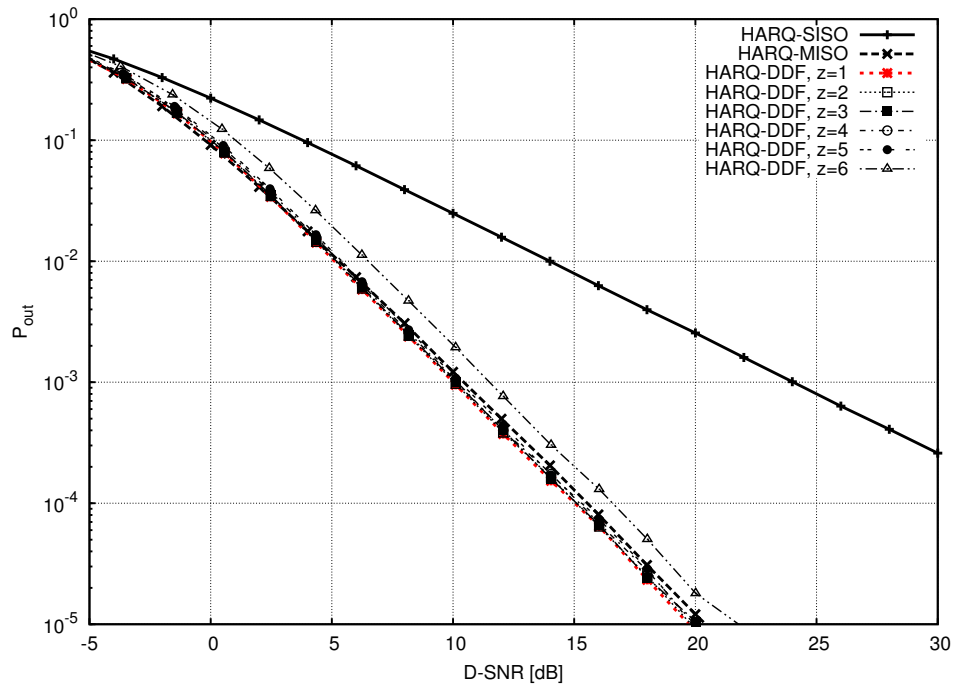


(a) Outage Probability

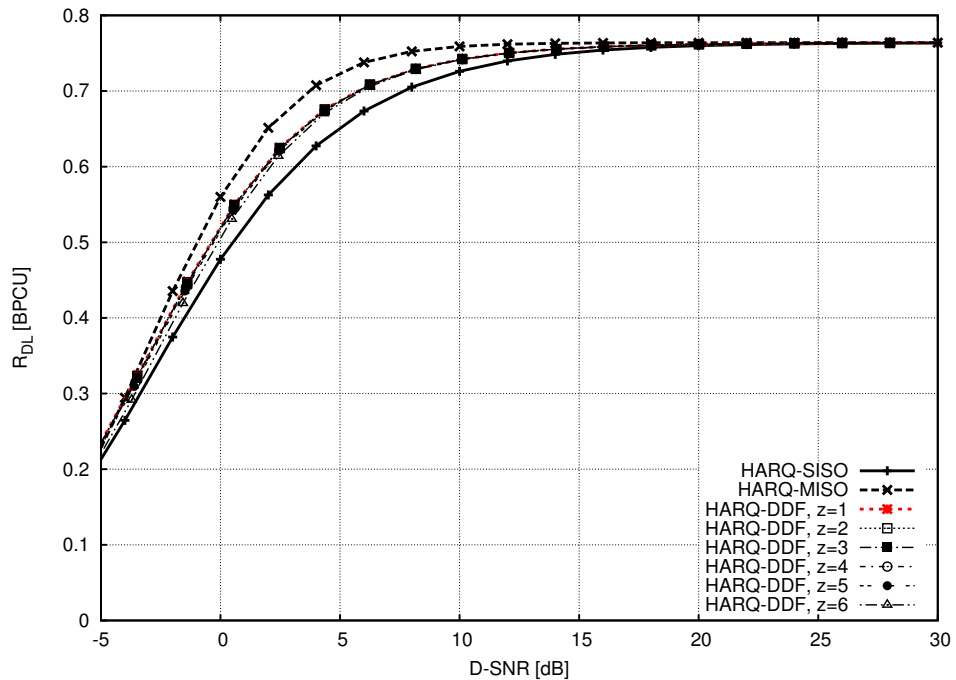


(b) Delay-limited throughput

**Figure 7.11:** Comparison of the outage probability and the delay-limited throughput applying the RCPC encoded NPA HARQ protocols and the TPA HARQ protocols.

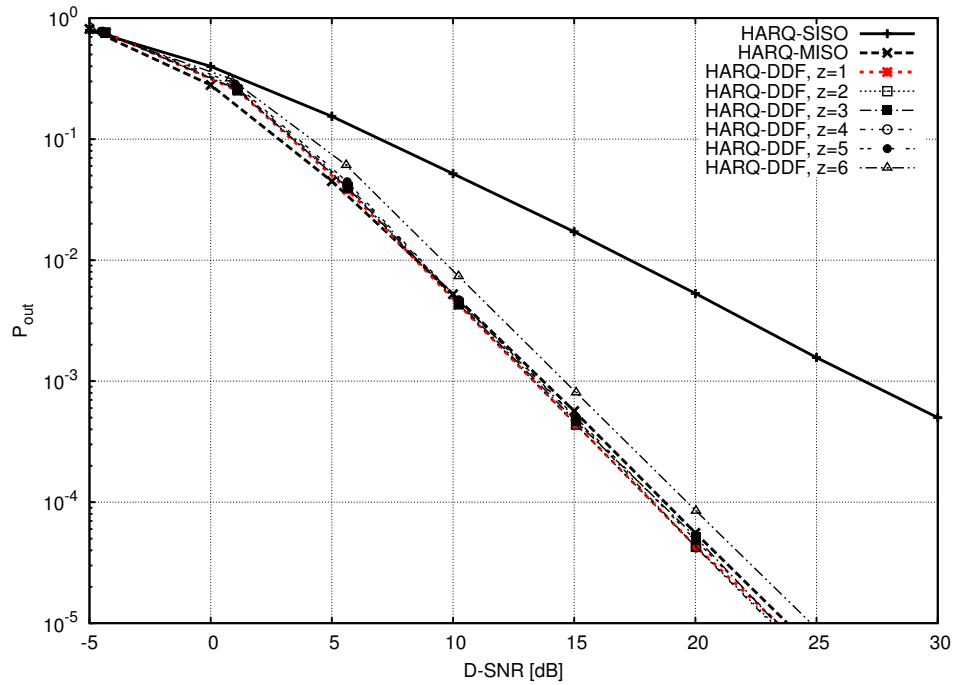


(a) Outage probability

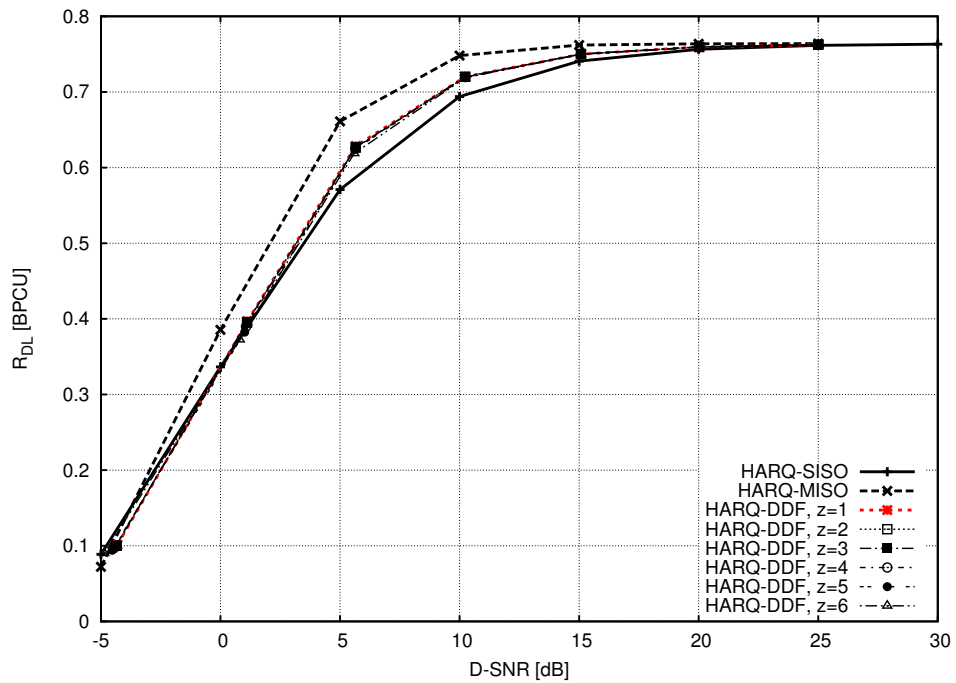


(b) Delay-limited throughput

**Figure 7.12:** Comparison of the outage probability and the delay-limited throughput of the HARQ-DDF protocol with reduced decoding cost at the relay and considering uniformly distributed BPSK channel inputs.



(a) Outage probability



(b) Delay-limited throughput

**Figure 7.13:** Comparison of the outage probability and the delay-limited throughput of the RCPC encoded HARQ-DDF protocol with reduced decoding cost at the relay.

## 7.5 Decoding Cost Reduction at the Relay for the HARQ-DDF Protocol

This section demonstrates the effect of decoding cost reduction at the relay for the HARQ-DDF protocol. To this end, the decoding instant sets at the source and the destination are selected as  $\mathcal{D} = \mathcal{D}_s = \mathcal{D}_d$ . Furthermore, the perforated decoding instant sets  $\mathcal{D}_r(z)$  applied at the relay are given as

$$\mathcal{D}_r(1) = \mathcal{D}, \quad (7.6)$$

$$\mathcal{D}_r(2) = \{1, 2, 4, 6, 8, 10, 12, 14, 16\}, \quad (7.7)$$

$$\mathcal{D}_r(3) = \{1, 2, 5, 8, 11, 14, 16\}, \quad (7.8)$$

$$\mathcal{D}_r(4) = \{1, 2, 8, 14, 16\}, \quad (7.9)$$

$$\mathcal{D}_r(5) = \{1, 8, 16\}, \quad (7.10)$$

$$\mathcal{D}_r(6) = \{1, 16\}, \quad (7.11)$$

where the decoding cost decreases with increasing  $z$ . Due to the structure of punctured convolutional codes and neglecting the computational cost due to depuncturing, it is assumed that the decoding cost in each ARQ round is constant. Consequently, according to (6.8) the decoding instant sets  $\mathcal{D}_r(z)$  are associated with the decoding cost factors

$$c_r(1) = 1, \quad c_r(2) = \frac{8}{15} \quad c_r(3) = \frac{6}{15} \quad c_r(4) = \frac{4}{15} \quad c_r(5) = \frac{2}{15} \quad c_r(6) = \frac{1}{15}.$$

Figure 7.12 depicts the outage probability and the delay-limited of the HARQ-DDF protocol considering uniformly distributed BPSK channel inputs. In terms of outage probability, it can be observed that the performance loss for  $z = 1$  to  $z = 5$  is negligible and that the HARQ-DDF protocol outperforms the HARQ-MISO protocol at high D-SNR. But for  $z = 6$ , the performance loss is significant and the HARQ-DDF protocol does not outperform the HARQ-MISO protocol.

In Figure 7.12b, it can be seen that the performance loss due to decoding cost reduction at the relay is negligible for all  $z$ . At low D-SNR, a small performance loss can be observed for  $z = 6$ .

Figure 7.13 depicts the outage probability and delay-limited throughput obtained by simulation of the RCPC encoded HARQ protocols. It can be observed

that the conclusions drawn for the performance measured considering equally distributed BPSK channel inputs are also valid for the RCPC encoded HARQ-DDF protocol.

Consequently, compared with  $z = 1$ , the decoding cost can be reduced to a factor of  $c(5) = \frac{2}{15}$  without a significant loss of outage probability and delay-limited throughput. If the measure of interest is the delay-limited throughput, the decoding cost can be reduced to a factor of  $c(6) = \frac{1}{15}$  with a small performance loss at low D-SNR only.

## 7.6 Decoding Cost Reduction at the Relay and the Destination

This section demonstrates the effect of decoding cost reduction at the destination for the HARDQ-MISO protocol and, at the relay *and* the destination for the HARQ-DDF protocol.

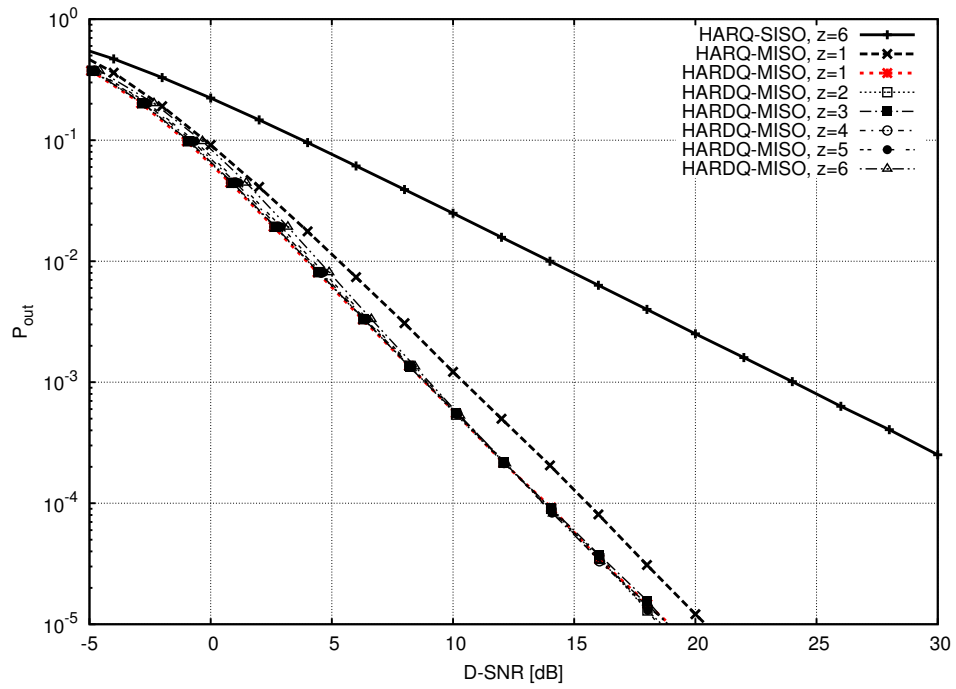
To this end, the decoding instant set at the source is selected as  $\mathcal{D} = \mathcal{D}_s$ . For the HARQ-DDF protocol, the decoding instant sets at the relay and the destination are selected as  $\mathcal{D}_d(z) = \mathcal{D}_r(z)$  given in (7.7) to (7.11). For the HARDQ-MISO protocol, the ARQ round after which the second antenna at the source starts to participate the transmission is selected as  $t = \min\{\mathcal{D}_d(z)\}$ . The associated decoding cost factors at the destination according to (6.9) are

$$c_d(1) = 1, \quad c_d(2) = \frac{9}{16} \quad c_r(3) = \frac{7}{16} \quad c_r(4) = \frac{5}{16} \quad c_r(5) = \frac{3}{16} \quad c_r(6) = \frac{2}{16}.$$

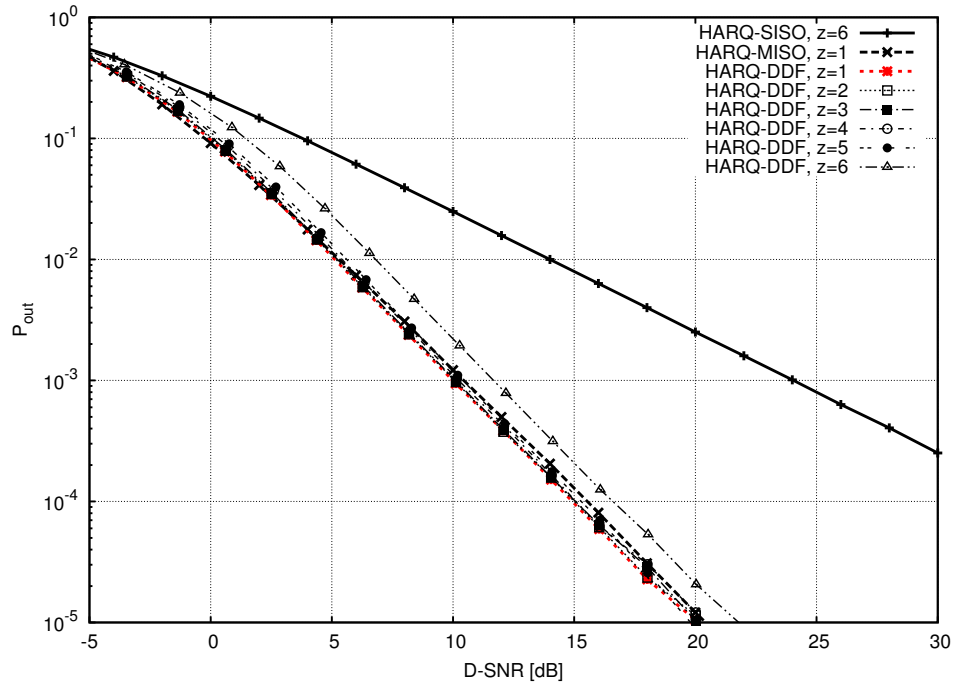
For comparison, the worst-case performance measure of the HARQ-SISO protocol achieved with  $z = 6$  and the best-case performance measure of the HARQ-MISO protocol achieved with  $z = 1$  is given.

### Outage Probability Considering Uniformly Distributed BPSK Channel Inputs

Considering uniformly distributed BPSK channel inputs, Figure 7.14 depicts the outage probability of the HARDQ-MISO and the HARQ-DDF protocol. For the HARDQ-MISO protocol, it can be observed that performance loss due to decoding cost reduction at the destination is negligible for  $z < 6$ . For  $z = 6$ ,

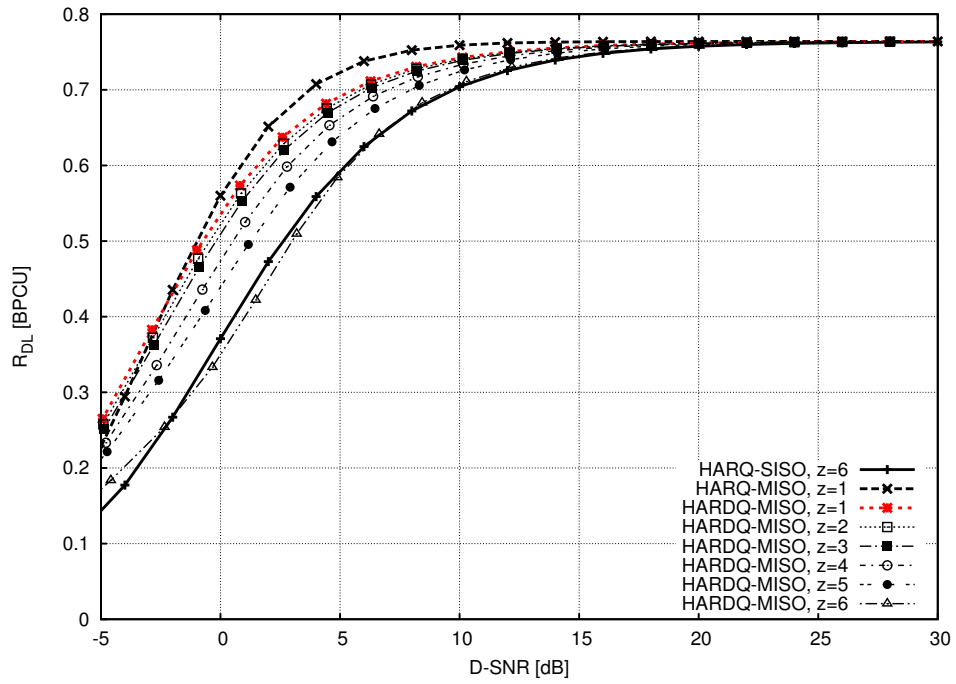


(a) HARQ-MISO protocol

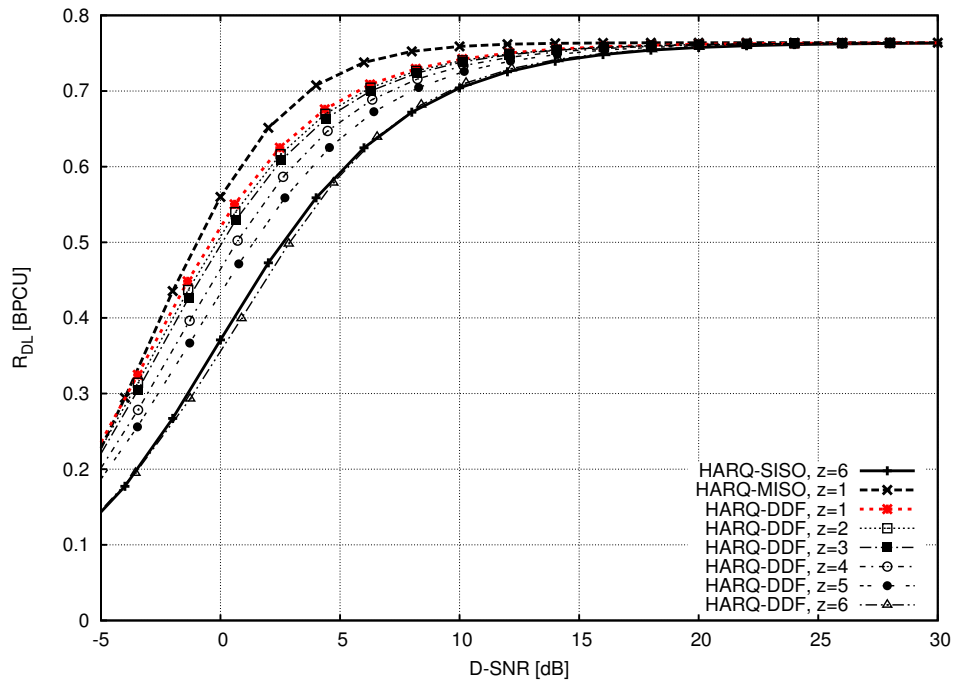


(b) HARQ-DDF protocol

**Figure 7.14:** Outage probability of the HARQ-MISO and HARQ-DDF protocol with reduced decoding cost at the relay and the destination considering uniformly distributed BPSK channel inputs.

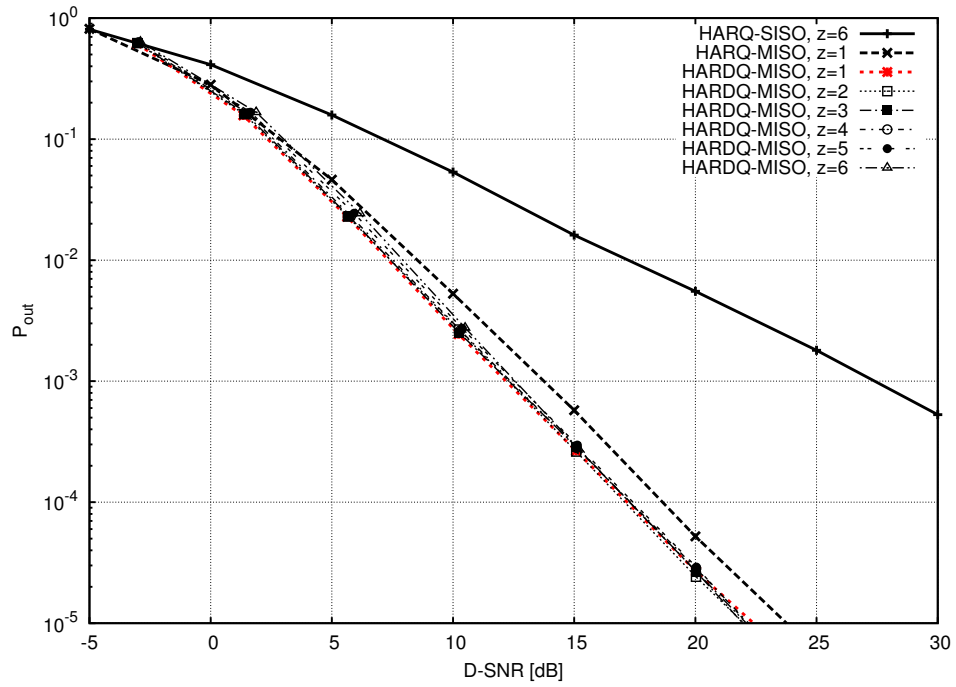


(a) HARQ-MISO protocol

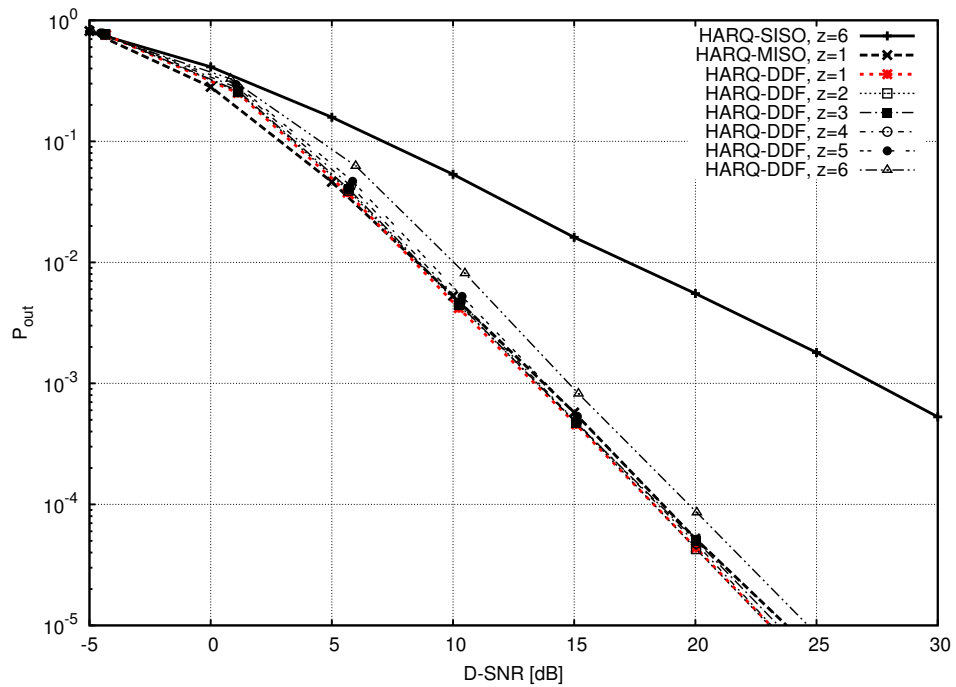


(b) HARQ-DDF protocol

**Figure 7.15:** Delay-limited throughput of the HARQ-MISO and HARQ-DDF protocol with reduced decoding cost at the relay and the destination considering uniformly distributed BPSK channel inputs.

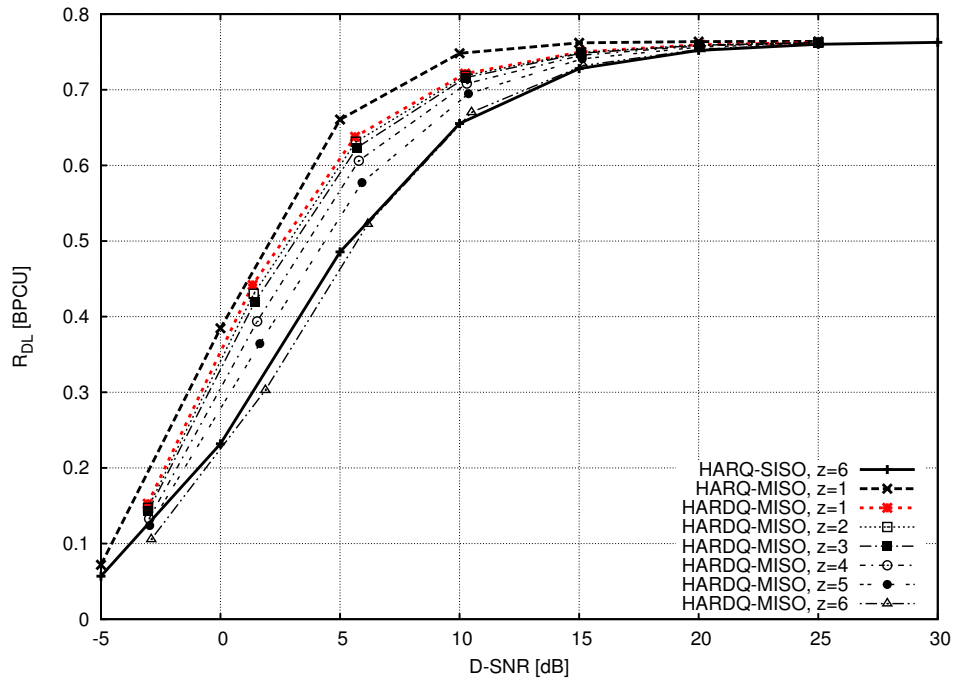


(a) HARDQ-MISO protocol

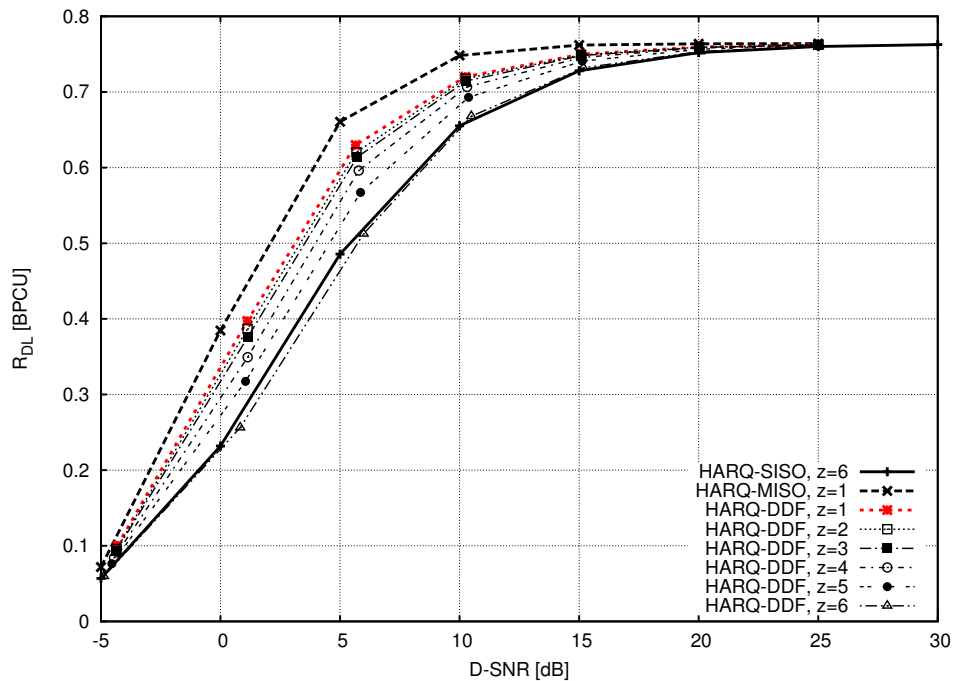


(b) HARQ-DDF protocol

**Figure 7.16:** Outage probability of the RCPC encoded HARDQ-MISO and HARQ-DDF protocol with reduced decoding cost at the relay and the destination.



(a) HARDQ-MISO protocol



(b) HARQ-DDF protocol

**Figure 7.17:** Delay-limited throughput of the RCPC encoded HARDQ-MISO and HARQ-DDF protocol with reduced decoding cost at the relay and the destination.

a small performance loss can be observed at low to medium D-SNR. However, at high D-SNR, no performance loss can be observed. Furthermore, for  $z = 1, 2, \dots, 6$  the HARDQ-MISO protocol outperforms the HARQ-MISO protocol with  $z = 6$ .

For the HARQ-DDF protocol, the performance loss in terms of outage probability is negligible for  $z < 4$  and small for  $z = 4, 5$ . But for  $z = 6$ , a significant performance loss can be observed. However, the comparison with the results discussed in Section 7.5 shows that this performance loss is caused by the decoding cost reduction at the relay rather than at the destination. In difference to the HARDQ-MISO protocol, the HARQ-DDF protocol outperforms the HARQ-MISO protocol with  $z = 6$  for  $z = 1, \dots, 4$ , only. Furthermore, in this range the performance difference to the HARQ-MISO protocol is small.

Considering uniformly distributed BPSK channel inputs, Figure 7.15 depicts the delay-limited throughput of the HARDQ-MISO and the HARQ-DDF protocol. In general it can be seen that both protocols show similar performance for all  $z$ , while the performance loss of the HARQ-DDF protocol in comparison with the HARDQ-MISO protocol is negligible. In comparison with  $z = 1$ , a small performance loss can be observed for  $z < 4$ . However, for  $z \geq 4$ , the performance loss is significant. For  $z = 1$  both the HARDQ-MISO and the HARQ-DDF protocol achieve the worst-case performance of the HARQ-SISO protocol.

Consequently, it can be concluded that the performance loss due to decoding cost reduction at the destination is negligible in terms of outage probability for all  $z$ . However, in terms of the delay-limited throughput the performance loss is small for  $z < 4$  only. Consequently, the decoding cost at the destination can be reduced to the factor  $c(3) = \frac{7}{16}$  without a significant performance loss in outage probability and a small performance loss in delay-limited throughput.

### Outage Probability of the RCPC Encoded HARQ Protocols

Figure 7.16 and Figure 7.17 depict the outage probability and the delay-limited throughput of the HARDQ-MISO and the HARQ-DDF protocol measured for the RCPC encoded communication system. Neglecting the performance offsets between the performance measured considering uniformly distributed channel inputs and the performance measured for the RCPC encoded HARQ protocols,

it can be observed that the conclusions drawn for the performance measured considering uniformly distributed BPSK channel inputs are also valid for the RCPC encoded HARQ protocol.

## 7.7 Summary

This chapter provides a comparison of the outage probability and the delay-limited throughput assuming uniformly distributed BPSK channel inputs and, of the outage probability and the delay-limited throughput measured for the RCPC encoded HARQ protocols. In general, it can be observed that the RCPC encoded HARQ protocols show very similar performance characteristics as the performance measured considering uniformly distributed BPSK channel inputs, neglecting the performance offsets due to a low memory of the convolutional code.

Section 7.3 provides a discussion of the performance of the HARQ protocols measured as a function of the SD-SNR and as a function of the D-SNR. To this end, several configurations with increasing  $x = t$  for the HARDQ-MISO protocol and, correspondingly, increasing  $x = \min\{\mathcal{D}_r\}$  for the HARQ-DDF protocol are selected. Comparing the performance of these configurations measured as a function of the SD-SNR and as a function of the D-SNR shows significant differences in the performance characteristics at low SD-SNR and low D-SNR. Measuring the performance as a function of the SD-SNR shows that the configuration  $x = 1$  outperforms all other configurations in terms of outage probability and delay-limited throughput. Measuring the performance as a function of the D-SNR shows that the configurations  $x \leq 4$  achieve equivalent performance at low D-SNR.

Furthermore, measuring the performance of the HARDQ-MISO protocol and of the HARQ-DDF protocol as a function of the D-SNR enables the comparison with the HARQ-SISO and the HARQ-MISO protocol on the system level. It is shown that the HARDQ-MISO and the HARQ-DDF protocol outperform the HARQ-MISO protocol at high D-SNR.

In comparison to the performance analysis considering a high-rate mother code given in Section 6, it is demonstrated that the RCPC encoded HARDQ-MISO protocol and RCPC encoded HARQ-DDF protocol do not achieve the

diversity of the HARQ-MISO protocol if  $x$  is close to the number of allowed ARQ rounds  $L$ . The performance measures given for Gaussian distributed channel inputs demonstrate that this difference stems from the upper bound on the mutual information of the corresponding channels given by the BPSK symbol constellation.

Section 7.4 provides a performance comparison of the NPA and the TPA protocol variants. For the high-rate code applied in the analysis in Section 6.3, it is shown that the NPA protocol variant outperforms the TPA protocol variant in terms of outage probability, but the TPA protocol variant outperforms the NPA protocol variant in terms of delay-limited throughput. In comparison, the performance measures given for the RCPC encoded HARQ protocols show that the NPA protocol variant outperforms the TPA protocol variant in terms of outage probability, but both variants achieve comparable performance in terms of delay-limited throughput. In comparison with the high rate analysis given in Section 6.3, it can be conjectured that this difference attributes the fact that the applied RCPC code provides only low code rates.

Section 7.5 and Section 7.6 consider the reduction of the computational decoding cost at the relay and at the destination. It is shown that the decoding cost can be reduced significantly, without a remarkable performance loss in outage probability and delay-limited throughput. These results are consistent with the high-rate analysis given in Section 6.4 and Section 6.5.

### Conclusion

---

This dissertation considers the design and analysis of the HARQ-DDF protocol for the quasi-static flat Rayleigh fading half-duplex relay channel. The performance measures of interest are the fixed-rate outage probability and the delay-limited throughput. Appropriate HARQ-SISO and HARQ-MISO protocols are given to benchmark the performance of the HARQ-DDF protocol. Furthermore, a novel variant of the HARQ-MISO protocol, the so-called HARDQ-MISO protocol is introduced.

The proposed HARQ protocols enable the application of rate assignment techniques considering unequal rate assignment for the source-to-relay and source-to-destination channel. This enables the scalability of computational cost at the relay and at the destination, and comes together with significant performance gains in terms of delay-limited throughput.

It is common practice to measure the fixed-rate outage probability and the delay-limited throughput of the cooperative relay channel as a function of the source-to-destination channel. However, it is outlined that this technique is inappropriate to benchmark the performance of the HARQ-DDF protocol against the HARQ-SISO and the HARQ-MISO protocol from an energy efficiency point

of view. Therefore, in [18] the TPA DDF protocol variant is used to enable the performance comparison of the DDF relay channel against the SISO and the MISO channel from an energy efficiency point of view. But this protocol variant complicates the DDF protocol and might not be feasible in practice. Instead, it is appropriate to consider the NPA protocol variant.

In order to include the energy efficiency perspective into the performance comparison of the HARQ-DDF and the HARDQ-MISO protocols against the HARQ-SISO and the HARQ-MISO protocols, this work recommends to measure the performance on the system level, i.e. the performance measures should be given as a function of the D-SNR.

The sequel briefly reviews the main contributions of this work and gives recommendations for future applications:

- Section 6.1 and Section 7.3 compare the performance characteristics of the HARQ-SISO, HARQ-MISO, HARDQ-MISO and the HARQ-DDF protocol measured on the one side as a function of the SD-SNR and on the other side measured as a function of the D-SNR. Taking the energy efficiency into account, this comparison reveals that the HARQ-DDF protocol and the HARDQ-MISO protocol outperform the HARQ-MISO protocol in terms of outage probability. Therefore, in case that the figure of merit is the outage probability, i.e. reliability, the HARQ-DDF protocol and the HARDQ-MISO protocol are preferable. On the other hand, in case that the figure of merit is the delay-limited throughput, the HARQ-MISO protocol should be used.
- Measuring the performance as a function of the D-SNR, it is demonstrated in Section 6.3 and Section 7.4 that the NPA protocols outperform the TPA protocols in terms of outage probability. However, considering high rate codes, the TPA protocols outperform the NPA protocols in terms of delay-limited throughput. Considering low rate codes the differences in delay-limited throughput are negligible. Consequently, in case that the figure of merit is the outage probability it is recommended to apply the NPA protocols. In case that the figure of merit is the delay-limited throughput it is recommended to apply the TPA protocols.
- In [31] it is demonstrated that code-rate assignment techniques enable to

gain performance in terms of throughput for the HARQ-SISO protocol using Gaussian channel inputs. These results are confirmed in Section 6.2 for the HARQ-MISO, HARDQ-MISO and the HARQ-DDF protocol. Furthermore, it is demonstrated that code-rate assignment techniques provide even more remarkable performance gains considering discrete channel inputs, as used in real-world applications.

Additionally, in Section 6.4, 6.5, 7.5 and 7.6 it is demonstrated that code-rate assignment techniques enable scalability of decoding cost with negligible performance loss.

Therefore, it is recommended that code design for the HARQ-MISO, HARDQ-MISO and the HARQ-DDF protocol takes the application of code-rate assignment techniques into account.

- Chapter 5 gives the closed form solutions for the fixed-rate outage probability and the delay-limited throughput for the HARQ-SISO, HARQ-MISO, HARDQ-MISO and the HARQ-DDF protocol considering code-rate assignment and Gaussian channel inputs. These results can be used for code-rate assignment optimization considering fixed-rate outage probability, delay-limited throughput and decoding cost. Furthermore, the closed-form solutions provide valuable performance benchmarks for real-world applications.
- In Chapter 7 the RCPC code is used to validate the performance properties investigated in Chapter 6 using a practical coding scheme. For real-world applications it is recommended to consider low-density parity-check codes and turbo codes since these codes are known to achieve better performance.

### Outlook Towards Future Work

---

The research carried out in this work applies the long-term quasi-static Rayleigh fading channel to model the land mobile radio channel and the WLAN channel. As discussed in Section 3.1, this channel model is not appropriate to model real-world scenarios. Thus, continuing research should consider the Suzuki process to obtain a more appropriate channel model.

Measuring the performance of the HARDQ-MISO and the HARQ-DDF protocol on the system-level as a function of the D-SNR enables the comparison against the HARDQ-MISO and the HARQ-DDF protocol from an energy efficiency perspective. However, this method enables the performance comparison on the system level within a large number of communication protocols, such as the corresponding non-HARQ protocols, the orthogonal DF protocols, and the non-orthogonal and orthogonal AF protocols. In context of this work, the performance comparison of the DDF protocol with the orthogonal DF protocols is of particular interest, since the DDF protocol comes together with a higher degree of complexity.

Furthermore, energy efficiency is the main objective in the field of green communication. In this context, the LTW DF protocol is embedded into cognitive

radio schemes to exploit cooperative diversity gains in [3, 17]. Since the DDF protocol outperforms the LTW DF protocol its application in cognitive radio systems is of particular interest. In this research the performance analysis should be carried out considering the D-SNR to enable the comparison of energy efficiency among different protocols on the system level.

In order to simplify the problem analysis in this work, the mobile wireless network is reduced to the single relay channel model. While this approach is appropriate for initial research activities, future research has to focus on the extension towards multiple relays and cooperative communication networks.

Furthermore, the computational cost analysis is of major importance for the practical application of a coding scheme in a communication system. In particular, in context of mobile wireless communication it is desirable to minimize the computational cost, since it has a major impact on power consumption and dissipation, and the required CPU clock rate. Throughout this work, computational cost is considered to be dominated by the decoding process. The Sections 6.4, 6.5, 7.6 and 7.5 give a performance analysis of the HARQ protocols considering the worst-case computational cost. However, for a comprehensive analysis, the decoding cost has to be computed considering the probability of decoding in a particular ARQ round. Using this result and the analysis given in Chapter 5, Chapter 6 and Chapter 7, an interesting research activity is to investigate the optimal trade-off between outage probability, delay-limited throughput and computational cost.

By perforation of the decoding instant sets applied at the relay it is demonstrated that the worst-case computational cost can be significantly reduced without sacrificing delay-limited throughput. However, a major performance loss in terms of outage probability can be observed. By perforation of the decoding instant sets applied at the destination it is demonstrated that a significantly reduced worst-case computational cost results in a small increase in outage probability while a significant impact on the delay-limited throughput can be observed. Due to these results, it can be conjectured that the optimization of the trade-off between outage probability, delay-limited throughput and computational cost can be performed independently for the relay and the destination.

Further related and promising research areas include transmit power opti-

mization techniques and rate optimization techniques as investigated in [31].

## References

---

- [1] Cisco, “Cisco visual networking index: Global mobile data traffic forecast update, 2013-2018,” Feb. 2014. [Online]. Available: [http://www.cisco.com/c/en/us/solutions/collateral/service-provider/visual-networking-index-vni/white\\_paper\\_c11-520862.pdf](http://www.cisco.com/c/en/us/solutions/collateral/service-provider/visual-networking-index-vni/white_paper_c11-520862.pdf)
- [2] A. Kumar, K. Singh, and D. Bhattacharya, “Green communication and wireless networking,” in *Green Computing, Communication and Conservation of Energy (ICGCE), 2013 International Conference on*, Dec. 2013, pp. 49–52.
- [3] D. Liu, W. Wang, and W. Guo, “‘green’ cooperative spectrum sharing communication,” *Communications Letters, IEEE*, vol. 17, no. 3, pp. 459–462, Mar. 2013.
- [4] M. Naeem, A. Anpalagan, M. Jaseemuddin, and D. Lee, “Resource allocation techniques in cooperative cognitive radio networks,” *Communications Surveys Tutorials, IEEE*, vol. 16, no. 2, pp. 729–744, Second 2014.
- [5] “Notice of proposed rule making and order,” FCC, Tech. Rep. 03-322, Dec 2003.
- [6] I. Akyildiz, W.-Y. Lee, M. C. Vuran, and S. Mohanty, “A survey on spectrum management in cognitive radio networks,” *Communications Magazine, IEEE*, vol. 46, no. 4, pp. 40–48, Apr. 2008.
- [7] M. Luo, Y. Chen, J. Zhang, and K. Lan, “Optimal power and time allocation in green cooperative cognitive radio network,” in *Signal Processing (ICSP), 2014 12th International Conference on*, Oct. 2014, pp. 123–127.

- [8] E. Telatar, “Capacity of Multi-antenna Gaussian Channels,” *European Transactions on Telecommunications*, vol. 10, pp. 585–595, 1999.
- [9] G. J. Foschini and M. J. Gans, “On limits of wireless communications in a fading environment when using multiple antennas,” *Wirel. Pers. Commun.*, vol. 6, no. 3, pp. 311–335, 1998.
- [10] S. M. Alamouti, “A simple transmit diversity technique for wireless communications,” *Selected Areas in Communications, IEEE Journal on*, vol. 16, no. 8, pp. 1451–1458, 1998.
- [11] A. Sendonaris, E. Erkip, and B. Aazhang, “User cooperation diversity. Part I. System description,” *Communications, IEEE Transactions on*, vol. 51, no. 11, pp. 1927–1938, Nov. 2003.
- [12] —, “User cooperation diversity. Part II. Implementation aspects and performance analysis,” *Communications, IEEE Transactions on*, vol. 51, no. 11, pp. 1939–1948, Nov. 2003.
- [13] J. Laneman and G. Wornell, “Distributed space-time-coded protocols for exploiting cooperative diversity in wireless networks,” *Information Theory, IEEE Transactions on*, vol. 49, no. 10, pp. 2415 – 2425, Oct. 2003.
- [14] J. Laneman, D. Tse, and G. Wornell, “Cooperative diversity in wireless networks: Efficient protocols and outage behavior,” *Information Theory, IEEE Transactions on*, vol. 50, no. 12, pp. 3062 – 3080, Dec. 2004.
- [15] J. Hagenauer, “Rate-compatible punctured convolutional codes (RCPC codes) and their applications,” *Communications, IEEE Transactions on*, vol. 36, no. 4, pp. 389 –400, Apr. 1988.
- [16] B. Makki, A. Graell i Amat, and T. Eriksson, “Green communication via power-optimized harq protocols,” *Vehicular Technology, IEEE Transactions on*, vol. 63, no. 1, pp. 161–177, Jan. 2014.
- [17] M. Naeem, K. Illanko, A. Karmokar, A. Anpalagan, and M. Jaseemuddin, “Power allocation in decode and forward relaying for green cooperative cognitive radio systems,” in *Wireless Communications and Networking Conference (WCNC), 2013 IEEE*, Apr. 2013, pp. 3806–3810.

- [18] K. Azarian, H. El Gamal, and P. Schniter, "On the achievable diversity-multiplexing tradeoff in half-duplex cooperative channels," *Information Theory, IEEE Transactions on*, vol. 51, no. 12, pp. 4152–4172, Dec. 2005.
- [19] —, "On the optimality of the ARQ-DDF protocol," *Information Theory, IEEE Transactions on*, vol. 54, no. 4, pp. 1718–1724, Apr. 2008.
- [20] L. Zheng and D. Tse, "Diversity and multiplexing: A fundamental tradeoff in multiple-antenna channels," *Information Theory, IEEE Transactions on*, vol. 49, no. 5, pp. 1073–1096, May 2003.
- [21] M. Yuksel and E. Erkip, "Multiple-antenna cooperative wireless systems: A diversity-multiplexing tradeoff perspective," *Information Theory, IEEE Transactions on*, vol. 53, no. 10, pp. 3371–3393, Oct. 2007.
- [22] K. Azarian, "Outage limited cooperative channels: Protocols and analysis," dissertation, Ohio State University, 2006. [Online]. Available: <https://etd.ohiolink.edu/>
- [23] R. Narasimhan, "Throughput-delay performance of half-duplex hybrid-ARQ relay channels," in *Communications, 2008. ICC '08. IEEE International Conference on*, 2008, pp. 986–990.
- [24] M. Khormuji and E. Larsson, "Cooperative transmission based on decode-and-forward relaying with partial repetition coding," *Wireless Communications, IEEE Transactions on*, vol. 8, no. 4, pp. 1716–1725, Apr. 2009.
- [25] K. Kumar and G. Caire, "Coding and decoding for the dynamic decode and forward relay protocol," *Information Theory, IEEE Transactions on*, vol. 55, no. 7, pp. 3186–3205, July 2009.
- [26] A. Murugan, K. Azarian, and H. E. Gamal, "Cooperative lattice coding and decoding in half-duplex channels," *Selected Areas in Communications, IEEE Journal on*, vol. 25, no. 2, pp. 268–279, Feb. 2007.
- [27] A. Ravanshid, L. Lampe, and J. Huber, "Dynamic decode-and-forward relaying using raptor codes," *Wireless Communications, IEEE Transactions on*, vol. 10, no. 5, pp. 1569–1581, May 2011.

- [28] S. Tian, Y. Li, and B. Vucetic, "A rateless code for dynamic decode-and-forward relaying in wireless relay networks," in *Wireless Communications and Networking Conference (WCNC), 2013 IEEE*, April 2013, pp. 3551–3556.
- [29] C. Hucher and P. Sadeghi, "Towards a low-complexity dynamic decode-and-forward relay protocol," *ArXiv e-prints*, Dec. 2010.
- [30] S. Maagh, J. Sharp, and T. Binnie, "The dynamic decode-and-forward channel: SNR allocation for fair performance analysis," in *Telecommunications Forum (TELFOR), 2013*, Nov. 2013, pp. 319–322.
- [31] C. Shen, T. Liu, and M. Fitz, "On the average rate performance of hybrid-ARQ in quasi-static fading channels," *Communications, IEEE Transactions on*, vol. 57, no. 11, pp. 3339–3352, Nov. 2009.
- [32] G. Caire and D. Tuninetti, "The throughput of hybrid-ARQ protocols for the Gaussian collision channel," *Information Theory, IEEE Transactions on*, vol. 47, no. 5, pp. 1971–1988, July 2001.
- [33] S. Sandhu and A. Paulraj, "Space-time block codes: A capacity perspective," *Communications Letters, IEEE*, vol. 4, no. 12, pp. 384–386, 2000.
- [34] G. Böcherer, "Capacity-achieving probabilistic shaping for noisy and noiseless channels," dissertation, RWTH Aachen, 2012. [Online]. Available: <http://www.georg-boecherer.de/capacityAchievingShaping.pdf>
- [35] E. Agrell and A. Alvarado, "Optimal alphabets and binary labelings for bicm at low snr," *Information Theory, IEEE Transactions on*, vol. 57, no. 10, pp. 6650–6672, Oct 2011.
- [36] D. Guo, S. Shamai, and S. Verdú, "Mutual information and minimum mean-square error in gaussian channels," *Information Theory, IEEE Transactions on*, vol. 51, no. 4, pp. 1261–1282, Apr. 2005.
- [37] S. Maagh and M. Sharif, "RCPC coding for the dynamic decode-and-forward channel," in *Microwaves, Communications, Antennas and Electronics Systems (COMCAS), 2011 IEEE International Conference on*, Nov. 2011, pp. 1–6.

- [38] J. G. Proakis and M. Salehi, *Digital Communications*, 5th ed. McGraw-Hill, 2008.
- [39] C. E. Shannon, "A mathematical theory of communication," *Bell system technical journal*, vol. 27, 1948.
- [40] R. G. Gallager, *Information Theory and Reliable Communication*. New York, NY, USA: John Wiley & Sons, Inc., 1968.
- [41] L. Ozarow, S. Shamai, and A. Wyner, "Information theoretic considerations for cellular mobile radio," *Vehicular Technology, IEEE Transactions on*, vol. 43, no. 2, pp. 359–378, May 1994.
- [42] X. Li, Y.-C. Wu, and E. Serpedin, "Timing synchronization in decode-and-forward cooperative communication systems," *Signal Processing, IEEE Transactions on*, vol. 57, no. 4, pp. 1444–1455, Apr. 2009.
- [43] E. Lindskog and A. Paulraj, "A transmit diversity scheme for channels with intersymbol interference," in *Communications, 2000. ICC 2000. 2000 IEEE International Conference on*, vol. 1, 2000, pp. 307–311 vol.1.
- [44] R. F. H. Fischer, *Precoding and Signal Shaping for Digital Transmission*. John Wiley & Sons, Inc., 2002.
- [45] B. Vucetic and J. Yuan, *Space-Time Coding*. New York, NY, USA: John Wiley & Sons, Inc., 2003.
- [46] S. Shamai and A. Wyner, "Information-theoretic considerations for symmetric, cellular, multiple-access fading channels. i," *Information Theory, IEEE Transactions on*, vol. 43, no. 6, pp. 1877–1894, 1997.
- [47] N. Lo, D. Falconer, and A. U. H. Sheikh, "Adaptive equalizer MSE performance in the presence of multipath fading, interference and noise," in *Vehicular Technology Conference, 1995 IEEE 45th*, vol. 1, July 1995, pp. 409–413 vol.1.
- [48] M. Tomlinson, "New automatic equaliser employing modulo arithmetic," *Electronics Letters*, vol. 7, no. 5, pp. 138–139, Mar. 1971.

- [49] H. Harashima and H. Miyakawa, “Matched-transmission technique for channels with intersymbol interference,” *Communications, IEEE Transactions on*, vol. 20, no. 4, pp. 774 – 780, Aug. 1972.
- [50] J. Cioffi, G. Dudevoir, M. Vedat Eyuboglu, and J. Forney, G.D., “MMSE decision-feedback equalizers and coding. I. equalization results,” *Communications, IEEE Transactions on*, vol. 43, no. 10, pp. 2582 –2594, Oct. 1995.
- [51] J. Cioffi, G. Dudevoir, M. Eyuboglu, and J. Forney, G.D., “MMSE decision-feedback equalizers and coding. II. coding results,” *Communications, IEEE Transactions on*, vol. 43, no. 10, pp. 2595 –2604, Oct. 1995.
- [52] N. Al-Dhahir and J. Cioffi, “MMSE decision-feedback equalizers: Finite-length results,” *Information Theory, IEEE Transactions on*, vol. 41, no. 4, pp. 961 –975, July 1995.
- [53] J. G. Proakis, C. M. Rader, F. Ling, and C. L. Nikias, *Advanced Digital Signal Processing*. Macmillan Publishing Company, 1992.
- [54] J. Proakis and J. Miller, “An adaptive receiver for digital signaling through channels with intersymbol interference,” *Information Theory, IEEE Transactions on*, vol. 15, no. 4, July 1969.
- [55] M. Patzold, U. Killat, Y. Li, and F. Laue, “Modeling, analysis, and simulation of nonfrequency-selective mobile radio channels with asymmetrical doppler power spectral density shapes,” *Vehicular Technology, IEEE Transactions on*, vol. 46, no. 2, pp. 494–507, May 1997.
- [56] H. Suzuki, “A statistical model for urban radio propagation,” *Communications, IEEE Transactions on*, vol. 25, no. 7, pp. 673–680, Jul 1977.
- [57] B. Lankl, A. Knopp, and M. Chouayakh, “Channel model and capacity for broadband indoor MIMO-WLAN systems based on measurements at 2.4 ghz,” *e&i Elektrotechnik und Informationstechnik*, vol. 122, no. 6, pp. 206–209, 2005.

- [58] M. Nakagami, "The m-distribution - a general formula of intensity distribution of rapid fading," in *Statistical Methods in Radio Wave Propagation*, W. C. Hoffman, Ed., Elmsford, NY: Pergamon, 1960.
- [59] X. Li and Q.-A. Zeng, "Capture effect in the IEEE 802.11 WLANs with Rayleigh fading, shadowing, and path loss," in *Wireless and Mobile Computing, Networking and Communications, 2006. (WiMob'2006). IEEE International Conference on*, June 2006, pp. 110–115.
- [60] V. Tarokh, N. Seshadri, and A. R. Calderbank, "Space-time codes for high data rate wireless communication: performance criterion and code construction," *Information Theory, IEEE Transactions on*, vol. 44, no. 2, pp. 744–765, 1998.
- [61] F. Oggier, J.-C. Belfiore, and E. Viterbo, "Cyclic division algebras: A tool for space-time coding," *Found. Trends Commun. Inf. Theory*, vol. 4, no. 1, pp. 1–95, 2007.
- [62] O. Tirkkonen and A. Hottinen, "Square-matrix embeddable space-time block codes for complex signal constellations," *Information Theory, IEEE Transactions on*, vol. 48, no. 2, pp. 384–395, 2002.
- [63] V. Tarokh, H. Jafarkhani, and A. R. Calderbank, "Space-time block codes from orthogonal designs," *Information Theory, IEEE Transactions on*, vol. 45, no. 5, pp. 1456–1467, 1999.
- [64] F. Oggier, G. Rekaya, J.-C. Belfiore, and E. Viterbo, "Perfect space-time block codes," *Information Theory, IEEE Transactions on*, vol. 52, no. 9, pp. 3885–3902, Sept. 2006.
- [65] T. M. Cover and J. A. Thomas, *Elements of Information Theory*, 2nd ed. Wiley-Interscience, 2006.
- [66] H. El-Gamal, G. Caire, and M.-O. Damen, "The MIMO ARQ channel: Diversity-multiplexing-delay tradeoff," *Information Theory, IEEE Transactions on*, Aug. 2006.
- [67] "SAR EVALUATION REPORT," FCC, Tech. Rep. BCG-E2642A, Sept 2013.

- [68] “SAR EVALUATION REPORT,” FCC, Tech. Rep. BCG-E2642A, Aug 2014.
- [69] R. Nabar, H. Bolcskei, and F. Kneubuhler, “Fading relay channels: performance limits and space-time signal design,” *Selected Areas in Communications, IEEE Journal on*, vol. 22, no. 6, pp. 1099–1109, Aug. 2004.
- [70] J. Zhang and Q. Zhang, “Stackelberg game for utility-based cooperative cognitive radio networks,” in *MobiHoc '09: Proceedings of the tenth ACM international symposium on Mobile ad hoc networking and computing*. New York, NY, USA: ACM, May 2009, pp. 23–32.
- [71] Y. Wang, G. Sun, and X. Wang, “A game theory approach for power control and relay selection in cooperative communication networks with asymmetric information,” in *Wireless Communications and Networking Conference Workshops (WCNCW), 2013 IEEE*, Apr. 2013, pp. 60–65.
- [72] B. Sirkeci-Mergen and A. Scaglione, “Randomized distributed space-time coding for cooperative communication in self organized networks,” June 2005, pp. 500 – 504.
- [73] M. Katz and S. Shamai, “Transmitting to colocated users in wireless ad hoc and sensor networks,” *Information Theory, IEEE Transactions on*, vol. 51, no. 10, pp. 3540–3563, Oct. 2005.
- [74] P. Mitran, H. Ochiari, and V. Tarokh, “Space-time diversity enhancements using collaborative communications,” *Information Theory, IEEE Transactions on*, vol. 51, no. 6, pp. 2041–2057, June 2005.
- [75] T. Tabet, S. Dusad, and R. Knopp, “Achievable diversity-multiplexing-delay tradeoff in half-duplex ARQ relay channels,” in *Information Theory, 2005. ISIT 2005. Proceedings. International Symposium on*, Sept. 2005, pp. 1828–1832.
- [76] S. Karmakar and M. Varanasi, “Diversity-multiplexing-delay tradeoff of a DDF protocol on a half-duplex ARQ relay channel,” in *Signals, Systems and Computers, 2009 Conference Record of the Forty-Third Asilomar Conference on*, Nov. 2009, pp. 1729–1733.

- [77] A. Chuang, A. Guillen i Fabregas, L. Rasmussen, and I. Collings, "Optimal throughput-diversity-delay tradeoff in MIMO ARQ block-fading channels," *Information Theory, IEEE Transactions on*, vol. 54, no. 9, pp. 3968–3986, Sept. 2008.
- [78] C. Shen and M. Fitz, "Hybrid ARQ schemes in multiple-antenna slow fading channels: A capacity perspective," in *Signals, Systems and Computers, 2008 42nd Asilomar Conference on*, Oct. 2008, pp. 1340–1344.
- [79] I. M. I. Habbab, M. Kavehrad, and C.-E. W. Sundberg, "Aloha with capture over slow and fast fading radio channels with coding and diversity," *Selected Areas in Communications, IEEE Journal on*, vol. 7, no. 1, pp. 79–88, 1989.
- [80] L. G. Roberts, "Aloha packet system with and without slots and capture," *SIGCOMM Comput. Commun. Rev.*, vol. 5, no. 2, Apr.
- [81] D. Chase, "Code combining—a maximum-likelihood decoding approach for combining an arbitrary number of noisy packets," *Communications, IEEE Transactions on*, vol. 33, no. 5, pp. 385–393, 1985.
- [82] A. Neubauer, J. Freudenberger, and V. Kuehn, *Coding Theory, Algorithms, Architecture and Applications*. John Wiley & Sons, Inc., 2007.
- [83] R. Comroe and J. Costello, D.J., "ARQ schemes for data transmission in mobile radio systems," *Selected Areas in Communications, IEEE Journal on*, vol. 2, no. 4, pp. 472–481, July 1984.
- [84] H. A. Ngo and L. Hanzo, "Hybrid automatic-repeat-request systems for cooperative wireless communications," *Communications Surveys Tutorials, IEEE*, vol. 16, no. 1, pp. 25–45, First 2014.
- [85] H. Y. Kong, H. V. Khuong, and D. H. Nam, "Exact error and outage probability formulas for Alamouti space time code  $2 \times j$ ," *Communications and Networks, Journal of*, vol. 9, no. 2, pp. 177–184, June 2007.
- [86] C. Shen and M. Fitz, "Hybrid ARQ in multiple-antenna slow fading channels: Performance limits and optimal linear dispersion code design," *In-*

- formation Theory, IEEE Transactions on*, vol. 57, no. 9, pp. 5863–5883, Sept. 2011.
- [87] H. Alves, R. Demo Souza, G. Brante, and M. Pellenz, “Performance of type-I and type-II hybrid ARQ in decode and forward relaying,” in  *Vehicular Technology Conference (VTC Spring), 2011 IEEE 73rd*, May. 2011, pp. 1–5.
- [88] C. Xiao and Y. Zheng, “On the mutual information and power allocation for vector Gaussian channels with finite discrete inputs,” in *Global Telecommunications Conference, 2008. IEEE GLOBECOM 2008. IEEE*, Nov. 2008, pp. 1–5.
- [89] L. Ozarow and A. Wyner, “On the capacity of the Gaussian channel with a finite number of input levels,” *Information Theory, IEEE Transactions on*, vol. 36, no. 6, pp. 1426–1428, Nov. 1990.
- [90] E. Baccarelli, “Asymptotically tight bounds on the capacity and outage probability for QAM transmissions over Rayleigh-faded data channels with CSI,” *Communications, IEEE Transactions on*, vol. 47, no. 9, pp. 1273–1277, Sep. 1999.
- [91] K. Nguyen, A. Fabregas, and L. Rasmussen, “Analysis and computation of the outage probability of discrete-input block-fading channels,” in *Information Theory, 2007. ISIT 2007. IEEE International Symposium on*, June 2007, pp. 1196–1200.
- [92] T. Cover and A. Gamal, “Capacity theorems for the relay channel,” *Information Theory, IEEE Transactions on*, vol. 25, no. 5, pp. 572–584, Sep. 1979.
- [93] A. Host-Madsen, “On the capacity of wireless relaying,” in *Vehicular Technology Conference, 2002. Proceedings. VTC 2002-Fall. 2002 IEEE 56th*, vol. 3, 2002, pp. 1333–1337 vol.3.
- [94] S. Maagh, M. Y. Sharif, and A. E. A. Almaini, “On the dynamic decode-and-forward relay listen-transmit decision rule in intersymbol interference channels,” in *Proceedings of the 9th WSEAS International Conference on*

- Data Networks, Communications, Computers*, ser. DNCOCO'10. Stevens Point, Wisconsin, USA: World Scientific and Engineering Academy and Society (WSEAS), 2010, pp. 26–29.
- [95] R. P. Brent, “An algorithm with guaranteed convergence for finding a zero of a function,” *The Computer Journal*, vol. 14, no. 4, pp. 422–425, Mar. 1971.
- [96] G. P. Lepage, “Vegas: An adaptive multidimensional integration program,” 1980.
- [97] *GNU Scientific Library Reference Manual - Third Edition*. Network Theory Ltd., 2009.
- [98] E. Zio, *The Monte Carlo Simulation Method for System Reliability and Risk Analysis (Springer Series in Reliability Engineering)*. Springer, 2012.
- [99] C. P. Robert and G. Casella, *Introducing Monte Carlo Methods with R (Use R!)*. Springer Verlag, 2009.
- [100] R. Demming and D. J. Duffy, *Introduction to the Boost C++ Libraries; Volume I - Foundations*. Datasim Education BV, 2010.
- [101] S. Loyka and G. Levin, “On outage probability and diversity-multiplexing tradeoff in MIMO relay channels,” *Communications, IEEE Transactions on*, vol. 59, no. 6, pp. 1731–1741, June 2011.
- [102] H. Lee, R. Heath, and E. Powers, “Information outage probability and diversity order of Alamouti transmit diversity in time-selective fading channels,” *Vehicular Technology, IEEE Transactions on*, vol. 57, no. 6, pp. 3890–3895, Nov. 2008.
- [103] B. Chalise and A. Czulwik, “Exact outage probability analysis for a multiuser MIMO wireless communication system with space-time block coding,” *Vehicular Technology, IEEE Transactions on*, vol. 57, no. 3, pp. 1502–1512, May 2008.

- [104] J. Perez, J. Ibanez, L. Vielva, and I. Santamaria, "Closed-form approximation for the outage capacity of orthogonal STBC," *Communications Letters, IEEE*, vol. 9, no. 11, pp. 961–963, Nov. 2005.
- [105] H. Zhang and T. Gulliver, "Capacity and error probability analysis for orthogonal space-time block codes over fading channels," *Wireless Communications, IEEE Transactions on*, vol. 4, no. 2, pp. 808–819, Mar. 2005.
- [106] S. Lin and D. J. Costello, *Error Control Coding*, 2nd ed. Prentice-Hall, Inc., 2004.
- [107] J. Cain, G. Clark, and J. Geist, "Punctured convolutional codes of rate  $(n-1)/n$  and simplified maximum likelihood decoding (corresp.)," *Information Theory, IEEE Transactions on*, vol. 25, no. 1, pp. 97 – 100, Jan. 1979.
- [108] D. Haccoun and G. Begin, "High-rate punctured convolutional codes for viterbi and sequential decoding," *Communications, IEEE Transactions on*, vol. 37, no. 11, pp. 1113–1125, 1989.
- [109] P. Frenger, P. Orten, T. Ottosson, and A. Svensson, "Multi-rate convolutional codes," Dept. of Signals and Systems, Chalmers University of Technology, Goteborg, Sweden, Technical Report 21, Apr. 1998.
- [110] A. Viterbi, "Error bounds for convolutional codes and an asymptotically optimum decoding algorithm," *Information Theory, IEEE Transactions on*, vol. 13, no. 2, pp. 260 – 269, Apr. 1967.
- [111] R. Fano, "A heuristic discussion of probabilistic decoding," *Information Theory, IEEE Transactions on*, vol. 9, no. 2, pp. 64–74, 1963.
- [112] L. Bahl, J. Cocke, F. Jelinek, and J. Raviv, "Optimal decoding of linear codes for minimizing symbol error rate (corresp.)," *Information Theory, IEEE Transactions on*, vol. 20, no. 2, pp. 284–287, 1974.
- [113] W. Peterson and D. Brown, "Cyclic codes for error detection," *Proceedings of the IRE*, vol. 49, no. 1, pp. 228–235, 1961.
- [114] G. Castagnoli, J. Ganz, and P. Graber, "Optimum cyclic redundancy-check codes with 16-bit redundancy," *Communications, IEEE Transactions on*, vol. 38, no. 1, pp. 111 –114, Jan. 1990.

- 
- [115] G. Castagnoli, S. Brauer, and M. Herrmann, "Optimization of cyclic redundancy-check codes with 24 and 32 parity bits," *Communications, IEEE Transactions on*, vol. 41, no. 6, pp. 883–892, 1993.
- [116] C. Berrou and A. Glavieux, "Near optimum error correcting coding and decoding: Turbo-codes," *Communications, IEEE Transactions on*, vol. 44, no. 10, pp. 1261–1271, 1996.
- [117] S. Nagaraj, "Generalized BICM for block fading channels," *Wireless Communications, IEEE Transactions on*, vol. 7, no. 11, pp. 4404–4410, 2008.

## Outage Probability

---

This chapter gives the derivation the outage probability of the HARQ-MISO channel, the HARDQ-MISO channel. To simplify notation, define the joint probability of two mutually independent, exponentially distributed random variables  $\gamma_0$  and  $\gamma_1$  with respective mean  $\sigma_0^2$  and  $\sigma_1^2$  as

$$G(\gamma_0, \gamma_1) = \frac{1}{\sigma_0^2 \sigma_1^2} e^{-\frac{\gamma_0}{\sigma_0^2} - \frac{\gamma_1}{\sigma_1^2}}. \quad (\text{A.1})$$

### A.1 Outage Probability of the HARQ-MISO protocol

The mutual information of the complex Alamouti encoded MISO channel with two transmit antennas at the source and a single receive antenna at the destination is given as

$$I^{(2)} = \log_2(1 + \rho(\gamma_0 + \gamma_1)), \quad (\text{A.2})$$

where  $\rho$  denotes the SNR at the destination and  $\gamma_0$  and  $\gamma_1$  denote the exponentially distributed channel gains with mean  $\sigma_0^2$  and  $\sigma_1^2$ , respectively. Then, the

outage probability is defined as

$$P_{\text{out}}^{(2)} = \Pr(I^{(2)} < R) \quad (\text{A.3})$$

$$= \Pr\left(\gamma_0 + \gamma_1 < \frac{2^R - 1}{\rho}\right), \quad (\text{A.4})$$

where  $R > 0$  and  $\rho > 0$ .

For  $\sigma_0^2 = \sigma_1^2 = 0$  the expectation of the mutual information becomes

$$\mathbb{E}[I^{(2)}] = 0, \quad (\text{A.5})$$

i.e., no reliable communication across the MISO channel is possible, and therefore the outage probability is given as

$$P_{\text{out}}^{(2)} = 1, \quad \sigma_0^2 = 0, \sigma_1^2 = 0. \quad (\text{A.6})$$

For  $\sigma_0^2 = 0$  and  $\sigma_1^2 > 0$ , or  $\sigma_1^2 = 0$  and  $\sigma_0^2 > 0$  the MISO channel effectively represents the SISO channel with the outage probabilities

$$P_{\text{out}}^{(2)} = 1 - e^{-\frac{2^R - 1}{\rho\sigma_0^2}}, \quad \sigma_0^2 > 0, \sigma_1^2 = 0, \quad (\text{A.7})$$

$$P_{\text{out}}^{(2)} = 1 - e^{-\frac{2^R - 1}{\rho\sigma_1^2}}, \quad \sigma_0^2 = 0, \sigma_1^2 > 0. \quad (\text{A.8})$$

For  $\sigma = \sigma_0^2 = \sigma_1^2$  (A.4) can be solved using the Erlang distribution as

$$P_{\text{out},\text{MISO}} = 1 - \left(1 + \frac{2^R - 1}{\rho\sigma^2}\right) e^{-\frac{2^R - 1}{\rho\sigma^2}}, \quad \sigma^2 = \sigma_0^2 = \sigma_1^2. \quad (\text{A.9})$$

For  $\sigma_0^2 > 0$ ,  $\sigma_1^2 > 0$  and  $\sigma_0^2 \neq \sigma_1^2$  the outage probability (A.4) is given by the solution of

$$P_{\text{out},\text{MISO}} = \int_{\gamma_0=0}^M \int_{\gamma_1=0}^{\beta(\gamma_0)} G(\gamma_0, \gamma_1) d\gamma_0 d\gamma_1, \quad (\text{A.10})$$

where the integral limits

$$M = \frac{2^R - 1}{\rho}, \quad (\text{A.11})$$

and

$$\beta(\gamma_1) = M - \gamma_1 \quad (\text{A.12})$$

are defined by the condition  $\gamma_0 + \gamma_1 < \frac{2^R - 1}{\rho}$ . Then, the solution of (A.10) is

$$P_{out,MISO} = \frac{1}{\sigma_0^2 \sigma_1^2} \int_{\gamma_0=0}^M \int_{\gamma_1=0}^{\beta(\gamma_0)} e^{-\frac{\gamma_0}{\sigma_0^2} - \frac{\gamma_1}{\sigma_1^2}} d\gamma_0 d\gamma_1 \quad (\text{A.13})$$

$$= \frac{1}{\sigma_0^2} \int_{\gamma_0=0}^M e^{-\frac{\gamma_0}{\sigma_0^2}} \left[ 1 - e^{-\frac{\beta(\gamma_0)}{\sigma_1^2}} \right] d\gamma_0 \quad (\text{A.14})$$

$$= \frac{1}{\sigma_0^2} \int_{\gamma_0=0}^M e^{-\frac{\gamma_0}{\sigma_0^2}} d\gamma_0 - \frac{1}{\sigma_0^2} \int_{\gamma_0=0}^M e^{-\frac{\gamma_0}{\sigma_0^2} - \frac{\beta(\gamma_0)}{\sigma_1^2}} d\gamma_0 \quad (\text{A.15})$$

$$= 1 - e^{-\frac{M}{\sigma_0^2}} - \frac{1}{\sigma_1^2} \int_{\gamma_0=0}^M e^{-\frac{\gamma_0}{\sigma_0^2} - \frac{M-\gamma_0}{\sigma_1^2}} d\gamma_0 \quad (\text{A.16})$$

$$= 1 - e^{-\frac{M}{\sigma_0^2}} - \frac{e^{-\frac{M}{\sigma_1^2}}}{\sigma_1^2} \int_{\gamma_0=0}^M e^{-\gamma_0 \frac{\sigma_1^2 - \sigma_0^2}{\sigma_0^2 \sigma_1^2}} d\gamma_0 \quad (\text{A.17})$$

$$= 1 - e^{-\frac{M}{\sigma_0^2}} - \frac{\sigma_0^2}{\sigma_1^2 - \sigma_0^2} e^{-\frac{M}{\sigma_1^2}} \left[ 1 - e^{-M \frac{\sigma_1^2 - \sigma_0^2}{\sigma_0^2 \sigma_1^2}} \right], \quad (\text{A.18})$$

where in step

1. (A.14) the integral is solved for  $\gamma_1$ ,
2. (A.15) the remaining integral is split up for readability,
3. (A.16) the left-hand-side integral is solved and  $\beta(\gamma_0)$  is back-substituted in the right-hand side integral,
4. (A.17) the constant  $e^{-\frac{M}{\sigma_1^2}}$  is moved in front the integral,
5. (A.18) the integral is solved for  $\gamma_0$ .

Therefore, the probability density function  $P_{\text{out,MISO}}$  is given as

$$P_{\text{out,MISO}} = \begin{cases} 1, & \sigma_0^2 = 0, \sigma_1^2 = 0, \\ 1 - e^{-\frac{2^{R-1}}{\rho\sigma_0^2}}, & \sigma_0^2 > 0, \sigma_1^2 = 0, \\ 1 - e^{-\frac{2^{R-1}}{\rho\sigma_1^2}}, & \sigma_0^2 = 0, \sigma_1^2 > 0, \\ 1 - \left(1 + \frac{2^{R-1}}{\rho\sigma^2}\right) e^{-\frac{2^{R-1}}{\rho\sigma^2}}, & \sigma^2 = \sigma_0^2 = \sigma_1^2, \\ 1 - e^{-\frac{M}{\sigma_0^2}} - \frac{\sigma_0^2}{\sigma_1^2 - \sigma_0^2} e^{-\frac{M}{\sigma_1^2}} \left[1 - e^{-M \frac{\sigma_1^2 - \sigma_0^2}{\sigma_0^2 \sigma_1^2}}\right], & \sigma_0^2 > 0, \sigma_1^2 > 0, \sigma_0^2 \neq \sigma_1^2. \end{cases} \quad (\text{A.19})$$

## A.2 Outage Probability of the HARDQ-MISO protocol

Let  $l$  denote the current ARQ round,  $t$  the ARQ round in which both antennas are used for transmission, and define  $l \in \mathcal{D}_d$  throughout this chapter. Then, the mutual information accumulated up to ARQ round  $l$  of the channel between the source and the destination, and considering the HARDQ-MISO protocol is given as

$$I^{(3)}(l) = \begin{cases} I^{(1)}, & t \geq l, \\ \frac{R(l)}{R(t)} I^{(1)} + \frac{R(t) - R(l)}{R(t)} I^{(2)}, & t < l. \end{cases} \quad (\text{A.20})$$

For any  $l \leq t$  the second antenna does not participate in transmission and therefore the outage probability is defined by the SISO channel as

$$P_{\text{out}}(l|l \leq t) = \Pr[I^{(3)}(l) < R(l)] = 1 - e^{-\frac{2^{R(l)} - 1}{\rho_1 \sigma_0^2}}. \quad (\text{A.21})$$

For  $l > t$  the outage probability is

$$P_{\text{out}}(l|l > t) = \Pr(I^{(3)}(l) < R(l)) \quad (\text{A.22})$$

$$= \Pr\left(\gamma_1 + \gamma_0 < \frac{2^\phi - 1}{\sigma_2}\right) \quad (\text{A.23})$$

$$= \int_{\gamma_0=0}^M \int_{\gamma_1}^{\beta(\gamma_0)} G(\gamma_0, \gamma_1) d\gamma_0 d\gamma_1 \quad (\text{A.24})$$

$$= 1 - e^{-\frac{M}{\sigma_0^2}} - \frac{1}{\sigma_0^2} \int_{\gamma_0=0}^M e^{-\frac{\gamma_0}{\sigma_0^2} - \frac{\beta(\gamma_1)}{\sigma_1^2}} d\gamma_0, \quad (\text{A.25})$$

where the derivation follows the same steps 1 to 3 as used in the derivation of (A.14) and  $\phi$  is

$$\phi = 2^{\frac{R(l)R(t)}{R(t)-R(l)} - \frac{R(l)}{R(t)R(l)}} \log(1 + \rho_1 \gamma_0). \quad (\text{A.26})$$

However,  $M$  is given as

$$M = \left\{ \gamma : R(l) = \frac{R(l)}{R(t)} \log_2(1 + \rho_1 \gamma) + \left(1 - \frac{R(l)}{R(t)}\right) \log_2(1 + \rho_2 \gamma) \right\}, \quad (\text{A.27})$$

and  $\beta(\gamma_0)$  is derived as

$$R(l) = \frac{R(l)}{R(t)} \log_2(1 + \rho_1 \gamma_0) + \frac{R(t) - R(l)}{R(t)} \log_2(1 + \rho_2(\gamma_0 + \gamma_1)) \quad (\text{A.28})$$

$$\frac{R(l)R(t)}{R(t) - R(l)} = \frac{R(l)}{R(t) - R(l)} \log_2(1 + \rho_1 \gamma_0) + \log_2(1 + \rho_2(\gamma_0 + \gamma_1)) \quad (\text{A.29})$$

$$2^{\frac{R(l)R(t)}{R(t)-R(l)}} = (1 + \rho_1 \gamma_0)^{\frac{R(l)}{R(t)-R(t)}} (1 + \rho_2(\gamma_0 + \gamma_1)) \quad (\text{A.30})$$

$$\beta(\gamma_0) = \frac{2^{\frac{R(l)R(t)}{R(t)-R(l)}}}{\rho_2 (1 + \rho_1 \gamma_0)^{\frac{R(l)}{R(t)-R(l)}}} - \frac{1}{\rho_2} - \gamma_0 = \gamma_1. \quad (\text{A.31})$$

### A.2.1 Upper and lower bounds for $M$

The upper integration limit  $M$  given in A.27 can be obtained numerically by solving

$$\frac{R(l)}{R(t)} \log_2(1 + \rho_1 \gamma) + \left(1 - \frac{R(l)}{R(t)}\right) \log_2(1 + \rho_2 \gamma) - R(l) = 0 \quad (\text{A.32})$$

for  $\gamma$ , using Brents root finding algorithm [95]. To this end, upper and lower bounds on  $\gamma$  are required to confine the search interval. In order to derive pragmatic bounds differ the three cases  $\rho_1 = \rho_2$ ,  $\rho_1 < \rho_2$  and  $\rho_1 > \rho_2$ .

**Case:**  $\rho_1 = \rho_2$

For  $\rho_1 = \rho_2 = \rho$  the integration limit is

$$M = \frac{2^{R(l)} - 1}{\rho}. \quad (\text{A.33})$$

**Case:**  $\rho_1 < \rho_2$

In this case (A.32) can be upper bounded as

$$\left(1 - \frac{R(l)}{R(t)}\right) \log_2(1 + \rho_2 \gamma) - R(l) < 0, \quad (\text{A.34})$$

which results in

$$\gamma < \frac{2^{\frac{R(l)R(t)}{R(t)-R(l)} - 1}}{\rho_2}. \quad (\text{A.35})$$

A lower bound is given by defining  $\rho_1 := \rho_2$ . Then, (A.32) becomes

$$\frac{R(l)}{R(t)} \log_2(1 + \rho_2 \gamma) + \left(1 - \frac{R(l)}{R(t)}\right) \log_2(1 + \rho_2 \gamma) - R(l) > 0 \quad (\text{A.36})$$

and the lower bound is given as

$$\gamma > \frac{2^{R(l)} - 1}{\rho_2}. \quad (\text{A.37})$$

Therefore, in case  $\rho_1 < \rho_2$  the search interval can be confined as

$$\frac{2^{R(l)} - 1}{\rho_2} < \gamma < \frac{2^{\frac{R(l)R(t)}{R(t)-R(l)}} - 1}{\rho_2}. \quad (\text{A.38})$$

**Case:**  $\rho_1 > \rho_2$

In this case (A.32) can be upper bounded by defining  $\rho_1 := \rho_2$  as

$$\frac{R(l)}{R(t)} \log_2(1 + \rho_2 \gamma) + \left(1 - \frac{R(l)}{R(t)}\right) \log_2(1 + \rho_2 \gamma) - R(l) < 0, \quad (\text{A.39})$$

which results in

$$\gamma < \frac{2^{R(l)} - 1}{\rho_2}. \quad (\text{A.40})$$

The lower bound can be derived as

$$0 = \frac{R(l)}{R(t)} \log_2(1 + \rho_1 \gamma) + \left(1 - \frac{R(l)}{R(t)}\right) \log_2(1 + \rho_2 \gamma) - R(l) \quad (\text{A.41})$$

$$= \frac{R(l)}{R(t)} \log_2(1 + \rho_1 \gamma) + \log_2(1 + \rho_2 \gamma) - \frac{R(l)}{R(t)} \log_2(1 + \rho_2 \gamma) - R(l) \quad (\text{A.42})$$

$$> \frac{R(l)}{R(t)} \log_2(1 + \rho_1 \gamma) + \log_2(1 + \rho_2 \gamma) - R(l) \quad (\text{A.43})$$

$$> \frac{R(l)}{R(t)} \log_2(1 + \rho_1 \gamma) + \log_2(1 + \rho_1 \gamma) - R(l), \quad (\text{A.44})$$

where in step (A.44)  $\rho_2 := \rho_1$ . Then, the lower bound is

$$\gamma > \frac{2^{\frac{R(l)R(t)}{R(t)+R(l)}} - 1}{\rho_1}. \quad (\text{A.45})$$

Therefore, in case  $\rho_1 > \rho_2$  the search interval can be confined as

$$\frac{2^{\frac{R(l)R(t)}{R(t)+R(l)}} - 1}{\rho_1} < \gamma < \frac{2^{R(l)} - 1}{\rho_2}. \quad (\text{A.46})$$

### Comparison of Closed-Form and Simulation Results for the TPA HARQ Protocols

---

Considering Gaussian channel inputs, Figure B.1 and Figure B.2 depict the outage probability and delay-limited throughput of the TPA HARQ protocols as a function of the D-SNR and compare the closed-form results against the Monte Carlo simulation results. The HARQ protocols are configured according to Section 5.7.1. Both figures demonstrate the agreement of the closed-form and the simulation results.

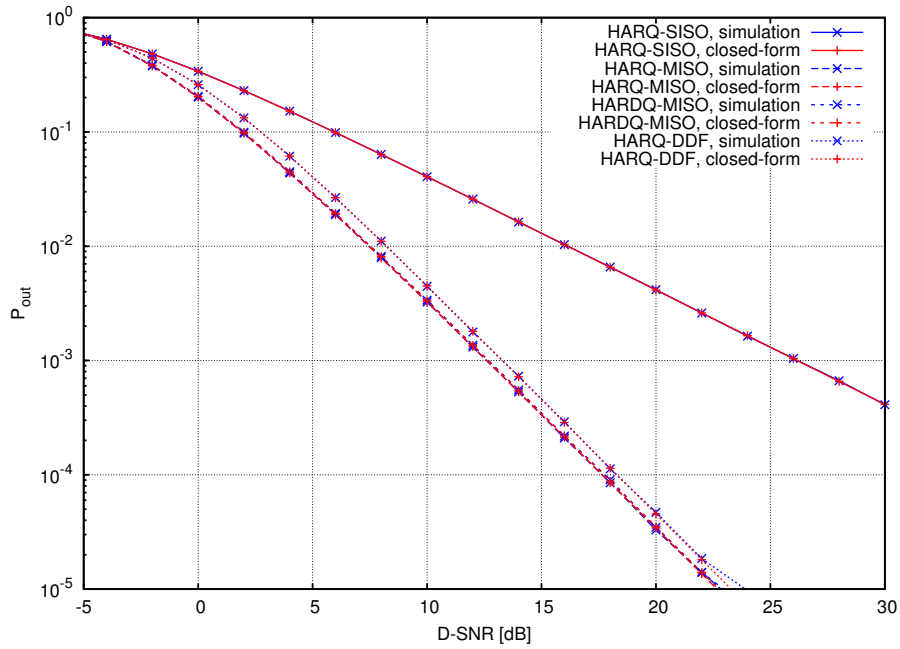


**Figure B.1:** Outage probability of the TPA HARQ protocols measured as a function of the D-SNR. The Monte Carlo simulation results verify the closed-form expressions given in Chapter 5.

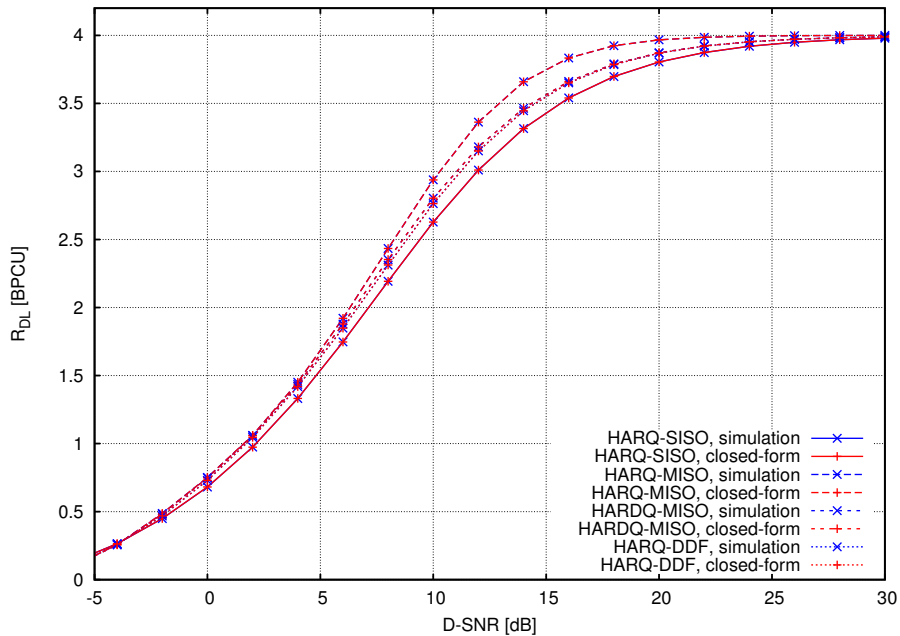


**Figure B.2:** Delay-limited throughput of the TPA HARQ protocols measured as a function of the D-SNR. The Monte Carlo simulation results verify the closed-form expressions given in Chapter 5.

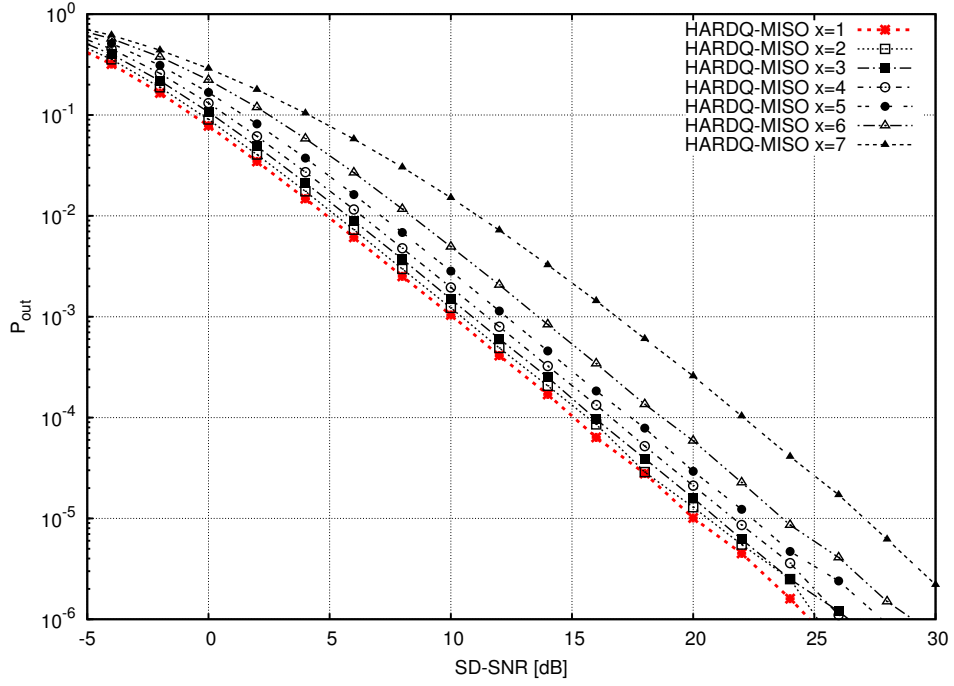
### Numerical Performance Analysis Considering SD-SNR and D-SNR

---

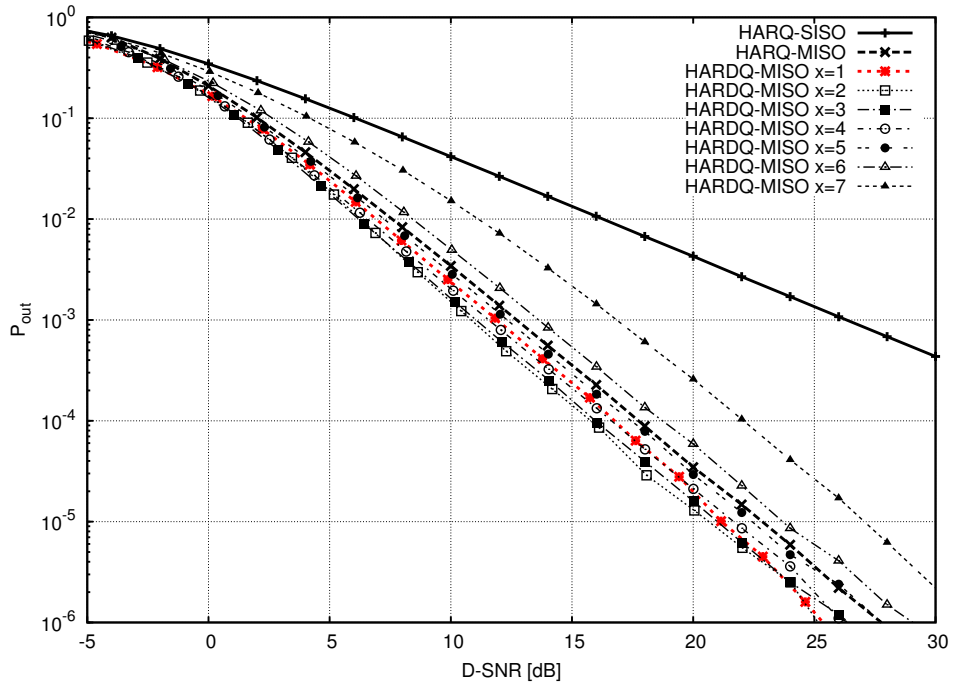
#### C.1 $\mathcal{C}_{\text{non-opt}}$ and 16-QAM Channel Inputs

Section 6.1 compares the performance of the HARQ protocols measured as a function of the SD-SNR and the D-SNR for the non-optimized codebook  $\mathcal{C}_{\text{non-opt}}$  and assuming Gaussian channel inputs. Correspondingly, this section gives the performance comparison assuming uniformly distributed 16-QAM channel inputs.

Figure C.1 and Figure C.2 depict the outage probability measured as a function of the SD-SNR and the D-SNR for the HARDQ-MISO and the HARQ-DDF protocol, respectively. The HARDQ-MISO protocol shows the same performance characteristics as observed for the assumption of Gaussian channel inputs. However, in comparison to Section 6.1, the performance measured for the HARQ-DDF protocol with configuration  $x = 1$  in Figure C.2 does not show to achieve the performance of the configurations  $x = 2$  and  $x = 3$  at high D-SNR.

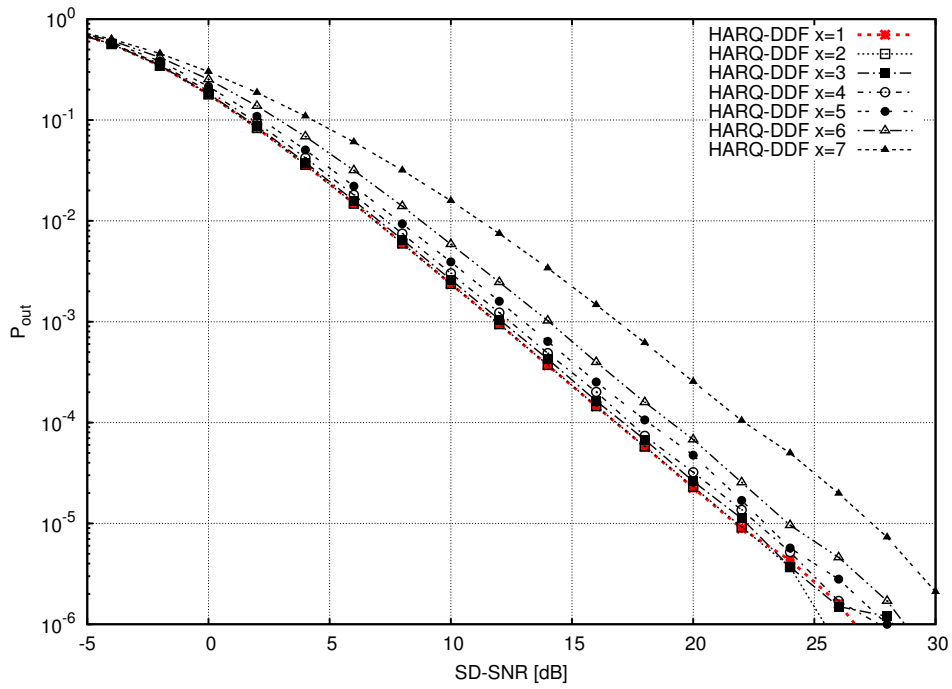


(a) Outage probability as a function of the SD-SNR

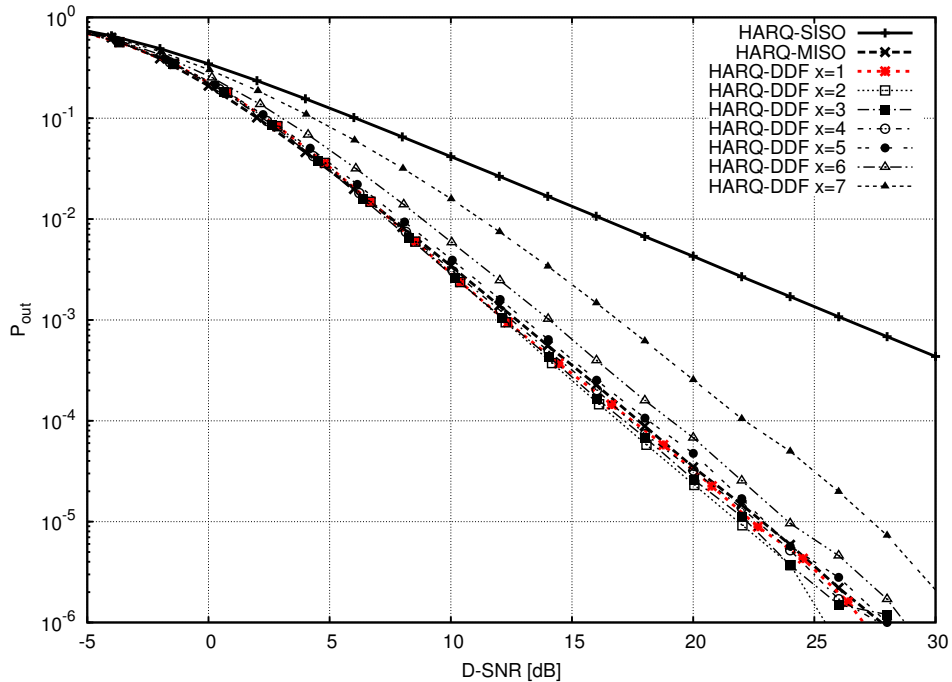


(b) Outage probability as a function of the D-SNR

**Figure C.1:** Comparison of the outage probability measured as a function of the SD-SNR and D-SNR for the HARQ-MISO protocol considering uniformly distributed 16-QAM channel inputs and increasing  $t = x$ .

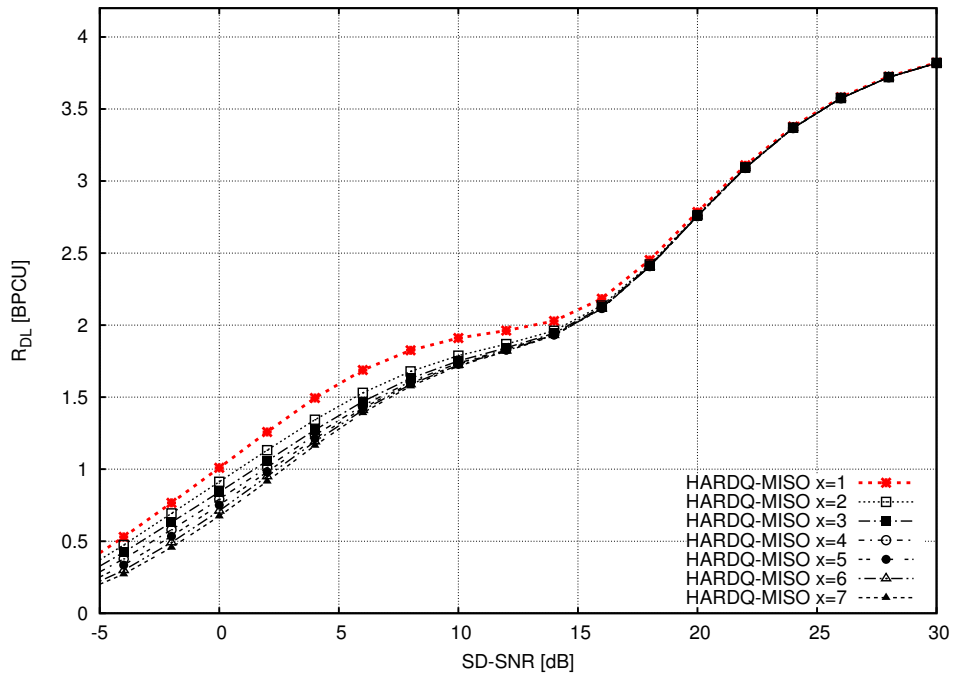


(a) Outage probability as a function of the SD-SNR

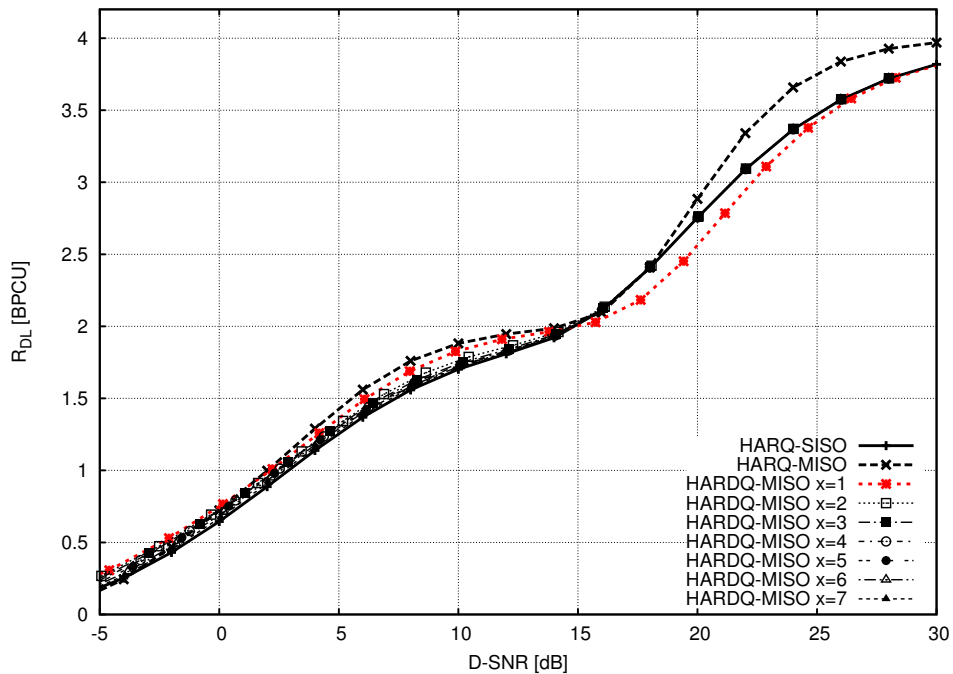


(b) Outage probability as a function of the D-SNR

**Figure C.2:** Comparison of the outage probability measured as a function of the SD-SNR and D-SNR for the HARQ-DDF protocol considering uniformly distributed 16-QAM channel inputs and increasing  $\min\{D_r\} = x$ .

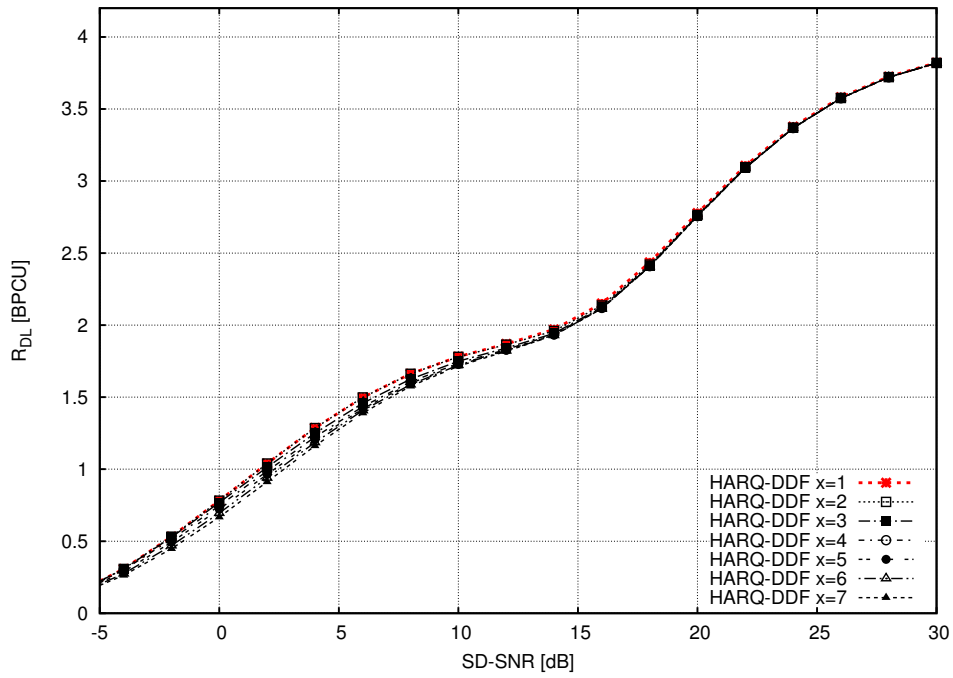


(a) Delay-limited throughput as a function of the SD-SNR

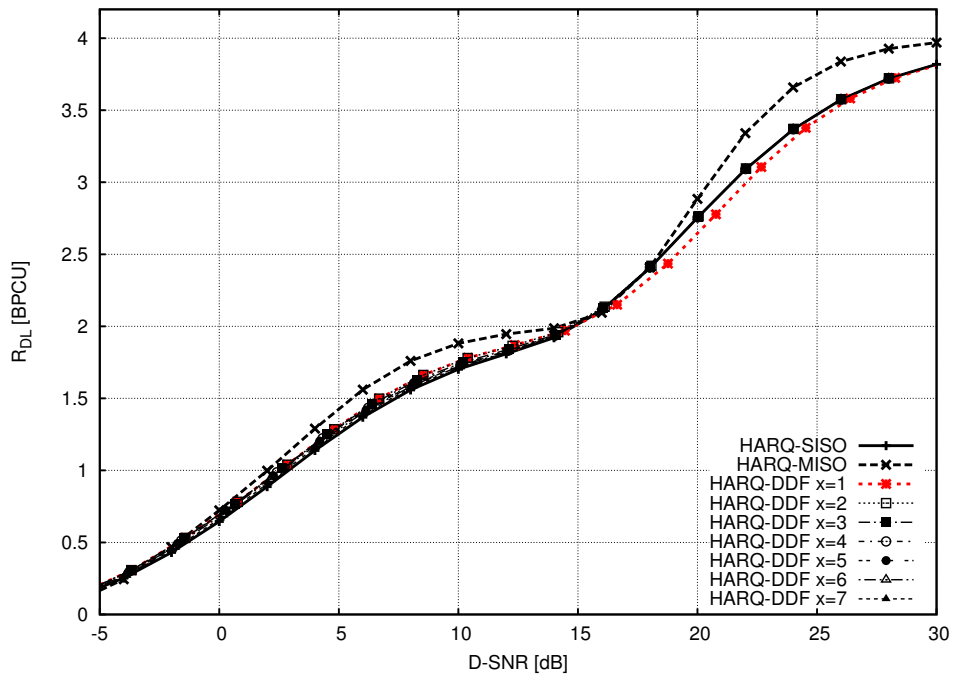


(b) Delay-limited throughput as a function of the D-SNR

**Figure C.3:** Comparison of the delay-limited throughput measured as a function of the D-SNR and the SD-SNR for the HARQ-MISO protocol considering uniformly distributed 16-QAM channel inputs and increasing  $t$ .



(a) Delay-limited throughput as a function of the SD-SNR



(b) Delay-limited throughput as a function of the D-SNR

**Figure C.4:** Comparison of the delay-limited throughput measured as a function of the D-SNR and the SD-SNR for the HARQ-DDF protocol considering uniformly distributed 16-QAM channel inputs and increasing  $\min\{D_r\}$ .

Figure C.3 and Figure C.4 depict the delay-limited throughput measured as a function of the SD-SNR and the D-SNR for the HARDQ-MISO and the HARQ-DDF protocol. In comparison to Section 6.1, a significant kink can be observed at  $R_{\text{DL}} = 2$  which is caused by the non-optimized rate function  $R_{\text{non-opt}}(l)$  given in (6.1). Section 6.2 shows that this characteristic can be abolished by the application of the optimized mother code  $\mathcal{C}_{\text{opt}}$  associated with the code rate function  $R_{\text{opt}}(l)$  given in (6.2).

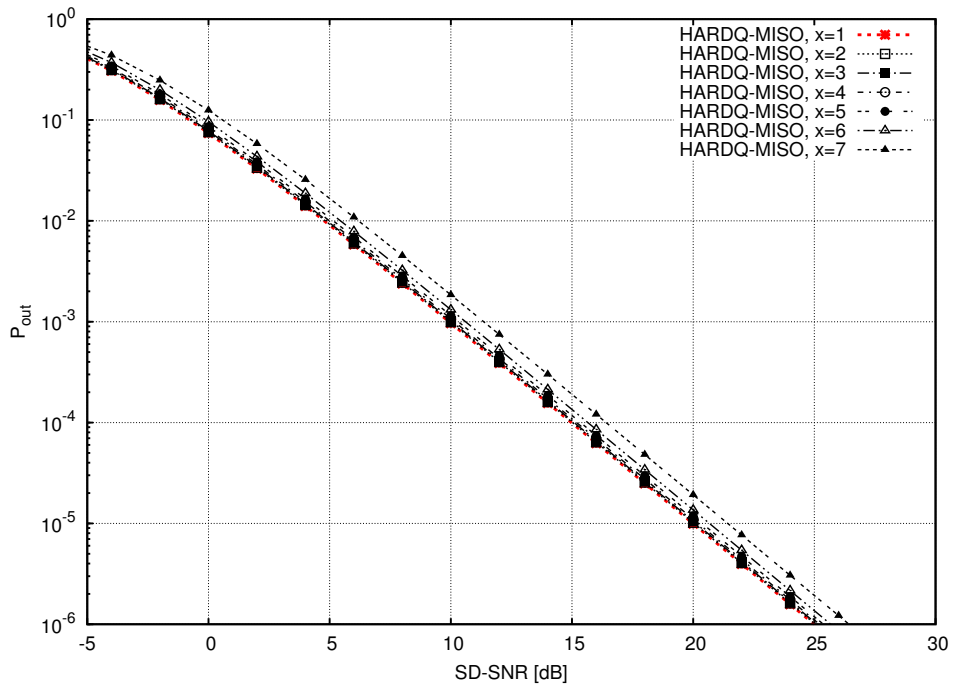
## C.2 $\mathcal{C}_{\text{opt}}$ and Gaussian Channel Inputs

Section 6.1 compares the performance of the HARQ protocols measured as a function of the SD-SNR and the D-SNR for the non-optimized codebook  $\mathcal{C}_{\text{non-opt}}$  assuming Gaussian channel inputs. Correspondingly, this section gives the performance comparison for the optimized code book  $\mathcal{C}_{\text{opt}}$ .

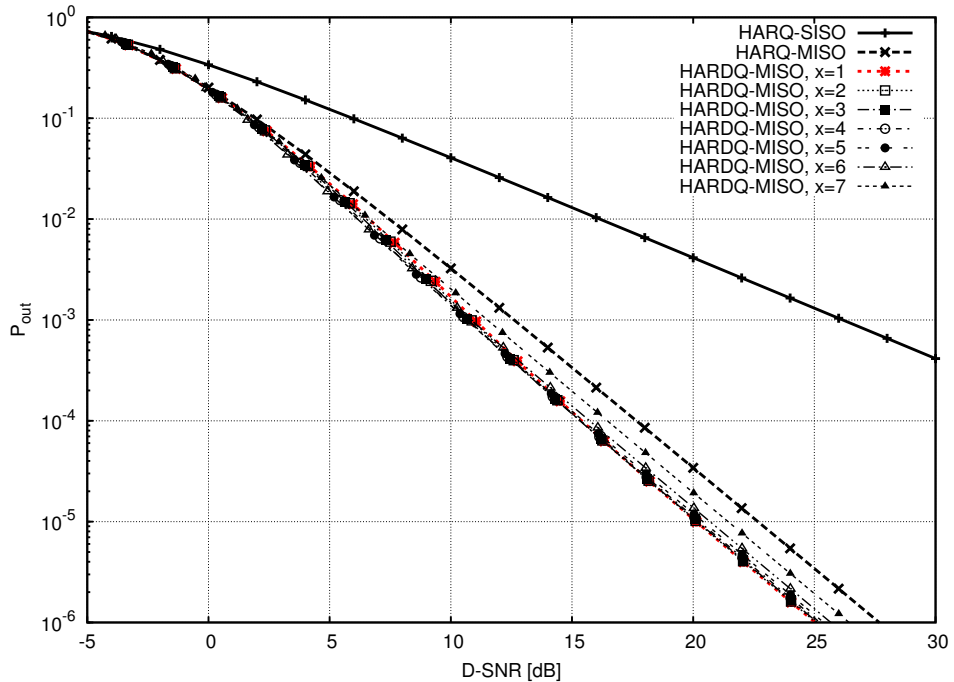
### C.2.1 HARDQ-MISO Protocol

Considering Gaussian channel inputs, Figure C.5 and Figure C.6 depict the outage probability and the delay-limited throughput of the HARDQ-MISO protocol, respectively. With respect to the comparison of the performance measured as a function of the SD-SNR against the performance measured as a function of the D-SNR, it can be observed that the application of the optimized codebook  $\mathcal{C}_{\text{opt}}$  shows similar performance characteristics as the application of the non-optimized codebook  $\mathcal{C}_{\text{non-opt}}$ .

Figure C.9 depicts the outage probability measured as a function of the SD-SNR and the D-SNR for the HARDQ-MISO protocol. In comparison to the performance obtained for the non-optimized codebook  $\mathcal{C}_{\text{non-opt}}$  it can be observed that the performance loss for increasing  $x$  is significantly smaller. However, in comparison with the configuration  $x = 1$ , a significant performance loss can be observed for  $x = 7$ . Furthermore, in comparison to Figure C.9a, measuring the outage probability as a function of the D-SNR as depicted in Figure C.5b shows no performance loss at low D-SNR. This characteristic is consistent with the observation for the non-optimization codebook given in Section 6.1. In comparison to Section 6.1, the optimized codebook outperforms the HARQ-MISO protocol for all configurations  $x$  in terms of outage probability.

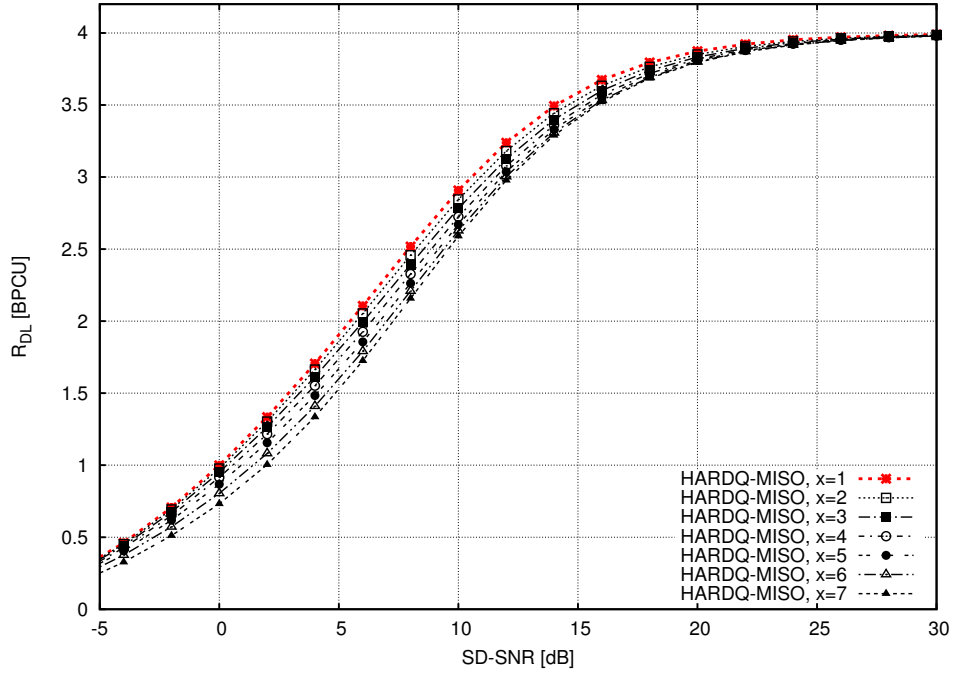


(a) Outage probability as a function of the SD-SNR

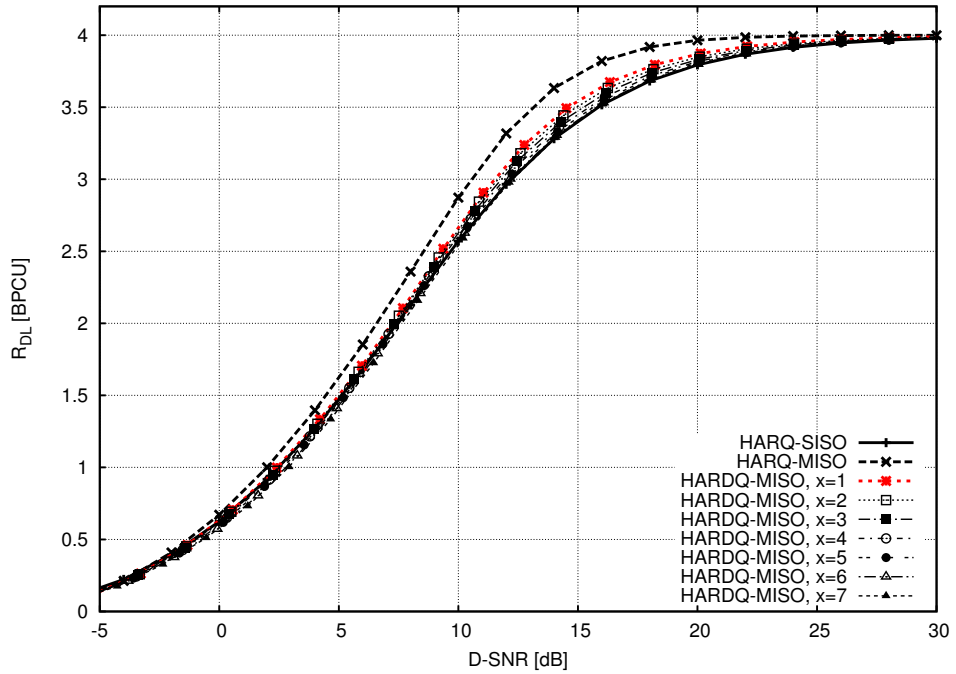


(b) Outage probability as a function of the D-SNR

**Figure C.5:** Comparison of the outage probability measured as a function of the SD-SNR and the D-SNR for the HARDQ-MISO protocol considering Gaussian channel inputs and increasing  $t = x$ .

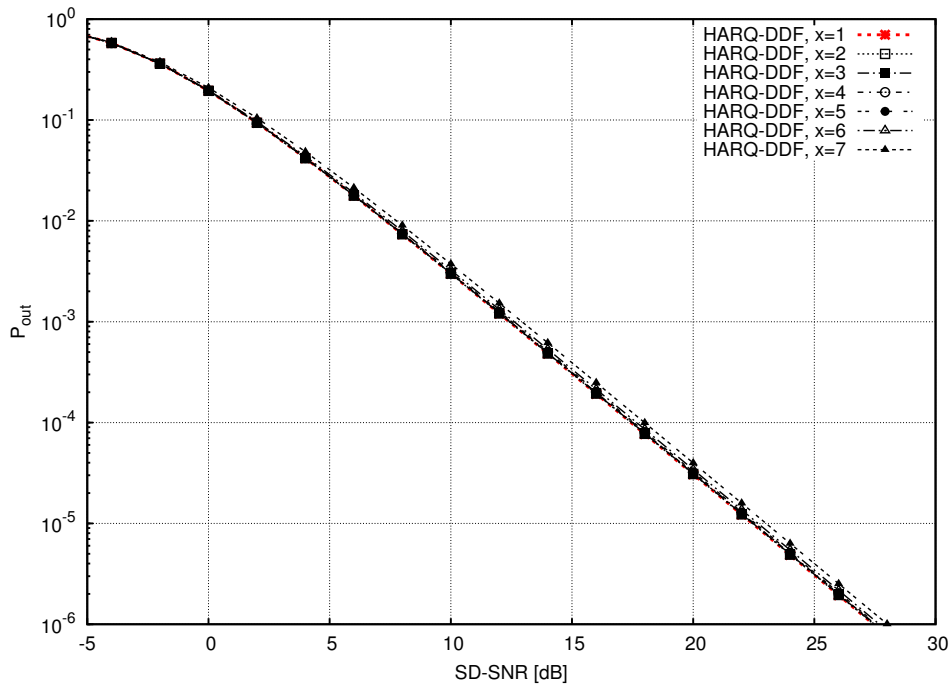


(a) Delay-limited throughput as a function of the SD-SNR

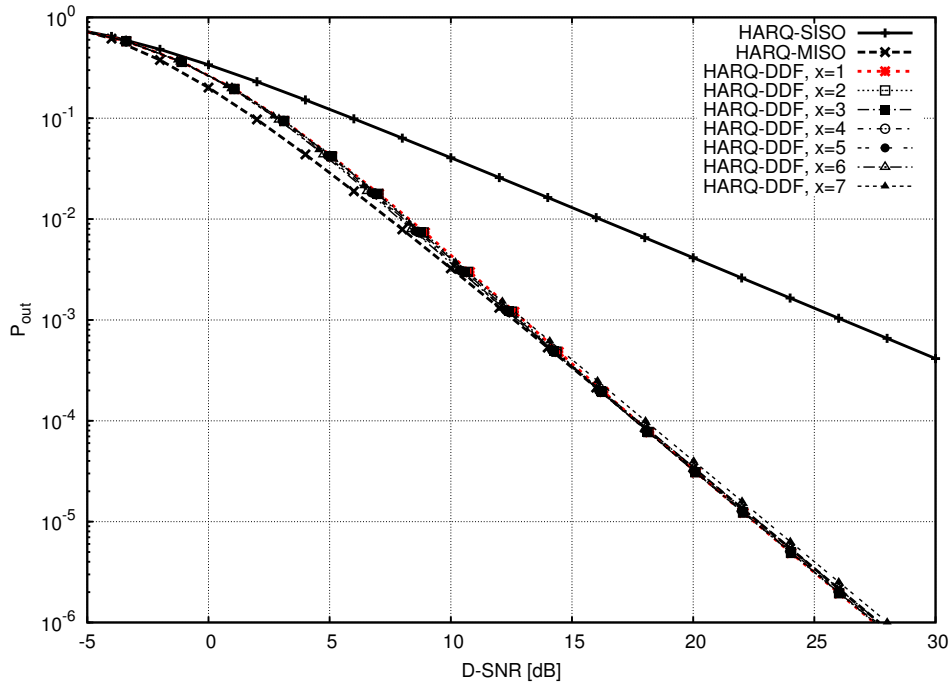


(b) Delay-limited throughput as a function of the D-SNR

**Figure C.6:** Comparison of the delay-limited throughput measured as a function of the SD-SNR and the D-SNR for the HARQ-MISO protocol considering Gaussian channel inputs and increasing  $t = x$ .

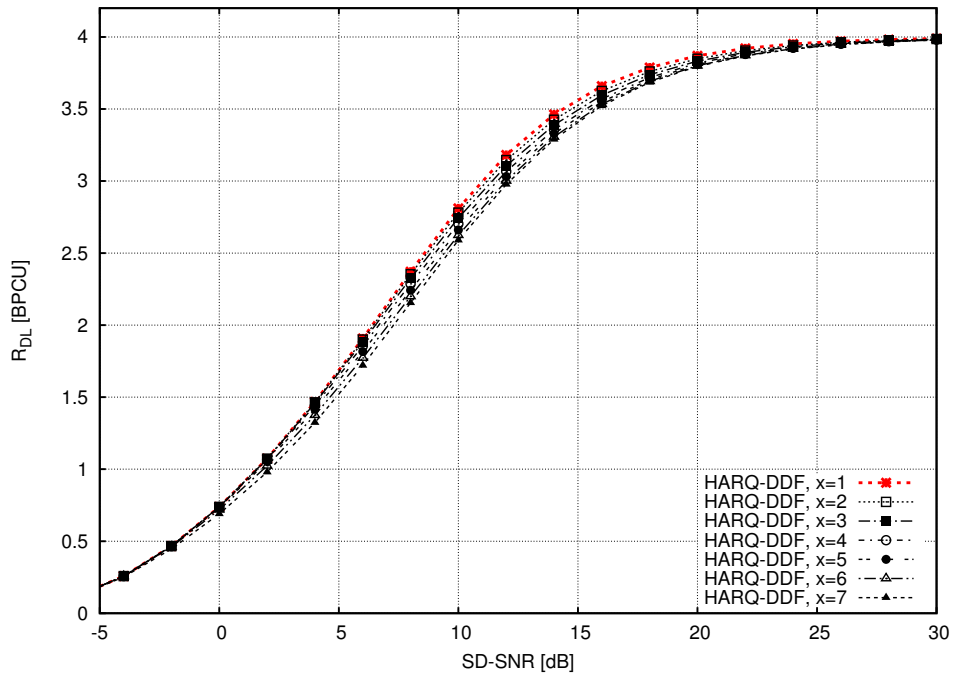


(a) Outage probability as a function of the SD-SNR

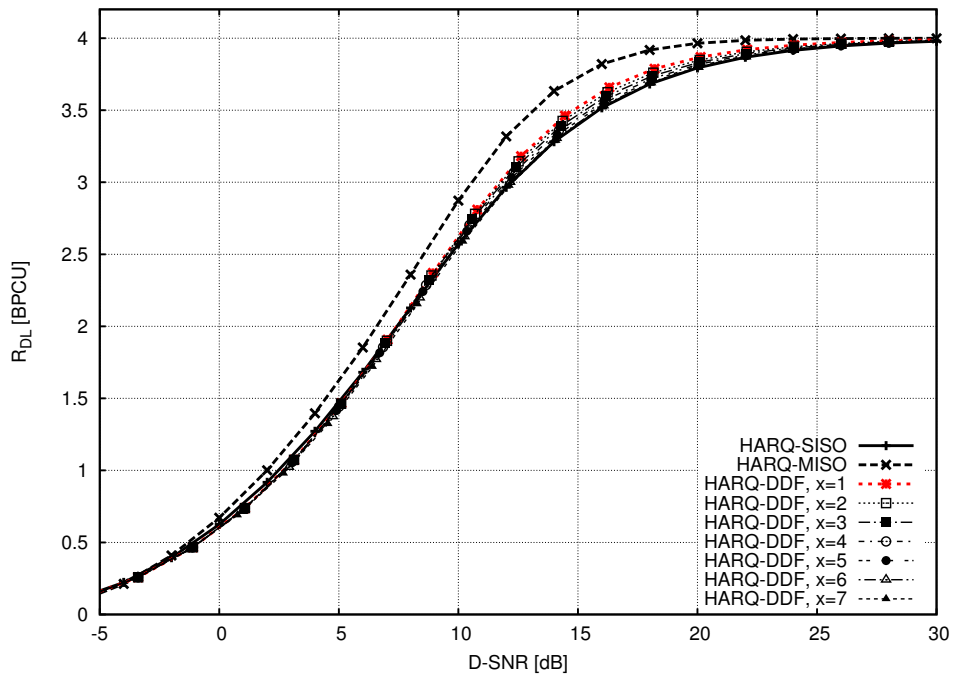


(b) Outage probability as a function of the D-SNR

**Figure C.7:** Comparison of the outage probability measured as a function of the SD-SNR and the D-SNR for the HARQ-DDF protocol considering Gaussian channel inputs and increasing  $\min\{D_r\} = x$ .



(a) Delay-limited throughput as a function of the SD-SNR



(b) Delay-limited throughput as a function of the D-SNR

**Figure C.8:** Comparison of the delay-limited throughput measured as a function of the SD-SNR and the D-SNR for the HARQ-DDF protocol considering Gaussian channel inputs and increasing  $\min\{D_r\} = x$ .

Correspondingly, Figure C.10 depicts the delay-limited throughput measured as a function of the SD-SNR and the D-SNR. While it is demonstrated in Section 6.1 that the HARQ-SISO protocol outperforms the HARDQ-MISO protocol for configuration  $x = 1$ , it can be observed in Figure C.10b that the optimized codebook  $\mathcal{C}_{\text{opt}}$  outperforms the HARQ-SISO protocol at medium to high D-SNR.

### C.2.2 HARQ-DDF Protocol

Considering Gaussian channel inputs, Figure C.7 and Figure C.8 depict the outage probability and the delay-limited throughput of the HARQ-DDF protocol, respectively. With respect to the comparison of the performance measured as a function of the SD-SNR against the performance measured as a function of the D-SNR, it can be observed that the application of the optimized codebook  $\mathcal{C}_{\text{opt}}$  shows similar performance characteristics as the application of the non-optimized codebook  $\mathcal{C}_{\text{non-opt}}$ .

Figure C.11 depicts the outage probability measured as a function of the SD-SNR and the D-SNR for the HARQ-DDF protocol. It can be observed that both performance measures show the same characteristics from low to high D-SNR. While a significant increase in performance loss with increasing  $x$  can be observed in Section 6.1, the application of the optimized codebook shows a small performance loss for the configuration  $x = 7$  only.

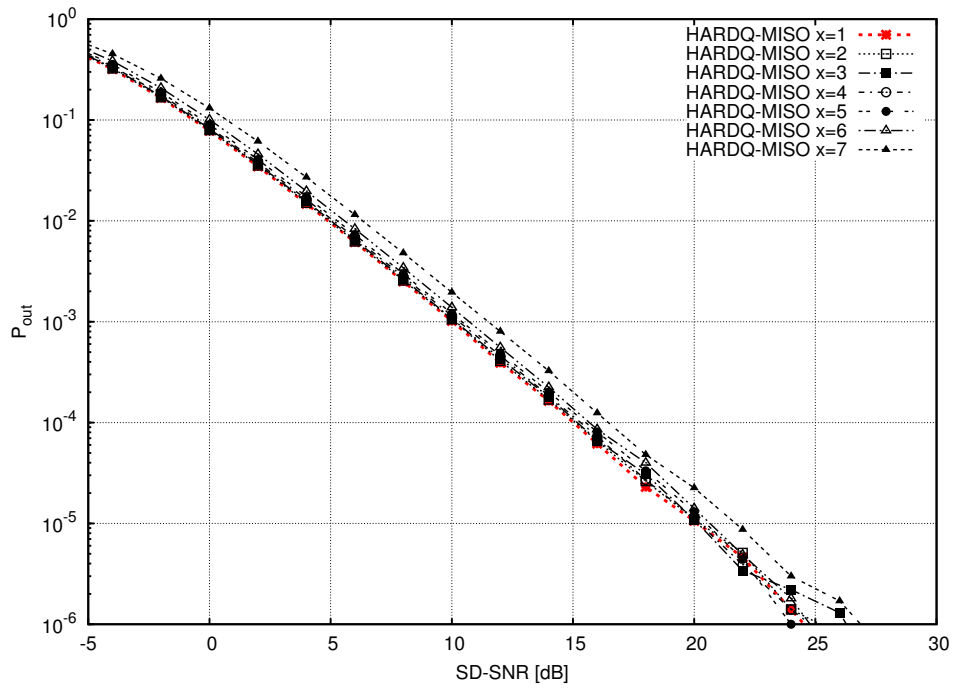
Correspondingly, Figure C.12 depicts the delay-limited throughput measured as a function of the SD-SNR and the D-SNR. In Section 6.1 it is demonstrated that the application of the non-optimized codebook allows to achieve at most the performance of the HARQ-SISO protocol. However, Figure C.8b shows that the application of the optimized codebook enables to outperform the HARQ-SISO protocol at medium to high D-SNR.

## C.3 $\mathcal{C}_{\text{opt}}$ and 16-QAM Channel Inputs

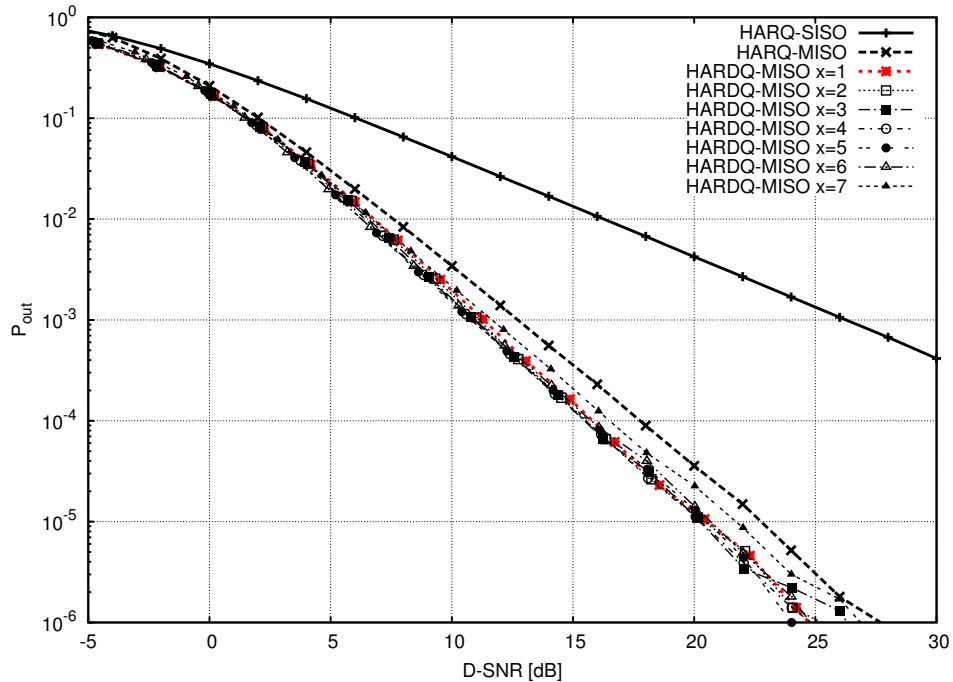
Section 6.1 compares the performance of the HARQ protocols measured as a function of the SD-SNR and the D-SNR for the non-optimized codebook  $\mathcal{C}_{\text{non-opt}}$  assuming Gaussian channel inputs. Correspondingly, this section gives

the performance comparison for the optimized code book  $\mathcal{C}_{\text{opt}}$  and assuming uniform distribution of 16-QAM channel inputs.

Figure C.9 and Figure C.10 depict the outage probability and the delay-limited throughput of the HARDQ-MISO protocol, respectively. It can be observed that the application of uniform distributed 16-QAM channel inputs gives the same performance characteristics as observed for Gaussian channel inputs in Section C.2. However, in terms of delay-limited throughput, Figure C.10b shows that the application of 16-QAM channel inputs results in a significant performance loss at medium D-SNR in comparison with Gaussian channel inputs. Furthermore, the performance gains over the HARQ-SISO protocol are smaller. These observations are also valid for the corresponding performance measures of the HARQ-DDF protocol depicted in Figure C.11 and Figure C.12

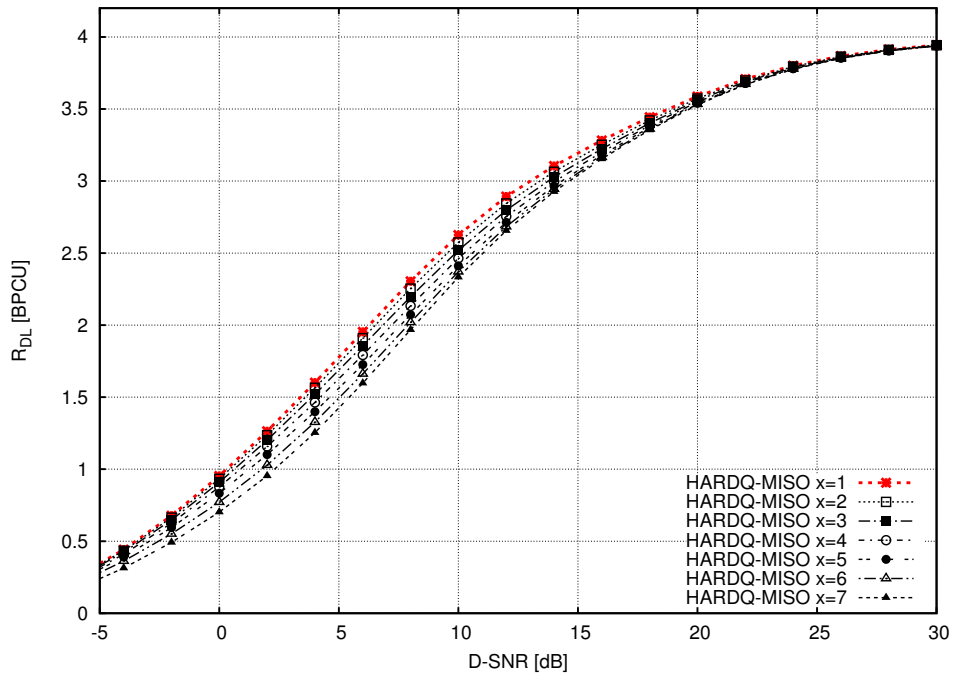


(a) Outage probability as a function of the SD-SNR

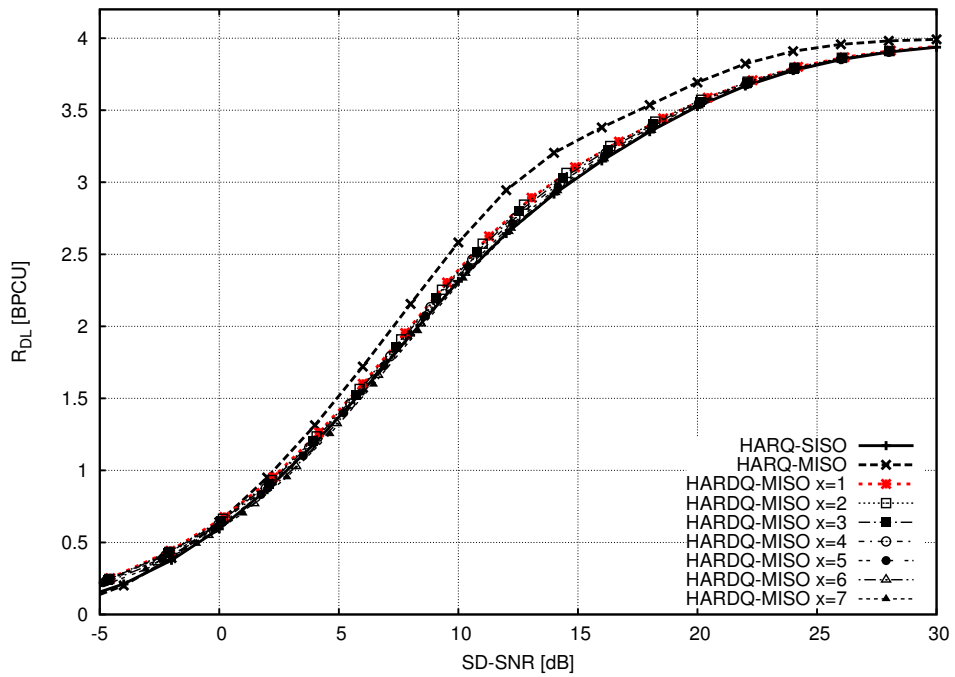


(b) Outage probability as a function of the D-SNR

**Figure C.9:** Comparison of the outage probability measured as a function of the SD-SNR and the D-SNR for the HARQ-MISO protocol considering uniformly distributed 16-QAM channel inputs and increasing  $t = x$ .

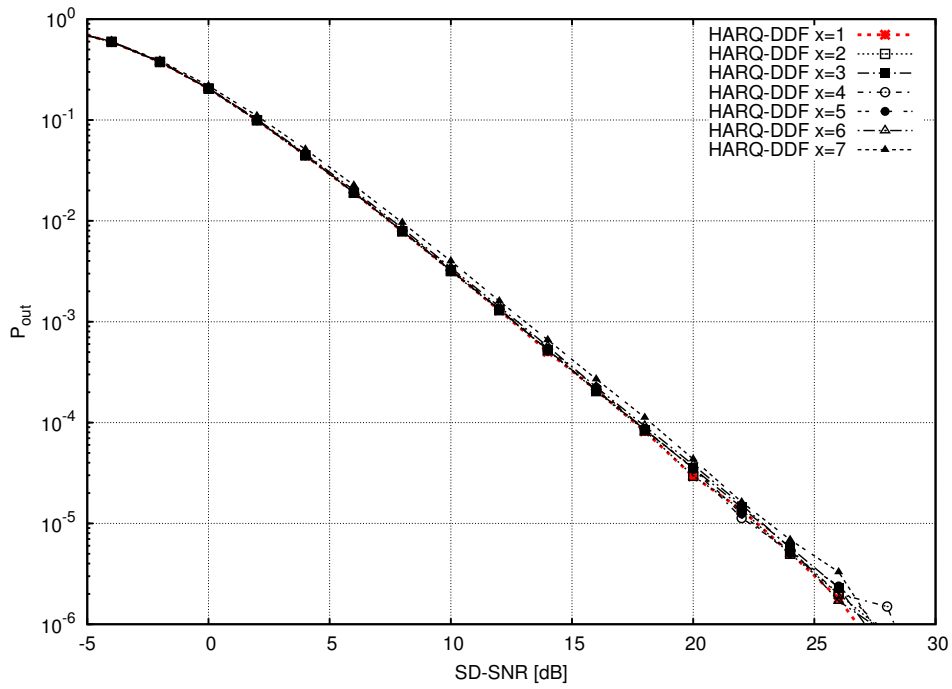


(a) Delay-limited throughput as a function of the SD-SNR

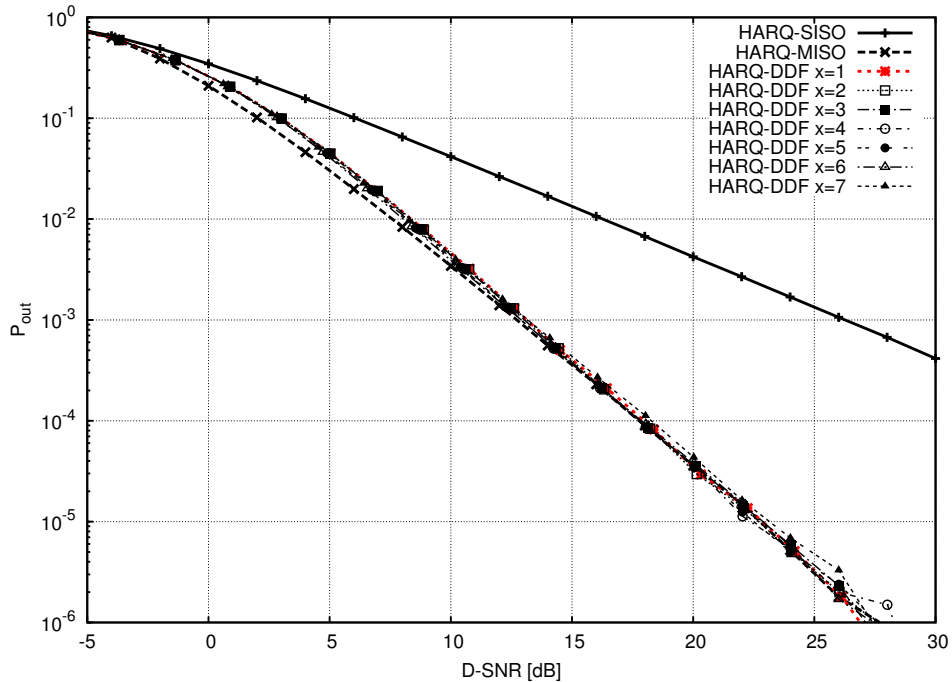


(b) Delay-limited throughput as a function of the D-SNR

**Figure C.10:** Comparison of the delay-limited throughput measured as a function of the SD-SNR and the D-SNR for the HARQ-MISO protocol considering uniformly distributed 16-QAM channel inputs and increasing  $t = x$ .

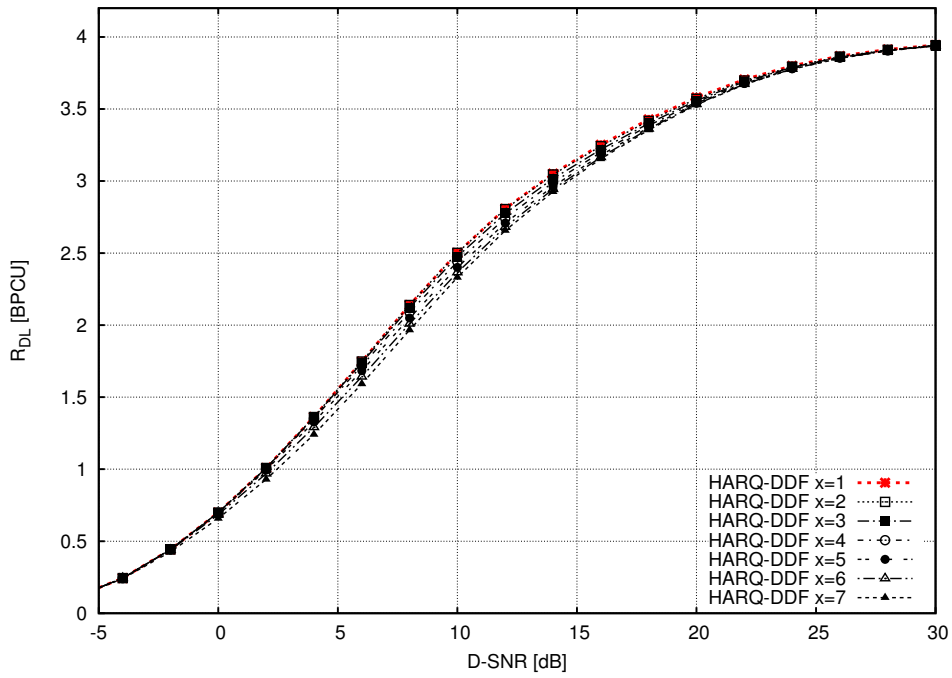


(a) Outage probability as a function of the SD-SNR

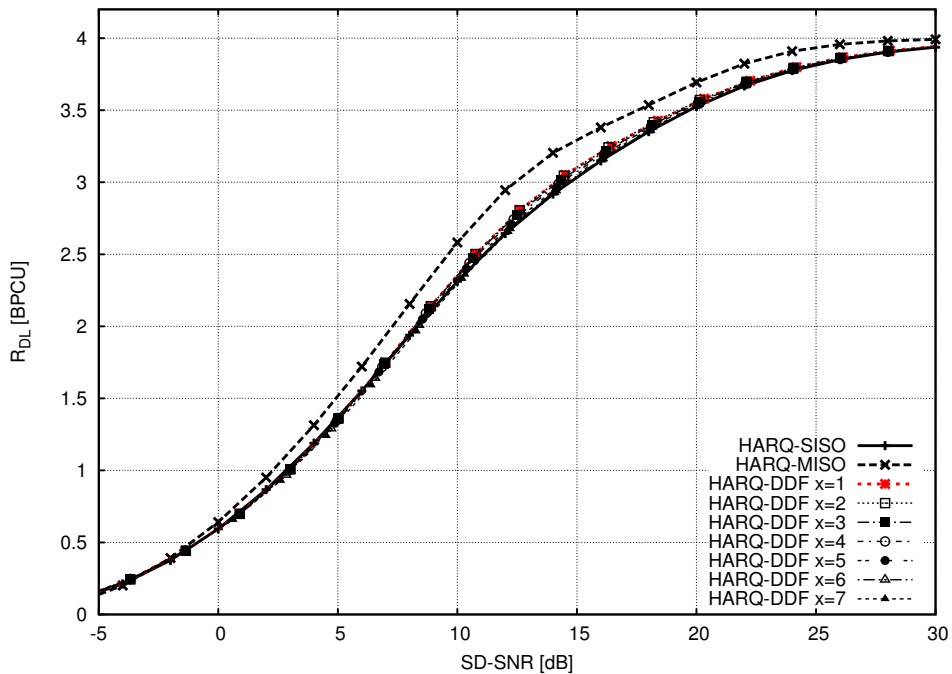


(b) Outage probability as a function of the D-SNR

**Figure C.11:** Comparison of the outage probability measured as a function of the SD-SNR and the D-SNR for the HARQ-DDF protocol considering uniformly distributed 16-QAM channel inputs and increasing  $\min\{D_r\} = x$ .



(a) Delay-limited throughput as a function of the SD-SNR



(b) Delay-limited throughput as a function of the D-SNR

**Figure C.12:** Comparison of the delay-limited throughput measured as a function of the D-SNR and the SD-SNR for the HARQ-DDF protocol considering uniformly distributed 16-QAM channel inputs and increasing  $\min\{D_r\} = x$ .

### Performance of the RCPC Encoded HARQ Protocols With Increasing Memory

---

This appendix compares the performance measured for the RCPC encoded HARQ protocols against the performance measured for Gaussian channel inputs, and for uniformly distributed BPSK channel inputs. The performance of the RCPC encoded HARQ protocols is improved by increasing the code memory size. To this end, consider the RCPC mother code  $C_{\text{RCPC}}(3, 1, v)$  associated with the code rate function  $R(l)$  given in (7.5). On the one hand, the performance considering Gaussian channel inputs is computed using the closed-form expressions given in Chapter 5. On the other hand, the performance considering uniformly distributed BPSK channel inputs is measured using the Monte Carlo simulation method as discussed in Chapter 5.7. The performance of the RCPC encoded HARQ protocols is measured using the Monte Carlo simulation method for code memory sizes of  $v = 2, 4, 6$ .

Figure D.1, Figure D.2, Figure D.3 and Figure D.4 depict the corresponding performance measures in terms of outage probability and delay-limited throughput for the HARQ-SISO, HARQ-MISO, HARQ-MISO and the HARQ-DDF protocol, respectively. It can be observed that the assumption of the Gaussian

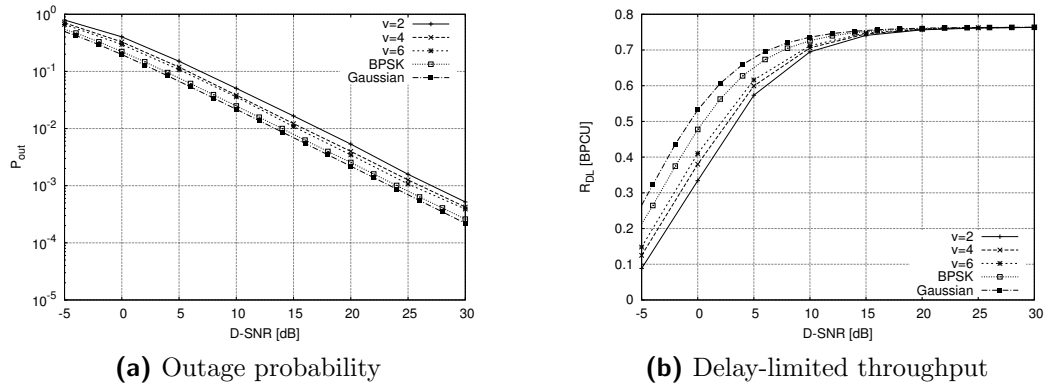


**Figure D.1:** HARQ-SISO protocol: comparison of the achievable performance and the performance applying RCPC coding with memory  $v = 2, 4, 6$ .

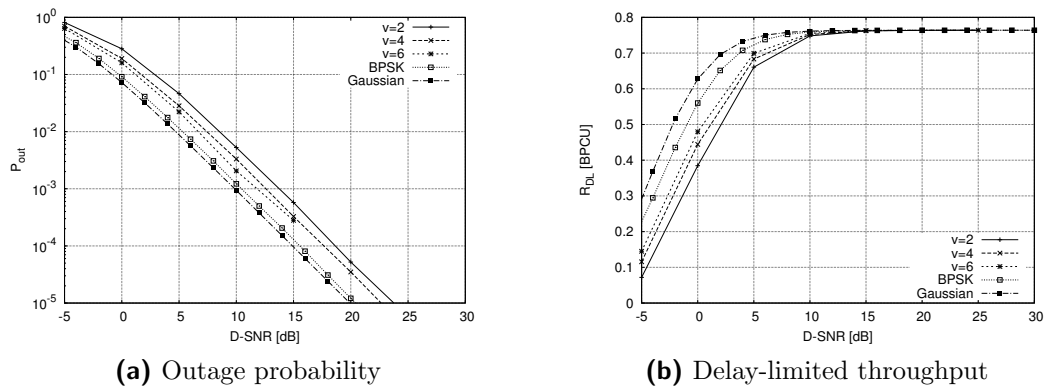


**Figure D.2:** HARQ-MISO protocol: comparison of the achievable performance and the performance applying RCPC coding with memory  $v = 2, 4, 6$ .

channel inputs is superior than the assumption of uniformly distributed BPSK channel inputs. It is noteworthy that the Alamouti code is not capacity achieving. Therefore, the performance considering Gaussian channel inputs gives the *achievable* performance with respect to Alamouti encoding. However, it can be observed that the RCPC encoded HARQ protocols do not give the achievable performance measures. But increasing the code memory order  $v$  significantly improves the performance measured for the RCPC encoded HARQ protocols.

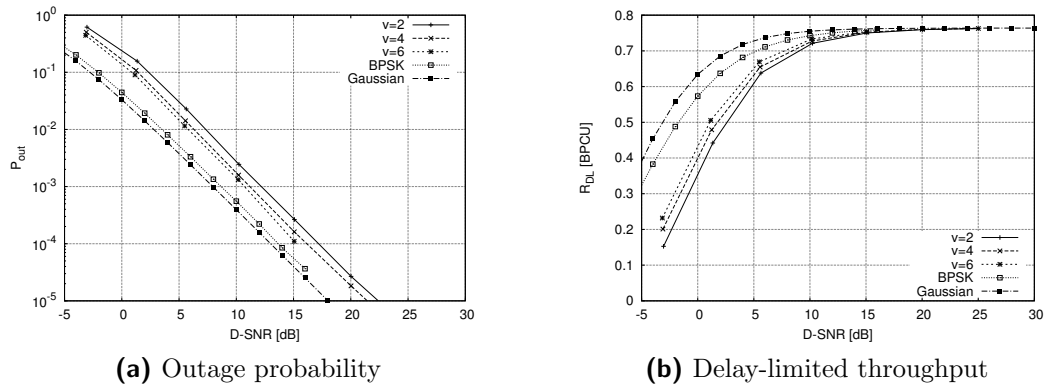


**Figure D.3:** HARQ-MISO protocol: comparison of the achievable performance and the performance applying RCPC coding with memory  $v = 2, 4, 6$ .

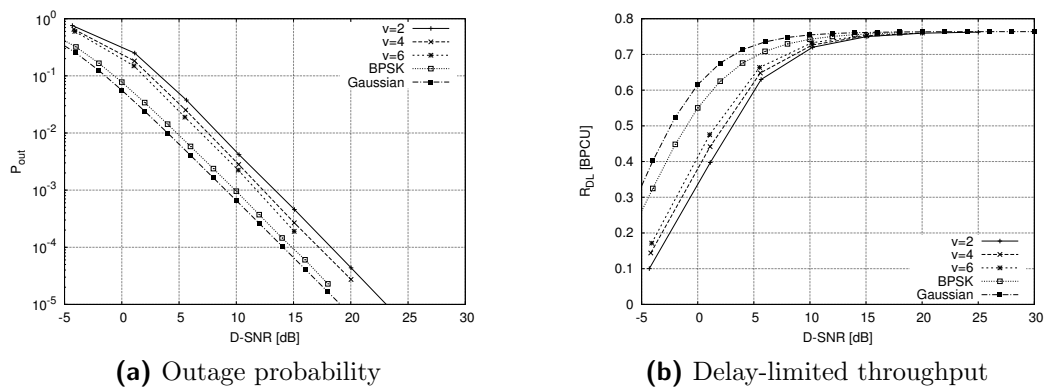


**Figure D.4:** HARQ-DDF protocol: comparison of the achievable performance and the performance applying RCPC coding with memory  $v = 2, 4, 6$ .

### Publications

---

#### **E.1 On the Dynamic Decode-and-Forward Relay Listen-Transmit Decision Rule in Intersymbol Interference Channels**

This conference paper was presented and accepted for publication on the *9th WSEAS International Conference on DATA NETWORKS, COMMUNICATIONS, COMPUTERS (DNCOCO '10)* that took place in November 3-5, 2010.









## **E.2 RCPC Coding for the Dynamic Decode-and-Forward Channel**

This conference paper was presented and accepted for publication on the *3rd International Conference on IEEE Conference on Microwaves, Communications, Antennas and Electronic Systems* (IEEE COMCAS 2011) that took place in November 7-9, 2011.













### **E.3 The Dynamic Decode-and-Forward Channel: SNR Allocation For Fair Performance Analysis**

This conference paper was presented and accepted for publication on the *21st Telecommunications forum TELFOR 2013* (IEEE TELFOR 2013) that took place in November 26-28, 2013.







